Palaeoenvironmental reconstruction of South African hominin-bearing cave deposits using stable isotope geochemistry

Philip J. Hopley

THE UNIVERSITY
of LIVERPOOL

Thesis submitted in accordance with the requirements of the University of Liverpool for the degree of Doctor of Philosophy. I declare that the content of this thesis is my own work and that it has not been submitted for examination at any other university.

2nd June 2004

Philip Jeffrey Hopley

ABSTRACT

The influence of climate change on early hominin speciation, extinction and migration is a central issue in the study of human evolution. To evaluate the role of climatic change in early hominin evolution it is of paramount importance to develop continuous and high-resolution terrestrial climate proxies from early hominin sites.

Plio-Pleistocene flowstones from South African hominin sites have been studied using stable isotopes of oxygen and carbon to develop a record of early hominin habitat change. A petrological and geochemical study of the flowstones shows the presence of primary aragonite, primary calcite and secondary (diagenetic) calcite. The identification of primary calcite flowstones was required to ensure the preservation of climatic signals within the speleothems.

Two long (2.4 m and 1.5 m) primary calcite flowstone sequences from the Makapansgat Valley, the Buffalo Cave flowstone and the Makapansgat Limeworks Member 1b (Collapsed Cone flowstone), were used to develop an oxygen and carbon isotope time series. The chronology of both flowstones was based on an established magnetostratigraphy (Herries, 2003), and the Buffalo Cave flowstone chronology was further constrained using UV annual-banding and time-series analysis. The orbitally tuned climate record from Buffalo Cave flowstone dates from 2 Ma to 1.5 Ma.

The incorporation of carbon isotopes into the speleothem carbonate was modelled using the $\delta^{13}C$ value of co-occurring organic matter as an indicator of the $\delta^{13}C$ value of palaeovegetation. This model indicates a high host-rock proportion of approximately 50% and enables the $\delta^{13}C$ values of the speleothem carbonate to be interpreted in terms of palaeovegetation: -8‰ indicates a purely C_3 palaeovegetation and –1‰ a purely C_4 palaeovegetation. Based on this model and the measured $\delta^{13}C$ values of organic matter, the Collapsed Cone flowstone was deposited in a purely C_3 environment, whereas the Buffalo Cave flowstone was deposited in a mixed C_3 and C_4 environment which varied from a C_4 dominated to C_3 dominated vegetation. The Buffalo Cave flowstone shows a shift towards a more C_4 grass dominated environment at 1.7 Ma which is similar in magnitude and timing to that observed in South African faunal and east African palynological records.

Stable isotope and microwear analysis of fossil rodent teeth from the Makapansgat Limeworks enabled mid-Pliocene palaeodiets and palaeoenvironments to be reconstructed. The palaeoenvironment had a greater forest cover than in the present day and also supported a significant proportion of savannah (C_4) grasses.

The origin of C_4 grasses is marked by a worldwide carbon isotope shift in the mid to late Miocene and a synchronous restructuring of terrestrial faunas. Details of the origin and spread of C_4 grasses were determined by combining the stable isotope data from this study with published records of late Neogene C_4 grass distribution. As predicted by the temperature and pCO_2 constraints on C_4 grass distribution, C_4 grasses first occurred in low latitudes in the mid-Miocene and continued to spread into mid-latitudes until the early Pliocene. This is circumstantial evidence to suggest that the spread of C_4 grasslands may have been a causal factor in the development of hominin bipedalism.

TABLE OF CONTENTS

LIST OF FIGURES

AKNOWLEDGEMENTS

I would like to thank my supervisors Jim Marshall and Alf Latham for all their help throughout this project. Thanks also to Steve Crowley for his help on all aspects of this work and to Jim Ball for assistance in the lab. Thanks to Lee Berger, Ron Clarke, Heidi Fourie, Andre Keyser, Kevin Kuykendall and Mike Raath for access to the speleothem and teeth specimens. Thanks to Kevin Kuykendall and Kay Reed for including me in their Makapansat field school and to Kevin for his help with the sampling and for letting me stay at his house. Thanks to Lee Berger, Darryl deRuiter, Kevin Kuykendall, Rodrigo LaCruz, Tim Partridge and Francis Thackeray for their help in the field at the Cradle of Humankind sites. Thanks to Mary Leslie at the South African Heritage Resources Agency (SAHRA) for the granting of permits to export the specimens out of South Africa.

Thanks to Kees Veltkamp for help with the SEM and for taking the SEM micrographs. Thanks to Andy Baker for use of the fluorescence spectrophotometer and UV microscope at the University of Newcastle, and for his help and advice. Thanks to Sarah James and Jacqui Duffett at the NERC ICP-AES facility at Royal Holloway, University of London for their help with the analysis and correction of the trace element data. Thanks to Paul Middlestead and Gilles St Jean at the University of Ottawa for running the dissolved organic carbon isotopic analyses and to the British Cave Research Association (BCRA) research fund for financing these samples. Thanks to Andy Herries for sharing his palaeomagnetic data and speleothem samples. Special thanks go to Graham Weedon for performing the spectral analyses, for producing the time-series analysis figures and for his help discussing and interpreting the time-series data. My PhD work was funded by NERC studentship NER/A/2000/04058.

I'd like to thank Joanne Walker, Dan Barnes, Andy Herries, Martin Gratton and Sally Reynolds for their help and friendship during this work. Thanks to my parents and sisters and to Lydia and the Mansons for their support over the last three years.

THESIS OVERVIEW

This thesis is an investigation of South African Plio-Pleistocene palaeoclimatic change, and the influence of these climatic changes on events in early hominin evolution.

Chapter 1 introduces and evaluates the existing theories that suggest specific links between palaeoclimatic change and early human evolution. Possible methods for testing the Savannah Hypothesis, the idea that the earliest hominins evolved in response to an expanding savannah ecosystem, are suggested.

Chapter 2 reviews previous palaeoenvironmental studies at the South African hominin sites and the problems encountered, such as time-averaged deposits, low-resolution environmental records and qualitative palaeo-environmental proxies.

The following chapters of this thesis document the attempt to create a detailed record of temperature and vegetation change based on the study of oxygen and carbon isotopes in flowstones (secondary calcite deposits) and fossil teeth from the South African cave-sites:

Chapter 3 provides the first detailed study of the South African Plio-Pleistocene speleothems. This petrographic and geochemical study indicates that both primary and diagenetic (secondary) speleothems are present within the cave deposits. Therefore, if any meaningful palaeoclimatic data is to be retrieved from these caves, it is important to develop criteria for the identification of primary calcite speleothems. Primary calcite flowstones can be identified petrographically but they are not common within the South African hominin sites. There are a number of thin primary calcite flowstones within the caves studied, but only two thick (>1m) sequences of primary calcite flowstone have been found to date, both from the Makapansgat Valley – Member 1b basal flowstone boss of the Makapansgat Limeworks and the basal flowstone of Buffalo Cave.

Chapter 4 investigates the carbon isotope geochemistry of these two flowstone deposits using the isotopic composition of co-occurring organic carbon inclusions and speleothem carbonate to distinguish the host-rock carbon

contribution from the carbon isotopic composition derived from soil CO_2 (and therefore from the palaeovegetation). Firstly, the isotopic equilibrium precipitation of the flowstones is established using growth layer and duplicate analyses. Then, by comparing the approximate carbon isotope composition of palaeovegetation (as determined from the organic matter inclusions) with the carbon isotope compostion of co-occurring speleothem carbonate, it is possible to model the percentage of host-rock contribution to the speleothem carbonate. Using the modelled host-rock contribution, the carbon isotopic composition of palaeovegetation can be determined from speleothem carbonate samples that lack co-occurring organic-matter data. The carbon isotopic composition of palaeovegetation indicates the proportion of C_4 and C_3 vegetation in the local palaeoenvironment and therefore the percentage of savannah grasses (C_4) versus trees and shrubs (C_3).

Chapter 5 shows the construction of an oxygen and carbon isotope time series for the Buffalo Cave and Collapsed Cone flowstones based on the palaeomagnetic stratigraphy of Herries (2003). The Buffalo Cave chronology is further constrained by combining UV annual-band measurements and spectral analysis to develop an orbitally tuned isotopic record between 1.5 and 2.0 Ma. The Buffalo Cave flowstone shows a carbon isotope shift at 1.7 Ma indicating a mean increase in the percentage of C_4 grasses in the local palaeoenvironment from approximately 25% to 50%. The timing and magnitude of this vegetational shift is in agreement with isotopic evidence from South African fossil teeth (Luyt, 2001; Luyt and Lee-Thorp, 2003) and this event is also recorded in east Africa (Bonnefille, 1995). The carbon isotope oscillations in the Buffalo Cave flowstone occur over precession (19-23ka) and obliquity (41ka) periodicities indicating rapid fluctuations in vegetation cover from grass-dominated to woodland-dominated ecosystems. At all levels within the time series, a mixture of C_3 and C_4 vegetation is recorded. These rapid variations in vegetation structure have not been recorded in carbon isotope studies of fossil teeth, which suggests that most of the South African faunal deposits are time-averaged with respect to environmental conditions.

The Collapsed Cone flowstone shows little isotopic variation, indicating a less variable late Miocene / early Pliocene palaeoenvironment. Carbon isotope values are light and invariant indicating a predominantly C_3 palaeoenvironment.

Between the early/Pliocene and early Pleistocene represented by these two flowstones, savannah grasses first arrived in the Makapansgat valley.

Chapter 6 is a study of carbon isotopes in fossil rodent teeth from the oldest faunal deposits of the Makapansgat valley – the Rodent Corner and Exit Quarry repositories – two mid-Pliocene deposits that offer the potential to refine the timing of the origin of C_4 grasses at Makapansgat (and by inference, the South Africa highveld). Reconstruction of the rodent palaeodiets using carbon isotopes and dental microwear analysis indicates that C_4 grasses were present in small proportions in the diet of these mid-Pliocene rodents. Therefore, C_4 grasses originated in the Makapansgat valley between the mid-Pliocene and the Miocene/Pliocene boundary (approx. 3.5 to 5 Ma).

Chapter 7 places the new data regarding the origin of C_4 grasses in South Africa within the global picture of C_4 grass expansion. The Cerling *et al.* (1997) model of C_4 grass evolution and expansion predicts a latitudinal control on the timing of C_4 origin due the dominance of C_4 grasses at high temperatures. For C_4 grasses to spread into mid-latitudes, the Cerling *et al.* (1997) model predicts a decrease in atmospheric CO_2 concentrations (a control of C_4 grass distribution). This chapter plots all published data on the global distribution of C_4 grasses from the mid-Miocene to recent. The mid-latitude sites of South Africa (this thesis), Northern North America, China and Namibia are the only localities to show the origin of C_4 grasses to be as late as 4-5Ma - in agreement with the Cerling *et al.* (1997) model. This shows that C_4 grasses expanded over millions of years from low latitudes to mid-latitudes and that the latter phases of this expansion coincided with the evolution of hominin bipedalism. This may be indicative of a causal relationship, in agreement with the Savannah Hypothesis of human origins.

References:

Bonnefille, R. (1995). A reassessment of the Plio-Pleistocene pollen record of east Africa. *In* "Paleoclimate and evolution with emphasis on human origins." (E. S. Vrba, G. H. Denton, T. C. Partridge, and L. H. Burckle, Eds.), pp. 299-310. Yale University Press, New Haven.

Cerling, T. E., Harris, J. M., MacFadden, B. J., Leakey, M. G., Quade, J., Eisenmann, V., and Ehleringer, J. R. (1997). Global vegetation change through the Miocene/Pliocene boundary. *Nature* **389,** 153-158.

Herries, A. I. R. (2003). "Magnetostratigraphic seriation of South African hominin palaeocaves." Unpublished PhD thesis, University of Liverpool.

Luyt, J. (2001). "Revisiting the palaeoenvironments of the South African hominid-bearing Plio-Pleistocene sites: New isotopic evidence from Sterkfontein." Unpublished MSc thesis, University of Cape Town.

Luyt, C. J., and Lee-Thorp, J. A. (2003). Carbon isotope ratios of Sterkfontein fossils indicate a marked shift to open environments c. 1.7 Myr ago. *South African Journal of Science* **99,** 273-275.

Chapter 1. Early hominin evolution and climate change - a review of competing models.

1.1. Introduction

There are numerous potential causal factors behind an evolutionary event, some of the more easily conceptualised include inter and intra-specific competition, sexual selection, disease, migration, climatic change and random or contingent events. Of all of these possible causes, the broad category of climatic change is the only potential cause that is largely independent of individuals and species and can be investigated using wholly independent lines of evidence. There are a large number of studies of Earth history that have attempted to relate biotic change to environmental change, but only a handful of studies that have successfully demonstrated a conclusive causal link between events in the geosphere and biosphere. The most successful case studies involve large global events that have an unquestionably large impact on life (e.g. Alverez *et al.*, 1980; Ryder, 1996; McLeod and Keller, 1996). The smaller the global event, the subtler the effects on the biota are likely to be, and the harder it is to demonstrate the causation.

Each stage of human evolution, from the origin of bipedalism in the earliest hominin species to the migration of modern humans out of Africa, has been tentatively linked to an episode of climatic change. It is unlikely that all of these postulated links between climate and evolution can be demonstrated to be true, whether or not there truly was a link in the past. However, the case study of climatic control on the origins of the earliest hominins (synonymous with the origins of bipedalism) may prove to be an exception. The late Neogene was a period of significant global change, which saw the evolution of the first savannah grasses and the replacement of tropical forest ecosystems by the savannah ecosystem. In response to these changes, the tropical mammalian fauna became savannah adapted as the familiar savannah mammal lineages evolved. If early humans can be shown to have evolved in response to the development of the savannah ecosystem, then a causal link is likely.

There are a number of competing hypotheses (as discussed below) that attempt to explain early hominin morphology and diversity as predictable responses to Quaternary climatic changes. The models differ in the climatic parameters considered to exert control over evolutionary processes, and in the hominin morphologies and macro-evolutionary patterns expected to develop in response to these climatic changes. Part 1. of this chapter introduces and evaluates the competing hypotheses of climatic control on early hominin evolution. The Savannah Hypothesis is of particular relevance to the palaevegetation evidence presented in the later chapters of this thesis. Part 2. of this chapter focuses on defining the Savannah Hypothesis and suggesting methods for testing the hypothesis. In the light of existing evidence, the validity of the Savannah Hypothesis is discussed.

1.2. Models of palaeoclimatic change and hominin evolution

1.2.1. Climatic forcing of hominin evolution

Evolutionary hypotheses relating to the influence of palaeoclimatic change on events in human evolution can be grouped in two opposing catagories - intrinsic and extrinsic forcing. The former states that evolution is controlled by processes intrinsic to the species in question, and would continue unaltered in a hypothetical world of constant environments (also known as the Red Queen hypothesis, Van Valen, 1973). In contrast, the extrinsic approach states that environmental forcing is the driving force behind macroevolutionary change (also known as the Court Jester hypothesis, Barnosky, 2001). Many intermediate hypotheses can lie between these two end-member states, as it is important to evaluate the degree to which intrinsic and extrinsic factors have contributed to an evolutionary event. Therefore, by developing detailed records of coeval environmental and biotic changes it is possible to investigate the influence of the former on the latter. A lack of correlation between the environmental and biotic records is good evidence for a lack of climatic forcing; however, a correlation between the two records may be coincidence rather than causality. Therefore, to assess the likelihood of a causal relationship in co-occurring evolutionary and environmental events, it is important to model and test the expected influence of the environmental change on macroevolutionary events.

The specific evolutionary events of the origin and evolution of the early hominins have been subjected to a number of models of climatic forcing which span the full range of climatically controlled, Court Jester models, to evolutionary controlled, Red Queen models. The following sections review the more prominent models of the hominin macroevolutionary response to climatic change.

Intrinsic factors

The Autocatalytic hypothesis of hominin evolution (McKee, 1999) takes a strictly microevolutionary approach to human evolution. McKee (1999) states

the importance of selective events intrinsic to an individual, such as parental nurturing and social status, over events more removed from the individual such as vegetational and climatic change. In a similar vein to Van Valen's (1973) Red Queen hypothesis, in which evolutionary novelty and direction are controlled by competition between individuals and species, the Autocatalyst model takes a highly intrinsic approach. However, the Autocatalysis model has difficulty in denying all influence of environmental change. For example McKee (1999) admits that the transition from a forest to a forest-savannah mosaic would have given selective advantage to a hypothetical common ancestor of *Pan* and *Australopithecus* that had modified its locomotory behaviour to include aspects of forest-floor locomotion:

"It is true that had the environment not changed, and savanna had not become available, the process may have taken a different direction, but such processes would not have been halted."

McKee is stating that environmental change can alter the direction of evolution, but that climatic change is not essential for evolutionary change. Few evolutionary theorists would take such an extreme extrinsic approach to state that evolution cannot occur without climatic change – the extrinsic argument is that macroevolutionary trends (more so than microevolutionary change) are modulated and sorted by climatic events. Therefore, if the Autocatalytic model accepts the existence of both intrinsic and extrinsic forcing, the argument is an issue of the relative importance of the two forcing mechanisms. The relative importance of intrinsic and extrinsic factors can potentially be tested, given new and detatiled environmental and faunal evidence.

Chaline *et al.* (2000) highlight the importance of developmental changes in providing the morphological developments of human evolution (following Gould, 1977; Vrba, 1994 etc.), such as the neotenous origin of the cranio-facial contraction necessary for an efficient bipedal gait. These intrinsic factors clearly indicate the origin of specific morphological novelties, but are not sufficient to explain the success of the novelties in an ecological context. Chaline *et al.* (2000) therefore take a combined intrinsic and extrinsic approach

by highlighting the importance of extrinsic factors in determining the relative fitness of these neotenic traits, and in providing the geographic isolation necessary for allopatric speciation. By viewing all macroevolutionary change through the sorting process of its ecological and environmental context, many researchers have adopted a strict extrinsic approach to causation of mammalian evolution, as discussed below.

Extrinsic approaches

There are two broad scenarios for the environmental forcing of hominin evolution based on marine environmental evidence – the Faunal Turnover hypothesis and the Variability Selection hypothesis. Both are based on the same records of global climate change, but highlight periods of increased global cooling in the former and increased climatic variability in the latter. Perhaps the greatest problem facing these models is the assumption that the same global climatic changes observed in the marine record occur in tropical terrestrial regions. For example, there is mounting evidence that late Quaternary tropical and sub-tropic terrestrial climates have varied over precessional timescales, rather than the eccentricity and obliquity cycle variations observed over the same period in the marine record (Clemens *et al.*, 1991; Partridge *et al.*, 1997).

1.2.2. The Turnover Pulse Hypothesis

The Faunal Turnover Hypothesis states that pulses of macroevolutionary change in the African terrestrial fauna occur at times of global cooling, as recorded in the marine oxygen isotope record. The term "turnover pulse" refers to a simultaneous increase in extinction and speciation to levels significantly above background rates. The Turnover Pulse hypothesis has been tested using a database of bovid species from the African Plio-Pleistocene (Vrba, 1997, 1992, 1995b), which show a period of increased faunal turnover at 2.5 Ma. Vrba (1995b) suggests that this turnover event occurred in response to the onset of Northern Hemisphere glaciation at 2.5 Ma and that it may have lead both to the increase in hominin species diversity and to the first use of stone tools observed

at this time. However, Behrensmeyer *et al.* (1997) question the validity of the Vrba (1995b) dataset on the basis of the inclusion of poorly dated South African specimens and due to the presence of sampling and taphonomic biases. The Behrensmeyer *et al.* (1997) dataset takes these problems into account and shows the most significant increase in Plio-Pleistocene faunal turnover in Africa to occur between 2.5 Ma and 1.7 Ma.

The causal link between climatic change and episodes of faunal turnover in the Turnover Pulse hypothesis is based on the argument that speciation and extinction events are predominantly controlled by climatic changes. Allopatric speciation is considered by most evolutionary biologists to be the dominant mode of speciation (Carson, 1987) and implicitly involves habitat change. An ancestral population is fragmented by a climatic or physical barrier into two populations (vicariance) that then undergo independent micro-evolutionary change. If this separation occurs for a suitable number of generations then the two populations may become reproductively isolated as separate species. If this model of speciation dominates biotic evolution, then it highlights the importance of ecological change in the process of speciation. The shifting of vegetational belts with glacial and interglacial climatic changes and the migration of land mammals with their preferred habitat provides ample possibilities for the development of vicariant populations. It is within these vicariant populations that allopatric speciation is expected to occur.

Species extinction is also envisaged by Vrba (1992, 1995a) to occur within climatically induced vicariant populations. The difference between a vicariant population that leads to speciation and one that leads to extinction is dependent on the rapidity and severity of the climatic change and the intrinsic "evolvability" of the isolated population.

The Turnover Pulse hypothesis outlines both the theoretical link between climatic change and evolution and the expected patterns to be observed in the fossil record if the hypothesis is correct. However, with the current limitations of the fossil and climatic records it is not yet possible to prove or discount the Faunal Turnover hypothesis with any degree of certainty.

1.2.3. Variability Selection Hypothesis

The Variability Selection hypothesis of hominin evolution (Potts, 1996; 1998) is based on an alternative view of Quaternary global change. Whereas the Faunal Turnover hypothesis attempts to link faunal events in Africa to events of increased global cooling, the Variability Selection hypothesis is based on the recognition that the high levels of Quaternary climatic variability on Milankovitch timescales are far greater and more rapid than the gradual trend of Plio-Pleistocene global cooling. The Variability Selection hypothesis refers to the evolution of ecological flexibility (generalism) in response to Milankovitch scale climatic oscillations. The term Variability Selection (Potts, 1998) is applied specifically to the evolution of adaptive traits as a population experiences highly variable environments over many generations. The process of Variability Selection is envisaged to occur if, for example, there is more than one type of genetic variation that can result in survival and reproductive success in a given environment. One type of genetic variation may have a higher relative fitness in a specific environment, whereas the second type of genetic variation may have a high relative fitness in the habitat in which it first appeared, but also happens to be adaptive when the environmental conditions change. In this scenario, the second trait survives the environmental change and ultimately dominates in the population over long and variable time scales.

Testing the Variability Selection hypothesis and distinguishing it from natural selection may well prove difficult. Despite this, Potts (1998) cites possible examples of Variability Selection such as dietary and locomotory flexibility in extant African generalist mammals, and encephalisation and flexible social groupings in hominins. Potts (1998) is keen to label the later hominin traits of tool use, migration and encephalisation as Variability Selected; however there is no evidence to suggest that these traits are the result of anything other than natural selection. While some of these issues of climatic variability and evolution are thought provoking, it is all to easy to accuse the Variability Selection hypothesis of being anthropocentric. The Variability Selection hypothesis remains to be tested.

1.2.4. Climatic Theories of Hominin Adaptation

The Faunal Turnover and Variability Selection hypotheses of hominin evolution deal with the background of climatic change and its potential effects on hominin evolution. In contrast, the Aquatic-Ape and Savannah hypotheses are contrasting theories based on the principal ecological adaptations of early hominins. This alternative approach to the problem takes a morphological and adaptive approach to investigate changing hominin habitats through time.

The Aquatic-Ape Hypothesis

The Aquatic-Ape hypothesis (Hardy, 1960; Morgan, 1997; Roade *et al.*, 1991) states loosely that the human lineage has been shaped by a temporary phase of adaptation to a littoral habitat. Specific modern-human characteristics such as bipedalism, elongated lower limbs, reduction of body hair, high levels of subcutaneous fat and tears have all been attributed to an aquatic phase of human evolution (Morgan, 1972; 1991; 1997) between 6 and 3 Ma. The palaeoanthropological community has largely rejected the Aquatic Ape hypothesis (Langdon, 1997), as most of the claims are circumstantial and un-testable and are less parsimonious than the competing terrestrial hypotheses. Most of the aquatic features listed in support of the aquatic-ape hypothesis are based on comparisons of modern humans to aquatic organisms. Evidence such as the high water loss during urination and sweating in modern humans have been used to indicate the modern-human inability to occupy the savannah habitat:

"*physiologically, biochemically and histologically, we should be hopeless as savanna-dwellers. All of the former savanna supporters must swallow our earlier words.*" (Tobias, 1995 *in* Morgan, 1997).

However, the logic of this reasoning is flawed for two reasons. Firstly, observations on modern human populations can not simply be converted to assumptions about extinct hominin species – it is feasible that early hominins were undergoing selection for savannah adaptations, whereas later hominin species were undergoing selection for some aquatic adaptations. It is highly

unlikely that the whole hominin lineage was undergoing the same selection pressures for millions of years, and such ideas of evolutionary gradualism are being gradually removed from discussions of human evolution. Secondly, the vast majority of evidence put forward for aquatic adaptations relate to soft-tissues and therefore cannot be tested in extinct hominin species. Studies of diet and locomotory adaptations are the only sources of evidence available to determine the habitat adaptations of hominins and show little support for the Aquatic-Ape hypothesis.

The Savannah Hypothesis

The Savannah Hypothesis alludes to the apparent adaptations of hominins to a savannah habitat and often cites climatic change as a forcing mechanism that lead an arboreal ancestor to pursue a terrestrial way of life. This idea was expressed by Darwin (1874) who linked the origins of bipedalism with either a climatic change or a change in dietary preference:

"As soon as some ancient member in the great series of the Primates came to be less arboreal, owing to a change in its manner of procuring subsistence, or to some change in the surrounding conditions, its habitual manner of progression would have been modified: and thus it would have been rendered more strictly quadrupedal or bipedal."

Throughout the twentieth century, the Savannah Hypothesis in its various forms was the most cited hypothesis of early human evolution, but in the light of recent evidence has been questioned. Kingston *et al.* (1994) were among the first workers to apply carbon isotope techniques to hominin palaeoenvironments by studying palaeosol carbonate and organic matter in Kenya. In disagreement with the basic premise of the Savannah Hypothesis, this study showed that the East African environment had contained a mixture of woody and savannah vegetation for the last 15Ma – there was no evidence for the shift in vegetation from forest to savannah necessary for the Savannah Hypothesis. More evidence for a mixed vegetation in east Africa from the mid-Miocene onwards (Cerling and Hay, 1986; Cerling, 1992; Sikes *et al.*, 1999 etc.) lead some authors to the

conclusion that the Savannah Hypothesis was no longer a tenable explanation of human origins (Hill, 1987; Kingston *et al.*, 1994; Verhaegen and Puech, 2000). Recent morphological data suggests a mosaic of post-cranial adaptations in the australopithecines, indicating both an arboreal and terrestrial component to australopithecine locomotion (Clarke and Tobias, 1995; McHenry and Berger, 1998; Clarke, 1999). These studies suggest that early hominins were adapted to a mosaic of savannah and woodland rather than a purely grass-dominated savannah. With the apparent decline in popularity of the Savannah Hypothesis there has been resurgence in alternative hypotheses of early hominin evolution such as the Aquatic Ape hypothesis (Morgan, 1997; Verhaegen and Puech, 2000) and the Autocatalysis hypothesis of McKee (1999). However, the evidence for a savannah-mosaic environment does not disprove the central implication of the Savannah Hypothesis, which requires an increase in the proportion of savannah grassland relative to closed-woodland sufficient enough increase the fitness of a predominantly ground-dwelling primate.

Not all workers in the field have discounted the Savannah Hypothesis on the basis of carbon isotope evidence. Leakey and Harris (2003) highlight the importance of the general trend from woodland-dominated to savannah-dominated over millions of years during the late Miocene in restructuring the African mammalian fauna. While the origin and spread of savannah (C_4) grasses may not be a rapid switch from woodland to savannah, Leakey and Harris (2003) still suggest its potential role in the origins of hominin bipedalism:

"A dramatic change took place in the African biota between 7 and 5 million years ago. Shrinkage of the equatorial forests coincided with expansion of the modern C_4 savanna grassland flora – expedited by an expansion of the polar ice caps or a reduction in atmospheric concentration of carbon dioxide, or perhaps a combination of these and other events. Expansion of the C_4 biomass was a worldwide phenomenon, and in Africa it resulted in the emergence of the faunal elements that would dominate the later Cenozoic – including hippos, giant pigs, grazing antelopes, true giraffes and elephants, and, of course, man.

Early humans are restricted in distribution to Africa, and their acquisition of an upright bipedal striding gait, the hallmark of humanity,

appears to be at least circumstantially linked to the reduction of the equatorial forests and spread of grasslands on that continent." Leakey and Harris (2003).

This hypothesis of early human evolution modulated by global climatic changes is not given a specific name by Leakey and Harris (2003) but the basis premise of the scenario is one of savannah expansion resulting in the evolution of early hominin bipedalism – it is therefore a modification of the Savannah hypothesis. As they suggest, this link between the spread of C_4 grasses and hominin bipedalism could be circumstantial. The following section outlines possible avenues of research for testing this hypothesis.

1.3. Testing the Savannah Hypothesis

In order to evaluate the response of mammalian and hominin evolution to the late Neogene spread of the savannah biome, the simplest approach is to attempt to falsify the Savannah hypothesis. The following tests of the Savannah Hypothesis must be fulfilled if the Savannah Hypothesis is to be proven:

Test 1. – That there is a change in vegetational conditions significantly above background levels during the period and in the region of the evolution of early hominins.

Test 2. – That the (a) faunal and (b) hominin response to the observed vegetation change can be predicted based on appropriate macroevolutionary models.

Test 3. – That the expected biotic response only occurs during a period of vegetational change or at a magnitude that is significantly greater during the period of vegetational change than at times of little vegetational change.

Test 1 – Geological and Floral evidence for spreading savannah environments

Evidence for the replacement of forest environments by savannah grasslands in the late Neogene is crucial if the Savannah Hypothesis is to be a tenable theory. However, evidence for the spread of savannah grasslands is currently scarce and is often contradictory. Continuous records of palaeovegetation change from the late Neogene of Africa are rare. The input of pollen (Dupont and Leroy, 1995) and aeolian sediment (deMenocal and Bloemendal, 1995) into marine basins provides high-resolution, continuous records of African terrestrial vegetation change. However, the vegetation proxies are averaged over a regional or continental scale and cannot discern localised hominin-habitats. Discontinuous pollen records from east African hominin sites Bonnefille (1983 and 1995) provide insights into the floral composition of Hominin habitats, but cannot

offer a continuous record of vegetational change. Similarily, macrofloral specimens (e.g. Bamford, 1999) are important at individual hominin sites, but their rarity prevents comparisons between sites. Carbon isotopes in palaeosols and teeth can determine the proportion of savannah grasses in the local environment and have great potential to determine vegetation changes over time (e.g. Lee-Thorp *et al.*, 2000; Cerling, 1992). The palaeoenvrionmental interpretation of carbon isotopes in teeth is however limited by the selective feeding of mammalian species (Kingston, 1999). The study of carbon isotopes in palaeosols is limited by the stratigraphic distance between individual palaeosol horizons.

The existing data indicates that a mosaic of woodland and savannah components were present in tropical Africa since the mid-Miocene (Cerling and Hay, 1986; Cerling, 1992; Kingston *et al.*, 1994; Sikes *et al.*, 1999). Periods of increased savannah cover have been suggested at 2.5Ma (Dupont and Leroy, 1995; Bonnefille, 1995), 1.7Ma (Bonnefille, 1995; Cerling, 1992). There is currently little evidence for a marked increase in savannah grassland coinciding with the origins of early hominin bipedalism.

Test 2a - Faunal response to the spread of savannah grasslands

Previous studies have focussed on the micro- and macro-evolutionary response to rapid climatic and vegetational events (e.g. the Faunal Turnover hypothesis). There has been less consideration of faunal responses to gradual expansions of savannah grasslands, perhaps because the detection of a faunal response to a gradual event is much harder to determine. However, there is evidence to suggest that the formation of the savannah-ecosystem and the faunal response to this change lasted for millions of years. The following discussion of faunal and hominin responses to a gradually expanding savannah biome focuses on the gradual late Neogene increase in savannah-adapted species.

Hypsodonty

Hypsodonty, the development of high-crowned molar teeth, has traditionally been regarded as an adaptation to a specialist grazing niche because of its occurrence in many modern grazing taxa and the fact that high crowned teeth

are necessary when consuming grasses due to abrasion from phytoliths and ingested soil particles. It has been assumed that the late Neogene increase in hypsodont species was a response to the spread of savannah grasslands. However, this is disputed by the evidence for "precocious hypsodonty" (MacFadden *et al.*, 1996) in which hypsodont species are found in fossil faunas millions of years prior to the arrival of savannah grasses in the area (as determined from stable carbon isotopes). Stromberg (2002) has shown that hypsodonty has been present in North America since the Oligocene and that the hypsodont species were living in a purely C_3 grassland.

Recent work by Feranec (2003) questioned the assumption that hypsodonty is a specialisation to a grazing diet by comparing dietary variability data from carbon isotopes in fossil teeth of hypsodont and bunodont taxa. This study and other data on carbon isotopes in teeth indicates that hypsodont taxa have a range of dietary preferences from pure graze to pure browse. Feranec (2003) concludes that hypsodonty is not strictly a specialisation of obligate grazing but can be considered as a generalisation enabling a range of niches to be exploited. Jernvall and Fortelius (2002) studied the development of hypsodonty between 18 Ma and 8 Ma in western Europe, showing that the first significant increase in hypsodonty occurred at 11 Ma, prior to which hypsodont mammals are confined to only a few localities.

The rate of species migration is orders of magnitude greater than the rate at which C_4 grasses expanded their geographic range according to the Cerling *et al.* (1997) model so it is not surprising that hypsodonty becomes decoupled from the savannah environment, some hypsodont mammals being found well outside the latitudinal range of C_4 grasslands and shown to be adapted to a browsing niche.

Test 2(b) - Hominin response to the spread of savannah grasslands

Are early Hominins savannah-adapted?

As discussed above, little is known for sure about early hominin adaptations. Speculation regarding physiology and soft-tissue morphology can be moulded to fit contrasting hypotheses such as the Savannah Hypothesis or the Aquatic Ape

hypothesis and do not aid discussion. Restricting discussion to the fossil evidence, observable morphological adaptations include dietary, locomotory and perhaps behavioural adaptations.

Dietary adaptation

Cranio-dental morphology, dental microwear and stable isotopes provide evidence regarding early hominin dietary adaptation. The combination of these techniques has enabled a detailed reconstruction of the diet of the South African gracile and robust australopithecines. Future studies on other early hominin species will help to determine the range of early hominin dietary adaptations.

The robust cranio-dental morphology of *Australopithecus robustus* suggests that it was a dietary specialist adapted to a diet dominated by hard food items (Wood, 1986). This is supported by the dental microwear evidence for hard-object consumption in A. *robustus* (Grine and Kay, 1988) and a more frugivorous diet in A. *africanus*. Therefore, the separate dietary niche inferred for these two species is suggestive of quite different life-styles and possibly habitats.

Carbon isotope evidence shows that the diet of both South African australopithecine species contained components derived from both C_3 and C_4 vegetation (Lee-Thorp *et al.*, 1994; Sponheimer and Lee-Thorp, 1999; Lee-Thorp *et al.*, 2000). This indicates the proximity of savannah grasses to these early hominins and shows that there is no significant difference in the proportion of C_4 and C_3 plant derived carbon in the diet of the robust and gracile australopithecines. The origin of the C_4 grass dietary component is unlikely to have been derived directly from grass consumption due to the low nutritional benefits and the lack of the specialised morphologies necessary in a grazing primate. The C_4 grass component may instead indicate termite consumption, as suggested by the characteristic wear on bone tools from Swartkrans (Backwell and d'Errico, 2001; d'Errico *et al.*, 2001).

Bipedalism as an adaptation to a savannah habitat

Obligatory bipedalism has often been assumed to be a definitive adaptation to an open savannah environment. Early statements of the Savannah hypothesis suggested that bipedalism was selected for in a savannah environment, however, bipedalism is more accurately conceived as a pre-adaptation (or exaptation, following the terminology of Gould and Vrba, 1982). From this standpoint, the development of a bipedal gait is considered to have been selected for in a closed environment, to later prove adaptive in a more open environment. There is currently debate regarding the locomotary nature of the last common ancestor of the first bipeds between an arboreal ancestor and a quadrupedal or knuckle-walking ancestor (Rose, 1991; Richmond, 2001). Other possible scenarios for ancestral locomotion include wading (Aquatic Ape hypothesis) and arboreal bipedalism (Stanford, 2002). There is also uncertainty regarding the transition to bipedalism, as some authors see the origins of bipedalism as a single event while others suggest that there were locomotory intermediates such as knuckle-walking (Richmond, 2001). It has also been suggested that the australopithecines have a mosaic of arboreal and terrestrial locomotory adaptations, which enabled them to exploit both niches (McHenry and Berger, 1998). Future fossil finds will help to confirm the nature of locomotion in the earliest hominins and their last common ancestor.

The evolution of bipedalism can be viewed in the traditional interpretation of the Savannah hypothesis as a locomotory or dietary adaptation that developed in direct response to the new selection pressures of the spreading savannah environment. Alternatively, bipedalism can be viewed as driven by intrinsic factors such as heterochronic changes in cranio-dental morphology and the "occipital shift" required for a bipedal gait (Chaline *et al.*, 2000). However, if intrinsic factors were the source of the morphological novelties required for bipedalism, the adaptive benefits are still dependant on the selective environment and reproductive isolation of the population (indeed, the climatic controls on heterochrony are discussed by Vrba, 1994). Whether bipedalism evolved in response to the gradual replacement of forest by savannah or as an adaptive developmental mutation, the vicariant biogeography of the spreading

savannah mosaic must have been instrumental in the continued spread and speciation of the earliest hominins.

Potts (1998) suggests that the evidence for climatic variability, mosaic environments and the significant variation in vegetation cover between regions, makes it unlikely that Plio-Pleistocene hominins were adapted to a single habitat, be it savannah or woodland. However, the association of hominin species with a mixed environment does not *a priori* indicate an adaptation to a mixed environment. Micro-habitat specifity, and time and space averaging of the faunal and environmental data must be fully addressed before an association can be inferred. The habitat specifity of each hominin species is potentially testable, given more fossil evidence and higher temporal and spatial resolution of palaeoenvironmental reconstructions.

Dietary and locomotory evidence, the most important indicators of hominin ecomorphology, is far from conclusive but does suggest a mixture of woodland and savannah components in the habitat of early hominins. Further work will determine whether specific hominin species are more or less savannah-adapted.

1.4. Ecological analogues of Hominin adaptations

The most widely cited ecological analogue of early hominins are the theropithecines. They have a similar date of origin, a similar geographical distribution (both lineages have been essentially restricted to Africa) and a similar biology (both being medium-sized primates). The theropithecines, like the early hominins, are considered to be savannah-adapted.

Theropithecus

Theropithecus is regarded as a truly savannah-adapted primate genus and similarities or differences in the parallel evolutionary history of *Theropithecus* and early hominins can shed light on the debated palaeoecology of the early hominins. *Theropithecus* has been recorded in various parts of Africa from 4 Ma

to the present day (Pickford, 1993) and each of the six species (Jablonski, 1993) is considered on the basis of its postcranial anatomy to be more or less savannah adapted. *Theropithecus* is distinguished from other Papionini by a large number of derived gross anatomical features associated mostly with its adaptations to a highly terrestrial habitat and its unique feeding strategy of "manual grazing". Existing evidence suggests that *Theropithecus* shared a common ancestor most recently with Papio between 7 and 3.5 Ma ago. *Theropithecus brumpti* was the only species of *Theropithecus* that is considered to be a forest dweller based on its specialised masticatory apparatus (Jablonski, 1993) and its postcranial anatomy (Krentz, 1993). Lee-Thorp *et al.* (1989) indicate that *Theropithecus darti* from Swartkrans at approx. 1.7-1.9 Ma had a predominately C_4 grass component to its diet as does the modern *Theropithecus gelada.*

Therefore, the theropithecines and the hominins both show an approximately synchronous adaptive radiation in the late Neogene of Africa, both adapting at least partially to a savannah environment (Foley, 1993). The base of both clades are characterised by novel locomotory adaptations to a more open environment.

1.5. Macroevolutionary response of hominin adaptation to spreading grasslands

Adaptive radiation and the savannah hypothesis

Early hominin species diversity has recently been viewed as one or more adaptive radiations (Foley, 2002; Wood, 2002). The term adaptive radiation is used to describe a proliferation of closely related species or sub-species that share an adaptive novelty that enables the exploitation of a new or previously un-available habitat (Schluter, 2000). In the case of early hominin evolution the development of bipedalism was either an adaptive or exaptive novelty that enabled the exploitation of the developing savannah ecosystem. The earliest reported evidence of hominin bipedalism (Senut *et al.*, 2001; Brunet *et al.*, 2002) at 6-7 Ma is associated with a woodland-savannah mosaic (Pickford and

Senut, 2001; Zazzo et al, 2000; Vignaud *et al.*, 2002). The discovery of new early hominin species within the different regions of Africa suggests regional variations of these bipeds to different climatic regimes. For example, studies of post-cranial morphology by McHenry and Berger (1998) and Clarke and Tobias (1995) suggest that *Australopithecus africanus* in South Africa was more arboreal than *A. afarensis* in the east African rift valley. The radiation of early hominin species is consistent with the Resource-Use hypothesis of speciation (Vrba, 1987) which states that specialist species are more likely to belong to specious clades due to their greater susceptibility to allopatric speciation. The radiation of the *Theropithecines* (Jablonski, 1993) is a co-occurring adaptive radiation in which a shuffling locomotion and grazing diet are the successful adaptive mechanisms, rather than bipedalism in hominins.

Turnover Pulse vs Adaptive Radiation

An adaptive radiation, by definition, requires an increase of species diversity within a clade, therefore the rate of speciation must exceed extinction. New species within a radiating clade adapt to a range of habitats thereby spreading in geographic range, species diversity and number of individuals. In contrast, a Turnover Pulse requires speciation and extinction to be of a similarly high magnitude and to be above background rates of speciation and extinction during any given period of faunal turnover. A Turnover Pulse is a theoretical result of a rapid global event such as sudden global cooling or sudden loss of woodland habitat. The catastrophic event results in widespread extinction and also coincident allopatric speciation in response to fragmented and isolated populations.

The theoretical framework for the evolutionary response to a gradual spread of grasslands is that extinction rates are unlikely to be significantly above background rates. This is because the replacement of forest by grassland is only locally disruptive, enabling populations to migrate with their preferred conditions - it is unlikely to occur on a scale large enough to cause a series of co-occurring extinctions. The successful development of bipedalism and the rate of speciation in the earliest hominins was greater than the rate of extinction, resulting in the radiation of early hominins (Foley, 2002). The Turnover Pulse

hypothesis (Vrba, 1995) can explain the replacement of one hominin species by another, but with its requirement of sub-equal rates of speciation and extinction, it cannot account for the increasing species diversity observed in the early hominin fossil record. Therefore, the adaptive radiation of early hominins is more likely to have been a response to a gradual expansion of savannah grassland than to a sudden vegetational shift envisaged in the Faunal Turnover hypothesis.

1.6. Conclusions

A number of uncertainties remain regarding the specific events that lead to the origins of bipedalism, such as the selective pressures that resulted in bipedalism, the locomotory adaptations of the hominin common ancestor and the degree of bipedalism / arborality of the earliest hominins. Therefore, with current evidence it is impossible to evaluate the role of climatic change in the origins of the hominins with any degree of certainty. Future research must focus on both the detailed characterisation of changing hominin palaeoenvironments and the habitat specifity and adaptations of individual hominin species.

1.7. References

Alvarez, L. W., Alvarez, W., Asaro, F., and Michel, H. V. (1980). Extraterrestrial cause for the Cretaceous-Tertiary boundary extinction. *Science* **208,** 1095-1108.

Backwell, L. R., and d'Errico, F. (2001). First evidence of termite-foraging by Swartkrans early hominids. *Proceedings of the National Academy of Sciences, USA* **98,** 1358-1363.

Bamford, M. (1999). Pliocene fossil woods from an early hominid cave deposit, Sterkfontein, South Africa. *South African Journal of Science* **95,** 231-237.

Barnosky, A. D. (2001). Distinguishing the effects of the Red Queen and Court Jester on Miocene mammal evolution in the Northern Rocky Mountains. *Journal of Vertebrate Paleontology* **21,** 172-185.

Behrensmeyer, A. K., Todd, N. E., Potts, R., and McBrinn, G. E. (1997). Late Pliocene faunal turnover in the Turkana Basin, Kenya. *Science* **278,** 1589-1594.

Bonnefille, R. (1983). Evidence for a cooler and drier climate in the Ethiopian uplands towards 2.5 Myr ago. *Nature* **303,** 487-491.

Bonnefille, R. (1995). A reassessment of the Plio-Pleistocene pollen record of east Africa. *In* "Paleoclimate and evolution with emphasis on human origins." (E. S. Vrba, G. H. Denton, T. C. Partridge, and L. H. Burckle, Eds.), pp. 299-310. Yale University Press, New Haven.

Brunet, M., Guy, F., Pilbeam, D., Mackaye, H. T., Likius, A., Ahounta, D., Beauvilain, A., Blondel, C., Bocherens, H., Boisserie, J. R., De Bonis, L., Coppens, Y., Dejax, J., Denys, C., Duringer, P., Eisenmann, V. R., Fanone, G., Fronty, P., Geraads, D., Lehmann, T., Lihoreau, F., Louchart, A., Mahamat, A., Merceron, G., Mouchelin, G., Otero, O., Campomanes, P. P., De Leon, M. P., Rage, J. C., Sapanet, M., Schuster, M., Sudre, J., Tassy, P., Valentin, X., Vignaud, P., Viriot, L., Zazze, A., and Zellikefer, C. (2002). A new hominid from the Upper Miocene of Chad, Central Africa (vol 419, pg 145, 2002). *Nature* **418,** 801-801.

Carson, H. L. (1987). The process whereby species originate. *BioScience* **37,** 715-720.

Cerling, T. E., and Hay, R. L. (1986). An isotopic study of paleosol carbonates from Olduvai Gorge. *Quaternary Research* **25,** 63-78.

Cerling, T. E. (1992). Development of grasslands and savannas in east-Africa during the Neogene. *Palaeogeography, Palaeoclimatology, Palaeoecology (Global and Planetary Change Section)* **97,** 241-247.

Cerling, T. E., Harris, J. M., MacFadden, B. J., Leakey, M. G., Quade, J., Eisenmann, V., and Ehleringer, J. R. (1997). Global vegetation change through the Miocene/Pliocene boundary. *Nature* **389,** 153-158.

Chaline, J., Durand, A., Dambricourt Malasse, A., David, B., Magniez-Jannin, F., and Marchand, D. (2000). Were climatic changes a driving force in hominid evolution. *In* "Climates: Past and Present." (M. B. Hart, Ed.), pp. 185-198. Geological Society, London, London.

Clarke, R. J., and Tobias, P. V. (1995). Sterkfontein-Member-2 foot bones of the oldest south-African hominid. *Science* **269,** 521-524.

Clarke, R. J. (1998). First ever discovery of a well-preserved skull and associated skeleton of *Australopithecus*. *South African Journal of Science* **94,** 460-463.

Clarke, R. J. (1999). Discovery of complete arm and hand of the 3.3 million-year-old *Australopithecus* skeleton from Sterkfontein. *South African Journal of Science* **95,** 477-480.

Clemens, S., Prell, W., Murray, D., Shimmield, G., and Weedon, G. (1991). Forcing mechanisms of the Indian Ocean monsoon. *Nature* **353,** 720-725.

d'Errico, F., Backwell, L. R., and Berger, L. R. (2001). Bone tool use in termite foraging by early hominids and its impact on our understanding of early hominid behaviour. *South African Journal of Science* **97,** 71-75.

Darwin, C. (1874). "The descent of man; and selection in relation to sex." Crowell, New York.

deMenocal, P. B., and Bloemendal, J. (1995). Plio-Pleistocene climatic variability in subtropical African and the paleoenvironment of hominid evolution. *In* "Paleoclimate and evolution with emphasis on human origins." (E. S. Vrba, G. H. Denton, T. C. Partridge, and L. H. Burckle, Eds.), pp. 262-288. Yale University Press, New Haven.

Dupont, L. M., and Leroy, S. A. G. (1995). Steps toward drier climatic conditions in Northwestern Africa during the Upper Pliocene. *In*

"Paleoclimate and evolution with emphasis on human origins." (E. S. Vrba, G. H. Denton, T. C. Partridge, and L. H. Burckle, Eds.), pp. 289-298. Yale University Press, New Haven.

Feranec, R. S. (2003). Stable isotopes, hypsodonty, and the paleodiet of Hemiauchenia (Mammalia: Camelidae): a morphological specialization creating ecological generalization. *Paleobiology* **29,** 230-242.

Foley, R. A. (1993). African terrestrial primates: the comparative evolutionary biology of *Theropithecus* and the Hominidae. *In* "*Theropithecus*: the rise and fall of a primate genus." pp. 245-270. Cambridge University Press, Cambridge.

Foley, R. A. (2002). Adaptive radiations and dispersals in Hominin evolutionary ecology. *Evolutionary Anthropology* **11,** 32-37.

Gould, S. J. (1977). "Ontogeny and phylogeny." Harvard University Press, Cambridge.

Gould, S. J., and Vrba, E. S. (1982). Exaptation - a missing term in the science of form. *Paleobiology* **8,** 4-15.

Grine, F. E., and Kay, R. F. (1988). Early hominid diets from quantitive image analysis of dental microwear. *Nature* **333,** 765-768.

Hardy, A. (1960). Was man more aquatic in the past? *New Scientist* **7,** 642-645.

Hill, A. (1987). Causes of perceived faunal change in the later Neogene of East Africa. *Journal of Human Evolution* **16**: 583-596.

Jablonski, N. G. (1993). The phylogeny of *Theropithecus*. *In* "*Theropithecus*: the rise and fall of a primate genus." (N. G. Jablonski, Ed.), pp. 209-224. Cambridge University Press, Cambridge.

Jernvall, J., and Fortelius, M. (2002). Common mammals drive the evolutionary increase of hypsodonty in the Neogene. *Nature* **417,** 538-540.

Kingston, J. D., Marino, B. D., and Hill, A. (1994). Isotopic evidence for Neogene Hominid paleoenvironments in the Kenya rift valley. *Science* **264,** 955-959.

Kingston, J. D. (1999). Isotopes and environments of the Baynunah Formation, Emirate of Abu Dhabi, United Arab Emirates. *In* "Fossil Vertebrates of Arabia." (P. J. Whybrow, and A. Hill, Eds.), pp. 523. Yale University Press.

Krentz, H. B. (1993). Postcranial anatomy of extant and extinct species of *Theropithecus*. *In* "*Theropithecus*: the rise and fall of a primate genus." (N. G. Jablonski, Ed.), pp. 383-422. Cambridge University Press, Cambridge.

Langdon, J. H. (1997). Umbrella hypotheses and parsimony in human evolution: a critique of the Aquatic Ape Hypothesis. *Journal of Human Evolution* **33,** 479-494.

Leakey, M. G., and Harris, J. M. (2003). Lothagam: its significance and contributions. *In* "Lothagam: the dawn of humanity in eastern Africa." (M. G. Leakey, and J. M. Harris, Eds.), pp. 625-660. Columbia University Press, New York.

Lee-Thorp, J. A., van der Merwe, N. J., and Brain, C. K. (1989). Isotopic evidence for dietary differences between two extinct baboon species from Swartkrans. *Journal of Human Evolution* **18,** 183-190.

Lee-Thorp, J. A., van der Merwe, N. J., and Brain, C. K. (1994). Diet of *Australopithecus-robustus* at Swartkrans from stable carbon isotopic analysis. *Journal of Human Evolution* **27,** 361-372.

Lee-Thorp, J. A., Thackeray, J. F., and van der Merwe, N. (2000). The hunters and the hunted revisited. *Journal of Human Evolution* **39,** 565-576.

MacFadden, B. J., Cerling, T. E., and Prado, J. (1996). Cenozoic terrestrial ecosystem evolution in Argentina: Evidence from carbon isotopes of fossil mammal teeth. *Palaios* **11,** 319; 327.

MacLeod, N., and Keller, G. (1996). Cretaceous-Tertiary mass extinctions: biotic and environmental changes, pp. 575. W. W. Norton and Company, New York.

McHenry, H. M., and Berger, L. R. (1998). Body proportions in *Australopithecus afarensis* and A. africanus and the origin of the genus *Homo*. *Journal of Human Evolution* **35,** 1-22.

McKee, J. K. (1999). The autocatalytic nature of hominid evolution in African Plio-Pleistocene environments. *In* "African biogeography, climate change and human evolution." (T. Bromage, and F. Schrenk, Eds.), pp. 57-68. Oxford University Press, Oxford.

Morgan, E. (1972). "The descent of woman." Souvenir Press, London.

Morgan, E. (1991). Why a new theory is needed. *In* "The aquatic ape: fact or fiction." (M. Roede, J. Wind, J. M. Patrick, and V. Reynolds, Eds.), pp. 9-22. Souvenir Press, London.

Morgan, E. (1997). "The Aquatic Ape hypothesis." Souvenir Press, London.

Partridge, T. C., deMenocal, P. B., Lorentz, S., Paiker, M. J., and Vogel, J. C. (1997). Obital forcing of climate over South Africa: a 200,000-year rainfall record from the Pretoria Saltpan. *Quaternary Science Reviews* **16,** 1125-1133.

Pickford, M. (1993). Climatic change, biogeography, and *Theropithecus*. *In* "*Theropithecus*: the rise and fall of a primate genus." (N. G. Jablonski, Ed.), pp. 227-243. Cambridge University Press, Cambridge.

Pickford, M., and Senut, B. (2001). The geological and faunal context of Late Miocene hominid remains from Lukeino, Kenya. *Comptes Rendus de L'Academie des Sciences serie II fascicule a- Sciences de la Terre et des Planetes* **332,** 145-152.

Potts, R. (1996). Evolution and climate variability. *Science* **273,** 922-923.

Potts, R. (1998). Variability selection in hominid evolution. *Evolutionary Anthropology* **7,** 81-96.

Retallack, G. J., Wynn, J. G., Benefit, B. R., and McCrossin, M. L. (2002). Paleosols and paleoenvironments of the middle Miocene, Maboko Formation, Kenya. *Journal of Human Evolution* **42,** 659-703.

Richmond, B. G. (2001). Origin of human bipedalism: the knuckle-walking hypothesis revisited. *Yearbook of Physical Anthropology* **44.**

Roede, M., Wind, J., Patrick, J. M., and Reynolds, V. (1991). The aquatic ape: fact or fiction?, pp. 369. Souvenir Press, London.

Rose, M. D. (1991). The process of bipedalization in hominids. *In* "Origine(s) de la bipedie chez les hominides." (Y. Coppens, and B. Senut, Eds.), pp. 37-48. Editions du CNRS, Paris.

Ryder, G. (1996). "The Cretaceous-Tertiary event and other catastrophies in earth history." Geological Society of America, Boulder, Colorado.

Schluter, D. (2000). "The ecology of adaptive radiation." Oxford University Press, Oxford.

Senut, B., Pickford, M., Gommery, D., Mein, P., Cheboi, K., and Coppens, Y.

(2001). First hominid from the Miocene (Lukeino Formation, Kenya). *Comptes Rendus de L'Academie des Sciences serie II fascicule a-Sciences de la Terre et des Planetes* **332,** 137-144.

Sikes, N. E., Potts, R., and Behrensmeyer, A. K. (1999). Early Pleistocene habitat in Member 1 Olorgesailie based on paleosol stable isotopes. *Journal of Human Evolution* **37,** 721-746.

Sponheimer, M., and Lee-Thorp, J. A. (1999). Isotopic evidence for the diet of an early hominid, *Australopithecus africanus*. *Science* **283,** 368-370.

Stanford, C. (2002). Brief communication: arboreal bipedalism in Bwindi Chimpanzees. *American Journal of Physical Anthropology* **119,** 87-91.

Stromberg, C. A. E. (2002). The origin and spread of grass-dominated ecosystems in the late Tertiary of North America: preliminary results concerning the evolution of hypsodonty. *Palaeogeography, Palaeoclimatology, Palaeoecology* **177,** 59-75.

Van Valen, L. (1973). A new evolutionary law. *Evolutionary Theory* **1,** 1-30.

Verhaegen, M., and Puech, P.-F. (2000). Hominid lifestyle and diet reconsidered: paleo-environmental and comparative data. *Human Evolution* **15,** 151-162.

Vignaud, P., Duringer, P., Mackaye, H. T., Likius, A., Blondel, C., Boisserie, J. R., de Bonis, L., Eisenmann, V., Etienne, M. E., Geraads, D., Guy, F., Lehmann, T., Lihoreau, F., Lopez-Martinez, N., Mourer-Chauvire, C., Otero, O., Rage, J. C., Schuster, M., Viriot, L., Zazzo, A., and Brunet, M. (2002). Geology and palaeontology of the Upper Miocene Toros-Menalla hominid locality, Chad. *Nature* **418,** 152-155.

Vrba, E. S. (1987). Ecology in relation to speciation rates: some case histories of Miocene-Recent mammal clades. *Evolutionary Ecology* **1,** 283-300.

Vrba, E. S. (1992). Mammals as a key to evolutionary theory. *Journal of Mammalogy* **73,** 1-28.

Vrba, E. S. (1994). An hypothesis of heterochrony in response to climatic cooling and its relevance to early hominid evolution. *In* "Integrative Paths to the Past-Paleoanthropological Advances in Honor of F. Clark Howell." (R. S. Corruccini, and R. L. Ciochon, Eds.), pp. 345-376. Prentice Hall, Englewood Cliffs, NJ.

Vrba, E. S. (1995a). On the connections between paleoclimate and evolution. *In* "Paleoclimate and evolution with emphasis on human origins." (E. S. Vrba, G. H. Denton, T. C. Partridge, and L. H. Burckle, Eds.). Yale University Press, New Haven.

Vrba, E. S. (1995b). The fossil record of African Antelopes (Mammalia, Bovidae) in relation to human evolution and paleoclimate. *In* "On the connections between paleoclimate and evolution." (E. S. Vrba, G. H. Denton, T. C. Partridge, and L. H. Burckle, Eds.), pp. 385-424. Yale University Press, New Haven.

Vrba, E. S. (1997). Species' habitats in relation to climate, evolution, migration and conservation. In, Huntley, B., Cramer, W., Morgan, A. V., Prentice, H. C. and Allen, J. R. M. *(eds.), Past and future rapid environmental changes: the spatial and evolutionary responses of terrestrial biota, NATO ASI Series I: Global Environmental Change* **47,** 275-286.

Wood, B. A. (1986). Were the robust Australopithecines dietary specialists? *South African Journal of Science* **82,** 86-87.

Wood, B. (2002). Palaeoanthropology: Hominid revelations from Chad. *Nature* **418,** 133-135.

Zazzo, A., Bocherens, H., Brunet, M., Beauvilain, A., Billiou, D., Mackaye, H. T., Vignaud, P., and Mariotti, A. (2000). Herbivore paleodiet and paleoenvironmental changes in Chad during the Pliocene using stable isotope ratios of tooth enamel carbonate. *Paleobiology* **26,** 294-309.

Chapter 2. Palaeoenvironmental reconstruction at South African hominin sites.

2.1. Introduction

The discovery of the Taung Child in the Buxton Limeworks near Kimberley, South Africa in 1924 and the recognition by Raymond Dart (1925) of its unique blend of ape-like and human-like features was a landmark in human evolutionary studies (Tobias, 2000). The Taung Child became the type specimen for the genus and species *Australopithecus africanus* and was placed within the primate family, Hominidae, along with its sister genus *Homo*. Since this discovery, numerous early hominin specimens have been discovered in four African regions: the east African rift valley, South Africa, Chad in North-Central Africa and Malawi in south-eastern Africa. The South African hominins have been collected from the dolomitic karst deposits of north-eastern South Africa from Taung in the south-west to Makapansgat in the North East (see Fig. 2.1.). The vast majority of the hominin fossils come from the cave breccias of Sterkfontein and Swartkrans near the city of Krugersdorp in the Gauteng Province. The South African hominins have been assigned to three species, *Australopithecus africanus*, *Australopithecus robustus* and *Homo* sp. and are now represented by more than 500 individuals (Tobias, 2000). The South African hominins are often very well preserved as indicated by the virtually complete skeleton of the recently discovered "Little Foot" from Sterkfontein (Clarke, 1998). This contrasts with the often fragmentary remains from the open air sites elsewhere in Africa.

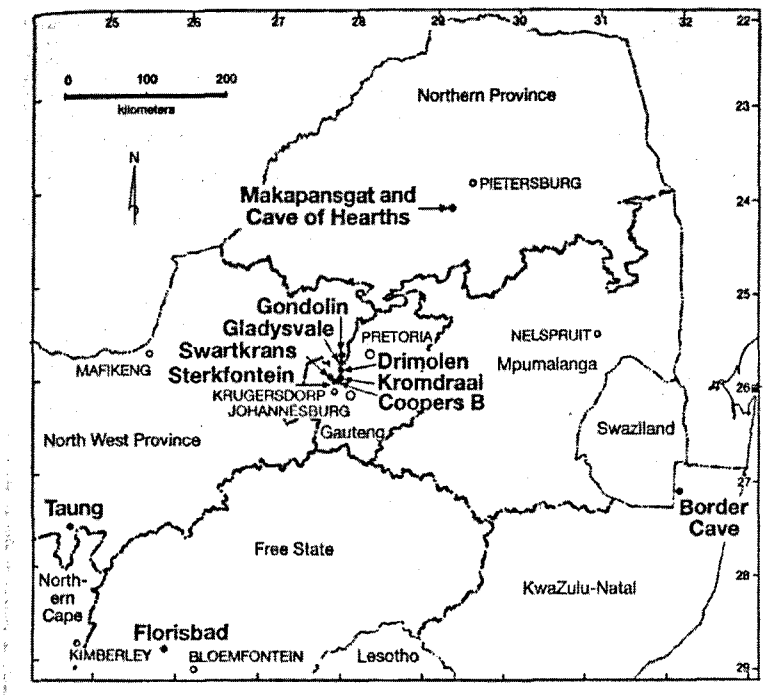

Figure. 2.1. Map of northern South Africa showing the locality of the principal Plio-Pleistocene hominin-bearing cave deposits

2.2. Cave stratigraphy and dating

It has proved difficult to establish a precise chronology of the South African cave sediments, due to the lack of suitable material for radiometric age-estimation in these cave deposits. The most commonly used dating method has been faunal correlation with the well established biostratigraphy of the eastern African fluvio-lacustrine Plio-Pleistocene succession (e.g. McKee, 1995a,b). The absolute age of the east African sediments and fauna is constrained by potassium-argon dating of the interbedded volcaniclastic sediments. The faunal-correlation method of dating the South African hominin sites is based on the assumption that first and last occurrence of each taxon is recorded in both South Africa and east Africa at the same time. Given the distance between the two regions and the low number of shared species, the faunal-correlation method can only offer an approximate relative age.

Recent attempts have been made to date the cave breccias by identifying palaeomagenetic reversals within the cave sequence and constraining the palaeomagnetic sequence with the existing faunal-correlation age estimates (McFadden *et al.*, 1979; Partridge *et al.*, 1999, Partridge *et al.*, 2000 and Herries,

2003). Because this method relies on faunal-correlation, there remains a degree of interpretation of the age as indicated by Berger *et al.* (2002).

Burial dating using the radioactive decay of cosmogenic ^{26}Al and ^{10}Be in quartz in cave sediment has also been applied to the Sterkfontein caves (Partridge *et al.*, 2003) with a reported age of approximately 4 Ma for the "Little-Foot" skeleton. While this technique seems promising, more work is needed before the dates will be widely accepted. There is also the potential of dating the South African speleothems using U/Pb dating as indicated by Richards *et al.* (1998), and work is currently in progress at Leeds University.

An understanding of cave stratigraphy and geology is important for a fuller understanding of the cave chronology, taphonomy and palaeoenvironments. Cave stratigraphy can be highly complex and with the current lack of absolute dating, it can be difficult to identify the sequence of depositional events and the presence of sedimentary hiatuses. Despite the complexity of individual cave-fills, a general model of cave formation and infilling has been developed for the South African hominin sites (Brain, 1958; Brink and Partridge, 1965). First is the formation of the cavern below the water table; second is speleothem precipitation as the water table is lowered; third is an influx of sediment when the cave becomes open to the surface; and fourth is the infilling of the entire cavern with roof-collapse breccia and surface-derived sediment.

With this basic model of cave formation in mind, the sedimentary sequences of each of the South African caves have been divided into a series of members on the basis of gross sedimentological characteristics (Brain, 1958; Partridge, 2000). While the member system of Partridge (2000) is well established and widely referred to in the literature, it has been suggested by some authors that these layer-cake stratigraphies are rather simplistic (Maguire *et al.*, 1985; Latham *et al.*, 1999; Latham *et al.*, 2003). The existence of separate repositories within a cave can result in contemporaneous deposits that differ significantly in their sedimentological characteristics. Therefore caution must be exercised when interpreting sedimentological characteristics in terms of a chronostratigraphy.

2.3. Previous palaeoenvironmental studies at the South African hominin sites

Numerous investigations on the palaeoenvironment of the South African hominin sites have been undertaken since their discovery, using a wide range of geological, faunal and floral evidence. As discussed in Rayner *et al.* (1993), the early studies often discussed palaeoclimates in terms of modern-day conditions such as wetter/dryer or warmer/colder. Little attempt was made to quantify these reconstructions or to test these proxies in the present day. Rayner *et al.* (1993) list the 40 previous studies undertaken at Makapansgat (see Fig. 2.2.) and show that 10 studies suggest wetter conditions than today, 8 studies suggest similar conditions to today and 18 studies suggest drier conditions (4 studies are inconclusive). They suggest that this lack of consensus may reflect fluctuating environmental conditions within the cave sequence.

Table 1 Summary of previous palaeoenvironmental conclusions

Wetter	Similar	Drier	Inconclusive
Dart, 1948 (O)	King, 1951 (I)	Dart, 1952 (I)	Wells & Cooke, 1957 (O)
Ewer, 1956 (O)	Meester, 1955 (O)	Oakley, 1954 (O)	Ewer & Cooke, 1964 (O)
Cooke, 1957 (I)	Ewer, 1958 (O)	Bosazza, 1957 (I)	Cooke, 1978 (O)
De Graaff, 1958 (O)	De Graaff, 1961 (O)	Oakley, 1957 (I)	Partridge, 1985 (I)
Vrba, 1975 (O)	Klein, 1977 (O)	Brain, 1958 (I)	
Howell, 1978 (O)	Partridge, 1980 (I)	Howell, 1959 (I)	
Butzer, 1980 (I)	Peters & Maguire, 1981 (O)	Robinson, 1961 (O)	
Turner, 1980 (I)	Partridge, 1982 (I & O)	Bond, 1963 (I)	
Levinson, 1985 (O)		Cooke, 1963 (I)	
Cadman & Rayner, 1989 (O)		Robinson, 1963 (O)	
		Cooke, 1964 (I)	
		Brain & Meester, 1964 (I)	
		Brain, 1967 (I)	
		Butzer, 1971 (I)	
		Butler & Greenwood, 1976 (O)	
		Butzer, 1978 (I)	
		Kitching, 1980 (O)	
		Bender, 1990 (O)	

Studies were based on either inorganic (I) or organic (O) data.

Table 2.2. A summary of previous palaeoenvironmental conclusions from organic and inorganic sources at the Makapansgat Limeworks (Rayner *et al.*, 1993).

Within the last twenty years there have been renewed attempts to obtain more robust and more detailed palaeoclimatic information. Cadman and Rayner (1989) and Zavada and Cadman (1993) have used palynological evidence from Makapansgat breccias to suggest forest conditions and fluctuating environmental conditions at approximately 3 Ma. However, Scott (1995 and 2002) questions the validity of these results based on the presence of exotic *Pinus* pollen which indicates the presence of recent contaminants. Scott (1995) also re-interprets the pollen spectra of Cadman and Rayner (1989) and Zavada and Cadman (1993), indicating that it contains components of arboreal and non-arboreal pollen, and that the assemblage is highly suggestive of modern contamination. Scott (1995) also studied 23 hyena coprolites from the Makapansgat Member 3 breccia and concluded that the pollen assemblege is indistinguishable from the modern pollen assemblage of Makapansgat and is similar to the spectra of Cadman and Rayner (1989). To avoid the problems of modern pollen contamination in cave breccias, Scott and Bonnefille (1986) analysed the pollen spectra of speleothems from Sterkfontein and Kromdraai and showed that they were lacking in modern contaminants. While the non-porous nature of the speleothem increases the likelihood of fossil pollen being preserved, the pollen yields can be low and Scott (1995) warns of the destruction of pollen assemblages during the recrystalisation of speleothem.

The only plant macrofossils discovered in the South African hominin sites are silicified wood from Sterkfontein Member 4 (Bamford, 1999). Two species of wood have been identified by Bamford (1999), the liana *Dichapetalum* cf. *mombuttense* and the shrub *Anastrabe integerrima*, neither of which is found at Sterkfontein today. Lianas require external physical support for their growth and are common components of forests indicating that a gallery forest component was present at Sterkfontein in the late Pliocene.

There have been many attempts to use the fossil faunas to reconstruct palaeoenvironments at the South African hominin sites (see references within Rayner *et al.*, 1993) but here the focus is on the most informative of these studies. When interpreting fossil assemblages in terms of palaeoenvironments, it must be assumed that the time represented by each assemblage is environmentally homogenous, that the area inhabited by the fauna is restricted to one climate / habitat zone and that the accumulation agent selected its prey

randomly with respect to environmental indicators (Vrba, 1980). The final assumption is one of taxonomic uniformity, that the extinct taxa approximate their extant relatives in terms of habitat specifity and dietary behaviour (Sponheimer *et al.*, 1999).

Fossil bovids have been a focus of palaeoenvironmental research because they are a ubiquitous component of the Plio-Pleistocene faunas and they are a group consisting of numerous species adapted to diverse habitats from rainforest to desert. Vrba (1980) introduced the Alcelaphine / Antilopine (AA) index as a proxy for open habitats. The alcelaphine and antilopine tribes are predominantly found in open and/or arid environments so the minimum number of individuals belonging to these tribes as a percentage of the number of individuals in the entire bovid assemblage is an indication of the openness of the modern environment (Vrba, 1980). When applied to the South African hominin sites, accepting the above assumptions, the AA index indicates that the younger sites (Swartkrans, Kromdraai) are indicative of open environments whereas the older sites (Sterkfontein Type Site and Makapansgat Member 3) have a greater degree of bush and tree cover.

Rather than focusing solely on bovids, Reed (1998) conducted a study of the eco-morphology of the entire fauna at Makapansgat Members 3 and 4 and concluded that the fauna represents a bushland vegetation with elements of edaphic grasslands and riparian woodlands. While Reed (1998) interprets the faunal assemblage as representing a life-assemblage, it is likely that the wide range of habitats inferred from this study represents a time-averaged death-assemblage sampled from a range of climatic conditions.

Cranio-dental eco-morphology uses the premise that the morphological characteristics of the dentition and cranium are indicative of dietary adaptations (Reed 1998). Since diet is linked to habitat tolerance, dietary reconstructions are palaeoenvironmental as well as behavioural indicators. A second line of palaeodietary evidence comes from carbon isotope studies of fossil teeth which determine the proportion of C_3 vegetation (trees, bushes, shrubs, herbs and temperate grasses) from C_4 vegetation (savannah grasses and sedges). By combining eco-morphology and stable isotopes, a detailed palaeodietary reconstruction can be achieved (MacFadden and Shockey, 1997; Sponheimer *et al.*, 1999). Using this approach at Makapansgat Members 3 and 4, Sponheimer

et al. (1999) are able to show that dietary and habitat inferences based on the principal of taxonomic uniformity are not always accurate. Using the new dietary evidence from stable isotopes in fossil bovids, Luyt and Lee-Thorp (2003) have been able to modify the Alcelaphine / Antelopine index of Vrba (1980) to produce a more accurate index of open environments.

While the accuracy of fauna-based palaeoenvironmental reconstructions is improving, there remains a number of limitations in the application of these techniques to the South African Plio-Pleistocene. Firstly, the temporal resolution of the faunal deposits is poor. There is no record of internal stratification within each cave breccia member, so the fauna from each member represents an unknown period of deposition, perhaps exceeding 100 ka. With so little temporal resolution, there is no indication of palaeoclimatic variability on shorter timescales. Any palaeoclimatic data obtained from the fossil faunas must be considered as an average of climatic change over the period of deposition.

The second problem is concerned with the interpretation of palaeodiets as a proxy for palaeovegetation. Selective feeding, migration and immigration are confounding factors that must be considered when interpreting carbon isotope data from fossil teeth (Kingston, 1999). These problems are best addressed by collecting data from a wide range of taxa with varied feeding strategies, and assessing the proportion of different feeding types within a faunal deposit. However, interpretating the abundance or proportion of certain taxa as palaeoenvironmental indicators depends on the assumptions discussed in Vrba (1980), such as taphonomic bias and time and space averaging.

Palaeoenvironmental reconstructions based on geological data have the potential to offer a more representative record of climatic changes, independently of faunal biases. Many studies have focused on the sedimentological characteristics of the South African cave breccias (King, 1951, Dart, 1952, Brain, 1958,) and have come to conflicting conclusions regarding the Plio-Pleistocene climate. The accuracy of these studies has often been limited by the lack of a suitable framework for identifying climatic parameters in cave sediments. Brain (1958) addressed this problem by studying the sedimentological characteristics of modern dolomite soils formed under a variety of climatic conditions and comparing these soils to the Plio-Pleistocene

cave breccias. Parameters used by Brain (1958) included sand grain angularity, proportion of dolomite fragments, soil colour, sediment grading and chert-quartz ratios. These indicators can be used at best as a qualitative indicator of palaeoclimate, however the interpretation of these climatic proxies is ambiguous, as discussed by Brain (1958) and Smith *et al.* (1995).

Study of sedimentary sequences within the cave deposits of South Africa has lead to some interesting hypotheses. Turner (1980) identified sequences of coarse sandstone interbedded with siltstone and fine sandstone at Rodent Corner, Makapansgat Limeworks, and interpreted these sequences as periods of suspension sedimentation interrupted by episodes of storm-derived coarse sandstone deposition. However, Turner (1980) did not indicate variations in the frequency and magnitude of these events, nor was the cause of these events discussed. Brain (1995) outlines the hypothesis that the sedimentation at Swartkrans and the other australopithecine cave sites is controlled by glacial-interglacial cycles. In this model, cave breccias are accumulated during interglacials and are punctuated by an erosional hiatus formed during glacial periods. Brain (1995) cites evidence from the late-Pleistocene to Holocene records of South Africa to suggest that cycles of temperature and rainfall amount are responsible for these episodes of deposition and erosion. Testing this model is currently hampered by the lack of chronological data.

2.4. Thesis Aims

With the focus of previous geological research on cave breccias, the South African speleothems have been neglected, despite their great potential as a palaeoenvironmental archive. The palaeosols from east African hominin sites have provided carbon isotope data that reflects hominin habitats independently of the biases of carbon isotopes in fossil teeth, but equivalent sedimentological data is currently lacking from the South African hominin sites. Carbon and oxygen isotope data from the South African speleothems has the potential to provide a far greater degree of temporal resolution for Plio-Pleistocene climate change than that obtained from palaeosols or fossil teeth.

The aim of this thesis is to investigate the potential of the South African Plio-Pleistocene speleothems as palaeoenvironmental archives. This requires a study of the preservation state of the speleothems based on petrographic and stable isotope data (see Chapter 3). It is also necessary to justify the interpretation of oxygen and carbon isotope signatures as palaeoenvironmental proxies for each speleothem studied (see Chapters 3 and 4). After these issues were addressed, it proved possible to develop high-resolution records of climatic change from the South African speleothems (see Chapter 5). These speleothems provide new insights into the palaeoecology of South Africa and its influence on events in early hominin evolution (see Chapters 5, 6 and 7).

2.5. References

Bamford, M. (1999). Pliocene fossil woods from an early hominid cave deposit, Sterkfontein, South Africa. *South African Journal of Science* **95,** 231-237.

Berger, L. R., Lacruz, R., and de Ruiter, D. J. (2002). Brief Communication: revised age estimates of *Australopithecus*-bearing deposits at Sterkfontein, South Africa. *American Journal of Physical Anthropology* **119,** 192-197.

Brain, C. K. (1958). The Transvaal ape-man-bearing cave deposits. *Transvaal Museum Memoir* **11,** 131.

Brain, C. K. (1995). The influence of climatic changes on the completeness of the early hominid record in Southern African caves, with particular reference to Swartkrans. *In* "Paleoclimate and evolution with emphasis on human origins." (E. S. Vrba, G. H. Denton, T. C. Partridge, and L. H. Burckle, Eds.), pp. 451-458. Yale University Press, New Haven.

Brink, A. B. A., and Partridge, T. C. (1965). Transvaal karst : some considerations of development and morphology, with special reference to sinkholes and subsidences on the Far West Rand. *South African Geographical Journal* **47,** 11-34.

Cadman, A., and Rayner, R. J. (1989). Climate change and the appearance of *Australopithecus africanus* in the Makapansgat sediments. *Journal of Human Evolution* **18,** 107-113.

Clarke, R. J. (1998). First ever discovery of a well-preserved skull and associated skeleton of *Australopithecus*. *South African Journal of Science* **94,** 460-463.

Dart, R. A. (1925). *Australopithecus africanus*: the man-ape of South Africa. *Nature* **115,** 195-199.

Dart, R. A. (1952). Faunal and climatic fluctuations in the Makapansgat Valley: their relation to the geological age and promethean status of *Australopithecus*. *In* "Proceedings of the Pan-African Congress on

Prehistory, Nairobi, 1947." (L. S. B. Leakey, and S. Cole, Eds.), pp. 96-106. Blackwell, Oxford.

Herries, A. I. R. (2003). "Magnetostratigraphic seriation of South African hominin palaeocaves." Unpublished PhD thesis, University of Liverpool.

King, L. C. (1951). The geology of the Makapan and other caves. *Transactions of the Royal Society of South Africa* **33,** 121-151.

Kingston, J. D. (1999). Isotopes and environments of the Baynunah Formation, Emirate of Abu Dhabi, United Arab Emirates. *In* "Fossil Vertebrates of Arabia." (P. J. Whybrow, and A. Hill, Eds.), pp. 523. Yale University Press.

Latham, A. G., Herries, A., and Kuykendall, K. (2003). The formation and sedimentary infilling of the Limeworks cave, Makapansgat, South Africa. *Palaeontologia Africana* **39**: 69-82.

Latham, A. G., Herries, A., Quinney, P., Sinclair, A., and Kuykendall, K. (1999). The Makapansgat Australopithecine site from a speleological perspective. In, Pollard, A. M. (ed.) Geoarchaeology: exploration, environments, resources. *Geological Society of London, Special Publications* **165,** 61-77.

Luyt, C. J., and Lee-Thorp, J. A. (2003). Carbon isotope ratios of Sterkfontein fossils indicate a marked shift to open environments c. 1.7 Myr ago. *South African Journal of Science* **99**.

MacFadden, B. J., and Shockey, B. J. (1997). Ancient feeding ecology and niche differentiation of Pleistocene mammalian herbivores from Tarija, Bolivia: morphological and isotopic evidence. *Paleobiology* **23,** 77-100.

Maguire, J. M., Schrenk, F., and Stanistreet, I. G. (1985). The lithostratigraphy of the Makapandsgat Limeworks Australopithecine site: some matters arising. *Annals of the geological survey of South Africa* **19,** 37-51.

McFadden, P. L., Brock, A., and Partridge, T. C. (1979). Palaeomagnetism and the age of the Makapansgat hominid site. *Earth and Planetary Science Letters* **44,** 373-382.

McKee, J. K. (1995a). Further chronological seriations of southern African Pliocene and Pleistocene mammalian faunal assemblages. *Palaeontologia Africana* **32,** 11-16.

McKee, J. K., Thackeray, J. F., and Berger, L. R. (1995b). Faunal assemblage seriation of southern African Pliocene and Pleistocene fossil deposits. *American Journal of Physical Anthropology* **96,** 235-250.

Partridge, T. C. (2000). Hominid-bearing cave and tufa deposits. *In* "The Cenozoic of Southern Africa." (T. C. Partridge, and R. R. Maud, Eds.), pp. 100-130. Oxford University Press, Oxford.

Partridge, T. C., Granger, D. E., Caffee, M. W., and Clarke, R. J. (2003). Lower Pliocene Hominid Remains from Sterkfontein. *Science* **300,** 607-612.

Partridge, T. C., Latham, A. G., and Heslop, D. (2000). Appendix on magnetostratigraphy of Makapansgat, Sterkfontein, Taung and Swartkrans. *In* "The Cenozoic of Southern Africa." (T. C. Partridge, and R. R. Maud, Eds.), pp. 126-129. Oxford University Press, Oxford.

Partridge, T. C., Shaw, J., Heslop, D., and Clarke, R. J. (1999). The new hominid skeleton from Sterkfontein, South Africa: age and preliminary assessment. *Journal of Quaternary Science* **14,** 293-298.

Rayner, R. J., Moon, B. P., and Masters, J. C. (1993). The Makapansgat Australopithecine environment. *Journal of Human Evolution* **24,** 219-

231.

Reed, K. E. (1998). Using large mammal communities to examine ecological and taxonomic structure and predict vegetation in extant and extinct assemblages. *Paleobiology* **24,** 384-408.

Richards, D. A., Bottrell, S. H., Cliff, R. A., Strohle, K., and Rowe, P. J. (1998). U-Pb dating of a speleothem of Quaternary age. *Geochimica et Cosmochimica Acta* **62,** 3683;3688.

Scott, L. (1995). Pollen evidence for vegetational and climatic change in southern Africa during the Neogene and Quaternary. *In* "Paleoclimate and evolution with emphasis on human origins." (E. S. Vrba, G. H. Denton, T. C. Partridge, and L. H. Burckle, Eds.), pp. 65-76. Yale University Press, New Haven.

Scott, L. (2002). Grassland development under glacial and interglacial conditions in southern Africa: review of pollen, phytolith and isotope evidence. *Palaeogeography, Palaeoclimatology, Palaeoecology* **177,** 47-57.

Scott, L., and Bonnefille, R. (1986). Search for pollen from the hominid deposits of Kromdraai, Sterkfontein and Swartkrans: some problems and preliminary results. *South African Journal of Science* **82,** 380-382.

Smith, I. W. S., Laing, M., Thackeray, J. F., and Watson, V. (1995). X-ray powder diffraction study of fossils and associated breccias from the Sterkfontein Valley. *South African Journal of Science* **91,** 589;596.

Sponheimer, M., Reed, K. E., and Lee-Thorp, J. A. (1999). Combining isotopic and ecomorphological data to refine bovid paleodietary reconstruction: a case study from the Makapansgat Limeworks hominin locality. *Journal of Human Evolution* **36,** 705-718.

Tobias, P. V. (2000). The fossil hominids. *In* "The Cenozoic of Southern Africa." (T. C. Partridge, and R. R. Maud, Eds.), pp. 252-276. Oxford University Press, Oxford.

Turner, B. R. (1980). Sedimentological characteristics of the "red muds" at Makapansgat limeworks. *Palaeontologia Africana* **23,** 51-58.

Vrba, E. S. (1980). The significance of bovid remains as indicators of environment and predation patterns. *In* "Fossils in the making. Vertebrate taphonomy and paleoecology." (A. K. Behrensmeyer, and A. P. Hill, Eds.), pp. 247-271. University of Chicago Press, Chicago.

Zavada, M. S., and Cadman, A. (1993). Palynological investigations at the Makapansgat Limeworks - an Australopithecine site. *Journal of Human Evolution* **25,** 337-350.

Chapter 3. Speleothem preservation and diagenesis in South African hominin sites - Implications for Palaeoenvironments and geochronology

3.1. Abstract

Plio-Pleistocene flowstones from the Transvaal Province of South Africa have the potential to yield palaeoenvironmental and geochronological data of importance to palaeoanthropology. Both calcitic and aragonitic speleothems are common in the dolomite palaeo-karst. The tendency of aragonite speleothems to recrystallise to calcite prevents the use of these flowstones in palaeoenvironmental studies. This study outlines the methods for identification of primary aragonite, primary calcite and secondary calcite in palaeo-karst deposits using petrology, stable isotopes and trace elements.

$\delta^{13}C$ values of the speleothem carbonate studied (primary and secondary calcite) range from +6 to –9‰ and $\delta^{18}O$ values range from –4 to –6‰. The data correspond to the meteoric calcite line of highly variable $\delta^{13}C$ and invariant $\delta^{18}O$. The enriched carbon isotope values are associated with the effects of recrystallisation and rapid outgassing of CO_2 during precipitation. Mg/Ca and Sr/Ca ratios differ between primary and secondary calcite speleothems and can be used in primary calcite and aragonite to determine the trace element composition of past cave waters. Trace element and stable isotopic signatures distinguish primary calcite from secondary calcite and offer insights into geochemical aspects of the recrystallisation process and the past cave environment. The primary calcite speleothems yield the pristine geochemical signals that are essential for palaeoenvironmental interpretation.

3.2. Introduction

The palaeo-caves of the Gauteng and Limpopo Provinces of South Africa have yielded hundreds of specimens of Plio-Pleistocene hominins and thousands of faunal specimens, and stone tools (Tobias, 2000). The geological context of

these finds is important in terms of palaeoenvironmental reconstruction and dating of the hominin-bearing cave deposits. Cave breccias have been the focus of previous geological research (Brain, 1958, Herries *et al.*, in press, Partridge, 1979, Schrenk, 1984) due to their direct association with the fauna. However, the resistance to post-depositional alteration and the incremental growth of speleothems (secondary cave precipitates) makes them suitable for geochemical techniques such as uranium-lead dating (Richards *et al.*, 1998) and palaeoenvironmental reconstruction using stable isotopes (Gascoyne, 1992).

Before any geochemical technique is applied to speleothem deposits, it is of paramount importance to identify any post-depositional (diagenetic) alteration (Jones *et al.*, 1995) that might have modified the primary geochemical signal. Most studies of late Pleistocene speleothems indicate that diagenetic alteration is minimal (e.g. McDermott *et al.*, 1999, Frisia *et al.*, 2000, Holmgren *et al.*, 1999). However, the precipitation of meta-stable aragonite in dolomitic caves often results in the dissolution of aragonite and subsequent precipitation of secondary calcite, the more stable calcium carbonate polymorph (Folk and Assereto, 1976; Bar-Matthews *et al.*, 1991; Frisia *et al.*, 1993; Frisia, 1996; Railsback *et al.*, 1997; Frisia *et al.*, 2002). This study uses petrology, stable isotopes and trace element geochemistry to characterise speleothem diagenesis in the South Afrcian hominin sites, and to provide guidelines for distinguishing between diagenetic calcite and the desired primary calcite flowstones.

3.3. Diagenesis and Geochemistry

The stable isotope and cation chemistry of meteoric water percolating through karst terrains is modified by the effects of rock-water interaction, uptake of organically derived CO_2 and mineralogical differences within the host-rock. Variations in the dominance of these factors produce diverse chemical conditions within the meteoric water system that have the potential to identify the sub-environments of speleothem deposition and of speleothem diagenesis. Water-rock interaction can occur in an *open* or water dominated system (low water-rock interaction) or in a *closed* system (high water-rock interaction). In open systems, the speleothem will be precipitated with stable isotope and trace element compositions reflecting meteoric waters, whereas with increasingly

closed systems, the speleothem geochemistry will reflect the geochemical composition of the host-rock. Flowstone precipitation occurs in a sub-aerial cave environment proximal to the reservoir of soil CO_2 and is therefore expected to have a host-rock contribution of less than 50% (Hendy, 1971). Typical speleothem host-rock contribution is considered to range from 10-20% (Genty and Massault, 1997). In contrast, speleothem diagenesis occurs either in sub-aqueous environments or in wet sub-aerial environments (through thin films of water) and diagenetic fluids can range in composition from open system meteoric waters to closed system groundwaters that have undergone higher degrees of water-rock interaction. The *meteoric calcite line* model of Lohmann (1988) predicts that the geochemistry of speleothems subjected to diagenesis will be more variable and will indicate higher degrees of water-rock interaction than that of primary sub-aerial speleothems. This model specifically predicts an increase in $\delta^{13}C$, Sr/Ca and Mg/Ca values in diagenetically altered speleothem with increasing host-rock contribution, due to the heavy $\delta^{13}C$ value of carbonate host-rocks and their reservoir of Sr^{2+} and Mg^{2+} ions. In contrast, $\delta^{18}O$ is predominantly sourced from meteoric water and is therefore largely invariant.

The diagenetic modification of speleothems is most common in caves formed in dolomitic terranes where aragonitic speleothems are most likely to form (Assereto and Folk, 1979; Frisia, 1996; Frisia *et al.*, 1993; Bar-Matthews *et al.*, 1991, Cabrol and Coudray, 1982). The high Mg/Ca ratios, common to cave waters in dolomitic terrains, are thought to be the primary control on aragonite precipitation as they suppress calcite growth (Hill and Forti, 1997). Fischbeck and Müller (1971) show that when the Mg/Ca ratio reaches about 2.9, aragonite is the main calcium carbonate mineral to form, and that at a ratio of 4.4, it is the only calcium carbonate mineral to form. Temperature has also been considered as a control on aragonite precipitation (Moore, 1956), although the presence of aragonitic speleothems in cold, alpine caves suggests that temperature is not the main control on aragonite precipitation.

The aragonite-calcite transformation is a wet dissolution-repreciptiation reaction in which the degree of elemental exchange and textural change are dependant on the volume and composition of the diagenetic waters (Brand and

Veizer, 1980). The aragonite-calcite transformation usually occurs across thin films of aqueous solution with aragonite dissolving on one side and calcite precipitating on the other side. Most reaction zones are intra-granular pores which are too narrow to permit fluid flow, so that ion exchange between $CaCO_3$ and the pore fluid occurs by diffusion (Pingitore, 1982). The intra-granular pores are connected to the aquifer solution by much larger inter-granular pores comprising a volume of water orders of magnitude greater than the reaction zone solution and passing through the sediment by direct flow, the rate of which depends on the permeability and hydrostatic head. Therefore, carbonate diagenesis is often considered to be a two water system with recrystalisation occurring by diffusion across a thin water film within a micropore of a few microns in diameter that is connected by diffusion to the main aquifer solution (Brand and Veizer, 1980 and Pingitore, 1982). Whenever the textures of meta-stable grains are preserved at a fine scale in a diagenetic calcite, it is clear that the dissolution-reprecipitation process occurred via a thin film, the messenger film of Brand and Veizer (1980), and that that this most likely occurred in the vadose environment (Pingitore, 1982). In such circumstances, the diagenetic calcite is likely to have trace element and isotopic signatures similar to those of the dissolved aragonite.

In contrast, when fine textures are less well preserved, dissolution-reprecipitation may have occurred via a broad zone, the chalkification process of Pingitore (1976), in which the aquifer solution water was more intimately associated with the diagenetic site and lead to a blurring of the chemical distinction between the two water regimes. Phreatic environments can vary considerably in the openness of the diagenetic system from the "partly closed reaction zones" of Brand and Veizer (1980), in which the aquifer and diagenetic solutions are isolated, to open system conditions which occur along the path of aquifer flow where mass transport dominates. Therefore, the degree of textural preservation and the trace element chemistry of the diagenetic calcites are clues to the degree of isolation of the two water regimes for a particular phreatic setting.

The dolomitic caves of the Transvaal mountains in South Africa contain a mixture of aragonitic (Holmgren *et al.*, 1999) and calcitic speleothem (Talma *et*

al., 1974). The presence of aragonite was of little consequence in the stable isotope (Holmgren *et al.*, 1999 ; Repinski *et al.*, 1999) and trace-element (Finch *et al.*, 2001) studies of Cold Air Cave in the Makapansgat Valley of South Africa, as these Holocene stalagmites were predominantly composed of columnar crystals of primary aragonite. However, beyond the Holocene, aragonite diagenesis becomes a significant problem for palaeoclimatic reconstruction and chronological studies. Therefore, a study of the mineralogy and crystal fabrics of the Transvaal hominin sites was undertaken to assess the scale of the diagenesis and to determine the suitability of the flowstones for future stable isotope and geochronological work.

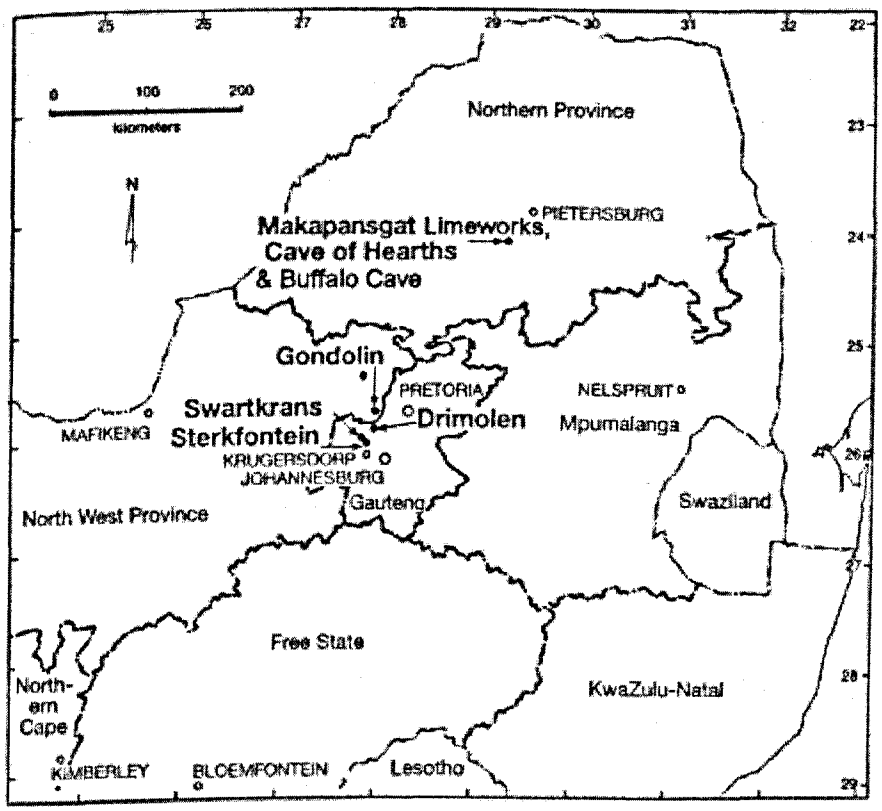

Figure 3.1. Locality map of South African hominin sites sampled for analysis of speleothem petrology

3.4. Materials

All samples were taken from speleothems of Plio-Pleistocene caves occurring within the Proterozoic Dolomites of the Transvaal Supergroup, north-eastern South Africa.

3.4.1. Makapansgat Valley

The Makapansgat Valley is located about 325 km north of Johannesburg in the Limpopo (Northern) Province, South Africa, approximately 4 km E.N.E. of Mokopane (formerly Potgietersrus). Palaeoclimatic reconstructions from aragonitic Holocene speleothems from Cold Air Cave in the Makapansgat Valley are well documented (Stevenson *et al.*, 1999; Holmgren *et al.*, 1999; 2003).

The Makapansgat Limeworks is a palaeocave containing speleothems and cave breccias that have been dated between >4 Ma and 2 Ma, on the basis of magnetostratigraphy (McFadden et al, 1979; Partridge et al, 2000; Herries, 2003). The cave is of palaeoanthropological interest as it has yielded australopithecine specimens (Dart, 1948) from the Member 3 Grey Breccia (Partridge, 2000), dated to approximately 2.5Ma. The stratigraphy and nomenclature in this study follows that of Partridge (2000) who have figured and described the geological units and localities within the cave. Representative speleothem samples were collected from the Collapsed Cone (CC), Entrance Quarry (EQ), Exit Quarry (XQ), Main Quarry (MQ) and the Original Ancient Entrance (OAE) repositories of Partridge (2000) and Latham *et al.* (2003). The Collapsed Cone flowstone is figured in Appendix 1.

Buffalo Cave is also situated in the Makapansgat Valley, 1.3 km south west of the Makapansgat Limeworks and is dated between 2 Ma and ~800 ka (Herries *et al.*, *in press*). The cave has yielded a Pleistocene fauna, predominately of grazing and browsing bovids (Kuykendall *et al.*, 1995). Samples of flowstone were restricted to the basal flowstone, a 3 m deep mined section of dark brown horizontally laminated calcite (figured in Appendix 1).

The Cave of Hearths is a Lower Palaeolithic site in the Makapansgat Valley. The sample collected from Rainbow Cave comes from a flowstone and breccia sequence isolated from the main Cave of Hearths deposits and is therefore of unknown age.

3.4.2. Krugersdorp

The cave sites of Sterkfontein, Swartkrans, Gondolin and Drimolen are all located within a few kilometres of each other, approximately six miles north of

Krugersdorp, Gauteng Province. Each site contains hominin remains (Tobias, 2000).

The excavation at Sterkfontein has yielded more than 500 hominin specimens belonging to at least three species (Tobias, 2000), making it one of the most important early hominin sites in the world. The cave deposits belonging to Members 1-5 have been dated at between 4 and 1.6 Ma (Partridge, 2000). The series of samples (STERK 16, 20, 21, 22) used in this study have been figured in Herries (2003) and are sourced from Bore Hole 5 and the Type Site (Partridge, 2000).

The Swartkrans cave deposits are younger than those of Sterkfontein, with Members 1-3 dated to approximately 1.8 – 1.0 Ma (Partridge 2000; McKee *et al.*, 1995) on the basis of faunal correlation with radiometrically dated fossil sequences from east Africa. Samples of basal flowstone were collected from an 80 cm thick sequence of horizontally laminated flowstone from the Member 1 Lower Bank deposits, immediately below the Member 1 Hanging Remnant as described and figured in Partridge (2000) and Appendix 1. This flowstone has been described as the basal or floor travertine by Brain (1958).

Gondolin is located approximately 20km N.W. of Sterkfontein and Swartkrans, near the town of Broederstroom and the cave breccias are dated at between 1.5 and 1.9 Ma on the basis of faunal correlation (Menter *et al.*, 1999). A sample from the Basal Collapse Breccia unit of (Menter *et al.*, 1999) was collected for analysis.

Drimolen is located approximately 7km north of the Sterkfontein valley and the bone-breccia deposits have been dated to between 2.0 and 1.5 Ma based on the composition of the faunal assembledge (Keyser *et al.*, 2000). A flowstone sample was collected from the Blocky Breccia deposit (Keyser *et al.*, 2000).

3.5. Methods

The speleothems collected from the above sites were first classified on the basis of gross morphology as either sub-aerial flowstones showing horizontally laminated growth layers or sub-aqueous mammillary speleothems showing a botryoidal habit. The speleothems were then cut parallel to the growth axis and

polished for the observation of gross crystal morphology, colour variations and layers of detritus. Thin sections of each speleothem were made and viewed under a polarizing microscope to investigate the calcite fabrics and mineralogy. X-ray diffraction (XRD) analysis was undertaken to determine the proportion of aragonite and calcite in a range of samples. A Siemens D500 diffractometer with a copper K-alpha radiation source was used. The percentage of the two $CaCO_3$ phases in the speleothems was estimated to ±2.5%, based on a calibration curve of known proportions of aragonite and calcite.

Samples for stable isotope and trace element analysis were drilled using a 1mm wide drill-bit perpendicular to the direction of speleothem growth, generating up to 10mg of powder, enabling aliquots of each sample to be used for stable isotope and trace element analysis. For stable isotope analysis, the powdered samples were pre-treated in an oxygen plasma asher to remove organic matter. The samples were then reacted to completion at 90°C with 100% phosphoric acid using an automated VG Isocarb preparation system. The CO_2 released by the reaction was cryogenically purified prior to the measurement of carbon and oxygen isotope ratios on an automated VG SIRA 12 mass spectrometer at the University of Liverpool. All data were corrected for ^{17}O effects following Craig (1957). Carbon and oxygen isotope data are reported in conventional delta (δ) notation in "parts per mil" (‰) relative to V-PDB (Coplen, 1995). Accuracy and reproducibility of the isotopic analyses was assessed by replicate analysis of BCS2 (internal calcite standard) against NBS-19 and two internal calcite standards. Long-term laboratory reproducibility is better than 0.1‰ for both isotope ratios.

For trace element analysis, aliquots of approximately 5 mg of powdered speleothem were dissolved in dilute nitric acid and analysed for Ca, Mg and Sr on a Perkin Elmer Optima 3300RL inductively coupled plasma atomic emission spectrometer (ICP-AES) at Royal Holloway, University of London. Analytical precision was determined using an internal speleothem standard. Reproducibility (2σ) of 1000 Mg/Ca and 1000 Sr/Ca molar ratios is ±0.65 and ±0.002 respectively.

3.6. Speleothem Terminology

Terms used in this study follow the nomenclature of Frisia (1996), Frisia *et al.* (1993) and Frisia *et al.* (2000):

Acicular: Needlelike; straight, thin, and much longer in one direction than in the other two. A common morphology of aragonite but also a possible morphology of calcite. Definitions vary, but commonly used to indicate that the crystals are more than 10 times as long as wide (González *et al.*, 1993).

Crystallite: A crystallite is the smallest crystal (it can be the size of a unit cell) that forms composite crystals (Kendall and Broughton, 1978).

Equant: Having nearly the same length in all directions. A common morphology of calcite, usually indicative of sub-aqueous precipitation. It is almost never observed in aragonitic speleothems.

Habit: Habit is the external form of crystallites as determined by growth kinetics. The most common habit of speleothem crystallites is rhombohedral (Gonzalez *et al.*, 1992).

Fabric: Fabric refers to the spatial orientation of crystallites and the relationships between them. Fabric differs from habit – for example, the columnar fabric commonly consists of the ordered stacking of rhombohedral (habit) crystallites.

Flowstones: Sheet-like speleothems that commonly have rippled, ribbed or crenulated surfaces and form when water flows on cave floors (Hill and Forti, 1997). Crystal orientation is commonly perpendicular to the growth surface of the speleothem.

Columnar Fabric: The term "columnar fabric" is used to describe elongated composite cystals wider than 10 μm (Kendall and Broughron, 1978) and with a length-to-width ratio $\leq$ 6:1 (e.g. Folk, 1965), straight boundaries, uniform

extinction, c axis perpendicular to the substrate and elongation along the c axis. The fabric rarely exhibits marked competitive growth phenomena (Kendall, 1993). Crystallites of each composite crystal have the same orientation.

Microcrystalline Fabric: This fabric forms milky, opaque and porous layers with up to 10% porosity. Crystallites that compose microcrystalline fabric are highly defective, being characterised by the presence of twins, lamellae and dislocations.

Dendritic Fabric: Dendritic fabric consists of branching polycrystals composed of stacked rhombohedral crystallites. The dendritic fabric derives its name from the branching spatial arrangement of the crystallites. Dendritic calcite has the highest density of defects such as dislocations, subgrain boundaries and twins. The fabric also shows high intercrystalline and intracrystalline porosity.

Calcareous Tufa Fabric: This porous fabric consists of aggregates of crystallites, rods, nanofibres and carbonate detritus. Crystallites (<2 μm in diameter) commonly coalesce into shrub-like aggregates. Calcareous tufa is well layered and contains rounded microsparite particles coated by isopachous cement. Common microstructures include lamellae, dislocations, and high intracrystalline porosity.

Lattice Deformation Fabric: This rare fabric, first described by Broughton (1983a) is characterized by curved or divergent crystallographic axis. An undulose or brush extinction is caused by curved domains that diverge from the axis of the speleothem. This lattice deformation can occur in calcitic and aragonitic speleothems and may be formed in a sub-aqueous environment.

Mimetic Replacement: This term was introduced by Frisia (1996) in analogy to the classification proposed for dolomite textures by Sibley & Gregg (1987). Mimetic phenomena preserve the original texture of the speleothem, whereby all the original components can be detected.

3.7. Petrology Results

Phases of $CaCO_3$ detected by XRD include low-magnesium calcite and aragonite. The approximate proportion of aragonite in the speleothems analysed ranged from 0% to 85%. Crystal morphology of the low-magnesium calcite can occur either as elongate drusy crystals, equant crystals or as a fine-grained micrite. The aragonite crystals are large (upto 5 cm in length) and are usually acicular in habit. XRD and petrological evidence indicates that calcite is by far the more dominant of the two calcium carbonate polymorphs present within the sampled specimens, although there are areas within the Makapansgat Limeworks stratigraphy that are rich in acicular aragonite or aragonite fans such as MAK LC04 from the Exit Quarry and the aragonite rich layers of the Original Ancient Entrance repository. XRD analysis indicates that the aragonite fans have been subjected to some degree of diagenetic alteration, containing at least 15% secondary calcite. Each of the speleothems studied differ macroscopically in terms of colour, mineralogy and texture but on the basis of petrographic features, each flowstone can be classified as belonging to one of the following primary or diagenetic fabrics.

3.7.1. Primary fabrics

Columnar Calcite Fabric

The columnar calcite fabric is the typical fabric of primary sub-aerial flowstones (e.g. Frisia *et al.*, 2000), and is by far the dominant fabrics of the Buffalo Cave, Rainbow Cave and Makapansgat Limeworks Member 1 flowstones (see Table 1.). The columnar calcite fabric is also intermittently present in the Swartkrans and Drimolen flowstones. Elongate columnar crystals are often greater than 1 cm in length and unit extinction of the crystallites dominates. Lateral overgrowths are common (see Figs. 3.2f and 3.3a) as are competitive growth fabrics following the deposition of thin mud or microcrystalline calcite layers.

Fluid-inclusions are present in this fabric, the most common types of inclusion being pseudopleochroic, linear and termination traces following the description of Broughton (1983b). Crystal zoning is evident in plane-polarized

Table 3.1.

Sample Name	Locality	Description (hand specimen)	Fabrics (thin section)	Environment of Precip-itation	Mode of Precipitation
MAK M1 CC	Makapansgat Limeworks, Member 1B flowstone boss, Collapsed Cone	Pure white, dense flowstone	Columnar calcite	Sub-aerial	Precipitation in Isotopic equilibrium with drip-water, as determined from growth layer analyses
MAK M1 NA	Makapansgat Limeworks, Member 1B, flowstone boss, North Alcove, Main Quarry	Pure white, dense flowstone	Columnar calcite	Sub-aerial	N/A
MAK M1 EQ	Makapansgat Limeworks, Member 1B, flowstone boss, Entrance Quarry / Main Quarry passage	Pure white, dense flowstone	Columnar calcite	Sub-aerial	N/A
MAK OAE B2	Makapansgat Limeworks, Member 1B, Original Ancient Entrance deposits	White, powdery flowstone layers interbedded with sugary light brown flowstone layers	Interbedded equant calcite, acicular aragonite, and mud rich layers	Probably sub-aerial and / or sub-aqueous aragonite prior to diagenesis	N/A
*MAK AM01	Makapansgat Limeworks, Member 1B, Original Ancient Entrance deposits	White, dense mammilary speleothem with thin red mud-rich layers	Lattice Deformation	Sub-aqueous	Some evaporation of cave pools (heavy $\delta^{18}O$) linked with periods of mud-influx
*MAK H03	Makapansgat Limeworks, Member 2, Classic Section	Light brown, porous, horizontally laminated flowstone	Equant calcite with aragonite relics	Sub-aerial aragonite and calcite prior to diagenesis	Recrystalisation of aragonite in groundwater with heavy $\delta^{13}C$ values
MAK LC03	Makapansgat Limeworks, Chimney repository, Exit Quarry	Pure white, dense mammilary speleothem.	Lattice Deformation,	Sub-aqueous	N/A
MAK LC04	Makapansgat Limeworks, Chimney repository, Exit Quarry	Brown-red colour, large needles of aragonite	Acicular aragonite with localised drusy calcite	Sub-aqueous	N/A
BUFF	Buffalo Cave[1], Basal Flowstone	Dark brown, horizontally laminated, dense flowstone with occassional thin white layers	Columnar and microcrystalline layers	Sub-aerial	Precipitation in Isotopic equilibrium with drip-water, as determined from growth layer analyses
RAINB	Rainbow Cave, Cave of Hearths	Cream coloured, dense flowstone	Columnar calcite	Sub-aerial	N/A
*STER 20	Sterkfontein, Member 2, Bore Hole 5	White, "sugary" flowstone	Equant calcite and mud-rich layers	Probably sub-aerial aragonite prior to diagenesis	Recrystalisation of aragonite in groundwater with heavy $\delta^{13}C$ values
*STER 21	Sterkfontein, Member 2, Bore Hole 5	Cream coloured flowstone consisting of interbedded mud-rich and "sugary" layers	Equant calcite with aragonite relics	Probably sub-aerial aragonite prior to diagenesis	N/A
*STER 22	Sterkfontein, Member 3b, Bore Hole 5	Cream coloured flowstone containing some elongate crystals	Acicular aragonite partly replaced by secondary calcite	Probably sub-aqueous aragonite prior to diagenesis	Recrystalisation of aragonite in groundwater with heavy $\delta^{13}C$ values
*STER 16	Sterkfontein, Interface between Members 4 & 5, Type Site	Cream coloured, interbedded flowstone	Interbedded acicular aragonite, secondary calcite, columnar calcite and mud-rich	Probably sub-aerial aragonite and calcite prior to diagenesis	N/A

			layers		
SWART HR	Swartkrans, Member 1A, Basal Flowstone underlying the Hanging Remnant	Interbedded white, dense flowstone and white "sugary" layers. Horizontally laminated and lacking in detritus	Columnar / equant	Sub-aerial calcite and aragonite prior to diagenesis	Precipitation of calcite possibly in isotopic equilibrium. Recrystallisation of aragonite in groundwater with heavy $\delta^{13}C$ values
DRIM D1	Drimolen, Basal flowstone.	Pure white flowstone with some "sugary" layers	Equant calcite with aragonite relics interbedded with columnar calcite	Sub-aerial calcite and aragonite prior to diagenesis	N/A
*GOND GB01	Gondolin[2], Flowstone from Basal Collapse Breccia Unit	Brown flowstone with some "sugary" and crystalline layers	Interbedded acicular aragonite, equant calcite and columnar calcite	Sub-aerial calcite and aragonite prior to diagenesis	Rapid Outgassing in a very open cave environment leading to very heavy $\delta^{13}C$ and $\delta^{18}O$ values

Table 3.1. (continued)

Table 3.1. Summary of sample locality, petrology and environmental interpretation. Cave member and locality nomenclature is from Partridge (2000) with the exception of [1] from Herries *et al.*, *in press* and [2] from Menter *et al.*, 1999. * refers to samples collected and described by Herries (2003). MAK M1 CC, BUFF and SWART HR are figured in Appendix 1. Speleothem fabrics are following the terminology of Frisia *et al.* (2000), see text for discussion. Mode of precipitation is based on a synthesis of the isotopic and petrographic data reported in this study.

light where fluid-inclusions outline the crystal faces and in UV-light where fluorescent banding is common due to the varying concentration and composition of organic acids (see Chapters 4 and 5).

Microcrystalline Fabric

Layers of white microcrystalline calcite up to 10mm thick occur intermittently throughout the Buffalo Cave flowstone sequence (BUFF). The micrite is composed of sub-rhombohedral crystals often displaying a random orientation of crystallites. The crystallites are often full of defects, displaying twins, lamellae and dislocations. Figure 3a indicates that microcrystalline layers in the Buffalo Cave flowstone are not significantly altered in isotopic composition relative to the adjacent columnar fabric. This finding is in agreement with Frisia *et al.* (2000) who, based on isotopic and petrographic studies of Alpine and Irish speleothems, conclude that the microcrystalline speleo-fabric tends to form in isotopic equilibrium. They suggest that microcrystalline fabrics form under

fluctuating discharge rates and periodic (seasonal) input of calcite growth inhibitors. Diagenetic microcrystalline calcite (e.g. Fig. 3.2d) can appear similar to the primary microcrystalline fabric, but aragonite relics and an equant mosaic are often present to distinguish these two fabrics.

Lattice Deformation Fabric

The distinctive Lattice Deformation Fabric (LDF) of Broughton (1983a) is the only known published record of this apparently rare speleo-fabric. Broughton (1983) found a number of speleothems displaying the fabric, but his specimens were without provenance data, preventing any inferences relating to the specific cave environment in which this fabric forms. The current study confirms Broughton's (1983) suggestion that the LDF, although rare, is a significant and widespread speleo-fabric.

The Lattice Deformation fabric occurs in MAK AM01, MAK OAE DB, MAK OAE B1, MAK OAE G2, all of which are mammilary (sub-aqueous) calcitic speleothems. All examples of this fabric display brush extinction (see Fig. 3.2e), which is absent from all the other fabrics. The direction of lattice curvature is variable but occurs in bundles of crystallites with sub-parallel axes of curvature. The recognition of layers of LDF within long sequences of flowstones is important, as it may be the best way of identifying short periods of sub-aqueous speleothem growth.

Dendritic Fabric

Dendritic crystals in speleothems are rare. Their formation has been attributed to the presence of micro-organisms (Jones and MacDonald, 1989; Jones and Kahle, 1986) and they have been found to form in isotopic disequilibrium with respect to source-water, perhaps due to irregular growth rates (Frisia *et al.*, 2000). There is no evidence of a dendritic speleo-fabric among the 60 thin sections sampled in this study which indicates that micro-organisms played little, if any, role in the precipitation of the South African speleothems studied here.

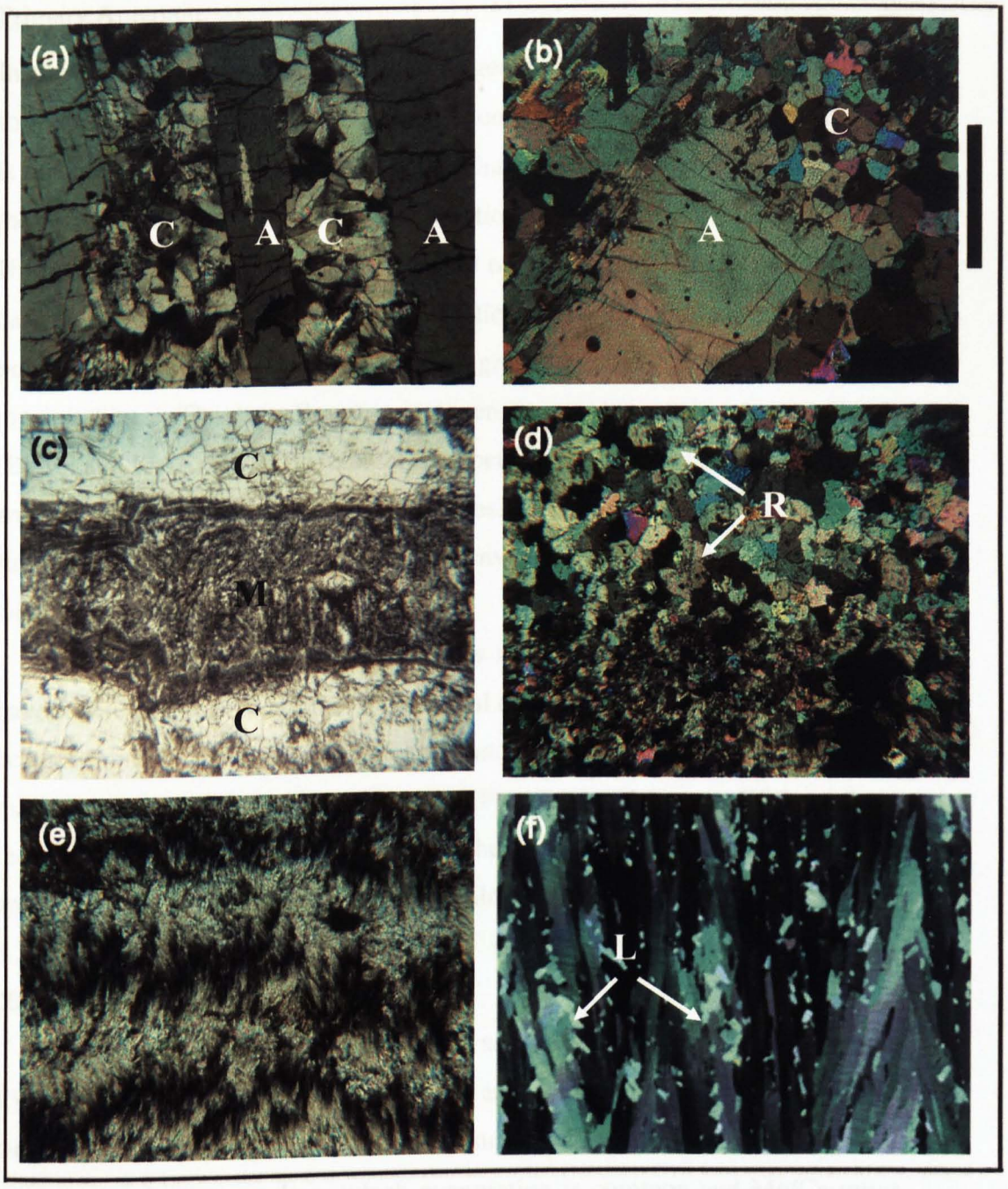

Figure 3.2. Secondary and primary fabrics in speleothems. (a) – (d) secondary fabrics; (e) and (f) primary calcite fabrics. (a) Primary aragonite (A) needles with secondary drusy calcite (C) crystals filling pore-spaces (MAK OAE). (b) Primary aragonite (A) dissolution and replacement with an equant calcite (C) mosaic (MAK OAE). (c) Rectangular aragonite crystal replaced by micrite (M) surrounded by drusy calcite (C) mosaic (MAK OAE). (d) Mosaic of secondary eqauant calcite crystals (MAK OAE). Intra-crystalline aragonite relics (R) are common. (e) Lattice deformation fabric of deformed calcite crystals formed in sub-aqueous mammilary speleothem (MAK AM01). (f) Primary columnar calcite crystals with competitive growth fabric and lateral overgrowths (L), a typical primary flowstone speleo-fabric (MAK M1 CC). Scale-bar is 2mm in length.

Primary Aragonite

In the Makapansgat Valley and the Krugersdorp sites, it is apparent that the formation of primary aragonite was common throughout the cave sequences and is not site or age specific. This indicates that the Mg/Ca ratio of the cave water, the primary control on aragonite precipitation (Fischbeck and Müller, 1971 and Hill and Forti, 1997), was highly variable over time and was dependant on the cave micro-environment. High Mg/Ca ratios are found in drip waters or cave-pools that have undergone significant degrees of evaporation or prior calcite precipitation. The two flowstone sequences without any aragonitic layers (BUFF and MAK M1 CC) are basal members of the cave-fill sequence and lack any significant detrital input or hiatuses. This indicates that these two flowstones were formed in closed cave environments free of evaporation and with a consistent water source.

Primary aragonite occurs either as small irregularly shaped relics that have retained little indication of the original crystal structure (Fig. 3.2d) or it can occur as predominately unaltered aragonite crystals that have preserved the majority of the original crystal structure (Fig. 3.2a). Based on XRD analysis, the most pristine aragonite-bearing speleothem from the studied sample contains approximately 85% aragonite and 15% calcite. This sample (Mak LC04; Fig. 3.2a) from the Makapansgat Limeworks is approximately 3.5 Ma (Herries, 2003).

The aragonite crystals in the Transvaal speleothems are often large (up to 15 cm long), are usually acicular in habit and often form in fan-shaped crystal bundles. These aragonite fans are usually associated with sub-aqueous precipitation in cave pools in which evaporation is common and Mg/Ca ratios can be high. The Original Ancient Entrance (OAE) repository at the Makapansgat Limeworks consists of a horizontally layered succession of mammilary speleothem, aragonitic fans and diagenetic calcite, precipitated in a large cave pool with fluctuating water levels (Latham *et al.*, 2003). The OAE is unusual in having so many large aragonitic fans in what is essentially their original condition (e.g. MAK LC04; Fig. 3.2a), although localised primary aragonite is also present at Sterkfontein in samples STER 22 and STER 16. In thin section, each crystallite of primary aragonite displays unit extinction, is

rectangular in shape and tends to be cross cut by large fractures (see Figs. 3.2.a,b). All the aragonite crystals show some degree of dissolution and replacement by one of the diagenetic fabrics described in Section 3.7.2.

Although all of the observed primary aragonite crystals are arranged in fans of sub-aqueous origin (e.g. Fig. 3.2a), it is possible that some of the thin layers of secondary calcite bounded by primary columnar calcite may have been precipitated as sub-aerial aragonitic flowstones prior to diagenetic alteration (e.g. Fig. 3.2d). Railsback *et al.* (1994) describe alternating layers of calcite and aragonite in a Holocene stalagmite from Botswana. The calcite-aragonite pairs represent one year of growth in an environment of highly seasonal rainfall in which the Mg/Ca ratio of the drip water is shown to fluctuate above and below the concentration required for aragonite precipitation. Similar alternations of aragonite and calcite may well have occurred in the Transvaal caves, either seasonally or quasi-periodically. If so, these sub-aerial aragonite crystallites would be considerably smaller than the sub-aqueous primary aragonitic fans discussed above, making them highly susceptible to diagenetic alteration and possibly explaining their absence in the studied samples. It is likely that the flowstones MAK H03, MAK OAE and SWART HR contained layers of sub-aerial aragonite, as there are fluid and organic inclusions preserved within the diagenetic mosaic of equant calcite crystals, which are most likely to have originated in a sub-aerial environment.

Primary Fabrics – summary

Evidence of primary fabrics is essential if stable isotope data is to be interpreted in terms of palaeoenvironments. While samples of primary aragonite can be used for palaeoenvironmental studies, care must be taken to sample from areas in which calcite replacement is minimal, as the two calcium carbonate polymorphs are intimately related in the primary aragonite samples (see Figs 3.2.a,b). The lattice deformation fabric of mammilary speleothem is composed of densely packed crystallites with negligible porosity or inclusions, and is therefore well suited for potential dating techniques. For stable isotope palaeoenvironmental studies, the sub-aerial columnar calcite fabric is most useful due to its formation in surface-derived waters that have not been

subjected to modification by evaporation or contact with cave-pool water or groundwater.

It can be seen from Figure 3.3a that isotopic values are not significantly altered by the passage from one primary fabric to another (in this case from columnar calcite to microcrystalline calcite) and that the oxygen and carbon isotope values can vary independently of the mineralogical changes. In the case of the speleothems in this study, primary fabrics have on average a more negative $\delta^{13}C$ value than secondary fabrics, due to the tendency of diagenetic processes to result in secondary calcite enriched in $\delta^{13}C$ (see Section 3.10.3. and Fig. 3.3.b).

3.7.2. Diagenetic Fabrics - Replacement of Aragonite by Calcite

The diagenetic replacement of aragonite by calcite has been comprehensively documented in the spelean environment (Assereto & Folk, 1979, Folk and Assereto, 1976; Frisia, 1996; Frisia *et al.*, 1993; Railsback *et al.*, 1997; Cabrol and Coudray, 1982). The transformation of aragonite into calcite can be assigned to one of two diagenetic processes. Calcitization of aragonite involves the preservation of aspects of the original aragonite texture, whereas dissolution-cementation is a two-stage process in which the original aragonitic texture is destroyed. Calcitization usually occurs across a very thin film of water (a few microns thick) under closed system conditions. In thin section, calcitization is typified by preservation of fluid and organic inclusions and aragonite relics within an equant calcite mosaic, whereas dissolution-cementation is typified by drusy calcite crystals filling the mould left by aragonite dissolution.

The Transvaal speleothems show a variety of diagenetic calcite fabrics resulting either from dissolution-cementation or calcitization of aragonite. This broad distinction is used to highlight the difference between an open diagenetic system in which dissolution-cementation is likely to dominate and a closed diagenetic system in which calcitization dominates.

Calcitization of aragonite

Equant calcite mosaics are a common product of aragonite replacement (see Figure 3.2.b&d) in the Transvaal speleothems and are present to some degree in most of the caves studied (Table 3.1). They contain aragonite relics and some

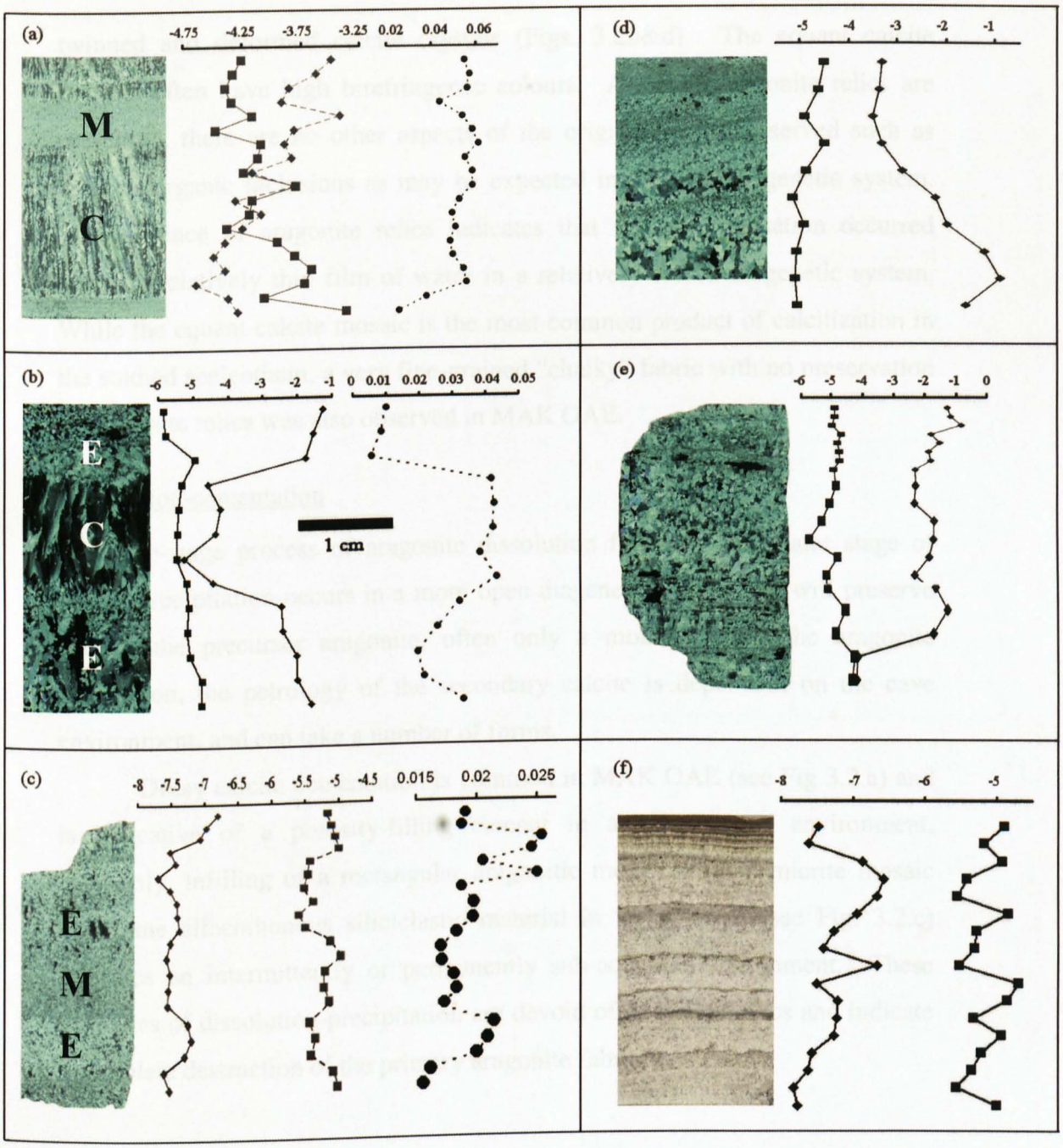

Figure 3.3. Thin sections of flowstones (a-e) and mammilary speleothems (f) with corresponding stable isotope and trace element data points. (a) BUFF A 71-91 showing columnar (C) and microcrystalline (M) speleo-fabrics, both primary calcite. The inverse δ18O and δ13C trends are not influenced by the microcrystalline fabric. (b) SWART HR D4 showing columnar calcite (C) overlain and underlain by secondary equant (E) calcite. The δ13C and Mg/Ca values are significantly altered by the change from primary to secondary calcite. (c) MAK OAE B2 consists of layers of equant (E) and microcrystalline (M) calcite, both secondary in origin as indicated by the low Mg/Ca ratios. (d) STERK 20 is mud-rich at the top of thin-section, and becomes dominated by an equant mosaic of secondary calcite towards the bottom of the thin-section. This change in fabric is reflected in the enriched δ13C values in the equant calcite mosaic. (e) MAK H03. consists of an equant mosaic of secondary calcite rich in aragonitic inclusions. The heavy carbon isotope values are typical of the secondary calcite speleothems studiesd (f) MAK AM01 is a mammilary speleothem in plane polarised light. The undulating $\delta^{18}O$ values indicate periodic evaporation that coincides with an increased mud input. This is suggestive of a fluctuating cave-pool depth, perhaps on a seasonal time-scale. Squares = $\delta^{18}O$, Diamonds = $\delta^{13}C$, Circles = Mg/Ca molar ratio. Scale bar as in (b).

twinned and deformed calcite crystals (Figs. 3.2b&d). The equant calcite crystals often have high birefringence colours. Although aragonite relics are preserved, there are no other aspects of the original fabric preserved such as fluid or organic inclusions as may be expected in a closed diagenetic system. The presence of aragonite relics indicates that the recrystalisation occurred across a relatively thin film of water in a relatively closed diagenetic system. While the equant calcite mosaic is the most common product of calcitization in the studied speleothem, a very fine-grained "chalky" fabric with no preservation of aragonite relics was also observed in MAK OAE.

Dissolution-cementation

This two-stage process of aragonite dissolution followed by a later stage of calcite precipitation occurs in a more open diagenetic system and will preserve less of the precursor aragonite, often only a mould. After the aragonite dissolution, the petrology of the secondary calcite is dependant on the cave environment, and can take a number of forms.

Drusy calcite cementation is common in MAK OAE (see Fig 3.2.a) and is indicative of a porosity-filling* cement in a sub-aqueous environment. Similarily, infilling of a rectangular aragonitic mold by drusy micrite mosaic and some allochthonous siliciclastic material in MAK OAE (see Fig. 3.2.c) indicates an intermittently or permanently sub-aqueous environment. These examples of dissolution-precipitation are devoid of aragonite relics and indicate a complete destruction of the primary aragonite fabric.

3.8. Stable Isotope Results

The primary calcite flowstones show $\delta^{13}C$ values ranging from –8.8‰ to –2.6‰ and $\delta^{18}O$ values ranging from –3.4‰ to –7‰ (Table 3.2. and Fig. 3.7.). The primary calcites show a different relationship between $\delta^{13}C$ and $\delta^{18}O$ depending on their age. Prior to ~4Ma the primary calcites have invariant $\delta^{13}C$ values (see Fig. 3.7) due to the lack of C_4 vegetation (see Chapters 4 & 5) and light $\delta^{18}O$ values. The post ~4Ma primary calcite flowstones show a negative correlation between $\delta^{13}C$ and $\delta^{18}O$ (see Fig. 3.7.). The secondary calcite speleothems show $\delta^{18}O$ values varying between –6‰ and –4‰ with a mean of -5‰ and $\delta^{13}C$

varying from –7.7‰ to 0.9‰ (see Fig. 3.6.). GOND GB01 has unusually heavy $\delta^{13}C$ and $\delta^{18}O$ values (+5.2‰ and –1.9‰ respectively) and is likely to have formed in a highly evaporative environment (see Fig. 3.8. and Section 3.10.4.).

		$\delta^{13}C$ ‰ PDB			$\delta^{18}O$ ‰ PDB			
Fabric	**Sample name**	**mean**	**min**	**max**	**mean**	**min**	**max**	**No. of analyses**
Primary Calcite	MAK M1 CC	-8.1	-8.8	-7.1	-5.7	-7.0	-4.5	239
	MAK M1 NA	-8.4	-8.6	-8.3	-6.0	-6.0	-6.0	3
	MAK M1 EQ	-7.9	-7.9	-7.8	-5.6	-5.7	-5.6	2
	BUFF	-5.0	-8.2	-2.6	-4.9	-6.5	-3.4	550
	RAINB	-3.6	-5.4	-2.6	-4.9	-5.4	-4.4	11
	MAK AM01	-7.3	-7.9	-6.6	-5.2	-5.6	-4.7	27
	MAK LC03	-6.8	-7.7	-5.6	-4.1	-4.9	-2.2	9
Primary Aragonite	MAK LC04	-6.2	-6.4	-6.0	-4.8	-4.9	-4.7	10
Secondary Calcite	MAK OAE B2	-7.4	-7.7	-6.8	-5.3	-5.6	-5.0	20
	MAK H03	-2.0	-4.2	-0.8	-4.9	-5.7	-4.3	19
	STERK 20	-2.4	-3.5	-0.9	-4.9	-5.1	-4.5	10
	STERK 21	-3.5	-3.9	-3.1	-4.7	-5.0	-4.3	5
Mixed Mineralogy	STERK 22	-0.4	-1.0	0.9	-4.6	-5.2	-4.2	10
	STERK 16	-5.1	-5.4	-4.5	-5.8	-6.7	-5.4	5
	SWART HR	-2.1	-4.2	0.8	-5.4	-6.2	-4.6	92
	DRIM D1	-4.5	-6.0	-3.5	-6.0	-6.4	-5.2	30
	GOND GB01	1.7	-1.3	5.2	-3.8	-5.3	-1.9	26

Table 3.2. Stable isotope results for primary calcite, primary aragonite and secondary calcite speleothems. Mixed mineralogy speleothems contain a mixture of fabrics, as indicated in Table 3.1.

3.9. Trace element Results

The 1000 Mg/Ca values in primary calcite speleothems vary between 23.9 and 89.2 and the 1000 Sr/Ca values vary between 0.0044 and 0.082 (Table 3.3. and Fig 3.4a). There is a positive correlation between 1000 Mg/Ca and 1000 Sr/Ca in all of the primary calcite flowstones (Fig. 3.4.a). The primary aragonite samples from MAK LC04 (85% aragonite) have low 1000 Mg/Ca values (from 1.23 to 1.70) and high 1000 Sr/Ca values (from 0.14 to 0.18) relative to the calcite samples as predicted by the partition coefficients of Sr and Mg into aragonite (Kinsman and Holland, 1969 and Oomori *et al.*, 1987). The secondary calcite flowstones (MAK OAE B2 and SWART HR D4) have

intermediate values between the aragonite and primary calcite end-members (Fig. 3.4.a) indicating either a variation in the degree of openness of the diagenetic system or a calcite-aragonite mixing trend or both. The depth-series record of 1000 Mg/Ca and $\delta^{18}O$ in the Buffalo Cave flowstone (Fig. 3.5.) displays a weak positive correlation with $\delta^{18}O$ ($r = 0.44$).

Fabric	Sample name	1000 Mg/Ca molar ratio			1000 Sr/Ca molar ratio			No. of analyses
		mean	min	max	mean	min	max	
Primary calcite	MAK M1 CC A1	41.4	33.9	49.3	0.0089	0.0070	0.0121	40
	MAK AM01	44.0	38.3	46.9	0.0055	0.0044	0.0065	9
	BUFF A	51.4	26.1	61.4	0.037	0.025	0.0823	21
	BUFF H	50.4	23.9	89.2	0.035	0.014	0.0762	90
Primary aragonite	MAK LC04	1.4	1.2	1.7	0.16	0.138	0.1798	10
Secondary calcite	MAK OAE B2	19.5	15.8	25.4	0.050	0.012	0.1336	20
Mixed Mineralogy	SWART HR D4	28.1	5.6	43.4	0.043	0.0091	0.2010	13

Table 3.3. Trace element results for primary calcite, primary aragonite and secondary calcite speleothems. SWART HR D4 contains a mixture of primary and secondary calcite, as described in Table 3.1. MAK LC04 is predominantly composed of primary aragonite, but contains small and variable proportions of secondary calcite (see Section 3.7.1.).

3.10. Discussion

3.10.1. Trace element partitioning in primary calcite speleothems

The incorporation of Mg and Sr in calcite depends on the initial composition of the precipitating solution and on their respective distribution coefficients (e.g. $Mg/Ca_{calcite}/Mg/Ca_{solution}$). The distribution coefficient of Mg depends mainly on temperature (Kats, 1973; Mucci and Morse, 1983; Burton and Walter, 1991; Huang and Fairchild, 2001), while the distribution coefficient of Sr depends mainly on the precipitation rate of the calcite (Lorens, 1981; Pingitore and Eastman, 1986; Huang and Fairchild, 2001) among other parameters. The primary calcite flowstones of this study contain Mg/Ca and Sr/Ca values that fit within the range reported for calcitic speleothems from other dolostone terrains (Bar-Matthews *et al.*, 1991 and Railsback *et al.*, 1994). The high Mg/Ca and low Sr/Ca ratios of the Transvaal calcitic speleothems differs significantly from values measured in speleothem from limestone or mixed dolomite/limestone terrains (e.g. Goede *et al.*, 1998; Roberts *et al.*, 1998; Bar-Matthews *et al.*, 1999; Hellstrom and McCulloch, 2000; Verheyden *et al.*, 2000; Huang *et al.*, 2001) as

is expected from the high Mg and low Sr content of the Transvaal Supergroup dolomite host-rock (Veizer et al, 1992). The Proterozoic Malmani dolomite host-rock is a stoichiometric dolomite, the dissolution of which is expected to lead to cave drip-water Ma/Ca ratios approaching unity. However, the presence of a fine-grained dolomitic cement between the dolomite rhombs, and its associated pore-space, makes the Malmani dolomite more susceptible to dissolution than most dolomites (Marker, 1981). There is currently little published data regarding the dominant processes of dolomite dissolution and groundwater composition in the Malmani dolomite, although a small sample of drip-water Mg/Ca ratios from the Transvaal caves varies between 0.8 and 8.3 (Talma *et al.*, 1974). It is currently uncertain whether this wide range of drip-water Mg/Ca values is related to dissolution processes or to evaporative modification of percolating water. Sr/Ca ratios in an aragonitic stalagmite (T7) from Cold Air Cave, Makapansgat Valley (Finch *et al.*, 2001), are shown to vary seasonally, but there is little discussion of the incorporation of Sr into the aragonite.

Values for Mg/Ca and Sr/Ca ratios of the solution from which the speleothem were precipitated were calculated using the partition coefficient for Mg (D_{Mg}) into calcite of 0.025 at 20°C and the partition coefficient for Sr (D_{Sr}) into calcite of 0.0675 (from Huang and Fairchild, 2001). The cave water compositions for Mg/Ca in primary calcite range from 0.96 to 3.56 with a mean of 1.66 and 1000 Sr/Ca values for the cave waters range from 0.066 to 1.22 with a mean of 0.402 (Fig. 3.4.b).

Fairchild *et al.* (2000) state that the primary controls on cave water chemistry are prior calcite precipitation, differential dissolution of calcite and dolomite, incongruent dolomite dissolution and selective leaching. In the present case study of Transvaal cave systems, differential dissolution of calcite and dolomite is minimal as the Malmani dolomite contains only localised beds of calcite (Veizer *et al.*, 1992 and Marker *et al.*, 1981). However, incongruent dolomite dissolution may preferentially release Ca from fresh dolomite surfaces during the early stages of dolomite dissolution, potentially increasing the Mg/Ca ratio of subsequent cave waters (Busenberg and Plummer, 1982). Since the partition coefficients for Mg and Sr are «1, the Mg/Ca and Sr/Ca ratios rise as calcite precipitation occurs, leading to the positive correlation of Mg/Ca and

Fig. 3.4.a Trace Elements in South African Flowstones

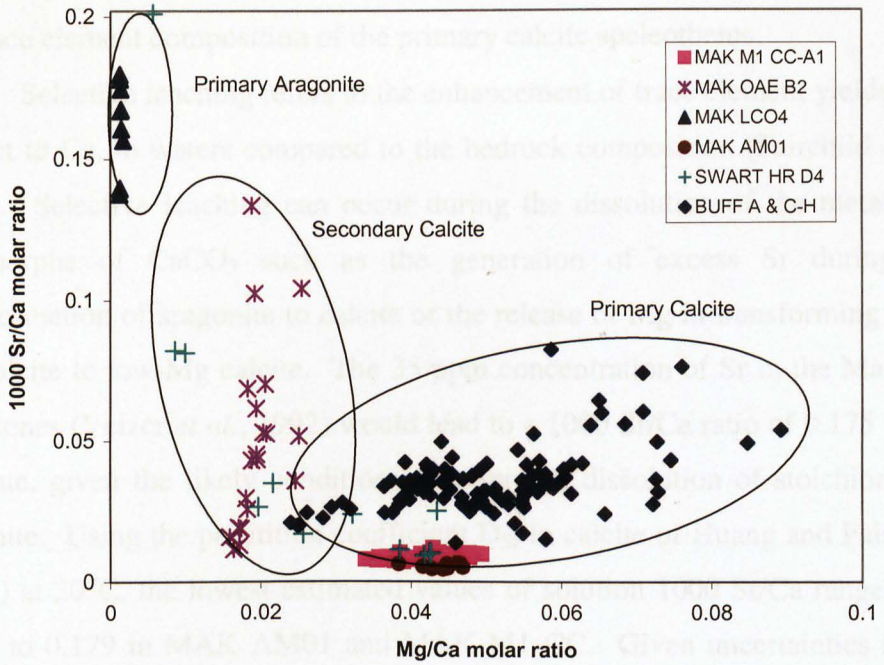

Fig. 3.4.b Calculated trace element composition of cave waters

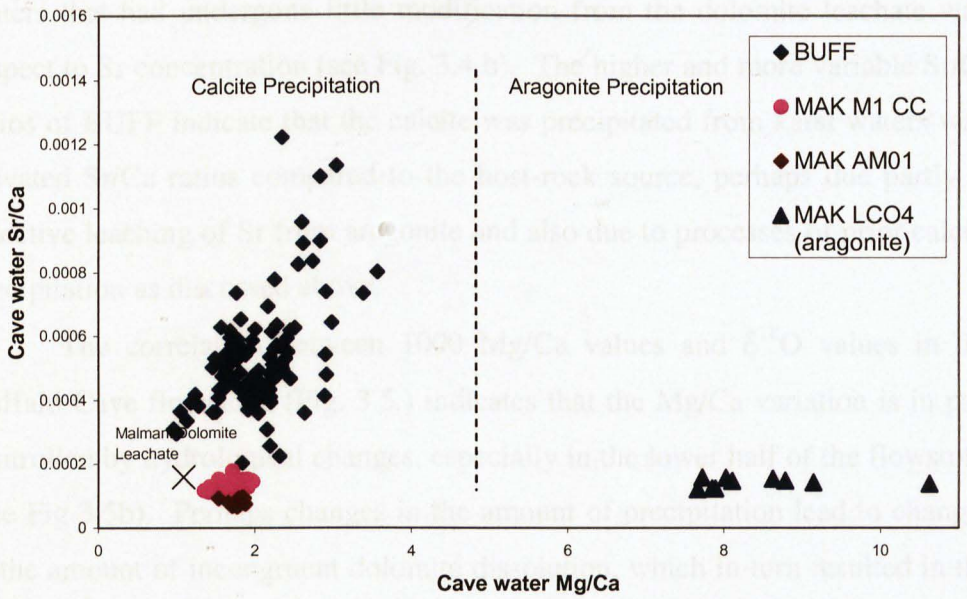

Figure 3.4. (a) Trace element composition of primary calcite, secondary calcite and aragonitic speleothem. Primary calcite has a trace element composition distinct from aragonite and secondary calcite. **(b)** Trace element composition of cave waters calculated using partition coefficients for calcite and aragonite (see Sections 3.10.1. and 3.10.2.). Aragonite is formed in cave waters with a Mg/Ca ratio greater than 4.6 (Fischbeck and Müller, 1971).

Sr/Ca (Fairchild *et al.*, 2000), as shown in the primary calcite samples of Figure 3.4.a. The correlation between Mg/Ca and Sr/Ca (Fig. 3.4.a) may indicate that the prior precipitation of calcite is a principal process responsible for modifying the trace element composition of the primary calcite speleothems.

Selective leaching refers to the enhancement of trace element yields with respect to Ca, in waters compared to the bedrock composition (Fairchild *et al.*, 2000). Selective leaching can occur during the dissolution of the metastable polymorphs of $CaCO_3$ such as the generation of excess Sr during the transformation of aragonite to calcite or the release of Mg in transforming high-Mg calcite to low-Mg calcite. The 35 ppm concentration of Sr in the Malmani dolostones (Veizer *et al.*, 1992) would lead to a 1000 Sr/Ca ratio of 0.175 in the leachate, given the likely condition of congruent dissolution of stoichiometric dolomite. Using the partitition coefficient D_{Sr} in calcite of Huang and Fairchild (2001) at 20°C, the lowest estimated values of solution 1000 Sr/Ca range from 0.066 to 0.179 in MAK AM01 and MAK M1 CC. Given uncertainties in the calculation of partition coefficients and in analytical measurements, the correspondence between the host rock Sr/Ca ratio and the minimum spelothem Sr/Ca indicates that MAK AM01 and MAK M1 CC were precipitated from karst waters that had undergone little modification from the dolomite leachate with respect to Sr concentration (see Fig. 3.4.b). The higher and more variable Sr/Ca ratios of BUFF indicate that the calcite was precipitated from karst waters with elevated Sr/Ca ratios compared to the host-rock source, perhaps due partly to selective leaching of Sr from aragonite and also due to processes of prior calcite precipitation as discussed above.

The correlation between 1000 Mg/Ca values and $\delta^{18}O$ values in the Buffalo Cave flowstone (Fig. 3.5.) indicates that the Mg/Ca variation is in part controlled by hydrological changes, especially in the lower half of the flowstone (see Fig 3.5b). Perhaps changes in the amount of precipitation lead to changes in the amount of incongruent dolomite dissolution, which in turn resulted in the observed Mg/Ca variation in the Buffalo Cave flowstone. Similarly, increased dissolution would have resulted in an increase in Sr leaching from aragonite. More work is required to identify the geochemical processes responsible for trace element variation in the South African primary speleothems.

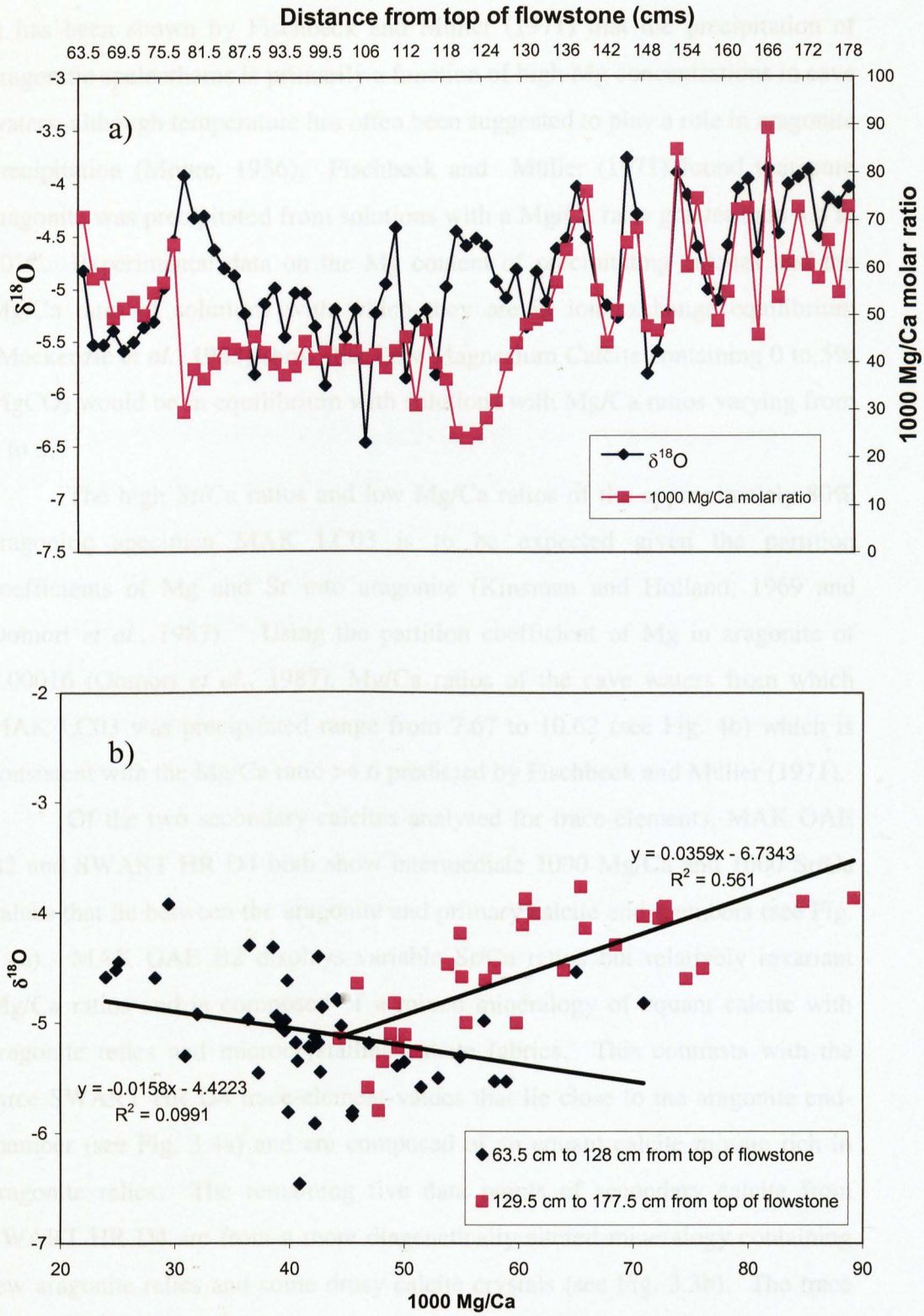

Figure 3.5. Mg/Ca and $\delta^{18}O$ depth-series and cross-plot for the Buffalo Cave flowstone. **a)** The time-series indicates a positive correlation between the two records below the depth of 1.29 m and a poor correlation above this level. **b)** By grouping the data above and below 1.29 m, the change in relationship between Mg/Ca and $\delta^{18}O$ at 1.29m is evident. See Sections 3.10.1. and 4.8.4 for discussion.

3.10.2. Trace elements in the aragonitic and secondary calcite flowstones

It has been shown by Fischbeck and Müller (1971) that the precipitation of aragonitic speleothems is primarily a function of high Mg concentrations in cave waters, although temperature has often been suggested to play a role in aragonite precipitation (Moore, 1956). Fischbeck and Müller (1971) found that pure aragonite was precipitated from solutions with a Mg/Ca ratio greater than 4.4 at 20°C. Experimental data on the Mg content of precipitating calcites and the Mg/Ca ratio of solutions with which they are in ion exchange equilibrium (Mackenzie *et al.*, 1983) show that Low Magnesium Calcite containing 0 to 5% $MgCO_3$ would be in equilibrium with solutions with Mg/Ca ratios varying from 0 to 3.

The high Sr/Ca ratios and low Mg/Ca ratios of the approximately 80% aragonitic specimen MAK LC03 is to be expected given the partition coefficients of Mg and Sr into aragonite (Kinsman and Holland, 1969 and Oomori *et al.*, 1987). Using the partition coefficient of Mg in aragonite of 0.00016 (Oomori *et al.*, 1987), Mg/Ca ratios of the cave waters from which MAK LC03 was precipitated range from 7.67 to 10.62 (see Fig. 4b) which is consistent with the Mg/Ca ratio >4.6 predicted by Fischbeck and Müller (1971).

Of the two secondary calcites analysed for trace-elements, MAK OAE B2 and SWART HR D4 both show intermediate 1000 Mg/Ca and 1000 Sr/Ca values that lie between the aragonite and primary calcite end-members (see Fig. 3.4a). MAK OAE B2 displays variable Sr/Ca ratios but relatively invariant Mg/Ca ratios and is composed of a mixed mineralogy of equant calcite with aragonite relics and microcrystalline calcite fabrics. This contrasts with the three SWART HR D4 trace-element values that lie close to the aragonite end-member (see Fig. 3.4a) and are composed of an equant calcite mosaic rich in aragonite relics. The remaining five data points of secondary calcite from SWART HR D4 are from a more diagenetically altered mineralogy containing few aragonite relics and some drusy calcite crystals (see Fig. 3.3b). The trace element data from these samples lies close to the primary calcite end-member (see Fig. 3.4a). Lying between these two secondary calcite layers is a 1.5 cm thick layer of primary columnar calcite from which five SWART HR D4 samples were derived (see Fig. 3.3b). Each of these samples have a trace

element composition typical of the primary calcite flowstones in this study (see Figs. 3.3b and 3.4a).

The increase in Sr/Ca and corresponding decrease in Mg/Ca observed in the aragonitic and secondary calcite speleothems (Fig. 3.4.a) is a mixing-trend between the primary aragonite and primary calcite end-members. The trace-element composition of the secondary calcite speleothems may also be indicative of the openness and environment of the diagenetic system, however with the current preliminary evidence, this cannot be determined.

3.10.3. Variable and heavy carbon isotope values in secondary calcite

Lohmann's (1988) model of meteoric vadose and phreatic cements and alteration products predicts that $\delta^{18}O$ values of secondary speleothem will be similar to that of primary calcite and indicative of meteoric water alteration whereas the $\delta^{13}C$ values will be highly variable and will increase with increasing degrees of rock-water interaction. This "inverted J-curve" or meteoric calcite line documents the enrichment of carbon isotopes with the increasing diagenesis of metastable assemblages until the host rock $\delta^{13}C$ values are reached. In the case of diagenesis within this study, most of the aragonite transformation has occurred under sub-aqueous conditions as determined by the equant and occasionally drusy nature of the replacement calcite. It is likely that the $\delta^{13}C$ values of the groundwater are approaching those of the host-rock due to long groundwater/cave-pool residence times. Contact of meta-stable minerals in the speleothems with groundwater/cave-pools that are undersaturated with respect to aragonite will result in aragonite dissolution and the precipitation of calcite. The variable $\delta^{13}C$ values and invariant $\delta^{18}O$ values of the South African secondary calcite flowstones are typical of the meteoric water line (see Fig.3.6.). The host rock $\delta^{18}O$ values and the meteoric water $\delta^{18}O$ values both have a mean value of –5‰ and therefore, $\delta^{18}O$ cannot be used to determine the degree of water-rock interaction.

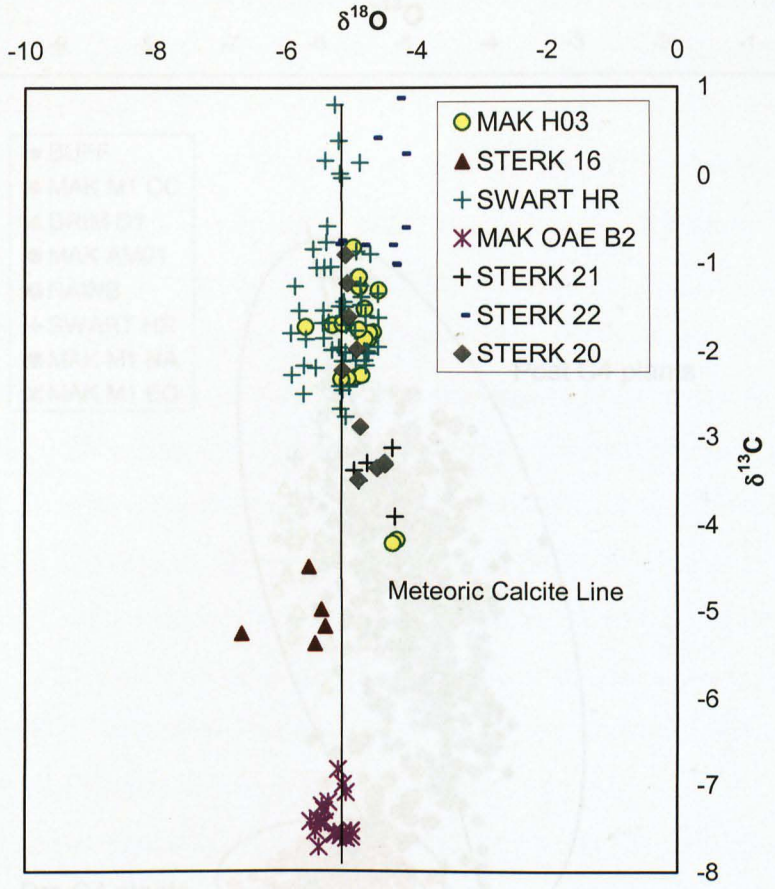

Figure 3.6. Cross-Plot of $\delta^{18}O$ and $\delta^{13}C$ in secondary calcite speleothem. The invariable $\delta^{18}O$ values and highly variable $\delta^{13}C$ values is typical of the Meteroic Calcite Line (Lohmann, 1988).

The flowstone specimens composed of a mosaic of secondary calcite crystals (MAK H03, MAK H03, STERK 21, 22 & 20, MAK OAE B2 and SWART HR D4) all contain the standard $\delta^{18}O$ values of $-5 \pm 1‰$ but have heavy $\delta^{13}C$ values of 0 to $-3.5‰$ (with the exception of MAK OAE B2 with mean $\delta^{13}C$ of -7.7, see below for discussion). The heavy $\delta^{13}C$ values of the diagenetic calcites is either an indication of heavy $\delta^{13}C$ values in the primary aragonite that have been retained in the diagenetic calcite due to a relatively closed diagenetic system, or is a result of recrystallisation in a moderately open system in contact with groundwater/cave-pool water with a heavy $\delta^{13}C$ value due to host-rock interaction and CO_2 outgassing.

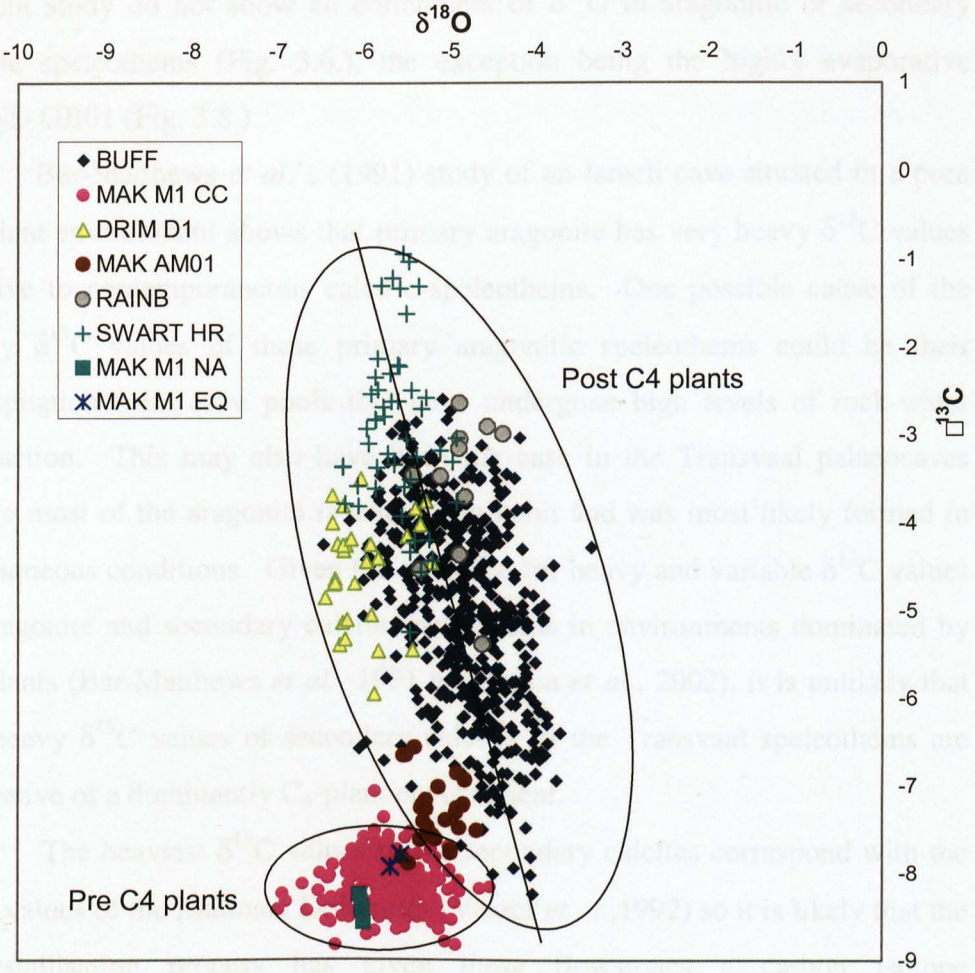

Figure 3.7. Cross-Plot of $\delta^{18}O$ and $\delta^{13}C$ in primary calcite flowstones. The flowstones are divided into two distinct groups based on the absence or presence of C4 plants at the time of speleothem formation (before ca. 4.5 Ma and after ca. 4.5 Ma respectively; see Section 3.8 and Chapters 5 and 7). Trend line in the post-C4 plant group differs from the Meteoric Calcite Line of Fig. 3.6.

The $\delta^{13}C$ equilibrium separation factor between aragonite and calcite is 1.7 ± 0.4‰ and is independent of temperature between 10 and 40°C (Romanek *et al.*, 1992). Bar-Matthews *et al.* (1991), Frisia *et al.* (2002) and Figure 3.3.b all show that the enrichment between aragonite and calcite layers can exceed this separation factor, indicating that other processes are contributing to the $\delta^{13}C$ enrichment of aragonitic speleothems. Frisia *et al.* (2002) show that $\delta^{13}C$ enrichment in aragonite is accompanied by $\delta^{18}O$ enrichment, indicating that kinetic processes such as prolonged degassing or evaporation were involved in precipitation of these speleothems and that this may have contributed to the

enriched $\delta^{13}C$ aragonite values. However, Bar-Matthews *et al.* (1991) and the present study do not show an enrichment of $\delta^{18}O$ in aragonitic or secondary calcite speleothems (Fig. 3.6.), the exception being the highly evaporative GOND GB01 (Fig. 3.8.).

Bar-Matthews *et al.*'s (1991) study of an Israeli cave situated in a pure C_3-plant environment shows that primary aragonite has very heavy $\delta^{13}C$ values relative to contemporaneous calcitic speleothems. One possible cause of the heavy $\delta^{13}C$ values of these primary aragonitic speleothems could be their precipitation from cave pools that have undergone high levels of rock-water interaction. This may also have been the case in the Transvaal palaeocaves where most of the aragonite is acicular in habit and was most likely formed in sub-aqueous conditions. Given the evidence for heavy and variable $\delta^{13}C$ values in aragonite and secondary calcite speleothems in environments dominated by C_3-plants (Bar-Matthews *et al.*, 1991 and Frisia *et al.*, 2002), it is unlikely that the heavy $\delta^{13}C$ values of secondary calcites in the Transvaal speleothems are indicative of a dominantly C_4-plant environment.

The heaviest $\delta^{13}C$ values of the secondary calcites correspond with the $\delta^{13}C$ values of the Malmani Dolomites (Veizer *et al.*,1992) so it is likely that the recrystallisation process has given these flowstones a carbon isotope composition that largely corresponds to a host-rock signal. It is likely that the trend towards host-rock $\delta^{13}C$ values in the secondary calcites is due to interaction with a fluid that had undergone a considerable amount of water-rock interaction, during the precipitation of primary aragonite or during the recrystallisation process or both.

3.10.4. Rapid Out-gassing of CO_2 – Gondolin

The Gondolin flowstone (GOND GB01) shows unusually heavy oxygen and carbon carbonate isotope values with a positive correlation (see Fig. 3.8.) that can only be attributed to rapid out-gassing of CO_2. This is the only case in the studied speleothems in which the $\delta^{18}O$ values deviate from the standard $-5 \pm 1‰$ and the $\delta^{13}C$ values are significantly heavier than the host-rock mean of $-1‰$. $\delta^{13}C$ values as high as $+5‰$ are unusual in speleothems and would usually be associated with speleothem formation in a environment lacking vegetation

cover (Dreybrodt, 1982), in which atmospheric CO_2 is the principal source of carbon. However, the high proportion of organic matter within GOND GB01 indicates that there was considerable vegetation cover in the vicinity of the cave. The gradient of the $\delta^{18}O/\delta^{13}C$ correlation is $\delta^{18}O = 0.44\ \delta^{13}C$ (Fig. 3.8.) which corresponds to experimental and measured instances of rapid outgassing of CO_2 (Fantidis and Ehhalt, 1970).

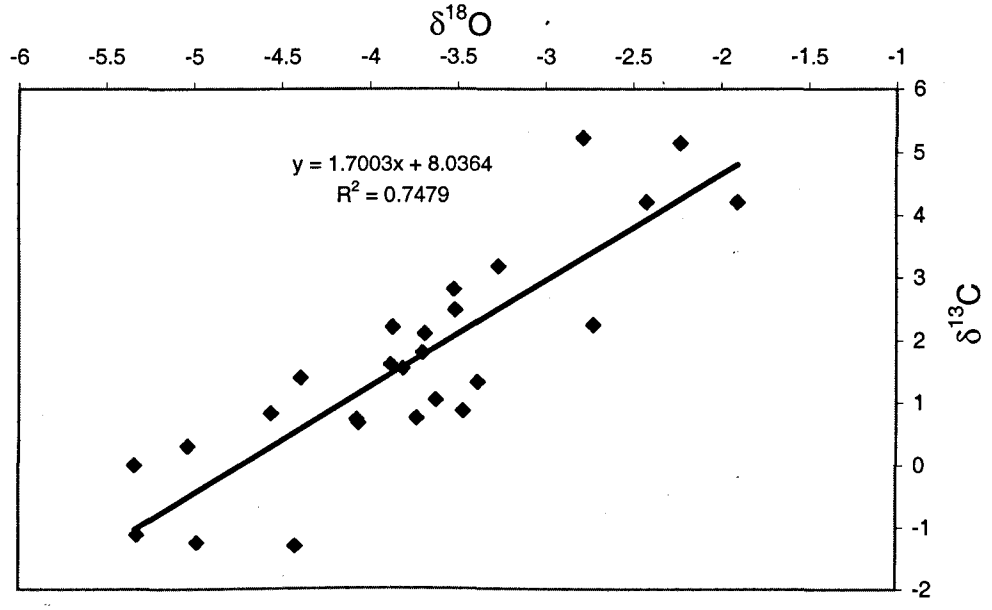

Figure 3.8. Heavy $\delta^{13}C$ and $\delta^{18}O$ values in a flowstone from Gondolin indicating rapid out-gassing of CO_2 during precipitation. The positive correlation between $\delta^{13}C$ and $\delta^{18}O$ corresponds to measured and experimental instances of rapid outgassing of CO_2 (Fantidis and Ehhalt, 1970).

3.11. Conclusions

Diagenetic flowstones dominate the South African Plio-Pleistocene hominin sites, to a degree previously unrecorded in any late Pleistocene speleothems. Secondary calcite can occur in layers of a few cm thickness, interbedded with primary calcite or in massive beds of >1m thickness. The different speleo-fabrics are formed in contrasting cave environments and can vary in their stable isotope and trace element composition. Some indication of the degree of diagenesis can be determined in hand-specimen from features such as crystal size and orientation (e.g. the difference between columnar and equant crystals of calcite). However, to distinguish between primary microcrystalline calcite and

secondary equant calcite, it is necessary to study the flowstone in thin section. The secondary nature of a flowstone can be determined from Mg/Ca and Sr/Ca ratios which are Mg-poor and Sr-rich relative to primary calcite flowstones.

The distinction between secondary and primary calcite flowstones can also be inferred from carbon and oxygen isotopes, although there is a high degree of overlap between the two groups (see Figs. 3.6. and 3.7.). The secondary flowstones follow the meteoric water line of (Lohmann, 1988) and therefore can show highly variable $\delta^{13}C$ values ranging from –8 to +1‰. As the primary flowstones reflect the carbon isotope composition of their dominant carbon source, soil derived CO_2, the $\delta^{13}C$ values vary from –9 to –1‰ as determined by fluctuations in the C_3 / C_4 vegetation proportion of soil CO_2. Primary calcite flowstones are also likely to show a negative correlation between $\delta^{18}O$ and $\delta^{13}C$ due to the apparent climatic control on these two variables in this region (see Fig 3.7. and Chapter 5.). It is evident from the petrology and trace element and stable isotope geochemistry of the primary calcite flowstones that they have the potential to yield radiometric dates and palaeoenvironmental proxies for environmental change, such as carbon and oxygen isotope records of vegetation and temperature change.

3.12. References

Assereto, R., and Folk, R. L. (1979). Diagenetic fabrics of aragonite, calcite, and dolomite in an ancient peritidal-spelean environment: Triassic calcare rosso, Lombardia, Italy. *Journal of Sedimentary Petrology* **50,** 371-394.

Bar-Matthews, M., Matthews, A., and Ayalon, A. (1991). Environmental controls of speleothem mineralogy in a karstic dolomitic terrain (Soreq Cave, Israel). *Journal of Geology* **99,** 189-207.

Bar-Matthews, M., Ayalon, A., Kaufman, A., and Wasserburg, G. J. (1999). The Eastern Mediterranean paleoclimate as a reflection of regional events: Soreq cave Israel. *Earth and Planetary Science Letters* **166,** 85-95.

Brain, C. K. (1958). The Transvaal ape-man-bearing cave deposits. *Transvaal Museum Memoir* **11,** 131.

Brand, U., and Veizer, J. (1980). Chemical diagenesis of a multicomponent carbonate system - 1: trace elements. *Journal of Sedimentary Petrology* **50,** 1219-1236.

Broughton, P. L. (1983a). Lattice deformation and curvature in stalactitic carbonate. *International Journal of Speleology* **13,** 19-30.

Broughton, P. L. (1983b). Secondary origin of the radial fabric in stalactitic

carbonate. *International Journal of Speleology* **13,** 43-66.

Burton, E. A., and Walter, L. M. (1991). The effects of P_{CO2} and temperature on magnesium incorporation in calcite in seawater and $MgCl_2$-$CaCl_2$ solutions. *Geochemica et Cosmochimica Acta* **55,** 777-785.

Busenberg, E., and Plummer, L. N. (1982). The kinetics of dissolution of dolomite in CO_2-H_2O systems at 1.5 to 65°C and 0 to 1 atm P_{CO_2}. *American Journal of Science* **282,** 45-78.

Cabrol, P., and Coudray, J. (1982). Climatic fluctuations influence the genesis and diagenesis of carbonate speleothems in southwestern France. *National Speleological Society Bulletin* **44,** 112-117.

Coplen, T. B. (1995). Reporting of stable carbon, hydrogen, and oxygen isotopic abundances. *In* "Reference and intercomparison materials for stable isotopes of light elements." pp. 31-34. International Atomic Energy Agency, TECDOC.

Craig, H. (1957). Isotopic standards for carbon and oxygen and correction factors for mass-spectrometric analysis of carbon dioxide. *Geochemica et Cosmochimica Acta* **12,** 133-149.

Dart, R. A. (1948). The Makapansgat proto-human *Australopithecus prometheus*. *American Journal of Physical Anthropology* **6,** 259-281.

Dreybrodt, W. (1982). A possible mechanism for growth of calcite speleothems without participation of biogenic carbon dioxide. *Earth and Planetary Science Letters* **58,** 293-299.

Fairchild, I. J., Borsato, A., Tooth, A. F., Frisia, S., Hawkesworth, C. J., Huang, Y. M., McDermott, F., and Spiro, B. (2000). Controls on trace element (Sr-Mg) compositions of carbonate cave waters: implications for speleothem climatic records. *Chemical Geology* **166,** 255;269.

Fantidis, J., and Ehhalt, D. H. (1970). Variations of the carbon and oxygen isotopic composition in stalagmites and stalactites: evidence of non-equilibrium isotopic fractionation. *Earth and Planetary Science Letters* **10,** 136-144.

Finch, A. A., Shaw, P. A., Weedon, G., and Holmgren, K. (2001). Trace element variation in speleothem aragonite: potential for palaeoenvironmental reconstruction. *Earth and Planetary Science Letters* **186,** 255-267.

Fischbeck, R., and Muller, G. (1971). Monohydrocalcite, hydromagnesite, nesquehonite, dolomite, aragonite, and calcite in speleothems of the Frankische Schweiz, Western Germany. *Contributions to Mineralogy and Petrology* **33,** 87-92.

Folk, R. L. (1965). Some aspects of recrystallization in ancient limestones. *In* "Dolomitization and limestone diagenesis." (L. C. Pray, and R. C. Murray, Eds.), pp. 14-48. Economic Paleontologists and Mineralogists.

Folk, R. L., and Assereto, R. (1976). Comparative fabrics of length-slow and length-fast calcite and calcitized aragonite in a Holocene speleothem, Carlsbad Caverns, New Mexico. *Journal of Sedimentary Petrology* **46,** 486-496.

Frisia, S., Bini, A., and Quinif, Y. (1993). Morphologic, crystallographic and isotopic study of an ancient flowstone (Grotta di Cunturines, Dolomites) -implications for paleoenvironmental reconstructions. *Speleochronos* **5,** 3-18.

Frisia, S. (1996). Petrographic evidences of diagenesis in speleothems: some examples. *Speleochronos* **7,** 21-30.

Frisia, S., Borsato, A., Fairchild, I. J., and McDermott, F. (2000). Calcite fabrics, growth mechanisms, and environments of formation in speleothems from the Italian Alps and southwestern Ireland. *Journal of Sedimentary Research* **70,** 1183-1196.

Frisia, S., Borsato, A., Fairchild, I. J., McDermott, F., and Selmo, E. M. (2002). Aragonite-calcite relationships in speleothems (Grotte de Clamouse, France): environment, fabrics, and carbonate geochemistry. *Journal of Sedimentary Research* **72,** 687-699.

Gascoyne, M. (1992). Palaeoclimate determination from cave calcite deposits. *Quaternary Science Reviews* **11,** 609-632.

Genty, D., and Massault, M. (1997). Bomb C-14 recorded in laminated speleothems: Calculation of dead carbon proportion. *Radiocarbon* **39,** 33-48.

Goede, A., McCulloch, M., McDermott, F., and Hawkesworth, C. (1998). Aeolian contribution to strontium and strontium isotope variations in a Tasmanian speleothem. *Chemical Geology* **149,** 37-50.

González, L. A., Carpenter, S. J., and Lohmann, K. (1992). Inorganic calcite morphology: roles of fluid chemistry and fluid flow. *Journal of Sedimentary Petrology* **62,** 382-399.

González, L. A., Carpenter, S. J., and Lohmann, K. C (1993). Columnar calcite in speleothems: Reply. *Journal of Sedimentary Petrology* **63**: 553-556.

Hellstrom, J. C., and McCulloch, M. T. (2000). Multi-proxy constraints on the climatic significance of trace element records from a New Zealand speleothem. *Earth and Planetary Science Letters* **179,** 287-297.

Hendy, C. H. (1971). The isotopic geochemistry of speleothems- I. The calculation of the effects of different modes of formation on the isotopic composition of speleothems and their applicability as palaeoclimatic indicators. *Geochemica et Cosmochimica Acta* **35,** 801-824.

Herries, A. I. R. (2003). "Magnetostratigraphic seriation of South African hominin palaeocaves." Unpublished PhD thesis, University of Liverpool.

Herries, A. I. R., Reed, K., Latham, A. G., and Kuykendall, K. L. (in press). The age of the Buffalo palaeocave fossil locality, Makapansgat, South Africa as determined by faunal correlation and magnetostratigraphy. *Quaternary Science Reviews.*

Hill, C., and Forti, P. (1997). The calcite-aragonite problem. *In* "Cave minerals of the world." (C. Hill, and P. Forti, Eds.), pp. 237-239. National Speleological Society, Alabama.

Hill, C., and Forti, P. (1997). "Cave minerals of the world." National Speleological Society, Alabama.

Holmgren, K., Karlen, W., Lauritzen, S. E., Lee-Thorp, J. A., Partridge, T. C., Piketh, S., Repinski, P., Stevenson, C., Svanered, O., and Tyson, P. D. (1999). A 3000-year high-resolution stalagmite-based record of palaeoclimate for northeastern South Africa. *Holocene* **9,** 295; 309.

Holmgren, K., Lee-Thorp, J. A., Cooper, G. R. J., Lundblad, K., Partridge, T. C., Scott, L., Sithaldeen, R., Talma, A. S., and Tyson, P. D. (2003). Persistent millennial-scale climatic variability over the past 25,000 years in Southern Africa. *Quaternary Science Reviews* **22**: 2311-2326.

Huang, Y., and Fairchild, I. J. (2001). Partitioning of Sr^{2+} and Mg^{2+} into calcite under karst -analogue experimental conditions. *Geochimica et Cosmochimica Acta* **65,** 47-62.

Huang, Y., Fairchild, I. J., Borsato, A., Frisia, S., Cassidy, N. J., McDermott, F., and Hawkesworth, C. J. (2001). Seasonal variations in Sr, Mg and P in modern speleothems (Grotta di Ernesto, Italy). *Chemical Geology* **175,** 429-448.

Jones, B., and Kahle, C. F. (1986). Dendritic calcite crystals formed by calcification of algal filaments in a vadose environment. *Journal of Sedimentary Petrology* **56,** 217-227.

Jones, B., and MacDonald, R. W. (1989). Micro-organisms and crystal fabrics in cave pisoliths from Grand Cayman, British West Indies. *Journal of Sedimentary Petrology* **59,** 387-396.

Jones, C. E., Halliday, A. N., and Lohmann, K. C. (1995). The impact of diagenesis on high-precision U-Pb dating of ancient carbonates: An example from the Late Permian of New Mexico. *Earth and Planetary Science Letters* **134,** 409-423.

Katz, A. (1973). The interaction of magnesium with calcite during crystal growth at 25-90°C and 1 atmosphere. *Geochimica et Cosmochimica Acta* **37,** 1563-1586.

Kendall, A. C., and Broughton, P. L. (1978). Origin of fabrics in speleothems composed of columnar calcite crystals. *Journal of Sedimentary Petrology* **48,** 519-538.

Kendall, A. C. (1993). Columnar calcite in speleothems - discussion. *Journal of Sedimentary Petrology* **63,** 550-552.

Keyser, A. W., Menter, C. G., Moggi-Cecchi, J., Pickering, T. R., and Berger, L. R. (2000). Drimolen: a new hominid-bearing site in Gauteng, South Africa. *South African Journal of Science* **96,** 193-197.

Kinsman, D. J. J., and Holland, H. D. (1969). The co-precipitation of cations with $CaCO_3$-IV. The co-precipitation of Sr^{2+} with aragonite between 16° and 96°C. *Geochemica et Cosmochimica Acta* **33,** 1-17.

Kuykendall, K. L., Toich, C. A., and McKee, J. K. (1995). Preliminary analysis of the fauna from Buffalo cave, northern transvaal, South Africa. *Palaeontologia Africana* **32,** 27-31.

Latham, A. G., Herries, A., Quinney, P., Sinclair, A., and Kuykendall, K. (1999). The Makapansgat Australopithecine site from a speleological perspective. In, Pollard, A. M. (ed.) Geoarchaeology: exploration, environments, resources. *Geological Society of London, Special Publications* **165,** 61-77.

Latham, A. G., Herries, A., and Kuykendall, K. (2003). The formation and sedimentary infilling of the Limeworks cave, Makapansgat, South Africa. *Palaeontologia Africana* **39**: 69-82.

Lohmann, K. C. (1988). Geochemical patterns of meteoric diagenetic systems and their application to studies of paleokarst. *In* "Paleokarst." (N. P. James, and P. W. Choquette, Eds.), pp. 58-81. Springer-Verlag, New York.

Lorens, R. B. (1981). Sr, Cd, Mn and Co distribution coefficients in calcite as a function of calcite precipitation rate. *Geochimica et Cosmochimica Acta* **45,** 553-561.

Mackenzie, F. T., Bischoff, W. D., Bishop, F. C., Loijens, M., Schoonmaker, J., and Wollast, R. (1983). Magnesian calcites: low temperature occurrence, solubility, and solid-solution behavior. *In* "Carbonates: Mineralogy and Chemistry." (R. J. Reeder, Ed.), pp. 97-144.

Marker, M. E. (1981). Aspects of the geology of two contrasted South African karst areas. *Transactions of the British Cave Research Association* **8,** 43-51.

McDermott, F., Frisia, S., Huang, Y. M., Longinelli, A., Spiro, B., Heaton, T. H. E., Hawkesworth, C. J., Borsato, A., Keppens, E., Fairchild, I. J., van der Borg, K., Verheyden, S., and Selmo, E. (1999). Holocene climate variability in Europe: Evidence from $\delta^{18}O$, textural and extension-rate variations in three speleothems. *Quaternary Science Reviews* **18,** 1021-1038.

McFadden, P. L., Brock, A., and Partridge, T. C. (1979). Palaeomagnetism and the age of the Makapansgat hominid site. *Earth and Planetary Science Letters* **44,** 373-382.

McKee, J. K., Thackeray, J. F., and Berger, L. R. (1995). Faunal assemblage seriation of southern African Pliocene and Pleistocene fossil deposits. *American Journal of Physical Anthropology* **96,** 235-250.

Menter, C. G., Kuykendall, K. L., Keyser, A. W., and Conroy, G. C. (1999). First record of hominid teeth from the Plio-Pleistocene site of Gondolin, South Africa. *Journal of Human Evolution* **37,** 299-307.

Moore, G. W. (1956). Aragonite speleothems as indicators of paleotemperature. *American Journal of Science* **254,** 746-753.

Mucci, A., and Morse, J. W. (1983). The incorporation of Mg^{2+} and Sr^{2+} into calcite overgrowths: influences of growth rate and solution composition. *Geochimica et Cosmochimica Acta* **47,** 217-233.

Oomori, T., Kaneshima, H., Maezato, Y., and Kitano, Y. (1987). Distribution coefficient of Mg^{2+} ions between calcite and solution at 10-50°C. *Marine Chemistry* **20**: 327-336

Partridge, T. C. (1979). Re-appraisal of lithostratigraphy of Makapansgat Limeworks hominid site. *Nature* **279,** 484-488.

Partridge, T. C. (2000). Hominid-bearing cave and tufa deposits. *In* "The Cenozoic of Southern Africa." (T. C. Partridge, and R. R. Maud, Eds.), pp. 100-130. Oxford University Press, Oxford.

Partridge, T. C., Latham, A. G., and Heslop, D. (2000). Appendix on magnetostratigraphy of Makapansgat, Sterkfontein, Taung and Swartkrans. *In* "The Cenozoic of Southern Africa." (T. C. Partridge, and R. R. Maud, Eds.), pp. 126-129. Oxford University Press, Oxford.

Pingitore, N. E. (1976). Vadose and phreatic diagenesis: processes, products and their recognition in corals. *Journal of Sedimentary Petrology* **46,** 985-1006.

Pingitore, N. E. J. (1982). The role of diffusion during carbonate diagenesis. *Journal of Sedimentary Petrology* **52,** 27-39.

Pingitore, N. E. J., and Eastman, M. P. (1986). The coprecipitation of Sr^{2+} with calcite at 25°C and 1 atmosphere. *Geochimica et Cosmochimica Acta* **50,** 2195-2203.

Railsback, L. B., Brook, G. A., Chen, J., Kalin, R., and Fleisher, C. J. (1994). Environmental controls on the petrology of a late Holocene speleothem from Botswana with annual layers of aragonite and calcite. *Journal of Sedimentary Research Section A-Sedimentary Petrology and Processes* **64,** 147-155.

Railsback, L. B., Sheen, S.-W., Rafter, M. A., Brook, G. A., and Kelloes, C. (1997). Diagenetic replacement of aragonite by aragonite in

speleothems: criteria for its recognition from Botswana and Madagascar. *Speleochronos* **8,** 3-11.

Repinski, P., Holmgren, K., Lauritzen, S. E., and Lee-Thorp, J. A. (1999). A late Holocene climate record from a stalagmite, Cold Air Cave, Northern Province, South Africa. *Palaeogeography, Palaeoclimatology, Palaeoecology* **150,** 269-277.

Richards, D. A., Bottrell, S. H., Cliff, R. A., Strohle, K., and Rowe, P. J. (1998). U-Pb dating of a speleothem of Quaternary age. *Geochimica et Cosmochimica Acta* **62,** 3683-3688.

Roberts, M. S., Smart, P. L., and Baker, A. (1998). Annual trace element variations in a Holocene speleothem. *Earth and Planetary Science Letters* **154,** 237-246.

Romanek, C. S., Grossman, E. L., and Morse, J. W. (1992). Carbon isotopic fractionation in synthetic aragonite and calcite: effects of temperature and precipitation rate. *Geochemica et Cosmochimica Acta* **56,** 419-430.

Schrenk, F. (1984). "New approaches to taphonomy and geology at the Makapansgat Limeworks hominid site, Transvaal, South Africa." Unpublished MSc thesis, University of the Witwatersrand.

Sibley, D. F., and Gregg, J. M. (1987). Classification of dolomite rock textures. *Journal of Sedimentary Petrology* **57,** 967-975.

Stevenson, C., Lee-Thorp, J. A., and Holmgren, K. (1999). A 3000-year isotopic record from a stalagmite in Cold Air Cave, Makapansgat Valley, Northern Province. *South African Journal of Science* **95,** 46-48.

Talma, A. S., Vogel, J. C., and Partridge, T. C. (1974). Isotopic contents of some Transvaal speleothems and their palaeoclimatic significance. *South African Journal of Science* **70,** 135-140.

Tobias, P. V. (2000). The fossil hominids. *In* "The Cenozoic of Southern Africa." (T. C. Partridge, and R. R. Maud, Eds.). Oxford University Press, Oxford.

Veizer, J., Clayton, R. N., and Hinton, R. W. (1992). Geochemistry of Precambrian carbonates: IV. Early Paleoproterozoic (2.25+-0.25Ga) seawater. *Geochemica et Cosmochimica Acta* **56,** 875-885.

Verheyden, S., Keppens, E., Fairchild, I. J., McDermott, F., and Weis, D. (2000). Mg, Sr and Sr isotope geochemistry of a Belgian Holocene speleothem: implications for paleoclimate reconstructions. *Chemical Geology* **169,** 131-144.

Chapter 4. Using $\delta^{13}C$ values of co-occurring organic matter and carbonate in South African Plio-Pleistocene Speleothems to model host-rock and palaeovegetation contributions.

4.1. Abstract

Organic carbon in two South African Plio-Pleistocene speleothems (Buffalo Cave flowstone and Collapsed Cone flowstone) has been identified using luminescence spectrophotometry. The early Pleistocene Buffalo Cave flowstone is rich in humic acids whereas the late Miocene/early Pliocene Collapsed Cone flowstone is rich in fulvic acids. The $\delta^{13}C$ value of the humic and fulvic fractions has been measured and used to model the host-rock contribution to the $\delta^{13}C$ value of co-occurring speleothem carbonate. Growth layer and duplicate analyses of the carbonate $\delta^{13}C$ and $\delta^{18}O$ indicate isotopic equilibrium precipitation of the flowstone carbonate, and Mg/Ca ratios suggest that $\delta^{13}C$ values are not controlled by variations in prior calcite precipitation or host-rock proportion. Results of the modelling indicate a high (ca. 50%) mean host-rock contribution, consistent with the high degree of soil productivity and dissolution expected in the Plio-Pleistocene South African cave sites. Using the modelled host-rock contribution, the $\delta^{13}C$ values of the speleothem carbonate provide an estimate of the proportion of C_4 plants in the local palaeoenvironment. This indicates that the Collapsed Cone flowstone was precipitated in an environment containing only C_3 vegetation, whereas the Buffalo Cave flowstone was formed in an environment of mixed C_3 and C_4 vegetation, ranging from 30% to 80% C_4 grasses.

4.2. Introduction

The formation of meteoric carbonate precipitates (including speleothems, palaeosols, calcretes) is so closely linked to biological production of CO_2 in the soil zone, that many studies of these deposits have used stable isotopes as indicators of vegetation change. C_4 vegetation (predominantly savannah grasses) is enriched in ^{13}C relative to C_3 vegetation (trees, shrubs, bushes and temperate

grasses), and this isotopic enrichment is preserved within meteoric carbonates. The carbon isotopic composition of meteoric carbonate can be used as an indicator of the carbon isotope composition of CO_2 derived from plant respiration and soil organic matter decomposition, and can therefore be used to estimate the proportion of C_3 vegetation and C_4 vegetation in past ecosystems. This technique has been successfully applied to palaeosol carbonates formed in geological terrains lacking carbonate rocks (Cerling and Hay, 1986; Cerling *et al.*, 1989) but has proved problematic in speleothem carbonate (Baker *et al.*, 1997). Secondary carbonate in karst environments is precipitated with an unknown proportion of carbon derived from the dissolution of the carbonate host-rock. The host-rock $\delta^{13}C$ values are usually heavy (marine limestone values are approximately 0‰) and therefore variation in the proportion of inorganic carbon incorporated in the speleothem will lead to enriched and variable $\delta^{13}C$ values of speleothem carbonate (Baker *et al.*, 1997) that have no relationship with the proportion of C_4 vegetation in the local environment.

Therefore, if $\delta^{13}C$ values of speleothems are to be used as indicators of palaeovegetation, then an assessment of the host-rock contribution to a particular speleothem is necessary. In the Holocene, host-rock contributions have been determined from ^{14}C activity measurements in U/Th dated speleothems (Genty and Massault, 1997 and 1999; Genty *et al.*, 1998 and 2001). This is possible because the carbonate host-rock is generally so old as to have a negligible ^{14}C activity, so that an increased proportion of host-rock derived carbon will increase the ^{14}C age estimate. Therefore, the discrepancy between ^{14}C and U/Th age estimates can be used as an estimate of the proportion of "dead carbon" derived from the carbonate host-rock. The dead carbon proportion (dcp) provides an approximate percentage of the host-rock contribution to the $\delta^{13}C$ of the speleothem carbonate (Genty and Massault, 1997 and 1999; Genty *et al.*, 1998 and 2001), and by inference, proportion of soil derived CO_2 contributing to the $\delta^{13}C$ value of a speleothem. The typical dcp in speleothems calculated by this method is between 10% and 20%, and can exceed 30% (see references in Genty and Massault, 1997; Genty *et al.*, 2001). The dcp is unlikely to exceed 50%, the equilibrium state of the reaction of carbonic acid with calcium carbonate (Hendy, 1971). The dcp is theoretically linked to the dissolution intensity and reaction

time during the host-rock and groundwater interaction - the more intense and complete the dissolution reaction, the higher the dcp (Genty *et al.*, 2001). Factors that control carbonate dissolution include soil thickness, karst geology, vegetation type and density, temperature, amount of precipitation and, most importantly, soil pCO_2 (Genty and Massault, 1997; Egli and Fitze, 2001). These factors combine to produce site-specific dissolution intensities, which may in part explain the low intra-site dcp variation observed by Genty and Massault (1997) and Genty *et al.* (2001). Genty and Massault (1997) suggest that in European sites of similar climate and geology, a greater dcp can be attributed to the presence of forest conditions. This is because soil pCO_2 is higher in a forest soil than under grassland due to the greater levels of root respiration and microbial organic matter decomposition under forested conditions.

In speleothems older than the lower limit of radiocarbon dating (approximately 45 ka), an alternative method for estimating the host-rock proportion is necessary. This study models the host-rock proportion in ancient speleothems by comparing the $\delta^{13}C$ values of co-occurring speleothem organic matter and carbonate extracted from speleothem. Assuming that the $\delta^{13}C$ value of speleothem organic matter approximates the $\delta^{13}C$ value of palaeovegetation (Elkins, 2002), the dead-carbon proportion can be estimated based on existing models of speleothem carbonate precipitation (Genty and Massault, 1999). The dead-carbon proportion can then be used to interpret speleothem carbonate $\delta^{13}C$ values in terms of the approximate proportion of C_4 grasses in the local palaeoenvironment. In order to model the host-rock proportion, it is important to characterise the organic matter present and to demonstrate that the speleothem carbonate was precipitated in isotopic equilibrium with soil pCO_2.

4.3. Carbon isotopes in speleothem carbonate

The carbon isotopic composition of speleothem carbonate depends on the specific and complex nature of the geochemical processes associated with recharge and carbonate dissolution/precipitation in karstic areas. This process is here divided into three stages, following the models of Hendy (1971) and Genty *et al.* (2001). First, there is the initial equilibration of recharge water with a CO_2 reservoir,

derived from soil organic matter or from the atmosphere if the site lacks a soil cover. Second is the subsequent dissolution of the carbonate host-rock, which may occur under fully open or closed system conditions or under some intermediate state between these two end-member situations. Under fully open system conditions CO_2 saturation and isotopic equilibrium is maintained between downward-percolating recharge water and the overlying CO_2 reservoir, whereas under fully closed system conditions the recharge water is initially equilibrated with a CO_2 reservoir but is then isolated from it prior to carbonate dissolution. Finally, there are the set of processes associated with the deposition of secondary carbonate in the cave. Depending on the environmental conditions at the time of deposition (which are dynamic and can change significantly over the time scale of speleothem deposition at any single drip site), precipitation of calcium carbonate can occur under conditions of isotopic equilibrium or of isotopic dis-equilibrium. Kinetic fractionation in speleothems has been linked to the water flow rate, the rate of CO_2 outgassing and/or evaporation (Fornaca-Rinaldi *et al.*, 1968; Hendy and Wilson, 1968; Fantidis and Ehhalt, 1970; Hendy, 1971) and its presence can be identified by isotopic measurements along individual growth layers. A positive correlation between $\delta^{13}C$ and $\delta^{18}O$ sampled across a growth layer can indicate rapid outgassing of CO_2 and heavy $\delta^{18}O$ values can indicate evaporation prior to calcite precipitation. The test for isotopic equilibrium is more rigorous if duplicate isotopic sequences are taken (in the direction of speleothem growth) from either a series of stalagmites within one cave (e.g. Holmgren *et al.*, 1999; Ayalon *et al.*, 2002) or a series of stalagmites within a region (e.g. Bar-Matthews *et al.*, 2003). It is also possible to duplicate analyses within a single flowstone by sampling from different sections of the flowstone. If the same isotopic excursions are found within the duplicates, then more confidence can be attached to the interpretation of the data in terms of local or regional palaeoclimates.

The Dulinski and Rosanski (1990) semi-dynamic model of speleothem precipitation has highlighted the importance of chemical kinetics in controlling the $\delta^{13}C$ composition of speleothems. The model distinguishes two phases in the precipitation process; the initial outgassing of the solution until CO_3^{2+} supersaturation is reached, and the subsequent precipitation of $CaCO_3$ resulting from further outgassing. The results of the modelling suggest that the $\delta^{13}C$

composition of speleothems is dependant on the time that has elapsed since the degassing of CO_2 commenced, as prolonged degassing results in dissolved organic carbon enriched in ^{13}C. Dulinski and Rosanski (1990) show that ten minutes after the start of speleothem calcite precipitation in a pure C_3 vegetation environment, $\delta^{13}C$ can range between –8‰ and –2‰, depending on temperature and pCO_2 conditions. Baker *et al.* (1997) suggest that extensive prior CO_2 degassing is likely in karst aquifers, where many fissures may be air-filled. Under these conditions, "residual" calcite with elevated $\delta^{13}C$ is likely to be deposited within the cave voids. Hellstrom and McCulloch (2000) state that the prior precipitation of calcite, and other factors related to the precipitation process (such as the flow rate of water over a speleothem), can be identified by comparing trace element and $\delta^{13}C$ records. An increase in the amount of prior calcite precipitation will increase the concentration of a trace element in solution, provided the distribution coefficient is significantly less than unity. With the increase in speleothem $\delta^{13}C$ during prolonged periods of outgassing, Hellstrom and McCulloch (2000) predict that a positive correlation between $\delta^{13}C$ and selected trace element concentrations within a speleothem depth-series may be indicative of significant and variable prior calcite precipitation.

4.4. Organic Matter incorporation into Speleothems

Organic matter is flushed from the soil and plants during times of high runoff (Baker *et al.*, 1997) and transported into the saturated zone of groundwater or into streams and rivers by surface runoff. In regions with a highly seasonal rainfall, seasonal flushing of organic matter is responsible for annual bands of high and low organic matter concentration within speleothems (Baker *et al.*, 1993; Baker *et al.*, 1999; Shopov *et al.*, 1994).

Organic-rich waters will eventually pass through the soil and epikarst zone and enter a cave where the organic acids are co-precipitated or adsorbed onto the surfaces of the forming speleothems. Organic molecules are preferentially adsorbed onto the surface of a growing calcite crystal rather than being taken up as fluid inclusions (Ramseyer *et al.*, 1997). In most aquatic systems (pH in the range of 4-8) the organic acids dissociate and have a negative charge. The calcite

surface has a zero point charge of 9, which means that in virtually all aquatic systems the calcite surface has a net positive charge. Therefore, calcite is an effective adsorbent for dissolved organic materials in natural waters (McGarry and Baker, 2000).

Organic acids make up about 60-70% of the total organic carbon in soils and 40-60% of the dissolved organic carbon in natural waters (Senesi *et al.*, 1991) and they can be defined according to their solubility in water. Fulvic acids (FA) are hydrophilic, being soluble in water at all pHs, while humic acids (HA) are more hydrophobic, being insoluble in aqueous solutions with pH < 2 and humins are insoluble in water at any pH (McGarry and Baker, 2000). Solubility is related to molecular weight, on the basis of which organic acids may also be differentiated. FAs have a lower molecular weight than HA, ranging from 500 to 2000 D. Organic acids are formed as one of the many products of humification, the transformation of macro-morphologically identifiable organic compounds into amorphous humic compounds (Zech *et al.*, 1997).

Most studies of speleothem organic matter have been based on the excitation and emission wavelengths of organic acid fluorescence (Baker *et al.*, 1998, McGarry and Baker, 2000). Humic acids have higher wavelengths of fluorescence excitation and emission and lower fluorescence intensities than fulvic acids due to the presence of higher molecular weight fractions in humic acids and the greater degree of aromaticity and polycondensation in humic acids (Senesi *et al.*, 1991). This technique is applied to solid speleothem samples and can be used to identify the relative proportions of humic and fulvic acids in a thin (~1mm) portion of speleothem calcite (Baker *et al.*, 1998). Ramseyer *et al.* (1997) have demonstrated that both hydrophilic and hydrophobic organic acids can be extracted from speleothems by acid dissolution of the speleothem carbonate. Acid dissolution with a weak acid minimises hydrolysis of the organic matter, enabling the speleothem organic matter to be studied spectroscopically (Ramseyer *et al.*, 1997) and isotopically (Elkins, 2002).

Most carbon isotopic studies of soil organic matter in the sedimentary record assume that the organic matter is well mixed and unaltered, representing the mean isotopic composition of the local biomass. Based on this assumption, variations in measured $\delta^{13}C$ values are often interpreted as changes in the mean

value of palaeovegetation (e.g. Krishnamurthy *et al.*, 1982; Guillet *et al.*, 1988; Ambrose and Sikes, 1991). However, Powers and Schlesinger (2002) show that an increase in $\delta^{13}C$ values is often observed with increasing depth in soil profiles from purely C_3 environments. Below depths of 20 cm, $\delta^{13}C$ values of soil organic matter can vary by up to 5.8‰ (Elheringer *et al.*, 2000; Powers and Schlesinger, 2002). Elheringer *et al.* (2000) suggest that $\delta^{13}C$ variations in soil organic matter may be related to the proportion of microbial and fungal carbon within the soil zone, as these organisms are enriched in $\delta^{13}C$ values relative to their substrate. Therefore, as the microbial and fungi derived components of soil organic matter increase with time, it is expected that the residual soil organic matter will become ^{13}C enriched as a result.

4.5. Soil organic matter and soil respiration –independent carbon pools

If the carbon isotopic composition of speleothem organic matter and carbonate are to be compared, then the carbon dynamics of organic and inorganic carbon in the soil zone must be considered. Specifically, it is important to assess the length of time that carbon species spend in the soil zone (turnover time) prior to their incorporation into speleothems as either organic carbon or as dissolved inorganic carbon.

Soil CO_2 is derived both from plant root respiration and from the microbial decomposition of organic matter (heterotrophic respiration). The CO_2 sourced from root respiration has a negligible turnover time, whereas CO_2 sourced from the decomposition of organic matter can have a turnover time ranging from months to 10s of years, depending of the organic fractions present and the local climatic conditions (Ehleringer *et al.*, 2000; Trumbore, 2000). Consumption of the most easily decomposable compounds (the labile component) occurs rapidly over periods of a few years (e.g. Bernoux *et al.*, 1998; Trumbore, 2000) and in combination with respired CO_2 gives soil CO_2 a typical age of between 1 and 30 years (Trumbore, 2000). In the case of tropical soils, the fast turnover of labile organic matter results in soil respiration dominated by carbon fixed less than 1 year ago (Trumbore, 2000). As soil CO_2 is well mixed by diffusion processes (Cerling *et al.*, 1989) its $\delta^{13}C$ value is expected to be an average of the $\delta^{13}C$

composition of the local biomass, with a small enrichment due to exchange with atmospheric CO_2. The transport of dissolved inorganic carbon species through the soil and into the karst aquifer will occur during periods of high rainfall. Therefore, depending on the rainfall regime and the residence time in the karst aquifer prior to entrance into the cave chamber, speleothem carbonate will usually contain soil-derived carbon that was fixed by photosynthesis less than a few years beforehand.

In contrast to the carbon of speleothem carbonate, the humic and fulvic acids that contribute to speleothem organic matter belong to the stable organic pool with long turnover times. Difficult to metabolise polymers such as hemiscelluloses, suberins, waxes and lignin (the stable component) contribute to the soil humus and constitute approximately 85% of the organic matter of a mineral soil (Schonwitz *et al.*, 1986). A third component, the refractory organic fraction, is composed of non-hydrolysable organic matter and can exhibit a very low turnover rate in excess of 8000 years (Poirier *et al.*, 2002).

Estimates of the turnover time of humic acids in the top 30 cm of soil in European temperate soils are 33 years (Lichtfouse *et al.*, 1995) and 10 years (Spaccini *et al.*, 2000). The turnover rate of humic and fulvic fractions in tropical ecosystems are less well known. Humid tropical and sub-tropical forest soils typically have a high turnover of soil organic matter due to intense biological activity which tends to result in a high concentration of low molecular weight organic matter (fulvic acids) in the soil (Dabin, 1982 in Almendros *et al.*, 2003; Chen and Chiu, 2000). The insolubility of humic acids in highly acidic forest soils also contributes to the dominance of fulvic acids at deeper levels in the soil (Chen and Chiu, 2000).

In a Botswanan savannah ecosystem, Almendros *et al.* (2003) show a much lower proportion of organic matter in the soil than in tropical forest soils, and a consistently greater proportion (up to 4 times) of humic acids than fulvic acids. Only a small amount of soil organic matter accumulates, but these carbon and nitrogen forms represent quite stable pools. Almendros *et al.* (2003) do not determine the age of the organic matter in the Botswanan savannah soils, but refractory organic matter in a Congolese savannah soil has been ^{14}C dated to approximately 8300 years (Poirier *et al.*, 2002). Almendros *et al.* (2003) suggest that the high temperatures, seasonality and susceptibility to fires of the tropical

climate are partly responsible for the low biodegradability of the humic material in tropical savannah soils.

It is evident from the luminescence of organic acid banding in speleothems (Baker *et al.*, 1993 and Shopov *et al.*, 1994), that organic acid incorporation into speleothems can occur in sub-annual bands. Although both the speleothem organic acids and speleothem carbonate are formed on sub-annual timescales, the two different sources of organic carbon can have vastly different turnover times. For example, Wassenaar *et al.* (1991) show that in a Canadian shallow groundwater system, dissolved organic carbon has a mean age of 3700 years old. This difference in carbon turnover time has been cited as a possible explanation for the lack of correspondence between the carbon isotopic composition of co-occurring organic matter and carbonate in some speleothems (Elkins, 2002). While carbon isotopic composition of soil CO_2 will respond to a hypothetical vegetational change within a few years, the humic and fulvic acid fractions may take centuries or millennia to respond to the change.

4.6. Locality and Materials

Two flowstone sequences were collected from the Makapansgat Valley in the Limpopo Province, South Africa (see Fig. 4.1. and Appendix 1.). The Collapsed Cone flowstone belongs to the basal flowstone boss (Latham *et al.*, 2003) from Member 1b (Partridge, 2000) of the Makapansgat Limeworks, dated to approximately 4 Ma using magnetostratigraphy (Herries, 2003). The Buffalo Cave flowstone, dated to approximately 1.2-1.8 Ma (Herries, 2003) is the basal flowstone unit of the Buffalo Cave sequence. Both flowstone sequences are continuous, largely free of detrital sediment and composed of columnar calcite crystals (see Chapter 3).

4.7. Methods

4.7.1. Fluorescence Spectrophotometry

Fluorescence wavelength measurements were undertaken on polished blocks of flowstone by scanning the sample with a Perkin-Elmer UV spectrophotometer at a spatial resolution of 0.5 mm. Scans were taken from representative portions of

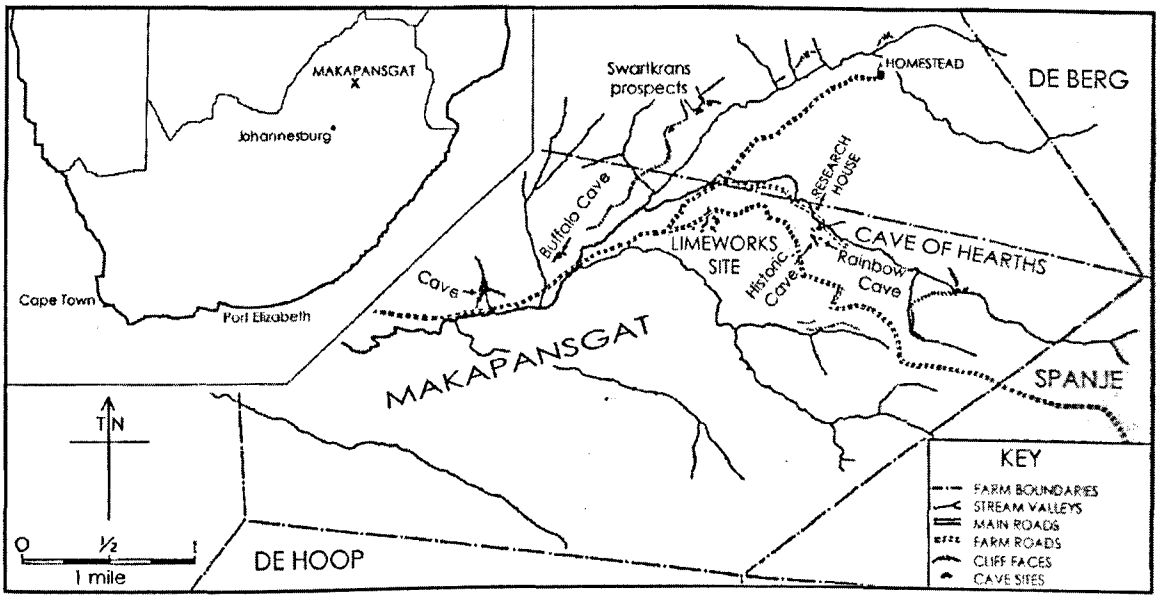

Figure 4.1. Map of the Makapansgat Valley, Limpopo Province, north-eastern South Africa. Includes the palaeo-karst localities sampled in this study, the Makapansgat Limeworks and Buffalo Cave (from Maguire, 1998).

each flowstone; 51 separate scans from the Collapsed Cone flowstone and 34 scans from the Buffalo Cave flowstone. The fluorescence properties of each scan were represented in the form of an excitation-emission-matrix (EEM) spectra in which fluorescence intensity is a function of excitation wavelength on one axis and emission wavelength on the other (Baker *et al.*, 1998; McGarry and Baker, 2000). The maximum intensity of an excitation-emission pair was recorded for each fluorescence centre.

4.7.2. Stable Isotopes in Speleothem Carbonate method

Samples for speleothem carbonate stable isotope analysis were removed from the flowstone using a diamond-tipped micro-drill. Samples were taken from the top, middle and bottom of each sample block used in the organic carbon method. This enabled direct comparison of the carbonate and organic carbon data. A series of eight carbonate samples were also taken along an individual growth layer of the Buffalo Cave and Collapsed Cone flowstone to test for isotopic equilibrium precipitation. In the case of the Buffalo Cave flowstone, the test for isotopic equilibrium was extended by taking duplicate stable isotopes profiles from two short depth-series along the growth axis of the flowstone. Depth-series A consists

of two series of 32 samples taken at 5mm intervals along the growth axis of the flowstone. The two duplicate profiles (BUFF W and X) are taken from the same level in the flowstone sequence (64 cm to 79.5 cm from the top of the sequence) and separated by a horizontal distance of 50 cm. Depth-series B was also sampled at 5 mm intervals and consists of two profiles of 36 samples (BUFF Y and Z) taken from between 216.5 cm and 234 cm from the top of the flowstone sequence, and separated by a horizontal distance of 73 cm.

For stable isotope analysis, the powdered samples were pre-treated in an oxygen plasma asher to remove organic matter. The samples were then reacted to completion at 90°C with 100% phosphoric acid using an automated VG Isocarb preparation system. The CO_2 released by the reaction was cryogenically purified prior to the measurement of carbon and oxygen isotope ratios on an automated VG SIRA 12 mass spectrometer at the University of Liverpool. All data were corrected for ^{17}O effects following Craig (1957). Carbon and oxygen isotope data are reported in conventional delta (δ) notation in "parts per mil" (‰) relative to V-PDB (Coplen, 1995). Accuracy and reproducibility of the isotopic analyses was assessed by replicate analysis of BCS2 (internal calcite standard) against NBS-19 and two internal calcite standards. Long-term laboratory reproducibility is better than 0.1‰ for both isotope ratios.

4.7.3. Mg/Ca ratio of Speleothem Carbonate

A depth-series of $\delta^{18}O$, $\delta^{13}C$ and Mg/Ca was obtained in order to determine if host-rock dissolution or prior calcite precipitation (as indicated by the Mg/Ca ratio) had any influence on $\delta^{13}C$ carbonate values. The depth-series consisted of 77 samples taken at intervals of 1.5 cm between 63.5 cm and 177.5 cm from the top of the flowstone sequence. Each drilled sample was divided into separate aliquots for stable isotope and trace element analysis. Approximately 5 mg of powdered sample was dissolved in dilute nitric acid and analysed for Ca, Mg and Sr on a Perkin Elmer Optima 3300RL inductively coupled plasma atomic emission spectrometer (ICP-AES) at the NERC facility at Royal Holloway, University of London. Analytical precision was determined using an internal speleothem standard. Reproducibility (2σ) of 1000 Mg/Ca and 1000 Sr/Ca molar ratios is ±0.65 and ±0.002 respectively.

4.7.4. Extraction and $\delta^{13}C$ analysis of organic compounds

5-15g of clean flowstone (approximately 1cm in vertical thickness) was crushed into small pieces in a pestle and mortar and added to a clean beaker containing 100 ml of 2M HCl. The samples were continuously stirred and more acid (4-6M HCl) was added until the reaction had ceased. Another 10 ml of 2M HCl was added to ensure all the carbonate had dissolved. The samples were allowed to outgas overnight and were then heated to 40°C in a water bath for one hour to remove excess dissolved CO_2.

The samples were separated based on the nature of the organic matter. Acid insoluble organic matter (e.g. humic acids) formed colloidal particles that settled to the bottom of the beaker and could be removed from the solution by centrifugation. Samples were centrifuged for 10 mins at 4000 rpm. Samples containing acid soluble organic matter (e.g. fulvic acids) produced no insoluble residue and could not be analysed using conventional methods, so they were subjected to wet oxidation using the persulfate wet oxidation method which converts dissolved organic compounds to CO_2 by chemical decomposition (Dafner *et al.*, 1999; Peltzer *et al.*, 1996). The isotopic composition of dissolved organic carbon was measured using a modified OI Analytical wet oxidation TOC analyser coupled with a continuous flow Finnigan MAT Delta Plus mass spectrometer at the University of Ottawa, Canada (St-Jean, 2003). Samples were calibrated against NBS 21 graphite and IAEA CH-6 sucrose international standards. Reproducibility of an internal humic acid standard (2σ) was ±0.25‰. Analytic precision (σ) of dissolved organic carbon is approximately ±0.5‰.

Samples that produced an insoluble residue (humic fraction) after centrifugation were rinsed twice with 2M HCL to remove dissolved salts and then freeze-dried. Carbon dioxide for carbon isotope ratio measurement was obtained by combusting the humic fraction with Cu(II)O and silver wire (to remove SO_2) in quartz tubes at 850°C for 2 hours. The resultant CO_2 was separated cryogenically and carbon isotope ratios were measured on an automated VG SIRA 12 mass spectrometer at the University of Liverpool. Accuracy and reproducibility were determined by replicate analysis of USGS 24 graphite standard and an internal humic acid standard. Long-term reproducibility (σ) of

USGS 24 was better than 0.06‰. Analytical precision of the internal humic acid standard (σ) was ±0.25‰, indicating that the carbonate dissolution and organic acid extraction procedure reduces the precision of the $\delta^{13}C$ measurements, perhaps due to partial hydrolysis of the organic matter.

4.8. Results and Interpretation

4.8.1. Fluorescence Photospectrometry

The Buffalo Cave flowstone and Collapsed Cone flowstone have fluorescence centres with mutually exclusive excitation and emission wavelengths. Each Buffalo Cave sample studied using this technique had peak fluorescence intensities at excitation wavelengths ranging from 382 to 392nm and emission wavelengths ranging from 453 to 470nm (Fig. 4.2.a). In contrast, the Collapsed Cone samples had peak fluorescence intensities at excitation wavelengths of 283-340nm and emission wavelengths of 381-409nm (Fig. 4.2.b). The shorter excitation and emission wavelengths of the Collapsed Cone flowstone are indicative of smaller molecules such as fulvic acids whereas the longer fluorescence wavelengths of the Buffalo Cave flowstone is indicative of larger molecules such as humic acids (Senesi *et al.*, 1991; Baker *et al.*, 1998).

The fluorescence photospectrometric data is consistent with the colour of the speleothems to the naked eye. The Buffalo Cave flowstone has a dark to light brown colour due to its humic acid inclusions, whereas the Collapsed Cone flowstone is pure white because the wavelength of luminescence of its fulvic acid inclusions is shorter than visible light. It is likely that the colour difference between the two flowstones is a function of the chemistry of their organic content.

4.8.2. Speleothem Organic Carbon $\delta^{13}C$

Buffalo Cave flowstone organic matter $\delta^{13}C$ values ranged from -27.3 to -21.1 with a mean value of -23.7, n = 27 (see Table 4.1.). Collapsed Cone flowstone organic matter $\delta^{13}C$ ranged from –31.6 to –25.5 with a mean value of -28.8, n = 7 (see Table 4.1.). C_3 plants (trees, shrubs and temperate grasses) have $\delta^{13}C$ values

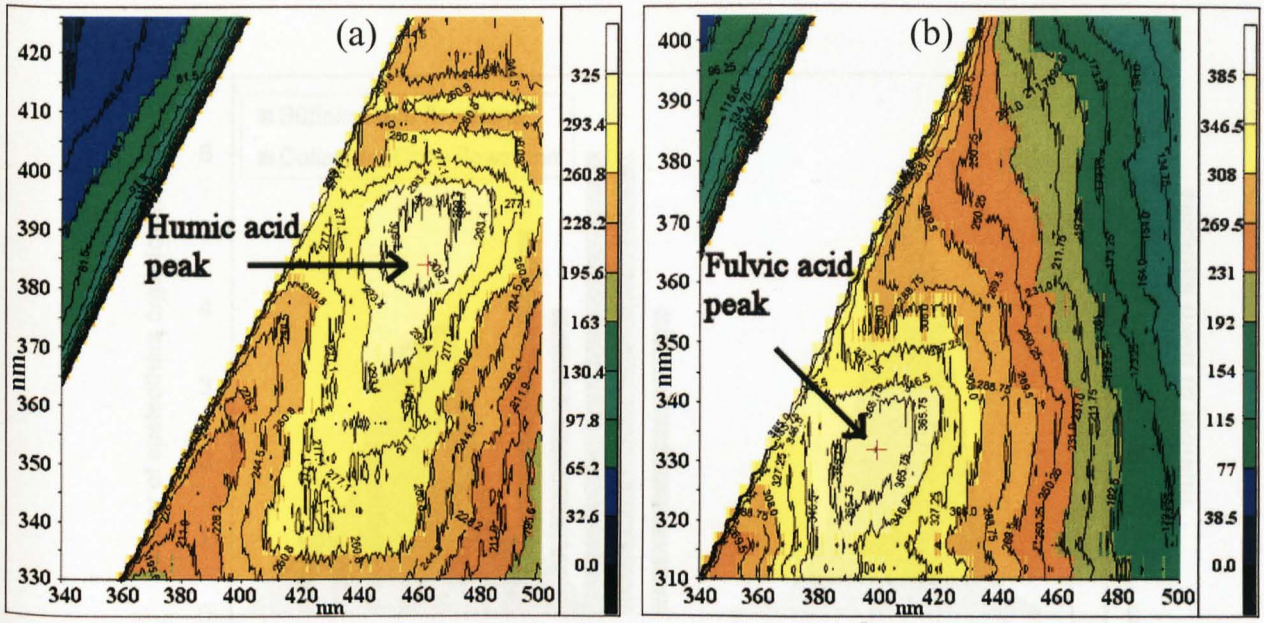

Figure 4.2. Typical Excitation-Emission Matrix (EEM) fluorescence spectra from (a) Buffalo Cave flowstone and (b) Collapsed Cone flowstone showing the presence of humic acids in the former and fulvic acids in the latter (see Section 4.8.1.).

in the range of –25 to –35‰, with a mean of ca. –28‰ (O'Leary, 1981 and 1988) whereas the C_4 plants (savannah grasses) typically vary between –16 and –10‰ with a mean of approximately 14‰ (Deines, 1980 and O'leary, 1988). As shown in Figure 4.3., the Collapsed Cone $\delta^{13}C$ organic matter values lie entirely within the range of modern day C_3 vegetation (Vogel *et al.*, 1978; O'Leary, 1981). It is likely that the observed variation in $\delta^{13}C$ of organic matter in the Collapsed Cone flowstone is indicative of the natural $\delta^{13}C$ variation of C_3 vegetation within the soil-zone (see Section 4.4.), although it is possible that the most enriched $\delta^{13}C$ values indicate a very small proportion of C_4 grasses within the local biomass (Fig. 4.3.). The Buffalo Cave flowstone organic matter $\delta^{13}C$ values are intermediate between the C_3 and C_4 vegetation end-members (Fig. 4.3.).

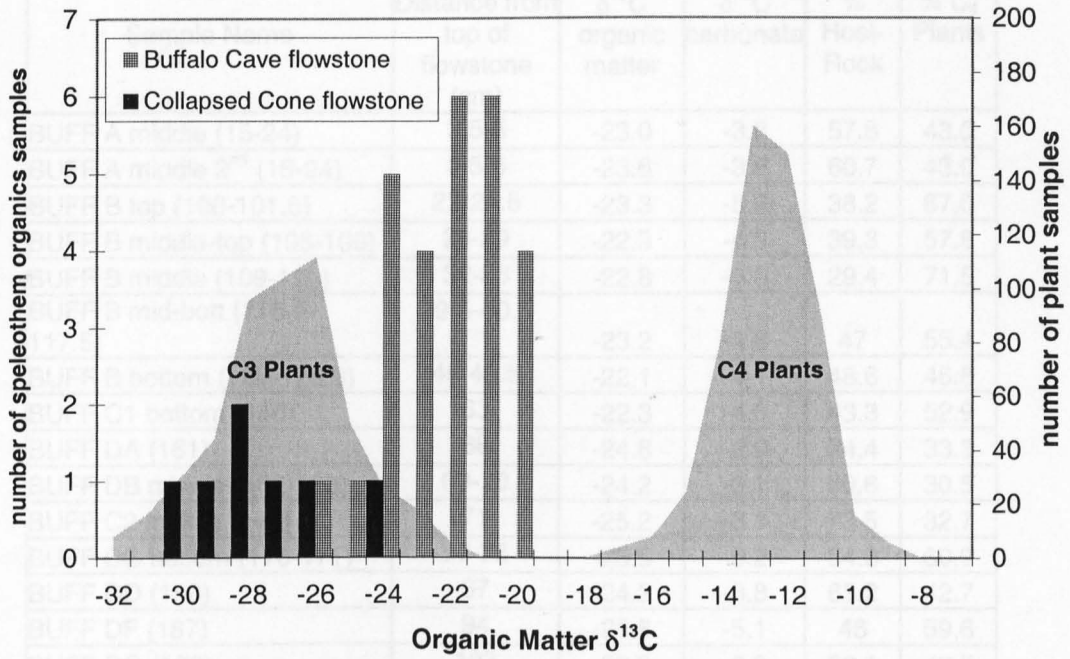

Figure 4.3. Frequency distribution of $\delta^{13}C$ for speleothem organic matter compared with C_3 and C_4 plant end-members. C_3 and C_4 plant distributions are a combination of data from Vogel *et al.* (1978), Deines (1980) and O'Leary (1988). The Collapsed Cone flowstone has a predominantly C_3 plant isotopic signal whereas the Buffalo Cone flowstone has a mixed C_3 and C_4 plant signal. This can be compared with the results of modelling the palaeovegetation signal within speleothem carbonate, as shown in Figure 4.9.

Low $\delta^{13}C$ values (< -30‰) are typical for C_3 forest plants that are affected by canopy or irradiance effects (Farquhar *et al.*, 1989). This suggests that the more depleted $\delta^{13}C$ values of the Collapsed Cone flowstone organic matter may be indicative of a closed or forested environment. However, $\delta^{13}C$ values of organic matter are known to vary depending on the organic fraction analysed (e.g.Rieley *et al.*, 1991; Freeman and Colarusso, 2001). Therefore, if the 1.2‰ depletion of humic and fulvic acids relative to total soil organic matter (Lichtfouse *et al.*, 1995a and b) is accounted for, the estimated mean $\delta^{13}C$ value of bulk soil organic matter is –27.6, close to mean C_3 vegetation $\delta^{13}C$ value of –28‰ (O'Leary, 1988).

Sample Name	Distance from top of flowstone (cm)	$\delta^{13}C$ organic matter	$\delta^{13}C$ carbonate	% Host-Rock	% C_4 Plants
BUFF A middle (15-24)	3.5-5	-23.0	-3.8	57.8	43.0
BUFF A middle 2nd (15-24)	3.5-5	-23.6	-3.8	60.7	43.0
BUFF B top (100-101.5)	23-24.5	-23.3	-5.6	38.2	67.0
BUFF B middle-top (105-106)	28-29	-22.3	-4.9	39.3	57.8
BUFF B middle (109-110)	32-33	-22.8	-6.0	29.4	71.5
BUFF B mid-bott (116.5-117.5)	39.5-40.5	-23.2	-4.8	47	55.4
BUFF B bottom (122-123.5)	45-46.5	-22.1	-4.1	48.6	46.8
BUFF C1 bottom (140)	63	-22.3	-4.6	43.3	52.9
BUFF DA (161)	68	-24.8	-2.9	74.4	33.3
BUFF DB middle (162-163)	69-70	-24.2	-3.1	70.6	30.5
BUFF C2 middle (148)	71	-25.2	-3.1	73.5	32.7
BUFF DC bottom (170-171)	77-78	-25.5	-5.2	54.6	60.9
BUFF DD (180)	87	-24.2	-3.8	63.2	42.7
BUFF DF (187)	94	-23.6	-5.1	46	59.6
BUFF DG (196)	103	-22.9	-3.9	56.1	43.5
BUFF DG (200.5-201)	107.5-108	-23.7	-4.4	54.4	50.5
BUFF E (225)	132	-21.8	-4.4	42.1	50.2
BUFF E (232)	139	-22.9	-5.9	31.5	70.8
BUFF E (234)	141	-27.3	-4.6	65.9	53.1
BUFF F (243)	150	-21.4	-3.5	52.2	74.1
BUFF F (256)	163	-25.1	-6.3	42.2	39.3
BUFF F (260)	167	-24.0	-6.7	31	76.7
BUFF F2 bottom (264)	171	-21.1	-6.2	7.2	81.4
BUFF H (J)(269.5-271)	176.5-178	-26.0	-6.7	43.3	81.7
BUFF K (286-287)	193-194	-25.3	-5.3	52.8	62.3
BUFF N1 (312.5-313.5)	200.5-201.5	-21.6	-4.1	44.8	46.8
BUFF N4 (344.5-345.5)	232.5-233.5	-25.8	-6.6	43.1	79.3
Coll Cone A1middle (41)	1	-25.5	-7.8	30.4	96.1
Coll Cone B block (99.5-101.5)	59.5-61.5	-29.1	-8.5	43	105.9
Coll Cone C2 2/2 (131)	91	-31.6	-8.0	54.4	98.4
Coll Cone C3 (156)	116	-29.1	-8.1	45.8	99.6
Coll Cone E4 middle	~160	-27.1	-7.8	39.4	96.6
Coll Cone F bottom	~180	-30.0	-8.4	47	103.9
Coll Cone G3 top	~200	-28.8	-8.2	43.9	101.6

Table 4.1. $\delta^{13}C$ values of co-occurring speleothem carbonate and organic matter for the Buffalo Cave and Collapsed Cone flowstones and the modelled host-rock contribution to $\delta^{13}C$ speleothem carbonate for each pair of samples. The variability of % Host-Rock values is attributed to the inherent variability of soil organic matter $\delta^{13}C$ and to its long turnover time (as discussed in Sections 4.4, 4.5). The % C_4 plants values are determined from the $\delta^{13}C$ carbonate values using the mean modelled host-rock proportion of 47% (as discussed in Section 4.9.; see Figs. 4.8, 4.9) and the known C_3 and C_4 plant $\delta^{13}C$ end-members (O'leary, 1989).

4.8.3. Speleothem Carbonate $\delta^{13}C$

Speleothem carbonate $\delta^{13}C$ shows mutually exclusive values in the Buffalo Cave flowstone (range: -2.7 to –7.5, mean = -4.7, n = 172) and the Collapsed Cone flowstone (range: -7.8 to –8.5, mean = -8.1, n = 7) as shown in Figs. 4.4. to 4.7. and Table 4.1. The growth layer tests (Fig. 4.4.) show low levels of isotopic variation along growth layers. The $\delta^{13}C$ and $\delta^{18}O$ values for the nine samples from the Collapsed Cone growth layer vary by 0.3‰ and 0.2‰ respectively, and the eight samples from the Buffalo Cave growth layer vary by 0.5‰ and 0.8‰ respectively. The two duplicate depth series carbonate analyses from Buffalo Cave (Fig. 4.5.) show strong agreement between the duplicated series, despite the lateral displacement of up to 73cms. Depth-series A is unusual in containing localised layers rich in phosphatic minerals (derived from bat guano), detrital sediment and small scale unconformable layers, in one of the duplicate series (BUFF X) whereas the other depth series (BUFF W) consists of the usual horizontally layered columnar calcite. The difference in the two speleothem fabrics is greatest in the bottom third of the depth series (74 to 79.5 cm from the top of the flowstone), and this is where the isotopic composition of the two records is seen to diverge (Fig. 4.5.a). Despite this divergence in the two records, there is a good agreement in the general trend of the two records indicating that the gross climatic signal is preserved despite the petrological differences. Depth-series B shows a very strong agreement between the duplicate isotopic records (Fig. 4.5.b). This indicates that the flowstone carbonate was precipitated under isotopic equilibrium conditions (Fig. 4.4.) and demonstrates that almost identical isotopic values are preserved over a horizontal distance of 73 cm in the direction of water flow (Fig. 4.5.).

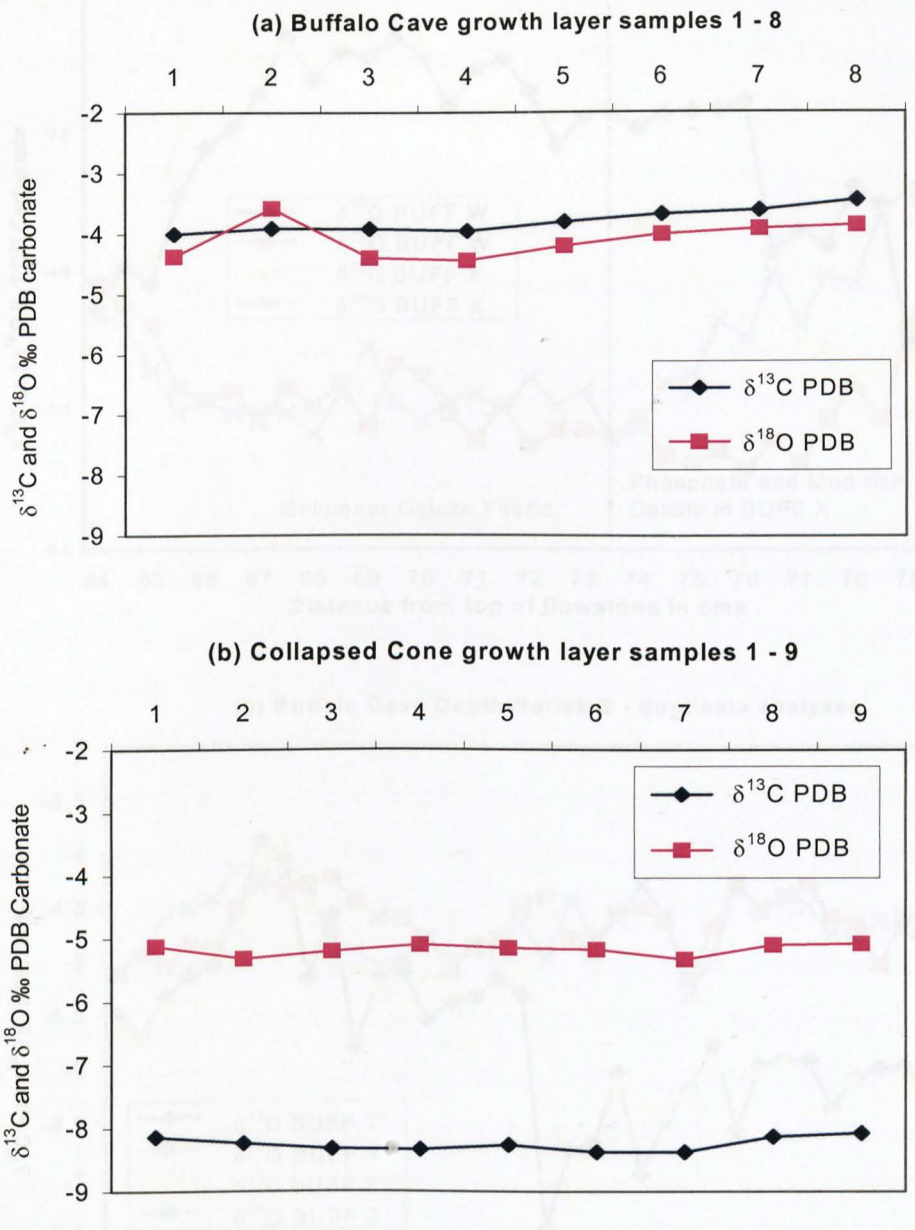

Figure 4.4. Growth layer tests for isotopic equilibrium precipitation of speleothem carbonate (Hendy and Wilson, 1986). (a) Buffalo Cave flowstone (b) Collapsed Cone flowstone. Samples taken at intervals of approximately 1cm.

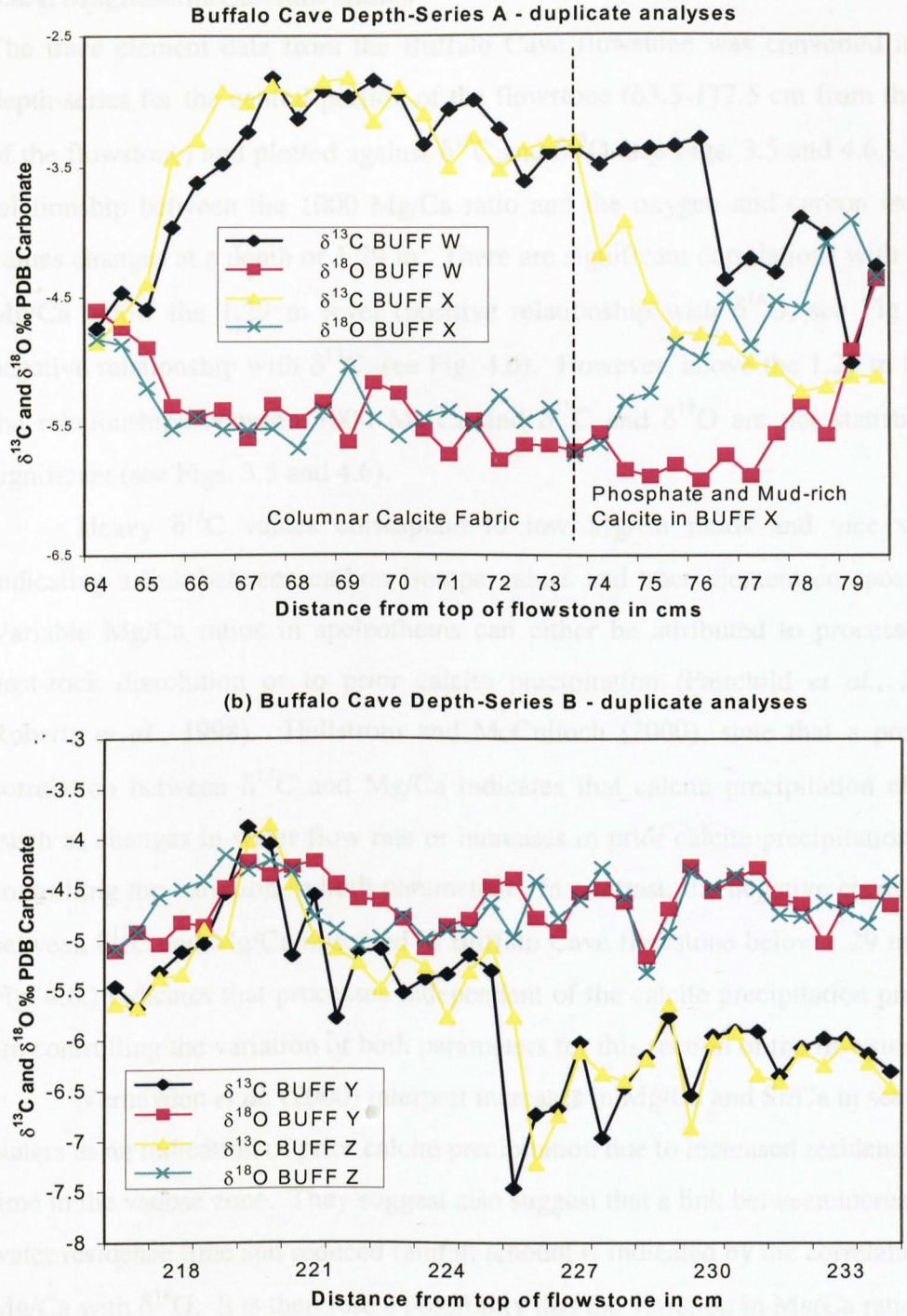

Figure 4.5. Duplicate stable isotope depth series from the Buffalo Cave flowstone as indicators of isotopic equilibrium precipitation. (a) The duplicate series of depth-series A were sampled from between 64 cm and 79 cm below the top of the flowstone and they are 50 cm apart horizontally. BUFF W consists of samples BUFF 140-156 and BUFF X consists of samples BUFF 156.5-172.5. (b) The duplicate series of depth-series B were sampled from between 216.5 cm and 234 cm below the top of the flowstone and they are 73 cm apart horizontally. BUFF Y consists of samples BUFF 290.5-308 and BUFF Z consists of samples BUFF 309.5-327.

4.8.4. Magnesium/Calcium Ratios

The trace element data from the Buffalo Cave flowstone was converted into a depth-series for the central portion of the flowstone (63.5-177.5 cm from the top of the flowstone) and plotted against $\delta^{13}C$ and $\delta^{18}O$ (see Figs. 3.5 and 4.6.). The relationship between the 1000 Mg/Ca ratio and the oxygen and carbon isotope values changes at a depth of 1.29 m. There are significant correlations with 1000 Mg/Ca below the 1.29 m level (positive relationship with $\delta^{18}O$, see Fig. 3.5; negative relationship with $\delta^{13}C$, see Fig. 4.6). However, above the 1.29 m level, the relationships between 1000 Mg/Ca and $\delta^{13}C$ and $\delta^{18}O$ are not statistically significant (see Figs. 3.5 and 4.6).

Heavy $\delta^{13}C$ values correspond to low Mg/Ca ratios and vice versa, indicating a link between carbon isotope values and trace element composition. Variable Mg/Ca ratios in speleothems can either be attributed to processes of host-rock dissolution or to prior calcite precipitation (Fairchild *et al.*, 2000; Roberts *et al.*, 1998). Hellstrom and McCulloch (2000), state that a positive correlation between $\delta^{13}C$ and Mg/Ca indicates that calcite precipitation effects (such as changes in water flow rate or increases in prior calcite precipitation) are controlling the variation in both parameters. In contrast, the negative correlation between $\delta^{13}C$ and Mg/Ca observed in Buffalo Cave flowstone below 1.29 m (see Fig. 4.6.) indicates that processes independent of the calcite precipitation process are controlling the variation of both parameters for this section of the flowstone.

Verheyden *et al.* (2000) interpret increases in Mg/Ca and Sr/Ca in seepage waters as an indication of prior calcite precipitation due to increased residence time in the vadose zone. They suggest also suggest that a link between increased water residence time and reduced rainfall amount is indicated by the correlation of Mg/Ca with $\delta^{18}O$. It is therefore a possibility that the variation in Mg/Ca ratios in the Buffalo Cave flowstone and its positive correlation with $\delta^{18}O$ below the 1.29 m level (Fig. 3.5) is a function of rainfall amount. As there are currently uncertainties regarding the relative magnitude of temperature and precipitation-amount variations on the magnitude and polarity of $\delta^{18}O$ variations in the Buffalo Cave flowstone (see Chapter 5), the relationship between $\delta^{18}O$ and Mg/Ca cannot yet be fully understood. If the climatic change represented by the $\delta^{18}O$ variation is controlling the variation in the Mg/Ca ratio, then the climatically controlled

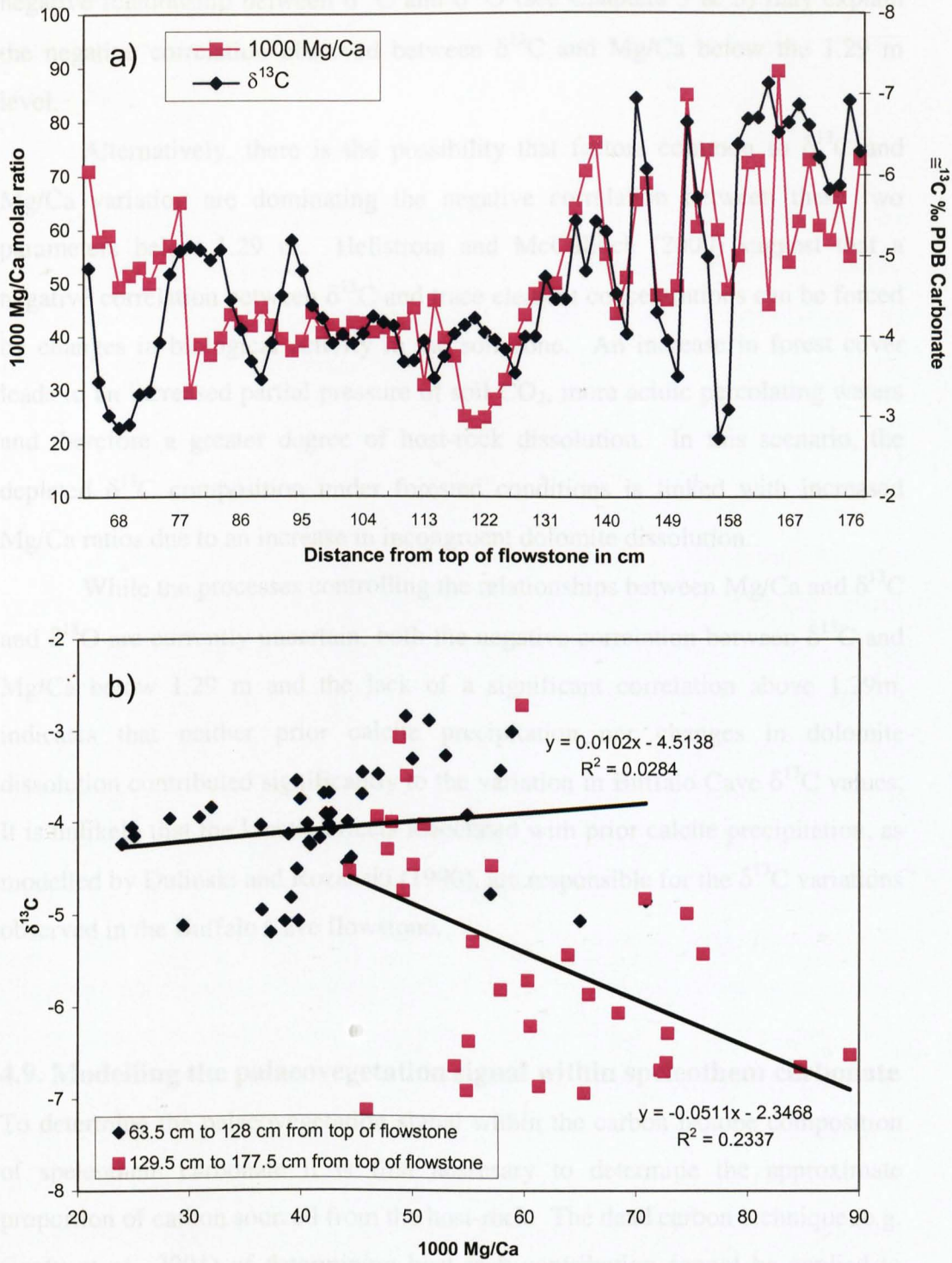

Figure. 4.6. Buffalo Cave flowstone Mg/Ca and $\delta^{13}C$ depth-series and cross-plot. **a)** Note that the $\delta^{13}C$ carbonate axis has been reversed to aid visualisation of the relationship between the two series. There is a negative correlation between $\delta^{13}C$ and Mg/Ca below 1.29 m and a weak positive correlation above 1.29 m. The lack of a significant positive correlation indicates that prior calcite precipitation was not a principal cause of $\delta^{13}C$ or Mg/Ca variation. **b)** There is a change in the relationship between $\delta^{13}C$ and Mg/Ca above and below 1.29 m. $\delta^{13}C$ values are on average lower below the 1.29 m level, as discussed in Chapter 5 (see Fig. 5.3.) See Fig. 3.5 for comparison with the $\delta^{18}O$ versus Mg/Ca relationship.

negative relationship between $\delta^{13}C$ and $\delta^{18}O$ (see Chapters 3 & 5) may explain the negative correlation observed between $\delta^{13}C$ and Mg/Ca below the 1.29 m level.

Alternatively, there is the possibility that factors common to $\delta^{13}C$ and Mg/Ca variation are dominating the negative correlation between these two parameters below 1.29 m. Hellstrom and McCulloch (2000) suggest that a negative correlation between $\delta^{13}C$ and trace element concentrations can be forced by changes in biological activity in the soil zone. An increase in forest cover leads to an increased partial pressure of soil CO_2, more acidic percolating waters and therefore a greater degree of host-rock dissolution. In this scenario, the depleted $\delta^{13}C$ composition under forested conditions is linked with increased Mg/Ca ratios due to an increase in incongruent dolomite dissolution.

While the processes controlling the relationships between Mg/Ca and $\delta^{13}C$ and $\delta^{18}O$ are currently uncertain, both the negative correlation between $\delta^{13}C$ and Mg/Ca below 1.29 m and the lack of a significant correlation above 1.29m, indicates that neither prior calcite precipitation nor changes in dolomite dissolution contributed significantly to the variation in Buffalo Cave $\delta^{13}C$ values. It is unlikely that the kinetic effects associated with prior calcite precipitation, as modelled by Dulinski and Rozanski (1990), are responsible for the $\delta^{13}C$ variations observed in the Buffalo Cave flowstone.

4.9. Modelling the palaeovegetation signal within speleothem carbonate

To determine the palaeovegetation signal within the carbon isotope composition of speleothem carbonate it is first nessesary to determine the approximate proportion of carbon sourced from the host-rock. The dead carbon technique (e.g. Genty *et al.*, 2001) of determining host-rock contribution cannot be applied to speleothems older than the Late Pleistocene. The extraction and isotopic measurement of organic matter in speleothems (as developed by Elkins, 2002) offers a new approach to determining the proportion of host-rock and soil CO_2 derived carbon in older speleothems. If the $\delta^{13}C$ value of organic matter in speleothems approximates the true value of palaeovegetation, then the following model enables the $\delta^{13}C$ value of speleothem carbonate to be corrected for the host

rock contribution. The model of the carbon isotope geochemistry of speleothem formation used here is based on Genty *et al.* (2001) and modified for the purposes of this study.

4.9.1. Modelling the relationship between speleothem organic matter and palaeovegetation

The relationship between the carbon isotopic composition of organic matter preserved in a speleothem and the carbon isotopic composition of palaeovegetation can be represented by:

$$\delta^{13}C_{palaeo\text{-}veg} = \delta^{13}C_{organics} + F_{org\text{-}toc} \quad (1)$$

where, *organics* refers to speleothem organic matter; *palaeo-veg* to past vegetation in the local cave environment; and *Forg-toc* to the fractionation factor between the organic fraction measured in the speleothem and total soil organic carbon. $F_{org\text{-}toc}$ is given a value of 1.2, as the humic and fulvic acid fractions have approximately 1.2‰ lower $\delta^{13}C$ values relative to bulk organic carbon (Lichtfouse *et al.* 1995a and b). This isotopic fractionation is either a function of the formation of the organic fractions or is due to isotopically distinct molecular components or both (Lichtfouse *et al.*, 1995b).

The $\delta^{13}C$ value of sedimentary organic matter is largely resistant to diagenetic alteration and is widely used to determine the proportion of C_3 and C_4 plants in past ecosystems (e.g. Beerling, 1997; Freeman and Colarusso, 2001; Ficken *et al.*, 2002). For the $\delta^{13}C_{organics}$ values measured to correspond to the $\delta^{13}C$ value of vegetation growing at the time of speleothem precipitation, the turnover time of the soil organic matter must be shorter than the period over which gross vegetational changes occur. The incremental growth of speleothems occurs sub-annually (e.g. Baker *et al.*, 1993), minimising the effects of time-averaging of environmental signals preserved within speleothem carbonate. In contrast, the turnover time of humic and fulvic acids can range from 10s of years to 1000s of years depending on the climate and soil chemistry (Paul and Clark, 1989). Almendros *et al.* (2003) show that soil organic matter from Botswanan savannahs (analogous to the South African savannah soils) are unusually resistant to biodegradation. This is also indicated by organic matter in a Congolese savannah

soil that has been dated to approximately 8300 years (Poirier *et al.*, 2002). Therefore, the presence of ancient humic and fulvic acid fractions in the soil may lead to $\delta^{13}C_{organics}$ values that are neither representative of the $\delta^{13}C$ value of vegetation nor of $\delta^{13}C_g$. The possibility of high turnover times of $\delta^{13}C_{organics}$ must be taken into account when interpreting the results of this model.

4.9.2. Modelling the distribution of carbon isotopes from vegetation to DIC

The microbial decomposition of plant matter in the soil releases CO_2 into the soil atmosphere with a $\delta^{13}C$ value that is essentially the same as the $\delta^{13}C$ value of the decaying vegetation (Reardon *et al.*, 1979; Dörr and Münnich, 1980; Cerling *et al.*, 1984; Schönwitz, 1986). The partial pressure of CO_2 (pCO_2) in a soil is typically an order of magnitude greater than atmospheric pCO_2, so diffusion will occur between the two reservoirs of CO_2. The $\delta^{13}C$ value of atmospheric CO_2 (approx. -6.5‰ in the early twentieth century; Fung *et al.*, 1997) is greater than the $\delta^{13}C$ value of vegetation, which results in isotopic exchange between these two reservoirs. Because of their different masses, $^{12}CO_2$ and $^{13}CO_2$ have different diffusion coefficients, leading to a predictable enrichment of the $\delta^{13}C$ value of soil CO_2, given known atmospheric and soil pCO_2 values. The combined result of this isotopic exchange and diffusive loss of $^{12}CO_2$ is a $\delta^{13}C$ enrichment of between 3‰ and 7‰ in soil CO_2 relative to soil organic matter, with a value of 4‰ being the typical observed and modelled value (Cerling, 1984; Dörr and Münnich, 1980; Genty *et al.*, 2001). Due to the greater pCO_2 of the soil atmosphere, only under poorly developed soils will the $\delta^{13}C$ value of atmospheric CO_2 contribute significantly to the isotopic composition of soil CO_2 (Cerling, 1984).

Therefore, the carbon isotope composition of soil CO_2 is calculated with the following fractionation model:

$$\delta^{13}C_g = \delta^{13}C_{organics} + F_{org\text{-}toc} + F_{respired\text{-}soil}\ ‰\ PDB \qquad (2)$$

where *g* refers to gaseous soil CO_2; and $F_{respired\text{-}soil}$ to the $\delta^{13}C$ enrichment in soil CO_2 relative to respired CO_2 as a consequence of diffusion between soil CO_2 and

atmospheric CO_2. $D_{respired\text{-}soil}$ is given a value of 4‰ following the modelling and experimental data of Cerling (1984).

Soil CO_2 dissolution and bicarbonate formation in percolating cave waters can be modelled, given the likely case of isotopic equilibrium between the soil CO_2 and the dissolved inorganic carbon (Hendy, 1971 and Deines *et al.*, 1974). The $\delta^{13}C$ fractionation is given by (Mook *et al.*, 1974):

$$\delta^{13}C_{DIC0} = \delta^{13}C_g + (-9483 * T^{-1} + 23.89)\ ‰\ PDB \qquad (3)$$

where DIC0 refers to dissolved inorganic carbon prior to host-rock dissolution, *g* refers to soil CO_2 and *T* = temperature in °K. In the absence of palaeotemperature estimates for the South African Plio-Pleistocene, the modern day mean annual temperature at Makapansgat of 18°C has been used in the model.

4.9.3. Calculating host-rock contribution:

The isotopic composition of dissolved CO_2 after dilution with host-rock carbon and prior to calcite precipitation can be derived from the $\delta^{13}C$ value of the speleothem calcite and the fractionation factor of $CaCO_3$ precipitation in the cave (Mook, 1980):

$$\delta^{13}C_{DIC} = \delta^{13}C_{carbonate} - (-4232 * T^{-1} + 15.1)\ ‰\ PDB \qquad (4)$$

where *DIC* refers to dissolved organic carbon after host-rock dilution and *carbonate* refers to speleothem calcite. This equation assumes that there is negligible prior calcite precipitation by CO_2 degassing in voids or microfissures in the unsaturated zone above the cave and that speleothem precipitation has occurred under isotopic equilibrium conditions. The isotopic equilibrium precipitation of the Buffalo Cave and Collapsed Cone flowstones has been demonstrated using growth layer and duplication tests (see Figs. 4.3. and 4.4. and Section 4.8.3.). The negative correlation between Mg/Ca ratios and $\delta^{13}C$ values

in the Buffalo Cave flowstone show that prior calcite precipitation was not a principal control on $\delta^{13}C$ variation (see Fig. 4.5 and Section 4.7.4.)

The percentage of host-rock carbon contribution to the speleothem calcite $\delta^{13}C$ can therefore be calculated from the difference in $\delta^{13}C$ before and after host-rock dissolution:

$$\%_{host\text{-}rock} = 100 * (\delta^{13}C_{DIC} - \delta^{13}C_{DIC0})/(\delta^{13}C_{lst} - \delta^{13}C_{DIC0}) \% \quad (5)$$

where *lst* is the host-rock and *%host-rock* is the percentage of host-rock carbon contribution to the dissolved inorganic carbon and speleothem calcite. The value of -0.9‰ for $\delta^{13}C_{lst}$ used in this model is the mean $\delta^{13}C$ value of the Malmani dolomite host-rock (Veizer *et al.*, 1992).

4.9.4. The modelled Host-Rock proportions:

From the measured values of co-occurring δ13Ccarbonate and δ13Corganics, eqns (2-5) have provided an estimate of the percentage of host-rock carbon contribution to δ13Ccarbonate, assuming that diagenesis and soil turnover times of the organic matter are minimal. The % host-rock values for the Collapsed Cone flowstone range from 30.4% to 54.4% with a mean of 43.4 whereas the Buffalo Cave flowstone values range from 7.2% to 74.4% with a mean of 48.6% (see Table 4.1. and Fig. 4.7.). It is evident from these results that the estimates of host-rock proportion are either imprecise or highly variable.

4.9.5. Precision of the Host-Rock proportions:

There is no significant relationship ($r = 0.16$; $n = 27$) between $\delta^{13}C_{carbonate}$ and $\delta^{13}C_{organics}$ values within the Buffalo Cave flowstone sample and a weak relationship ($r = 0.48$; $n = 7$) within the Collapsed Cone flowstone, indicating that the former value is not a simple function of the latter (see Fig 4.7.). This discrepancy between the two values is indicative of either a highly variable host-

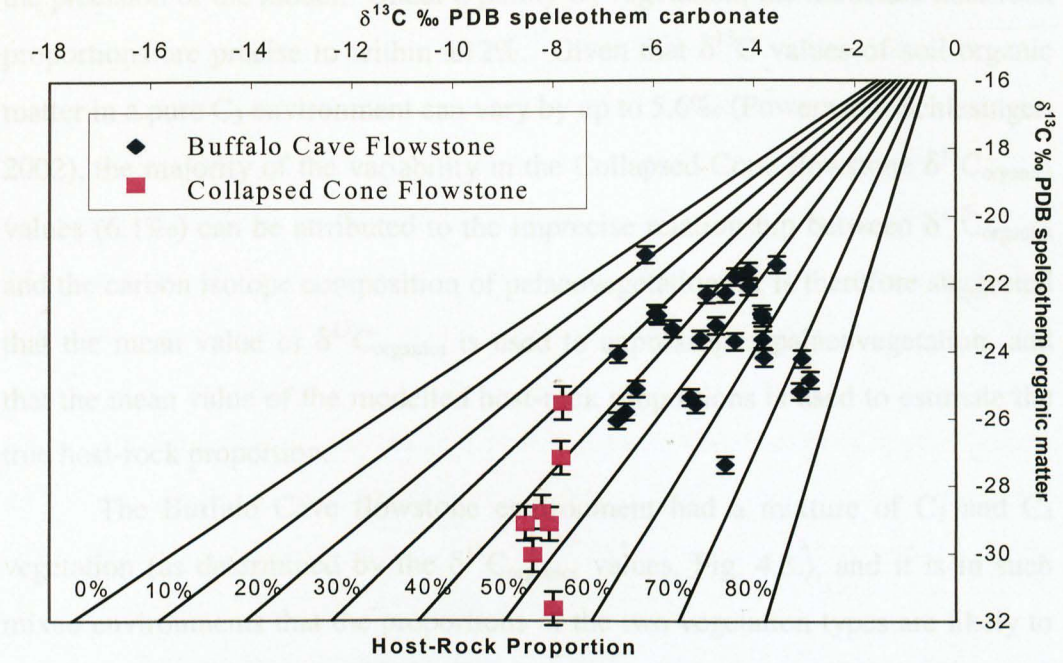

Figure 4.7. Cross-Plot of measured $\delta^{13}C$ values of co-occurring speleothem carbonate against speleothem organic matter for the Buffalo Cave and Collapsed Cone flowstones. The diagonal lines indicate the predicted relationship between $\delta^{13}C$ values of speleothem carbonate and organic matter with a range of host-rock contributions to speleothem carbon from 0% to 80%.

rock proportion or of $\delta^{13}C_{organics}$ values that are not precise indicators of palaeovegetation. These two possibilities are evaluated below.

Because all of the Collapsed Cone flowstone $\delta^{13}C_{organics}$ values lie within the $\delta^{13}C$ range of modern day C_3 vegetation (see Fig. 4.3.), and because the $\delta^{13}C_{carbonate}$ values are invariant and depleted in ^{13}C, it is apparent that the Collapsed Cone environment contained negligible proportions of C_4 grasses. As discussed above, the highly invariant $\delta^{13}C_{carbonate}$ composition of the Collapsed Cone flowstone (mean = –8.1‰; range = -7.1 to –8.8; s.d. = 0.28; n = 239; see Chapter 3) cannot have been controlled by significant variations in vegetation type, kinetic fractionation or host-rock contribution. In such a consistently C_3-dominated environment, a high turnover time of soil organic matter will not impact the correspondence between co-occurring $\delta^{13}C_{organics}$ and $\delta^{13}C_{carbonate}$ values, nor will it reduce the precision of the host-rock proportion modelling. Therefore, the variability within the modelled Collapsed Cone flowstone host-rock proportions (ranging from 30.4% to 54.4%) can be used as an indication of

the precision of the model. Under a purely C_3 vegetation, the modelled host-rock proportions are precise to within ±12%. Given that $\delta^{13}C$ values of soil organic matter in a pure C_3 environment can vary by up to 5.6‰ (Powers and Schlesinger, 2002), the majority of the variability in the Collapsed Cone flowstone $\delta^{13}C_{organics}$ values (6.1‰) can be attributed to the imprecise relationship between $\delta^{13}C_{organics}$ and the carbon isotope composition of palaeovegetation. It is therefore suggested that the mean value of $\delta^{13}C_{organics}$ is used to approximate palaeovegetation, and that the mean value of the modelled host-rock proportions is used to estimate the true host-rock proportion.

The Buffalo Cave flowstone environment had a mixture of C_3 and C_4 vegetation (as determined by the $\delta^{13}C_{organics}$ values, Fig. 4.3.), and it is in such mixed environments that the proportions of the two vegetation types are likely to vary (e.g. Boom *et al.*, 2002; Freeman and Colarusso, 2001). Changing proportions of C_3 and C_4 vegetation can explain the high degree of variability in measured $\delta^{13}C_{carbonate}$ values (mean = -8.2; range = -2.6‰ to -8.2‰; s.d. = 1.2‰; n = 550; see Chapter 3) in the Buffalo Cave flowstone. High organic matter turnover times in an environment of changing vegetation cover, will lead to a complete decoupling of the isotopic signals from the rapid turnover of soil CO_2-derived speleothem carbonate and the long turnover time of speleothem organic matter. This is the most likely explanation of the lack of correlation between $\delta^{13}C_{organics}$ and $\delta^{13}C_{carbonate}$ in the Buffalo Cave flowstone (r = 0.16; n = 27) and the high variability of modelled host-rock contributions.

4.9.6. Comparison with previous estimates of Host-Rock proportions:

Studies of the host-rock proportion of Holocene speleothems have used radiocarbon methods to determine the proportion of carbon sourced from ^{14}C "dead" host-rock. Genty and Massault (1997) show that published studies of speleothem dead-carbon proportions from Western Europe typically range from 10% to 25%. Higher dcp values (22%-38%) have been recorded in a Scottish stalagmite (Genty *et al.*, 2001) but have been attributed to old organic matter in the overlying peat increasing the "dead" ^{14}C signal. The positive relationship observed between $\delta^{13}C$ and dcp in several European cave sites indicates, as

expected, that an increased input of heavy carbon from host-rock dissolution results in heavier $\delta^{13}C$ values (Genty *et al.*, 2001). Very high dead carbon proportions (65-70%) have been found in modern stalactites from Castelguard Cave in the Columbia ice field, Canada, where the primary source of CO_2 for carbonate dissolution is atmospheric CO_2 (Gascoyne and Nelson, 1983). Two measurements of dcp in sub-tropical Holocene African speleothems come from Drotsky's Cave (dcp = 14%) in north-western Botswana (Railsback *et al.*, 1994) and Cango Caves (dcp = 17%) in the Cape Province of South Africa (Talma and Vogel, 1992). Cango Caves has had a mean annual temperature of approximately 18°C throughout the Holocene (Talma and Vogel, 1992) and is located within the transitional zone between the mixed C_3 and C_4 savannah vegetation and the purely C_3 environment of the Cape floral province.

The host-rock contributions modelled for the Pliocene and early Pleistocene flowstones in this study (mean of 47%) are higher than most of the dead carbon proportions calculated for Holocene speleothems (10-25%). This either indicates the presence of error within the model or indicates that these flowstones were precipitated with unusually high host-rock proportions. Host-rock proportions exceeding 50% are rarely observed (Genty *et al.*, 1999; Gascoyne and Nelson, 1983) and are considered unlikely given the equilibrium reaction between carbonic acid and calcium carbonate (Hendy, 1971). In tropical and sub-tropical karst environments, high temperatures and forest cover combine to greatly increase biological soil-CO_2 production, which leads to increased rates of limestone dissolution (Drake, 1980 and 1983). In such tropical environments, speleothems are expected to contain high host-rock proportions (Genty *et al.*, 2001). With the current lack of evidence for dcp in truly tropical karst (mean annual temperature >20°C, high rainfall and significant tree cover), this relationship remains to be demonstrated.

The disaggrement between the dcp of late Holocene speleothems from Southern Africa and the modelled host-rock proportions of the Plio-Pleistocene speleothems in this study is possibly a function of different palaeoclimatic conditions. For example, the volume of speleothem precipitation in the Plio-Pleistocene flowstones is far greater than the small stalagmites of the Holocene, suggesting that the Plio-Pleistocene temperature, precipitation and vegetation

conditions were more suited to the formation of massive speleothem deposits than Holocene palaeoclimates (as discussed in Latham *et al.*, 2003). Without palaeotemperature estimates for the Plio-Pleistocene flowstones, it is only possible to speculate that the high host-rock proportions are indicative of increased carbonate dissolution under higher temperatures and greater vegetation cover. Therefore a dcp of 40-50% in the Transvaal Plio-Pleistocene caves is feasible, but cannot yet be supported by independent evidence. A dcp study of Holocene stalagmites and flowstones from the Makapansgat Valley may help to determine local conditions of host-rock dissolution and carbon dynamics.

4.9.7. Reconstructing palaeovegetation using the estimated host rock proportion:

Given that the host-rock proportion is assumed to be constant at individual cave sites (Genty and Massault, 1997; Genty *et al.*, 2001), and that the range of modelled host-rock proportions can be attributed to long turnover times and variable $\delta^{13}C$ values of soil organic matter, the mean $\%_{host\text{-}rock}$ value offers the best approximation of host-rock contribution for both flowstones studied. Based on the above model, the mean $\%_{host\text{-}rock}$ value can be used to predict $\delta^{13}C_{palaeo\text{-}veg}$ for samples represented by $\delta^{13}C_{speleothem}$ values only. By inputting the known value of $\delta^{13}C_{speleothem}$ into equation (4) and the modelled $\%_{host\text{-}rock}$ value into equation (6) and working in order through equations (6), (3) and (7), an approximate value for $\delta^{13}C_{palaeo\text{-}veg}$ is obtained. Equation (6) is rearranged from equation (5) and equation (7) describes the relationship between vegetation and gaseous CO_2 in the soil:

$$\delta^{13}C_{DIC0} = (\delta^{13}C_{DIC} - (\%_{host\text{-}rock}/100)^* \delta^{13}C_{lst}) / (1-(\%_{host\text{-}rock}/100)) \text{ ‰ PDB} \quad (6)$$

$$\delta^{13}C_{palaeo\text{-}veg} = \delta^{13}C_g - F_{respired\text{-}soil} \text{ ‰ PDB} \quad (7)$$

Assuming an end-member linear mixing model in terms of $\delta^{13}C_{speleothem}$ for C_3 and C_4 photosynthesis it is possible to estimate the proportion of C_4 versus C_3 vegetation (e.g. Huang *et al.*, 2000; Boom *et al.*, 2002). O'Leary (1988) shows that the carbon isotopic composition of C_3 plants and C_4 plants have means of

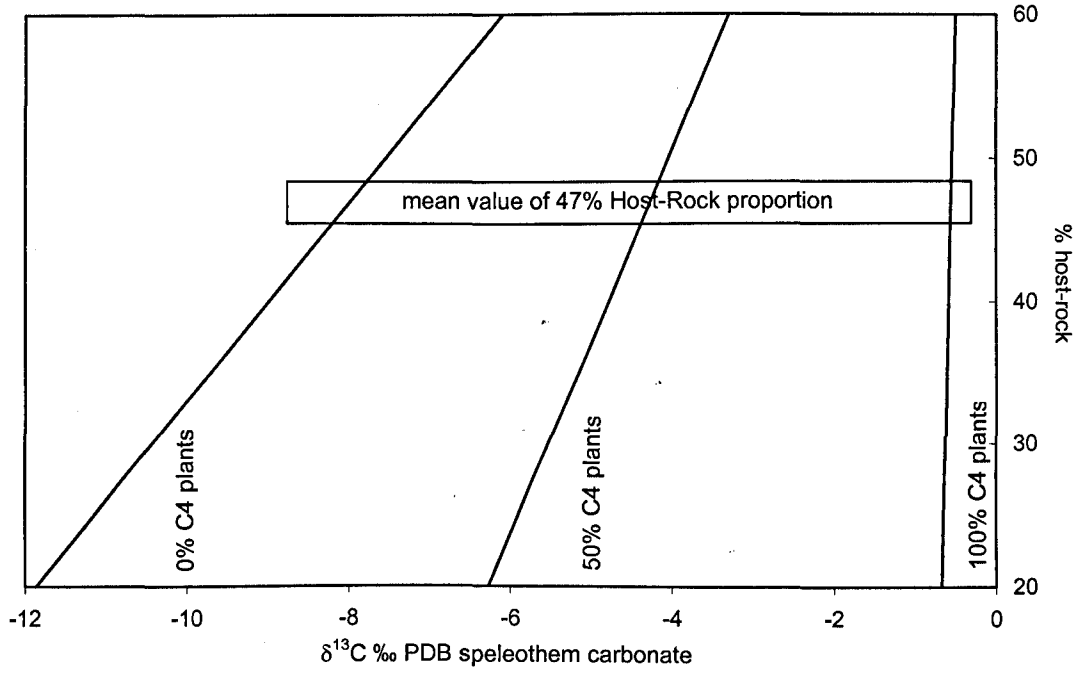

Figure 4.8. Modelled C_3 and C_4 plant end-member variation of speleothem carbonate $\delta^{13}C$ values with changing host-rock proportions. Contours indicate the proportion of C_4 plant input into speleothem carbonate with varying $\delta^{13}C$ and % Host-Rock values. Rectangle indicates the mean modelled host-rock proportion (47%) of the Buffalo Cave and Collapsed Cone flowstones. With this host-rock proportion, the corresponding C_3 and C_4 plant end-members for $\delta^{13}C$ speleothem carbonate are –8‰ and –0.6‰ respectively.

-28‰ and –14‰ and can vary by approximately 10‰ and 6‰ respectively (see Fig. 4.3.). This carbon isotope variability between different plant species and between different plant compounds (e.g. Rieley *et al.*, 1991; Freeman and Colarusso, 2001) with the same photosynthetic pathway, increases uncertainty when quantifying C_3 and C_4 plant proportions within an ecosystem. Despite this, the mean carbon isotope values of pure C_3 vegetation and pure C_4 vegetation (O'Leary, 1988) can be used to approximate the proportion of C_3 and C_4 plants in speleothem organic matter. Using the above model of speleothem formation, the proportion of C_3 and C_4 plants can then be determined from the carbon isotope composition of speleothem carbonate. Following Boom (2002), palaeovegetation

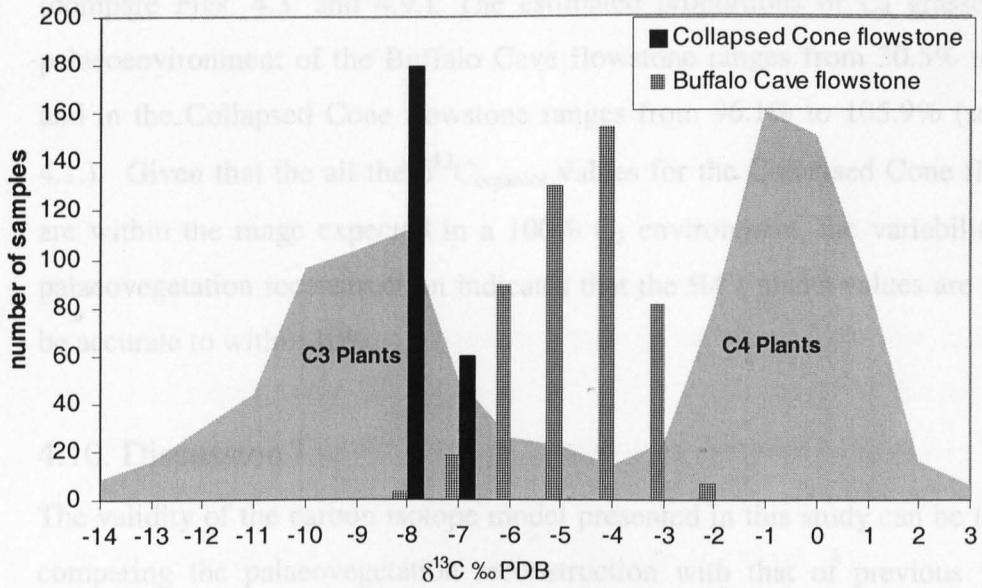

Figure 4.9. Frequency distribution of $\delta^{13}C$ for speleothem carbonate compared with the modelled C_3 and C_4 plant end-members following correction for the host-rock contribution. C_3 and C_4 plant end-member distributions are a combination of data from Vogel *et al.* (1978), Deines, (1980) and O'Leary, (1988). The $\delta^{13}C$ speleothem carbonate values are compiled from the Buffalo Cave and Collapsed Cone flowstones depth series (see Chapter 5). The Collapsed Cone flowstone has a predominantly C_3 plant isotopic signal whereas the Buffalo Cone flowstone has a mixed C_3 and C_4 plant signal. Comparison with Figure 4.3. indicates the same magnitude of vegetation shift between the two flowstones. The wider vegetation range of the Buffalo Cave flowstone is due to the larger number and greater resolution of the carbonate samples compared with the organic matter samples.

is defined in terms of a percentage of C_4 vegetation cover, % C_4 plants, as follows:

$$\% \, C_4 \text{ plants} = 100 - ((\delta^{13}C_{\text{C4 e-m}} - \delta^{13}C_{\text{carbonate}}) * (100 / (\delta^{13}C_{\text{C4 e-m}} - \delta^{13}C_{\text{C3 e-m}}))) \quad (8)$$

where e-m refers to the end-member carbon isotope value of pure C_3 or C_4 vegetation in speleothem carbonate. The speleothem carbonate C_3 and C_4 end-members (see Figs. 4.8. and 4.9.) of -8.0‰ and –0.6‰ respectively are derived from the C_3 plant and C_4 plant end-members of –28‰ and –14‰ (O'Leary, 1988), using the mean host-rock proportion of 47%. Therefore, any $\delta^{13}C_{\text{carbonate}}$ value can be converted to an approximate percentage of C_4 grasses (see Fig. 4.8.) using eqn (8). These speleothem carbonate palaeovegetation reconstructions are essentially the same as the reconstructions based on speleothem organic matter

(compare Figs. 4.3. and 4.9.). The estimated proportions of C_4 grasses in the palaeoenvironment of the Buffalo Cave flowstone ranges from 30.5% to 81.7% and in the Collapsed Cone flowstone ranges from 96.1% to 105.9% (see Table 4.1.). Given that the all the $\delta^{13}C_{organics}$ values for the Collapsed Cone flowstone are within the range expected in a 100% C_3 environment, the variability in the palaeovegetation reconstruction indicates that the $\%C_4$ plants values are likely to be accurate to within 10%.

4.10. Discussion

The validity of the carbon isotope model presented in this study can be tested by comparing the palaeovegetation reconstruction with that of previous workers. Numerous previous attempts have been made to reconstruct the palaeoenvironment of the Plio-Pleistocene cave deposits of South Africa based on sedimentological, floral, faunal and isotopic data. There are no fossil deposits in the Makapansgat Valley that correspond in age to the period of 1.8 Ma to 1.4 Ma represented by the Buffalo Cave flowstone or the approximately 4-5 Ma age of the Collapsed Cone flowstone. However, the hominin cave sites near Krugersdorp (e.g. Sterkfontein, Swartkrans; ~300 km south of Makapansgat) are located within a similar floral province in the present day (Acocks, 1953; Scholes, 1997), and are likely to have shared floral and faunal characteristics in the past. Therefore by taking the Plio-Pleistocene fossil record of the South African highveld as a whole, it is possible to develop a regional picture of Plio-Pleistocene palaeoecology. Evidence for gallery forests comes from silicified wood from Sterkfontein Member 4, as the liana *Dichapetalum* cf. *mombuttense* are common components of forests, requiring trees for external physical support (Bamford, 1999). Faunal evidence for closed woodland/forest conditions also comes from the presence of dedicated browsers. However, as indicated by stable isotope (Sponheimer et al, 1999; Lee-Thorp *et al.*, 2000; Van der Merwe *et al.*, 2003) and ecomorphological (Reed, 1998) evidence, each cave deposit has a significant component of C_4 grass consumers. Each cave deposit studied has yielded grassland and woodland components, indicating a mixed environment of C_4 grassland and C_3 woodland. The present study has also shown a mixed environment of C_3 and C_4 vegetation in the Early Pleistocene of South Africa.

The palaeovegetation of the Buffalo Cave flowstone has been shown to vary from a C_3 dominated to a C_4 dominated vegetation, with both vegetational groups present at all times.

Carbon isotope studies of fossil tooth enamel have provided detailed palaeodietary information from a number of South African cave deposits of various ages. However, converting the carbon isotope palaeodietary data into meaningful palaeoclimatic information requires the assumption that taphonomic biases and selective feeding are minimal (Kingston *et al.*, 1999; Sponheimer *et al.*, 1999). The Alcelaphine / Antelope (AA) index has been used as an indication of open savannah environments (Vrba, 1980), as these taxa are known to inhabit open environments in the present day. Subsequent carbon isotope evidence has indicated that some of the extinct Alcelaphine and Antelope taxa had a significant browsing component to their diet, enabling the AA index to be modified and improved (Luyt, 2001; Sponheimer, 2003). Luyt (2001) combines the existing isotopic and morphological data to create a C_4 grass index for the Plio-Pleistocene hominin sites. The values range from 30% to 80% C_4 grasses between 3 Ma and 1.4 Ma and therefore show close agreement with the range of values of 25% to 80% C_4 grasses at 1.6 Ma, as determined in the present study.

4.11. Conclusions

This study has extracted organic inclusions preserved within speleothem calcite and measured the isotopic composition of the organic matter. $\delta^{13}C$ values of speleothem organic matter indicate a change in the proportion of C_4 grasses in the local palaeoenvironment between the late Miocene/early Pliocene and the early Pleistocene (see Fig. 4.3.). The late Miocene/early Pliocene Collapsed Cone flowstone was formed under purely C_3 palaeovegetation conditions, whereas the early Pleistocene Buffalo Cave flowstone was formed within a mixed C_3 and C_4 palaeovegetation. These separate vegetation regimes are indicative of a large-scale climatic change in the late Neogene of South Africa.

These organic matter $\delta^{13}C$ measurements can be used to determine the palaeovegetion signal within speleothem carbonate, assuming the speleothems were precipitated under isotopic equilibrium conditions. $\delta^{13}C$ measurements of speleothem carbonate across growth layers and over duplicate records in the

direction of speleothem growth, have demonstrated the isotopic equilibrium precipitation of the flowstone carbonate. By modelling the carbon isotope offset between co-occurring carbonate and organic matter, it has been possible to determine an approximate host-rock contribution to the speleothem carbonate $\delta^{13}C$ values. Applying the mean host-rock contribution value to the carbon isotope model has enabled the speleothem carbonate $\delta^{13}C$ values to be converted into an approximate percentage of C_4 grasses in the local palaeoenvironment (see Fig. 4.9.). The modelled percentage of C_4 grasses corresponds well with existing faunal, floral and isotopic data from the late Neogene of South Africa.

4.12. References

Acocks, J. P. H. (1953). Veld types of South Africa. *Memoirs of the Botanical Survey of South Africa* **28,** 1-192.

Almendros, G., Kgathi, D., Sekhwela, M., Zancada, M.-C., Tinoco, P., and Pardo, M.-T. (2003). Biogeochemical assessment of resilient humus formations from virgin and cultivated Northern Botswana soils. *Journal of Agricultural and Food Chemistry* **51,** 4321-4330.

Ayalon, A., Bar-Matthews, M., and Kaufman, A. (2002). Climatic conditions during marine oxygen isotope stage 6 in the eastern Mediterranean region from the isotopic composition of speleothems of Soreq Cave, Israel. *Geology* **30,** 303-306.

Baker, A., Smart, P. L., Edwards, R. L., and Richards, D. A. (1993). Annual growth banding in a cave stalagmite. *Nature* **364,** 518-520.

Baker, A., Barnes, W. L., and Smart, P. L. (1996). Speleothem luminescence intensity and spectral characteristics: Signal calibration and a record of palaeovegetation change. *Chemical Geology* **130,** 65-76.

Baker, A., Ito, E., Smart, P. L., and McEwan, R. F. (1997). Elevated and variable values of C^{13} in speleothems in a British cave system. *Chemical Geology* **136,** 263-270.

Baker, A., Barnes, W. L., and Smart, P. L. (1997). Variations in the discharge and organic matter content of stalagmite drip waters in Lower Cave, Bristol. *Hydrological Processes* **11.**

Baker, A., Genty, D., and Smart, P. L. (1998). High-resolution records of soil humification and paleoclimate change from variations in speleothem luminescence excitation and emission wavelengths. *Geology* **26,** 903-906.

Baker, A., Proctor, C. J., and Barnes, W. L. (1999). Variations in stalagmite luminescence laminae structure at Poole's Cavern, England, AD 1910-1996: calibration of a palaeoprecipitation proxy. *Holocene* **9,** 683-688.

Bamford, M. (1999). Pliocene fossil woods from an early hominid cave deposit, Sterkfontein, South Africa. *South African Journal of Science* **95,** 231-237.

Bar-Matthews, M., Ayalon, A., Gilmour, M., Matthews, A., and Hawkesworth, C. J. (2003). Sea-land oxygen isotopic relationships from planktonic foraminifera and speleothems in the Eastern Mediterranean region and

their implication for paleorainfall during interglacial intervals. *Geochimica et Cosmochimica Acta* **67,** 3181-3199.

Beerling, D. J. (1997). Interpreting environmental and biological signals from the stable carbon isotope composition of fossilized organic and inorganic carbon. *Journal of the Geological Society, London* **154,** 303-309.

Bernoux, M., Cerri, C. C., Neill, C., and de Moraes, J. F. L. (1998). The use of stable carbon isotopes for estimating soil organic matter turnover rates. *Geoderma* **82,** 43-58.

Boom, A., Marchant, R., Hooghiemstra, H., and Sinninghe Damste, J. S. (2002). CO_2-and temperature-controlled altitudinal shifts of C4- and C3-dominated grasslands allow reconstruction of palaeoatmospheric pCO_2. *Palaeogeography, Palaeoclimatology, Palaeoecology* **177,** 151-168.

Cerling, T. E. (1984). The stable isotopic composition of modern soil carbonate and its relationship to climate. *Earth and Planetary Science Letters* **71,** 229-240.

Cerling, T. E., and Hay, R. L. (1986). An isotopic study of paleosol carbonates from Olduvai Gorge. *Quaternary Research* **25,** 63-78.

Cerling, T. E., Quade, J., Wang, Y., and Bowman, J. R. (1989). Carbon isotopes in soils and paleosols as ecology and paleoecology indicators. *Nature* **341,** 138-139.

Chen, J.-S., and Chiu, C.-Y. (2000). Effect of topography on the composition of soil organic substances in a perhumid sub-tropical montane forest ecosystem in Taiwan. *Geoderma* **96,** 19-30.

Coplen, T. B. (1995). Reporting of stable carbon, hydrogen, and oxygen isotopic abundances. *In* "Reference and intercomparison materials for stable isotopes of light elements." pp. 31-34. International Atomic Energy Agency, TECDOC.

Craig, H. (1957). Isotopic standards for carbon and oxygen and correction factors for mass-spectrometric analysis of carbon dioxide. *Geochemica et Cosmochimica Acta* **12,** 133-149.

Dafner, E., Sempere, R., Yoro, S. C., Agatova, A., and Cauwet, G. (1999). Application of the wet oxidation method for dissolved organic carbon analysis in the Southern Ocean. *Comptes Rendus de L'Academie des Sciences Serie II fascicule a- Sciences de la Terre et des Planetes* **329,** 345-350.

Deines, P., Langmuir, D., and Harmon, R. S. (1974). Stable carbon isotope ratios and the existence of a gas phase in the evolution of carbonate ground waters. *Geochimica et Cosmochimica Acta* **38,** 1147-1164.

Deines, P. (1980). The isotopic composition of reduced organic carbon. *In* "Handbook of Environmental Isotope Geochemistry." (P. Fritz, and J. C. Fontes, Eds.), pp. 329-406. Elsevier, Amsterdam.

Doane, T. A., Devêvre, O. C., and Horwáth, W. R. (2003). Short-term soil carbon dynamics of humic fractions in low-input and organic cropping systems. *Geoderma* **114,** 319-331.

Dörr, H., and Münnich, K. O. (1980). Carbon-14 and carbon-13 in soil CO_2. *Radiocarbon* **22,** 909-918.

Dulinski, M., and Rozanski, K. (1990). Formation of $^{13}C/^{12}C$ isotope ratios in speleothems: a semi-dynamic model. *Radiocarbon* **32,** 7-16.

Egli, M., and Fitze, P. (2001). Quantitative aspects of carbonate leaching of soils with differing ages and climates. *Catena* **46,** 35-62.

Ehleringer, J. R., Buchmann, N., and Flanagan, L. B. (2000). Carbon isotope ratios in belowground carbon cycle processes. *Ecological Applications* **10,** 412-422.

Elkins, J. T. (2002). "Use of $\delta^{13}C$ values of soil organic matter found in speleothems as a new proxy for paleovegetation and interpreting paleoclimate." Unpublished PhD thesis, The University of Georgia.

Fairchild, I. J., Borsato, A., Tooth, A. F., Frisia, S., Hawkesworth, C. J., Huang, Y. M., McDermott, F., and Spiro, B. (2000). Controls on trace element (Sr-Mg) compositions of carbonate cave waters: implications for speleothem climatic records. *Chemical Geology* **166,** 255-269.

Farquhar, G. D., Ehleringer, J. R., and Hubick, K. T. (1989). Carbon isotope discrimination and photosynthesis. *Annual Review of Plant Physiology and Plant Molecular Biology* **40,** 503-537.

Ficken, K. J., Wooller, M. J., Swain, D. L., Street-Perrott, F. A., and Eglinton, G. (2002). Reconstruction of a subalpine grass-dominated ecosystem, Lake Rutundu, Mount Kenya: a novel multi-proxy approach. *Palaeogeography, Palaeoclimatology, Palaeoecology* **177,** 137-149.

Filip, Z., Pecher, W., and Berthelin, J. (1999). Microbial utilization and transformation of humic acids extracted from different soils. *Journal of Plant Nutrition and Soil Science* **162,** 215-222.

Filip, Z., and Kubát, J. (2001). Microbial utilization and transformation of humic substances extracted from soils of long-term field experiments. *European Journal of Soil Biology* **37,** 167-174.

Fornaca-Rinaldi, G., Panichi, C., and Tongiorgi, E. (1968). Some causes of the variation of the isotopic composition of carbon and oxygen in cave concretions. *Earth and Planetary Science Letters* **4,** 321-324.

Freeman, K. H., and Colarusso, L. A. (2001). Molecular and isotopic records of C4 grassland expansion in the late Miocene. *Geochimica et Cosmochimica Acta* **65,** 1439-1454.

Fung, I., Field, C., Berry, J. A., Thompson, M. V., Randerson, J. T., Malmstrom, C. M., Vitousek, P. M., Collatz, G. J., Sellers, P. J., Randall, D. A., Denning, A. S., Badeck, F., and John, J. (1997). Carbon 13 exchanges between the atmosphere and biosphere. *Global Biogeochemical Cycles* **11,** 507-533.

Gascoyne, M., and Nelson, D. E. (1983). Growth mechanisms of recent speleothems from Castelguard Cave, Columbia Icefield, Alberta, Canada, inferred from a comparison of uranium-series and carbon-14 age data. *Arctic and Alpine Research* **15,** 537-542.

Genty, D., and Massault, M. (1997). Bomb C-14 recorded in laminated speleothems: Calculation of dead carbon proportion. *Radiocarbon* **39,** 33-48.

Genty, D., Vokal, B., Obelic, B., and Massault, M. (1998). Bomb ^{14}C time history recorded in two modern stalagmites - importance for soil organic matter dynamics and bomb ^{14}C distribution over continents. *Earth and Planetary Science Letters* **160,** 795-809.

Genty, D., and Massault, M. (1999). Carbon transfer dynamics from bomb-^{14}C and $\delta^{13}C$ time series of a laminated stalagmite from SW France - Modelling and comparison with other stalagmite records. *Geochimica et Cosmochimica Acta* **63,** 1537-1548.

Genty, D., Baker, A., Massault, M., Proctor, C., Gilmour, M., Pons-Branchu, E.,

and Hamelin, B. (2001). Dead carbon in stalagmites: Carbonate bedrock paleodissolution vs. ageing of soil organic matter. Implications for ^{13}C variations in speleothems. *Geochemica et Cosmochimica Acta* **65,** 3443-3457.

Guillet, B., Faivre, P., Mariotti, A., and Khobzi, J. (1988). The ^{14}C dates and $^{13}C/^{12}C$ ratios of soil organic matter as a means of studying the past vegetation in intertropical regions: examples from Colombia (South America). *Palaeogeography, Palaeoclimatology, Palaeoecology* **65,** 51-58.

Hellstrom, J. C., and McCulloch, M. T. (2000). Multi-proxy constraints on the climatic significance of trace element records from a New Zealand speleothem. *Earth and Planetary Science Letters* **179,** 287-297.

Hendy, C. H., and Wilson, A. T. (1968). Palaeoclimatic data from speleothems. *Nature* **219,** 48-51.

Hendy, C. H. (1971). The isotopic geochemistry of speleothems- I. The calculation of the effects of different modes of formation on the isotopic composition of speleothems and their applicability as palaeoclimatic indicators. *Geochemica et Cosmochimica Acta* **35,** 801-824.

Holmgren, K., Lauritzen, S. E., and Possnert, G. (1994). $^{230}Th/^{234}U$ and ^{14}C dating of a late Pleistocene stalagmite in Lobatse II cave, Botswana. *Quaternary Geochronology (Quaternary Science Reviews)* **13,** 111-119.

Holmgren, K., Lee-Thorp, J. A., Cooper, G. R. I., Lundblad, K., Partridge, T. C., Scott, L., Sithaldeen, R., Talma, A. S., Tyson, P. D. (2004). Persistent millennial-scale climatic variability over the past 25,000 years in Southern Africa. *Quaternary Science Reviews* **22**: 2311-2326.

Kingston, J. D. (1999). Isotopes and environments of the Baynunah Formation, Emirate of Abu Dhabi, United Arab Emirates. *In* "Fossil Vertebrates of Arabia." (P. J. Whybrow, and A. Hill, Eds.), pp. 523. Yale University Press.

Krishnamurthy, R. V., DeNiro, M. J., Pant, R. K. (1982). Isotope evidence for Pleistocene climatic changes in Kashmir, India. *Nature* **298**: 640-641.

Latham, A. G., Herries, A., and Kuykendall, K. (2003). The formation and sedimentary infilling of the Limeworks cave, Makapansgat, South Africa. *Palaeontologia Africana* **39**: 69-82.

Lee-Thorp, J. A., Thackeray, J. F., and van der Merwe, N. (2000). The hunters and the hunted revisited. *Journal of Human Evolution* **39,** 565-576.

Lichtfouse, E., Dou, S., Girardin, C., Grably, M., Balesdent, J., Behar, F., and Vandenbroucke, M. (1995). Unexpected ^{13}C-enrichment of organic components from wheat crop soils: evidence for the in situ origin of soil organic matter. *Organic Geochemistry* **23,** 865-868.

Lichtfouse, E., Dou, S., Houot, S., and Barriuso, E. (1995). Isotope evidence for soil organic carbon pools with distinct turnover rates - II. Humic substances. *Organic Geochemistry* **23,** 845-847.

Luyt, J. (2001). "Revisiting the palaeoenvironments of the South African hominid-bearing Plio-Pleistocene sites: New isotopic evidence from Sterkfontein." Unpublished MSc thesis, University of Cape Town.

Maguire, J. M. (1998). "Makapansgat: A guide to the Palaeontological and Archaeological sites of the Makapansgat Valley." The Dual Congress of the International Association for the study of Human Palaeontology and

International Association of Human Biologists, Sun City, Republic of South Africa.

McGarry, S. F., and Baker, A. (2000). Organic acid fluorescence: applications to speleothem palaeoenvironmental reconstruction. *Quaternary Science Reviews* **19,** 1087;1101.

Mook, W. G., Bommerson, J. C., and Staverman, W. H. (1974). Carbon isotope fractionation between dissolved bicarbonate and gaseous carbon dioxide. *Earth and Planetary Science Letters* **22,** 169-176.

Mook, W. G. (1980). Carbon 14 in hydrogeological studies. *In* "Handbook of Environmental Geochemistry." (P. Fritz, and J. C. Fontes, Eds.), pp. 49-74.

O'Leary, M. H. (1981). Carbon isotope fractionation in plants. *Phytochemistry* **20,** 553-567.

O'Leary, M. H. (1988). Carbon isotopes in photosynthesis. *BioScience* **38,** 328-336.

Paul, E. A., and Clark, F. E. (1989). Soil microbiology and biochemistry. Academic Press, San Diego, California, 273 pp.

Peltzer, E. T., Fry, B., Doering, P. H., McKenna, J. H., Norrman, B., and Zweifel, U. L. (1996). A comparison of methods for the measurement of dissolved organic carbon in natural waters. *Marine Chemistry* **54,** 85-96.

Poirier, N., Derenne, S., Balesdent, J., Rouzaud, J.-N., Mariotti, A., and Largeau, C. (2002). Abundance and composition of the refractory organic fraction of an ancient, tropical soil (Pointe Noire, Congo). *Organic Geochemistry* **33,** 383-391.

Powers, J. S. and W. H. Schlesinger (2002). Geographic and vertical patterns of stable carbon isotopes in tropical rain forest soils of Costa Rica. *Geoderma* **109**: 141-160.

Railsback, L. B., Brook, G. A., Chen, J., Kalin, R., and Fleisher, C. J. (1994). Environmental controls on the petrology of a late Holocene speleothem from Botswana with annual layers of aragonite and calcite. *Journal of Sedimentary Research Section A-Sedimentary Petrology and Processes* **64,** 147-155.

Ramseyer, K., Miano, T. M., D'Orazio, V., Wildberger, A., Wagner, T., and Geister, J. (1997). Nature and origin of organic matter in carbonates from speleothems, marine cements and coral skeletons. *Organic Geochemistry* **26,** 361-378.

Reardon, E. J., Allison, G. B., and Fritz, P. (1979). Seasonal chemical and isotopic variations of soil CO_2 at Trout Creek, Ontario. *Journal of Hydrology* **43,** 355-71.

Reed, K. E. (1998). Using large mammal communities to examine ecological and taxonomic structure and predict vegetation in extant and extinct assemblages. *Paleobiology* **24,** 384-408.

Rieley, G., Collier, R. J., Jones, D. M., Eglinton, G., Eakin, P. A., and Fallick, A. E. (1991). Sources of sedimentary lipids deduced from stable carbon-isotope analyses of individual compounds. *Nature* **352,** 425-427.

Roberts, M. S., Smart, P. L., and Baker, A. (1998). Annual trace element variations in a Holocene speleothem. *Earth and Planetary Science Letters* **154,** 237-246.

Scholes, R. J. (1997). Savanna. *In* "Vegetation of Southern Africa." (R. M. Cowling, D. M. Richardson, and S. M. Pierce, Eds.), pp. 258-277.

Cambridge University Press, Cambridge.

Schönwitz, R., Stichler, W., and Ziegler, H. (1986). $\delta^{13}C$ values of CO_2 from soil respiration on sites with crops of C3 and C4 type of photosynthesis. *Oecologia* **69,** 305-308.

Senesi, N., Miano, T. M., Provenzano, M. R., and Brunett, G. (1991). Characterization, differentation, and classification of humic substances by fluorescence spectroscopy. *Soil Science* **152,** 259-271.

Shopov, Y. Y., Ford, D. C., and Schwarcz, H. P. (1994). Luminescent microbanding in speleothems: high resolution chronology and paleoclimate. *Geology* **22,** 407-410.

Spaccini, R., Piccolo, A., Haberhauer, G., and Gerzaber, M. H. (2000). Transformation of organic matter from maize residues into labile and humic fractions of three European soils as revealed by ^{13}C distribution and CPMAS-NMR spectra. *European Journal of Soil Science* **51,** 583-594.

Sponheimer, M., Reed, K. E., and Lee-Thorp, J. A. (1999). Combining isotopic and ecomorphological data to refine bovid paleodietary reconstruction: a case study from the Makapansgat Limeworks hominin locality. *Journal of Human Evolution* **36,** 705-718.

St-Jean, G. (2003). Automated quantitative and isotopic (^{13}C) analysis of dissolved inorganic carbon and dissolved organic carbon in continuous-flow using a total organic carbon analyser. *Rapid Communications in Mass Spectrometry* **17,** 419-428.

Trumbore, S. (2000). Age of soil organic matter and soil respiration: radiocarbon constraints on belowground C dynamics. *Ecological Applications* **10**: 399-411.

van der Merwe, N., Thackeray, F., Lee-Thorp, J. A., and Luyt, J. (2003). The carbon isotope ecology and diet of *Australopithecus africanus* at Sterkfontein, South Africa. *Journal of Human Evolution* **44,** 581-597.

Veizer, J., Clayton, R. N., and Hinton, R. W. (1992). Geochemistry of Precambrian carbonates: IV. Early Paleoproterozoic (2.25+-0.25Ga) seawater. *Geochemica et Cosmochimica Acta* **56,** 875-885.

Verheyden, S., Keppens, E., Fairchild, I. J., McDermott, F., and Weis, D. (2000). Mg, Sr and Sr isotope geochemistry of a Belgian Holocene speleothem: implications for paleoclimate reconstructions. *Chemical Geology* **169,** 131;144.

Vogel, J. C., Fuls, A., and Ellis, R. P. (1978). The geographical distribution of Kranz grasses in South Africa. *South African Journal of Science* **74,** 209-215.

Vrba, E. S. (1980). The significance of bovid remains as indicators of environment and predation patterns. *In* "Fossils in the making. Vertebrate taphonomy and paleoecology." (A. K. Behrensmeyer, and A. P. Hill, Eds.), pp. 247-271. University of Chicago Press, Chicago.

Wassenaar, L. I., Aravena, R., Fritz, P., and Barker, J. F. (1991). Controls on the transport and carbon isotopic composition of dissolved organic carbon in a shallow groundwater system, Central Ontario, Canada. *Chemical Geology* **87,** 39-57.

Zech, W., Senesi, N., Guggenberger, G., Kaiser, K., Lehmann, J., Miano, T. M., Miltner, A., and Schroth, G. (1997). Factors controlling humification and mineralization of soil organic matter in the tropics. *Geoderma* **79,** 117 -161.

Chapter 5. Orbital forcing of hominin palaeo-environments in the early Pleistocene of South Africa

5.1. Abstract

Reconstructing Plio-Pleistocene African palaeoenvironments is important for models of early hominin evolution, but is often hampered by low-resolution or discontinuous climatic data. Here we present high-resolution stable oxygen and carbon isotope time-series data from two flowstones (secondary cave deposits) from the South African hominin-bearing Makapansgat Valley. The older of the two flowstones (Collapsed Cone flowstone) is dated by palaeomagnetism to approximately 4 Ma and the younger flowstone (Buffalo Cave flowstone) is dated to 1.5-2.0 Ma by a combination of palaeomagnetism, annual UV-band counting and orbital-tuning of the isotopic data.

The carbon isotope data is used as a proxy for the proportion of C_4 grasses in the local environment and the oxygen isotope data reflects a combined temperature and precipitation signal. The light and invariant $\delta^{13}C$ values of the Collapsed Cone flowstone indicate a predominantly C_3 vegetation in the Late Miocene / Early Pliocene, in contrast to the mixed C_3 and C_4 vegetation of the Early Quaternary Buffalo Cave flowstone. It is suggested that C_4 grasses became a significant part of the Makapansgat Valley ecosystem at approximately 4-5 Ma. Spectral analysis of the Buffalo Cave time-series indicates precessional (18-23 ka) control of the oxygen isotope data, as is typical for records of sub-tropical terrestrial climate. In contrast, the carbon isotope time-series is dominated by the obliquity (40 ka) periodicity, the dominant frequency of early Pleistocene global climatic change recorded in marine and ice-core records. This suggests that different aspects of the global climate system are forcing the proxy records of vegetation and precipitation/temperature change.

5.2. Introduction

Global climatic oscillations with Milankovitch periodicities are a dominant feature of the Late Neogene and have been viewed as driving forces in the evolution of African mammalian faunas, including hominins (e.g. Bromage and

Schrenk, 1995; Vrba, 1995; Potts, 1998; Zeitoun, 2000; Bobe and Eck, 2001; Barry *et al.*, 2002; Bobe *et al.*, 2002). In the absence of a long and detailed terrestrial record of global change, these models of climatically forced macroevolution use the marine palaeotemperature record (e.g. Shackleton, 1995) as the template onto which trends in mammalian evolution are fitted. The focus has been either on directional trends of global cooling (Vrba, 1992; 1995) or on the magnitude and frequency of climatic variability (Potts, 1996; 1998). These global climatic events have been held responsible for episodes of hominin speciation, extinction and migration. While there are sound theoretical and empirical reasons to link events in hominin evolution to periods of climatic change (Vrba, 1995b), it has yet to be demonstrated that the Late Neogene marine palaeoclimate record is a faithful proxy for sub-tropical and tropical African palaeoclimates. To the contrary, there is mounting evidence to show that tropical terrestrial climatic change is decoupled from the global ice-volume record of deep-sea $\delta^{18}O$ (e.g. Pokras and Mix, 1987; Clemens *et al.*, 1991; Partridge *et al.*, 1997). Previous proxy records of African climate change have been constructed from terrestrial components within marine sediment cores (deMenocal and Bloemendal, 1995; Dupont and Leroy, 1995) that produce space-averaged terrestrial records that cannot be linked to specific hominin habitats. This study provides the first long-record of terrestrial Late Neogene African climate change within a savannah-mosaic environment inhabited by early hominins. Comparing the record of climatic change in local hominin habitats to the global climatic record of marine oxygen isotopes will test the existing models of hominin evolution in response to global climatic change.

5.3. Southern African Pleistocene Palaeoclimates

Palaeoclimatic data for the Late Pleistocene of southern Africa comes from a broad range of faunal, floral and geological sources (as reviewed in Lee-Thorp and Talma, 2000; Tyson *et al.*, 2001; Scott, 2002). However, only a few of these datasets (e.g. Partridge *et al.*, 1997; Talma and Vogel, 1992; Holmgren *et al.*, 2003) provide time-series of necessary length and resolution to provide continuous information on glacial-interglacial climatic change. The 200,000-year Late Quaternary precipitation record of Partridge *et al.* (1997) from the Pretoria

Saltpan, South Africa, is the longest record of climatic change from Southern Africa. The rainfall proxy is based on the relationship between regional precipitation and soil texture, which is recorded as textural and compositional changes within the sedimentary sequence. This time-series is forced by orbital precession (23 ka), the dominant orbital periodicity observed in records from the northern and southern hemisphere subtropics (Clemens *et al.*, 1991; Prell and Kutzbach, 1987; Prell and Van Campo, 1986; Hooghiemstra, 1995; Partridge *et al.*, 1997). The geometry of orbital precession predicts that changes in summer insolation should be antiphase between hemispheres, and this is shown to be the case when the northern hemisphere and southern hemisphere records are compared (Partridge *et al.*, 1997).

The model of South African palaeoclimates of Tyson (1999) and Tyson and Preston-Whyte (2000) is based on observations of present-day weather patterns, Quaternary palaeoclimate data and Global Circulation Models (GCMs). The model posits warmer, wetter conditions being forced by changes originating in the easterly circulation of the tropics and cooler, drier conditions being brought about by an equator-ward expansion of the westerlies and their associated weather disturbances (see Fig. 5.1.).

The precessional cycle changes the time of year in which perihelion (when the Earth is nearest to the Sun) and aphelion (when the Earth is farthest from the Sun) occur. Currently, perihelion occurs in early January, in the southern hemisphere summer, and aphelion in early July, in the southern hemisphere winter. This causes the southern hemisphere summers and winters to be more severe and their northern hemisphere counterparts to be less so. At the extremity of the precessional cycle, as is the case in the present day, the thermal equator strengthens in the equatorial regions of Africa and moves towards the southern hemisphere. The temperature gradient between the equator and the South Pole strengthens, as does the Inter-Tropical Convergence Zone (ITCZ), and the tropical forcing of southern African climates is enhanced. Wetter conditions prevail, while drier conditions occur over Africa to the north of the equator (Tyson, 1999). In the present day, wetter conditions in mid-summer over Southern Africa are associated with enhanced northeasterly moisture transport, whereas under dry conditions, moisture transport is from the southwest. The Tyson (1999) model of South African palaeoclimates suggests that in cool, dry phases of the precessional

cycle such as the Late Glacial Maximum (LGM), moisture over South Africa was primarily sourced from the southwest.

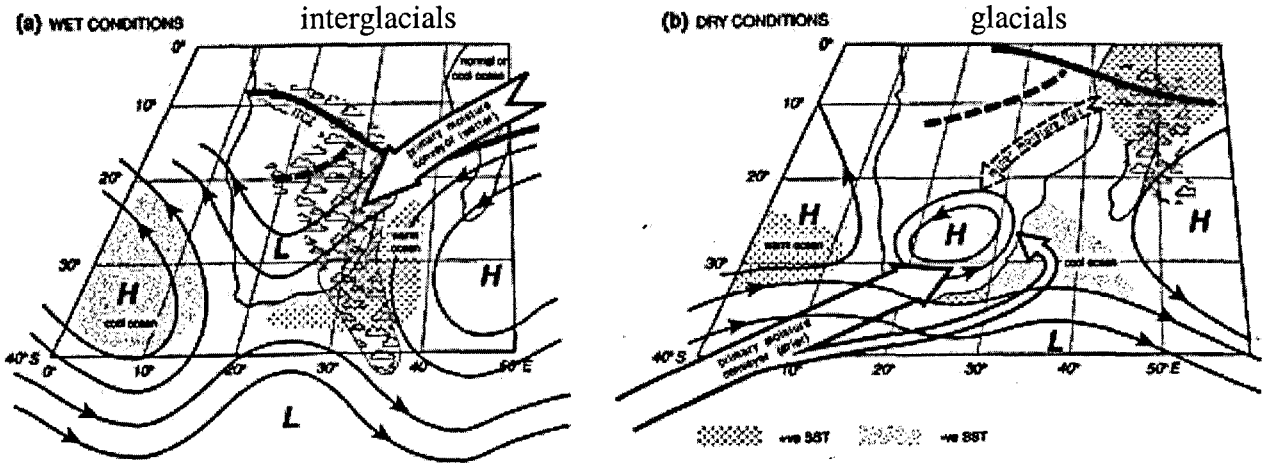

Figure 5.1. Glacial and interglacial palaeoclimates of Southern Africa (from Tyson and Preston-Whyte, 2000). This model, based on present-day weather patterns, posits (a) warmer and wetter conditions during interglacial periods and (b) cooler and drier conditions during glacial periods.

This hypothesis is supported by $\delta^{18}O$ water measurements in the Stampriet aquifer in Namibia that show enriched $\delta^{18}O$ values in the LGM compared to Holocene water values (Stute and Talma, 1997). This indicates a change in the dominant water source from the Indian Ocean in the Holocene to the Atlantic Ocean during the Late Glacial Maximum and therefore a change in $\delta^{18}O$ due to the continental effect (Stute and Talma, 1997; Tyson and Preston-Whyte, 2000). Enriched $\delta^{18}O$ values in the Holocene of the Stampriet aquifer can be explained by the short transport distance from the Atlantic Ocean and the depleted $\delta^{18}O$ values at the Late Glacial Maximum are due to the distant Indian Ocean water source. For sites to the east of the continent, such as the Pretoria Saltpan and the Makapansgat speleothems, the continental effect is likely to work in the opposite sense – i.e. heavy $\delta^{18}O$ values in the Holocene due to the proximity of the Indian Ocean moisture source, and depleted values at the last glacial maximum due to the continental effect from the Atlantic Ocean moisture source.

Data on the palaeoenvironments of South African hominins is derived either from the fauna, flora or geology of cave breccias. Many of the faunal specimens in the South African hominin sites were found in lime-dumps after the

caves were mined for lime in the early twentieth century, and lack stratigraphic context. In situ bone-breccias that survived the lime-mining intact tend to be poorly stratified, and represent unknown periods of deposition of tens to hundreds of thousands of years (McFadden *et al.*, 1979; Herries, 2003). Both in-situ and mined bone-breccias are given Member status within the stratigraphy of each cave deposit (e.g. Partridge, 1979 and 1978) and are defined on broad differences in sedimentological and palaeontological characteristics. Previous palaeo-environmental studies based on these bone-breccias have therefore lacked the temporal resolution required to investigate climatic change and early hominin palaeoecology on the scale of glacial-interglacial cycles.

Stable carbon isotopes of fossil teeth from South African Plio-Pleistocene cave breccias have shown the presence of both C_3 and C_4 vegetation in the local environment of each faunal Member studied (Van der Merwe and Thackeray, 1997; Sponheimer *et al.*, 1999; Lee-Thorp *et al.*, 2000). However, as discussed in Kingston (1999), selective feeding and taphonomic factors (Vrba, 1980) make converting isotopic palaeodietary data into meaningful palaeovegetational reconstructions problematic. Fossil macrofloras have only been found in Sterkfontein Member 4 (Bamford, 1999) and fossil pollen studies have been hindered by modern-day contamination (Scott, 1995).

This study investigates the early Pliocene and early Pleistocene palaeoclimates of South Africa using time-series of carbon and oxygen isotopes in flowstone sequences from the hominin-bearing Makapansgat Valley. In contrast to bone breccias, the speleothems offer a high-resolution and continuous stratigraphy. Carbon and oxygen isotope studies of speleothems offer the potential of high-resolution, semi-quantitative records of palaeovegetation, meteoric precipitation and the temperature of speleothem precipitation.

5.4. Oxygen isotopes in speleothems

When speleothem carbonate has been deposited under isotopic equilibrium conditions, the oxygen isotopic composition of the carbonate can be expressed as an equation consisting of two components - (1) the thermodynamic fractionation between cave drip water and speleothem carbonate, and (2) the drip water

function (Schwarcz, 1986; Lauritzen, 1995). The drip water function reflects the $\delta^{18}O$ value of precipitation at a site, which is dependant on the precipitation source, the transport history of the rain and the temperature of rain or snow formation in the atmosphere. Drip waters may also be modified by a seasonal interception bias in aquifer recharge above the cave (Yonge *et al.*, 1985).

The potential of speleothem $\delta^{18}O$ to yield palaeotemperature estimates is based on the thermodynamic fractionation of $\delta^{18}O$, which always has a negative response to temperature (i.e., heavier speleothem $\delta^{18}O$ values indicate decreasing temperature). In contrast, the drip-water function can respond either positively or negatively to temperature, depending on specifics of the regional meteorology. Therefore, the temperature response of speleothem $\delta^{18}O$ is entirely dependent on the relative magnitudes of the thermodynamic and drip-water functions, which can result in a net negative, positive or zero response of speleothem $\delta^{18}O$ with temperature (Holmgren *et al.*, 1999).

These problems can be overcome in one of several ways. First, measurement of $\delta^{18}O$ of water in speleothem fluid-inclusions can yield temperature values directly from the thermodynamic term (Schwarcz *et al.*, 1976; Matthews *et al.*, 2000; Dennis *et al.*, 2001; Fleitmann *et al.*, 2003). Second, an estimation of palaeowater $\delta^{18}O$ can be derived from other sources such as fossil aquifers (Talma and Vogel, 1992, Holmgren *et al.*, 2003), although mixing of the water may influence the results. Third, by comparing the $\delta^{18}O$ values of speleothem before and after a known temperature change, the sign of the relationship between temperature and speleothem $\delta^{18}O$ can be determined, assuming that it is constant throughout the time-series. Common temperature changes used include the transition from the last glacial maximum to the Holocene (Schwarcz, 1986) and the transition from the Little Ice Age to the present day (Holmgren *et al.*, 1999).

5.5. Carbon isotopes in speleothems as a palaeovegetation proxy

The relative abundance of C_3 and C_4 plants in modern-day South Africa is strongly influenced by the existence of two seasonally distinct climate systems (Vogel *et al.*, 1978; Lee-Thorp and Talma, 2000). C_4 grasses dominate the grassy vegetation of those areas receiving summer rainfall in the eastern and interior

regions of South Africa, with the exception of the high mountains along the eastern escarpment (Vogel *et al.*, 1978). C_3 grasses occur in the Fynbos region to the south west of South Africa, which receives the majority of its rainfall in the winter. A mixture of C_3 and C_4 grasses is found in the transition zone between the winter and summer rainfall zones. A shift in the range and intensity of the dominant atmospheric circulation systems would therefore change the distribution of these two vegetation systems (Lee-Thorp and Talma, 2000).

The photosynthetic yield of C_3 vegetation is restricted by high temperatures and low concentrations of atmospheric CO_2, due to the increase of photorespiration under these conditions (Ehleringer *et al.*, 1997). The C_4 photosynthetic pathway is effectively a CO_2-concentrating mechanism that enables C_4 plants to survive in these high temperature and low atmospheric pCO_2 conditions (Cerling *et al.*, 1998). Under lower temperatures and higher atmospheric pCO_2 conditions, C_3 plants out-compete C_4 plants due to the metabolic expense of the C_4 photosynthetic mechanism. The proportion of C_4 plants in an ecosystem is predictable if the conditions of atmospheric pCO_2 and temperature are known (Ehleringer *et al.*, 1997, Cerling *et al.*, 1997). This ecophysiology of C_3 and C_4 vegetation explains the restriction of C_4 grasses to the warm summer rainfall region and C_3 grasses to the cold winter rainfall region of present day South Africa (Vogel *et al.*, 1978, Lee-Thorp and Talma, 2000).

As a consequence of the C_4 photosynthetic pathway, the carbon isotope composition of C_4 plant matter is enriched in ^{13}C (O'leary, 1981; 1988), enabling the presence of C_4 photosynthesis to be detected in organic and inorganic carbon species derived from biological processes. The proportion of C_3 and C_4 vegetation in past ecosystems can be determined in fossil teeth (e.g. Lee-Thorp *et al.*, 2000) and sedimentary carbonates (e.g. Cerling *et al.*, 1989), as long as the effects of diagenetic alteration can be discounted. With reliable palaeo-temperature estimates, the proportion of C_4 plants within a sedimentary record can also be used as a proxy for atmospheric pCO_2 (Boom *et al.*, 2002).

5.6. Methods

5.6.1. Sampling, Stratigraphy and Chronology

Two continuous sequences of primary calcite flowstone (see Chapter 3) were obtained from palaeo-caves in the Makapansgat Valley (Limpopo Province) of South Africa. A 1.22 m long sequence was taken from the basal flowstone deposit of the Makapansgat Limeworks (referred to as Member 1b in Partridge, 2000; Partridge *et al.*, 2000) and a 2.41m long sequence from the basal flowstone of Buffalo Cave (Kuykendall *et al.*, 1995; Herries *et al.*, *in press*), situated 1 km to the west of the Makapansgat Limeworks. The basal flowstone unit (Member 1b) of the Makapansgat Limeworks consists of two flowstone bosses of up to 20 meters wide and approximately 10 m high (Latham *et al.*, 2003). The deposit was extensively mined in the early twentieth century, leaving disconnected outcrops of the flowstone which are now difficult to place within the stratigraphy of the unit (Latham *et al.*, 1999; Latham *et al.*, 2003). Therefore selected samples of Member 1b were taken from different localities within the cave to determine any isotopic trends or variability within the flowstone. All sequences and samples were composed of primary calcite deposited in sub-aerial conditions, as determined by the dominance of the columnar calcite fabric (see Chapter 3).

The age scale used in this study is based on the geomagnetic polarity reversals and faunal correlations of Partridge *et al.* (2000), Herries (2003) and Herries *et al.* (*in press*). The Member 1b basal flowstone of the Makapansgat Limeworks cannot be directly dated using palaeomagnetism because the flowstone is very pure and lacks detrital iron oxides. The Member 2 sediments unconformably overlying Member 1b flowstones are dated by palaeomagnetism to approximately 4 Ma (Partridge *et al.*, 2000 and Herries *et al.*, in press), giving the Member 1b flowstones a minimum age of approximately 4 Ma. Member 1b flowstones sampled in this study come from the Original Ancient Entrance repository immediately below the unconformable contact with Member 1b, and from the Collapsed Cone repository where a large block of Member 1b flowstone has detached from flowstone attached to the roof of the mined cave (see Appendix 1.). The sampled fallen block is derived from the outer layers of the basal stalagmite boss, indicating a younger age than the majority of the mined Member 1b deposit. The maximum age of the sampled specimens of Member 1b can

currently only be estimated based on speleothem growth rates, but are unlikely to be older than 5 Ma.

The Buffalo Cave flowstone is the basal unit of the Buffalo Cave sedimentary sequence. The flowstone appears to represent one phase of depositon, with the exception of a possible hiatus at a depth of 0.39 m (see Fig. 5.3), as indicated by a thin layer of bat guano. The cave sediments are dated using palaeomagnetism constrained by faunal correlation (Herries, 2003; Herries *et al.*, *in press*). Mud-rich sediments 3 m above the unconformable contact overlying the top of the flowstone sequence have a reversed polarity and have been placed within the Jaramillo event (0.99-1.07 Ma). A sample taken from the mud-rich sediments 30 cm above the Buffalo Cave flowstone has a reversed polarity typical of the Matuyama epoch, but its age cannot be constrained. The only sample within the Buffalo Cave flowstone to be sufficiently mud-rich for palaeomagnetic analysis is from 25 cms above the base of the flowstone sequence and has a normal polarity (Herries, 2003) indicative of the Olduvai chron (1.79-1.95 Ma). Using this limited palaeomagnetic data, it can be inferred that the Buffalo Cave flowstone was deposited in the early Pleistocene and was deposited over a period of less than a million years. This study refines the chronology of the Buffalo Cave flowstone by combining the existing magnetostratigraphic evidence with data from UV-fluorescent annual banding of organic matter and from the orbital-tuning of the stable isotope data.

5.6.2. Stable Isotope Methods

The Buffalo Cave flowstone (2.41 m long, 482 samples) and Collapsed Cone flowstone (1.22 m long, 239 samples) were sampled continuously for stable isotope analysis at 5 mm intervals using a diamond-tipped micro-drill with a diameter of 1.5 mm. The powdered samples were pre-treated in an oxygen plasma asher to remove organic matter. The samples were then reacted to completion at 90°C with 100% phosphoric acid using an automated VG Isocarb preparation system. The CO_2 released by the reaction was cryogenically purified prior to the measurement of carbon and oxygen isotope ratios on an automated VG SIRA 12 mass spectrometer at the University of Liverpool. All data were corrected for ^{17}O effects following Craig (1957). Carbon and oxygen isotope data are reported in conventional delta (δ) notation in "parts per mil" (‰) relative to

V-PDB (Coplen, 1995). Accuracy and reproducibility of the isotopic analyses was assessed by replicate analysis of BCS2 (internal calcite standard) against NBS-19 and two internal calcite standards. Long-term laboratory reproducibility is better than 0.1‰ for both isotope ratios.

5.6.3. UV-fluorescent banding methods

Additional dating evidence for the Buffalo Cave flowstone comes from measurement of UV-fluorescence bands of organic matter within the flowstone. Seven thin sections were cut from the top to the base of the Buffalo Cave flowstone and 3 thin sections from the Collapsed Cone flowstone. Each thin section was examined for luminescent bands using standard UV microscopy techniques (Baker *et al.*, 1993). Band widths were measured using a Zeiss Axiotech reflected light microscope with mercury vapour light source with a 320-420 nm excitation filter, black and white CCD camera and Image Pro Plus image analysis software.

The resolution of growth bands varied depending on the quality of the polish, so growth band measurements were taken from localised highly polished areas (see Fig. 5.4). Some regions of the flowstone lacked resolvable luminescent banding, probably because the UV-source was not powerful enough to excite weak luminescence (Baker *et al.*, 1993). Luminescent band-widths were measured at a magnification of x100, the highest magnification available. At lower magnifications, closely spaced laminae could not be resolved and appeared similar to individual luminescent bands. By measuring bandwidths at a magnification of x100, this problem was reduced although there were still multiple laminae visible that could not be resolved any further. In portions of the flowstone with greater growth rates, the luminescent banding was regularly spaced and produced a sinusoidal shaped greyscale curve, common in annual banding (Baker *et al.*, 1993 and 1999). If the UV banding can be interpreted as annual growth banding, then the measured band-widths can be used to approximate the growth rate of the speleothems. The estimated annual growth rates can then be combined with the spectral analysis and palaeomagnetic evidence to develop a high-resolution chronology for the Buffalo Cave flowstone.

5.6.4. Time-Series Analysis Methods

Spectral analysis

Spectral analysis was used to test for the presence of regular sedimentary cyclicity (as a function of thickness), which can be diagnostic of orbital-climatic cyclicity (Weedon, 1999). Trends in the mean and variance of a depth-series distort the spectral power at low frequencies (Weedon, 2003), so the data was detrended using a linear least-squares regression line (Press *et al.*, 1992) to remove the non-stationary mean. Spectral estimation was determined by the discrete Fourier transform method, using the Lomb-Scargle algorithm for irregularly spaced data (Press *et al.*, 1992). Statistical confidence intervals were determined by the robust first-order autoregressive method of Mann & Lees (1996). The Buffalo Cave flowstone spectra confirmed a change in accumulation rates that was obvious visually within the isotope records at a depth of approximately 1.29 m (see Fig. 5.3.). Individual spectra were then plotted for the isotopic data above and below the 1.29 m datum (Fig. 5.3.).

Cross-spectral analysis

The relationship between the $\delta^{13}C$ and $\delta^{18}O$ depth-series was assessed using coherency and phase spectra for both the Collapsed Cone and Buffalo Cave flowstones. Coherency is a measure of the similarity of the amplitude variations in two time-series determined at particular frequencies and ranges from 0 (zero coherency) to 1.0 (perfectly coherent). A phase spectrum describes the average difference in phase between two time-series at the frequencies of significant coherence. Phase difference ranges from +180° to -180°, with a zero phase difference indicating oscillations that are "in phase" and ±180° for oscillations that are in "anti-phase". Positive phase indicates that the first series leads the second, and negative phase that the first series lags the second. Coherency and phase spectra were based on the discrete Fourier transform spectral estimates for irregularly spaced data, and were generated using a modification (by G.P. Weedon, pers. comm.) of the Bloomfield (1976) algorithm.

Orbital Tuning

Band-pass filtering of the Buffalo Cave flowstone $\delta^{18}O$ depth-series at wavelengths of 9 cm (below 1.29 m depth) and 16 cm (above 1.29 m depth) was used to isolate the cycles associated with the shortest wavelength spectral peaks (see Fig. 5.6.b). Band-pass filtering was performed using the algorithm of Ifeachor & Jervis (1993) to implement the method of McClellan *et al.* (1973). Tuning of the filtered $\delta^{18}O$ record was based on dating constraints (magnetostratigraphy and UV-annual banding) and then on visually maximizing the agreement between the amplitude modulation of the filtered data with the amplitude modulation of Early Pleistocene solar insolation at 24° South (using the orbital solution of Berger and Loutre, 1991).

5.7. Results

5.7.1. Speleothem carbonate isotope results

Carbon isotope values from the Buffalo Cave flowstone range from –8.2‰ to –2.6‰ with a mean value of -5.0‰ (n = 483), whereas carbon isotope values from the Collapsed Cone range from –8.8‰ to –7.1‰ with a mean value of –8.1 (n = 239). The samples taken from elsewhere in the Makapansgat Limeworks Member 1 sequence (Original Ancient Entrance, North Alcove and the Entrance Quarry; see Section 5.6.1.) show $\delta^{13}C$ values ranging from –8.6 to -7.9‰, similar to those from the Collapsed Cone flowstone (see Table 3.2.). The significantly different carbon isotope signatures of the Buffalo Cave and Makapansgat Limeworks Member 1 flowstone records are illustrated by the fact that 96.4% of the Buffalo Cave $\delta^{13}C$ values lie outside the Collapsed Cone $\delta^{13}C$ range of values. Oxygen isotope values from the Buffalo Cave flowstone range from –6.5‰ to –3.4‰ with a mean value of –4.9‰ whereas oxygen isotope values from the Collapsed Cone range from –7.0‰ to –4.5‰ with a mean value of –5.7‰. Twenty one point 9 percent of the Buffalo Cave $\delta^{18}O$ values fall outside of the Collapsed Cone range of $\delta^{18}O$ values. The lower half of the Buffalo Cave record (2.6 m to 1.29 m) has significantly lower $\delta^{13}C$ values (mean = -4.4‰, s.d. = 0.75‰) than the upper half of the record (0 m to 1.29 m; mean = –5.7‰, s.d. = 1.0‰). This carbon isotope shift at 1.29 m punctuates the otherwise stationary oscillations of $\delta^{13}C$ above and below this level (see Fig. 5.3.).

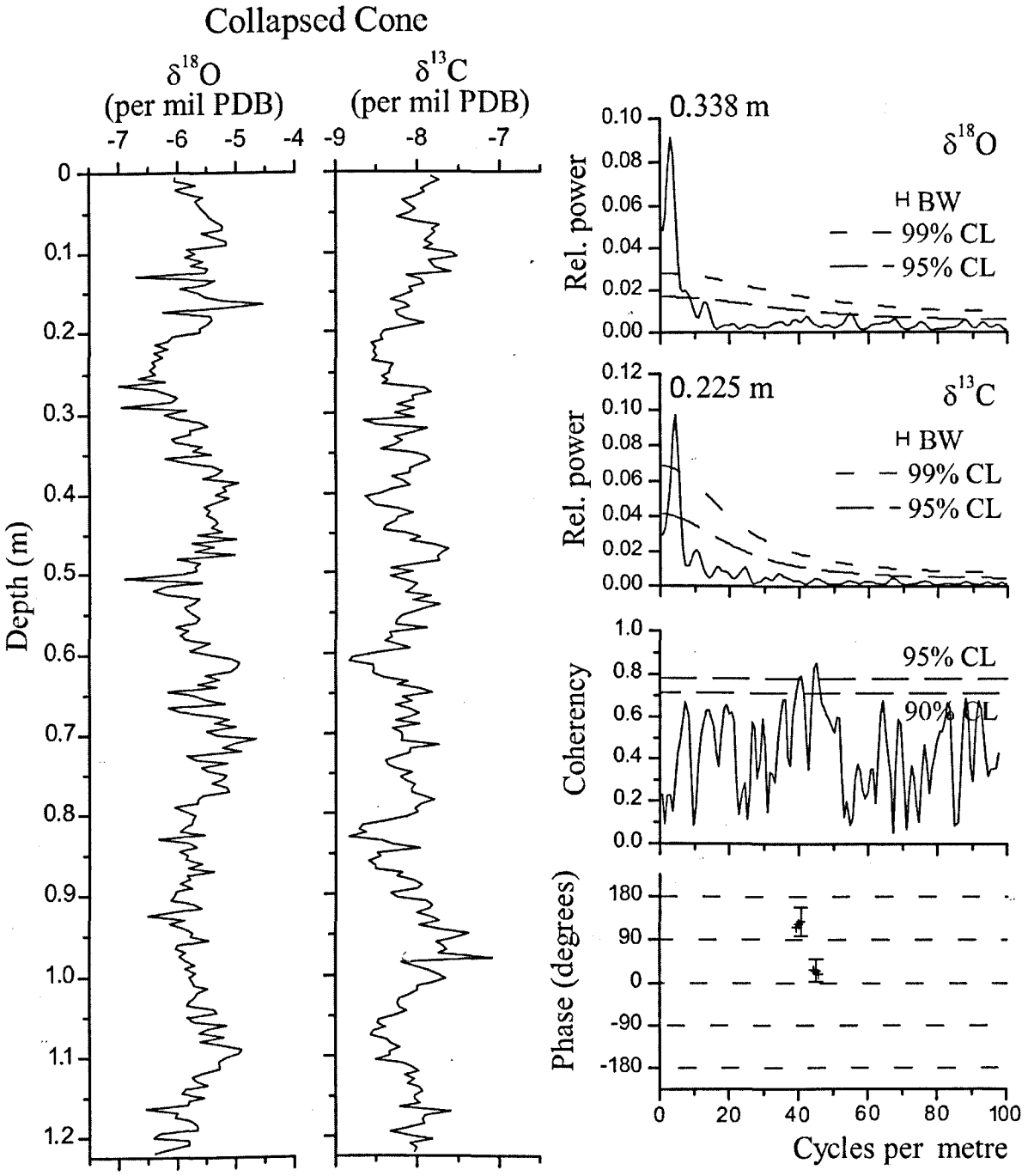

Figure 5.2. Collapsed Cone flowstone $\delta^{18}O$ and $\delta^{13}C$ depth-series, power spectra and cross-spectra. With less than six low-frequency cycles with wavelengths of 33.8 cms for $\delta^{18}O$ and 22.5 cms for $\delta^{13}C$, regular cyclicity of these spectral peaks cannot be demonstrated (see Section 5.7.3.). There are no statistically significant phase relationships at these frequencies. BW = bandwidth; CL = confidence level.

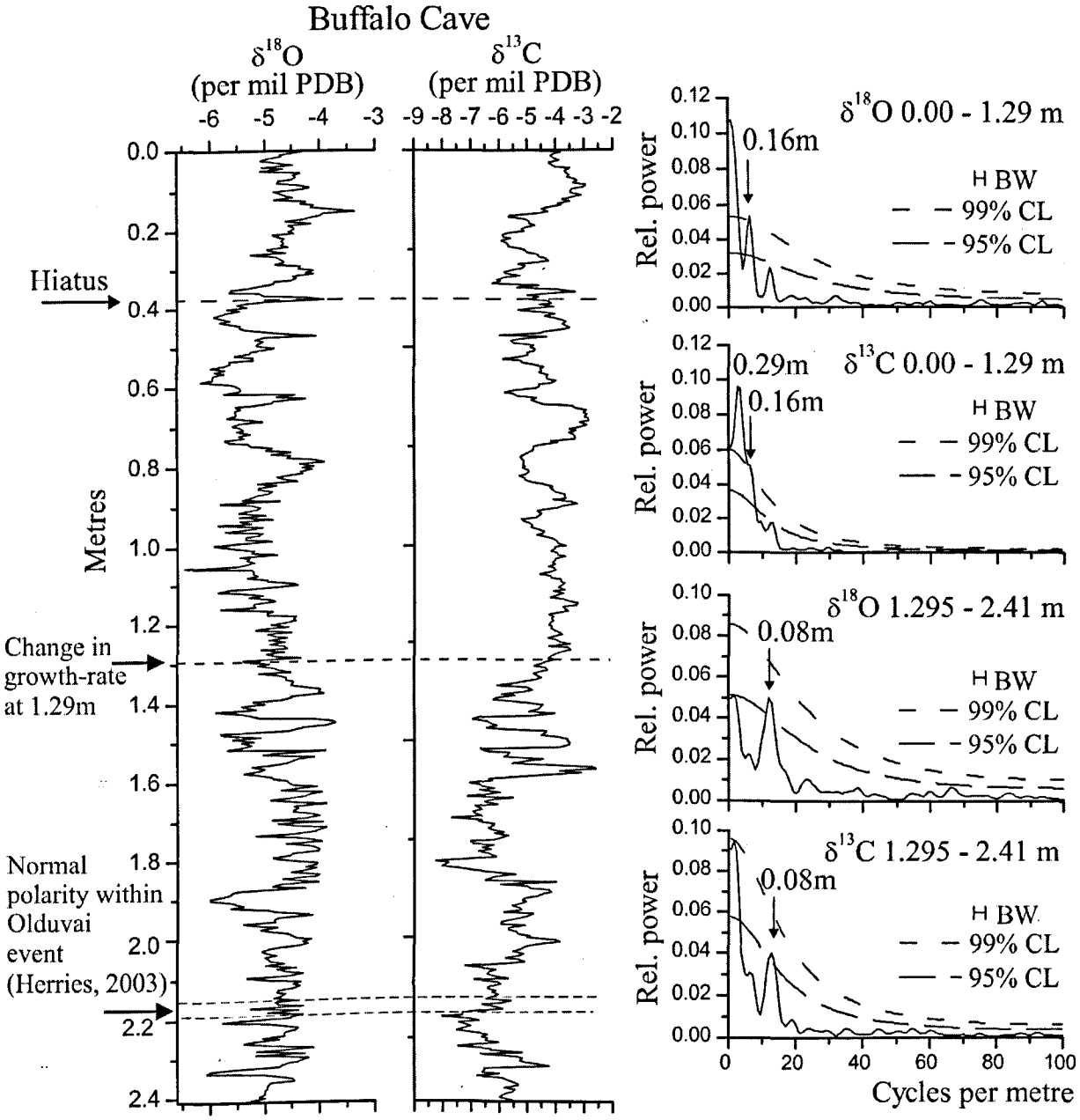

Figure 5.3. Spectral Analyses of Buffalo Cave flowstone $\delta^{18}O$ and $\delta^{13}C$ depth-series. The cycle frequency changes at a depth of 1.29m indicating a change in growth rate above and below this datum. Spectral peaks indicate cycles with wavelengths of 29cm, 16cm and 8cm. There are more than six 16cm and 8cm cycles, indicating regular cyclicity at these wavelengths (Weedon, 2003). Arrow indicates position of the palaeomagnetism sample (depth of 2.15 to 2.19m) placed within the Oluvai event (1.79-1.95Ma) by the magnetostratigraphy of Herries (2003), as discussed in Section 5.6.1. BW = bandwidth; CL = confidence level.

There is a strong negative correlation between $\delta^{13}C$ and $\delta^{18}O$ in the top two thirds of the Buffalo Cave flowstone sequence (Fig 5.3., Fig. 5.8.a and Section 5.7.3.).

5.7.2. UV-fluorescence annual banding results

Luminescent banding was present throughout the Buffalo Cave flowstone but was absent from the Collapsed Cone flowstone. The absence of luminescent banding from the Collapsed Cone flowstone is most likely due to the short wavelength of luminescence excitation (283-340 nm) of the organic matter (see Chapter 4.) that cannot be excited by the long wave UV light source (320-420 nm). Future study of the Collapsed Cone flowstone using a short wave UV light source may reveal luminescent banding, however there is also the possibility that luminescent banding will be shown to be less well developed in this flowstone due to a less seasonal palaeoclimate. The majority of growth bands in the Buffalo Cave flowstone were chevron shaped, reflecting the morphology of individual columnar calcite crystallites (see Fig. 5.4.). The thickness of the growth bands was often greatest in the direction of the long axis of crystal growth.

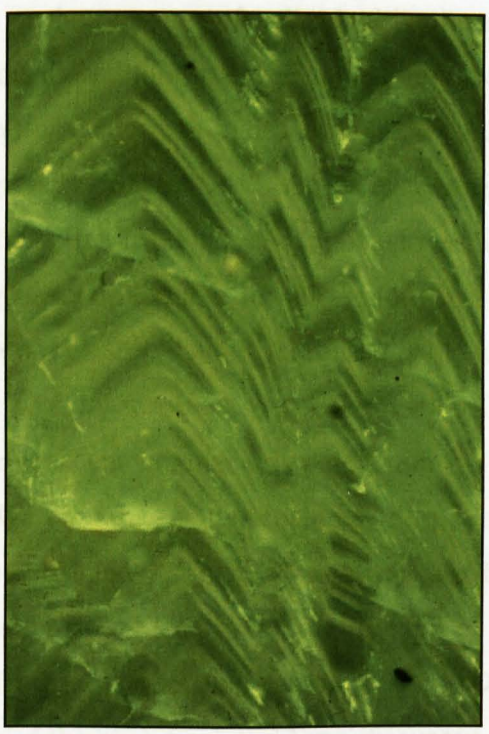

Figure 5. 4. UV growth banding in the Buffalo Cave flowstone. Blurred areas indicate poor polish with less well resolved banding. Some luminescent bands are composed of two or more closely spaced bands. Sample BUFF A; length of view is 0.9mm.

The measured band-widths were divided into two groups, above and below the 1.29 m level (see Fig. 5.5). A two sample T-Test indicates that the band-widths can be grouped into two significantly different populations (C.I. = 94.6) above the 1.29 m level (n = 81; mean = 10.89; standard deviation = 6.40) and below the 1.29 m level (n = 105; mean = 9.24; standard deviation = 4.77). This increase in mean band-width from below to above the 1.29 m level is consistent with the increase in growth rate at 1.29 m inferred from the spectral analysis of the stable isotope data. As discussed below (see Section 5.7.3.), the change in cyclicity in the stable isotope depth series (Fig. 5.3.) from a 16cm cycle above 1.29m to an 8cm cycle below 1.29m is suggestive of a doubling of the growth rate at the 1.29m datum.

The distribution of the 186 measured luminescent band-widths is skewed towards the shorter band-widths (see Fig. 5.5.). This skewed distribution suggests that the large band-widths are artefacts caused by apparently wide UV bands consisting of numerous unresolved UV annual bands. These wide bands can be excluded from the sample by taking the mode, rather than the mean, as the average annual band-width (see Fig. 5.5.).

Reasons for the lack of annual resolution could include a weak organic acid content in these layers or the presence of individual laminae that are too thin to be resolved by the techniques used this study. This phenomenon was observed in the Buffalo Cave flowstone when growth bands were measured at a magnification of x100, the highest magnification available. At lower magnifications, these closely spaced laminae could not be resolved and appeared as individual luminescent bands. By measuring bandwidths at a magnification of x100, this problem was reduced although there were still double laminae visible with a width of a few microns that could not be fully resolved. As discussed by Baker *et al.* (1999), the presence of double luminescent laminae in speleothem may either indicate intra-annual fluxes of dissolved organic matter such as storm events, or it may indicate two closely spaced annual bands. There is also the possibility of short hiatuses within the flowstone which could lead to the observation of less annual bands, and an under-estimation of the true time span of the deposit. Due to the slow growth rate of this flowstone and the analytical problems discussed above, the counting of luminescent bands should be considered to provide a minimum estimate of the true number of years of flowstone deposition.

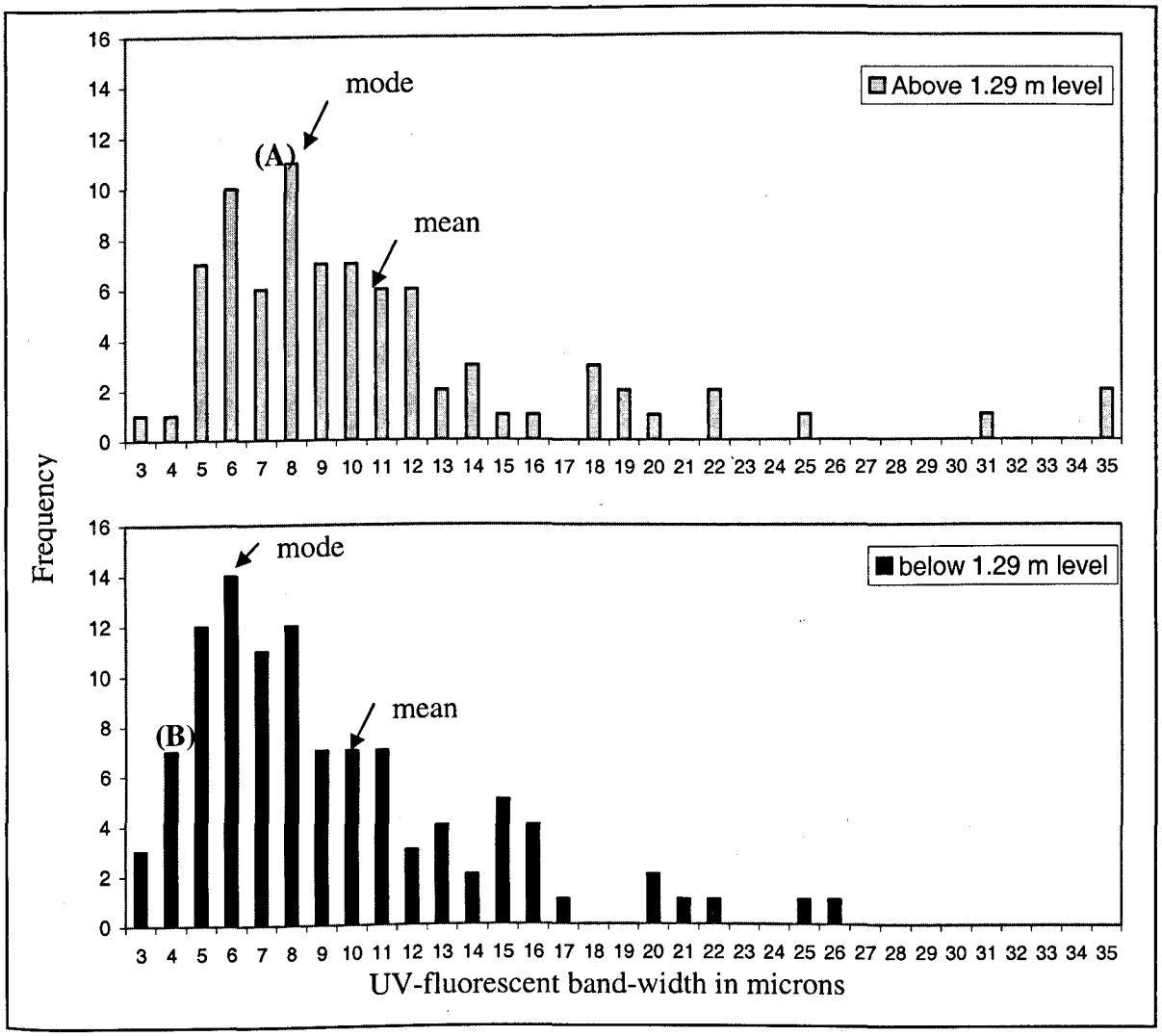

Figure 5.5. Buffalo Cave UV-fluorescence band-width frequency in microns, above and below the 1.29 m level. Mean and mode of both data sets are indicated. A two sample T-Test indicates that the two data sets are significantly different at the 94.6% Confidence Interval. It is likely that the tails of the skewed distributions represent thicker UV bands composed of unresolved growth layers (see Section 5.7.2.). (A) indicates the mean annual band-width of approx. 7.6 μm required above the 1.29 m level for the 16 cm and 29 cm cyclicities to be assigned to the ca. 20 ka cycle of orbital precession and the 40 ka cycle of obliquity respectively (see Section 5.7.4. and Table 5.1.). (B) indicates the mean annual band-width of 4 μm below the 1.29 m level required for the 8 cm cyclicity to be assigned to the ca. 20 ka cycle of orbital precession (see Section 5.7.4. and Table 5.1.).

5.7.3. Time-Series Analysis results

Collapsed Cone flowstone

The Collapsed Cone flowstone has spectral peaks above the 95% confidence level with wavelengths of 34 cm for $\delta^{18}O$ and 23 cm for $\delta^{13}C$ within the 122 cm depth-series (see Fig. 5.2.). At least six cycles at a particular wavelength are required to

demonstrate regular cyclicity (Weedon, 2003), so with only 3.6 and 5.3 oscillations respectively of these low frequency cycles, it is not possible to identify regular cyclicity within the Collapsed Cone flowstone depth-series at these frequencies. The coherency and phase relationships between $\delta^{18}O$ and $\delta^{13}C$ do not exceed the 90% confidence level at the 34 cm or the 23 cm cycle frequencies (see Fig. 5.2.). Therefore, with no regular cyclicity within the depth-series and no phase relationship between $\delta^{18}O$ and $\delta^{13}C$, time-series analysis of the Collapsed Cone flowstone cannot be taken any further with the existing dataset.

Buffalo Cave flowstone

The three spectral peaks above the 95% confidence level observed in the Buffalo Cave flowstone stable isotope depth-series have wavelengths of 29 cm and 16 cm above the 1.29 m datum and 8 cm below the 1.29 m datum (see Fig. 5.3.). There are more than six 16 cm and 8 cm cycles within the isotopic depth series, indicating regular periodicity at these frequencies (Weedon, 2003).

A visual comparison of the $\delta^{13}C$ and $\delta^{18}O$ depth-series for the Buffalo Cave flowstone (shown in Fig. 5.3.) indicates a dominant negative correlation (phase of ±180) above a depth of 1.6 m and the loss of this relationship below 1.6 m. Therefore, to investigate the relationship between $\delta^{13}C$ and $\delta^{18}O$ using cross-spectral analysis, the tuned Buffalo Cave record was divided into two sections above and below 1.6m. Figure 5.8a shows that above 1.6 m, the two isotopic records are coherent at both the precession (ca. 21 ka; 16 cm cycle) and obliquity (41 ka; 29 cm cycle) frequencies. At the precession frequency the two records are in anti-phase (phase = ±180°), but at the obliquity frequency $\delta^{18}O$ lags $\delta^{13}C$ by half a cycle (phase = -90°). Below 1.6m (Fig. 5.8.b), both the precession and obliquity frequencies are coherent and show different phase relationships. $\delta^{18}O$ leads $\delta^{13}C$ by half a cycle (phase = +90°) at the precessional frequency whereas at the obliquity frequency, the two records are approaching anti-phase (phase = +130° to +180°).

5.7.4. Establishing a Buffalo Cave Flowstone Chronology

The chronology of the Buffalo Cave flowstone shown in Figs 5.6., 5.7., 5.9. is based on geomagnetic polarity reversals, orbital tuning of spectral peaks and estimates of growth rates based on UV annual banding. By assuming that each UV-growth band represents one year's growth (as is documented in well dated speleothems – e.g. Baker *et al.*, 1993; Shopov *et al.*, 1994; Baker *et al.*, 1999), the mean UV band-width gives an approximation of the growth rate of the speleothem. The UV banding growth rate should fit with the growth rate inferred from palaeomagnetism and when used to convert the spectral peaks from cycles per cm to cycles per kilo-year should approximate Milankovitch periodicities.

Table 5.1. shows the expected mean annual growth rate of the flowstone if the three spectral peaks observed in the Buffalo Cave flowstone stable isotope depth-series above the 95% confidence level (wavelengths of 29 cm, 16 cm and 8 cm) are attributed to the precession, obliquity or eccentricity Milankovitch periodicities. In the top half of the flowstone (0-1.29 m), two significant spectral peaks, the 29 cm and 16 cm cycles, dominate the isotopic depth-series. The presence of two co-occurring spectral peaks aids in identification of the dominant Milankovitch periodicities. If the 29 cm and 16 cm cycles are attributed to the ca. 20 ka and 40 ka Milankovitch periodicities, then the speleothem must have a mean annual growth rate of 7.25 μm and 8 μm respectively (see Table 5.1.). These predicted mean annual growth rates lie between the mode (6 μm) and median (8 μm) values of observed UV annual band-widths above the 1.29 m level of the Buffalo Cave flowstone (see Fig. 5.5.). The only other possibility is that the 29 cm and 16 cm cycles represent the 100 ka and 40 ka Milankovitch periodicities respectively. This would require a low mean annual growth-rate of approximately 3.5 μm and would require eccentricity forcing (not observed in any palaeoclimate records older than 0.9 Ma – e.g. Shackleton, 1995).

If the entire flowstone was dominated by obliquity forcing of the 16cm and 8 cm cycles, then this would indicate that the entire flowstone was deposited over a period of approximately 880 ka (22 cycles at 40 ka), contrary to the palaeomagnetic evidence. If the top half of the flowstone (0-1.29 m) was dominated by the obliquity cycle and the bottom half of the flowstone (1.295-2.60 m) was dominated

Buffalo Cave Observed Spectral Peaks		Milankovitch Periodicities		
		100 ka	40 ka	20 ka
0 – 1.29 m	29 cm	2.9 μm	**7.25 μm**	14.5 μm
	16 cm	1.6 μm	4.0 μm	**8 μm**
1.295–2.60 m	8 cm	0.8 μm	2.0 μm	**4.0 μm**

Table 5.1. Calculated mean annual band-widths required for the Buffalo Cave depth-series spectral peaks to be attributed to individual Milankovitch periodicities. The calculated mean annual band-widths in bold of ~7.6 μm and 4 μm approximate the measured modal UV band-widths above and below the 1.29 m datum (Section 5.7.4 and Figure 5.5). The other calculated annual band-widths lie outside the range of measured UV band-widths. The co-occurring 29 cm and 16 cm cycles in the top half of the flowstone (0 - 1.29 m) can only be attributed to the 40 ka and 20 ka Milankovitch periodicities based both on the magnetostratrgraphy age-constraints (see Section 5.7.4) and due to the measured UV band-widths. Attributing the 8 cm cycle in the bottom half of the flowstone (1.295-2.60 m) to the shortest Milankovitch periodicity (20 ka) indicates a change in growth rate between the top and bottom portions of the flowstone.

by the precessional cycle, the flowstone would have been deposited over a period of approximately 660 ka, in agreement with the palaeomagnetic evidence. However, this would require a change in the dominant Milankovitch cycles at 1.29m, an event which has not been observed in any contempory palaeoclimate records (e.g. Shackleton, 1995).

The bottom half of the Buffalo Cave flowstone (1.295-2.60 m) has only one significant spectral peak, with a wavelength of 8 cm (see Fig. 5.3.). This short cycle is most likely to represent orbital precession, the shortest Milankovitch cycle (ca. 20 ka), and if so, it would have a mean annual growth rate of 4.5 μm (see Fig. 5.4.). This mean annual growth rate lies within the range of measured UV band-widths below the 1.29 m level (see Fig. 5.5.), but is located towards the short band-width end of the distribution. However, as discussed above, this may be because the true growth rate is slower than is indicated by the mean measured UV band-width due to poorly resolved banding and small hiatuses. Attributing both the 16 cm cycles (0-1.29 m) and the 8 cm cycles (1.295-2.60 m) to orbital precession results in a total of twenty-two precession cycles (21 ka) and indicates that the flowstone was precipitated over a period of approximately 460 ka, in agreement with the palaeomagnetic evidence.

If the 16 cm cycle in the top half of the flowstone and the 8 cm cycle in the bottom half of the flowstone are both attributed to the precession cycle (ca. 21 ka), then the bottom half of the flowstone must have precipitated with a slower growth rate than the top half. As discussed below and in Chapter 4, the carbon isotope values and Mg/Ca ratios of the Buffalo Cave flowstone also change at a depth of approximately 1.29 m, indicating a significant climatic and hydrologic change at this point in the record. It is possible that these changes are associated with an increase in the growth rate of the flowstone at 1.29 m.

The chronology of the Buffalo Cave flowstone can be further refined using the solar insolation solution of Berger and Loutre (1991) for mid-month January insolation at 24° South, and the existing magnetostratigraphy of Herries (2003). As discussed above, the palaeomagnetic stratigraphy of Herries (2003) places the Buffalo Cave flowstone between approximately 1.2 Ma and 2 Ma, based on the identification of the Olduvai event (1.79-1.95 Ma) 25 cm above the base of the flowstone (Fig. 5.3.). With the depth-series anchored to the Olduvai event at a depth of 2.15-2.19 m, there is only a 160 ka window into which the isotopic records can be tuned to the insolation time-series. The insolation solution at 24° South between 1.2 and 2.0 Ma (Berger and Loutre, 1991) is a close approximation of the orbital precession signal at this latitude. The record of orbital precession is marked by two high-amplitude episodes of eccentricity-modulation ending at 1.8 Ma and 1.7 Ma (see Fig. 5.6.c) that are clearly evident in the amplitude variations of the $\delta^{18}O$-filtered Buffalo Cave record (see Fig. 5.6.b).

Inability to separate the temperature signal from variations in the $\delta^{18}O$ composition of precipitation has hindered the identification of glacial versus interglacial periods within the Buffalo Cave flowstone $\delta^{18}O$ record (Sections 5.4 and 5.8.1). The orbital tuning shown in Figs. 5.6, 5.7 and 5.9 has been based on the assumption of a positive relationship between flowstone $\delta^{18}O$ and solar insolation which, as discussed in Section 5.8.1, may or may not be correct. This uncertainty does not affect the accuracy of the spectral analyses or the identification and interpretation of orbital forcing in the Buffalo Cave flowstone.

5.7.5. Spectral Analysis of Orbitally-Tuned Buffalo Cave flowstone

Once the filtered $\delta^{18}O$ depth series has been tuned to orbital precession (the dominant component of insolation at 24° South) and converted to a time series (Fig. 5.6. and Section 5.7.4), spectral power was re-analysed. As shown in Figure 5.7., the post-tuning spectral peaks are better resolved from background noise than the pre-tuning spectral peaks of Figure 5.3. The post-tuning precessional signal resolves into two components (22.8 ka and 19.4 ka), and both the precession and obliquity signals (40 ka) have increased power relative to the background. Pisias (1983) demonstrated using synthetic time-series that the tuning process does not artificially induce spectral power increases at the frequency of the tuned component relative to any other frequency; nor does the tuning process produce artificial spectral power increases at non-tuned frequencies. Therefore, the orbital tuning process is considered a valid technique for refining the time scale of geological records (Kominz and Pisias, 1979; Kominz *et al.*, 1979; Pisias, 1983) and can be used to identify the orbital signal within a time-series. Spectral analysis of the orbitally-tuned Buffalo Cave flowstone time-series indicates that the $\delta^{13}C$ and $\delta^{18}O$ records are dominated by different orbital parameters (Fig. 5.7.). The $\delta^{18}O$ record is dominated by orbital precession (19-23 ka) whereas the $\delta^{13}C$ record is dominated by the obliquity signal (40 ka).

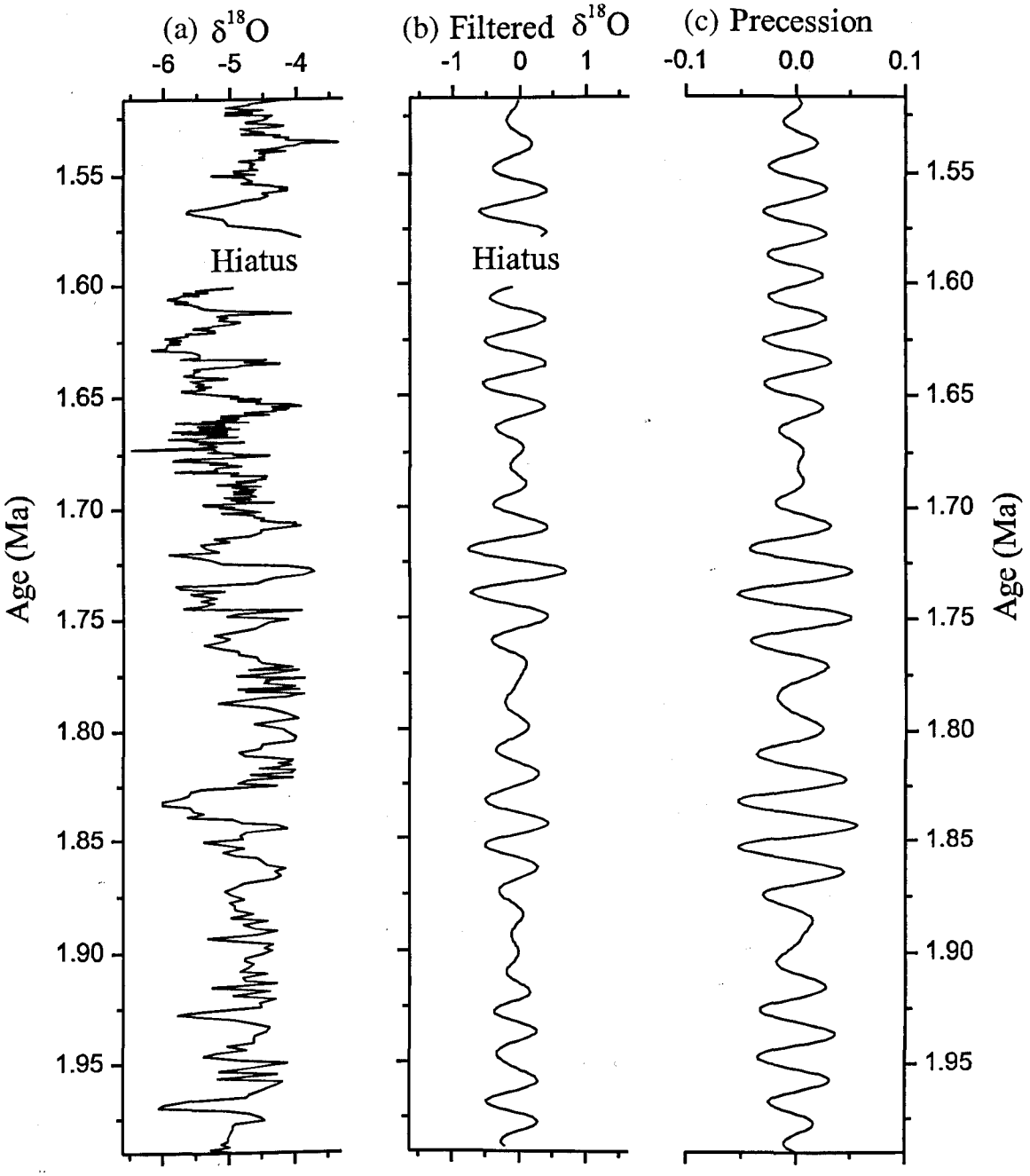

Figure. 5.6. Buffalo Cave flowstone $\delta^{18}O$ time series filtered and tuned to orbital precession at 24° South between 1.5 Ma and 2 Ma. (a) Buffalo Cave $\delta^{18}O$ time series (b) $\delta^{18}O$ time series filtered at wavelengths of 16cm (0-1.29m) and 8 cm (1.295-2.40 m) (c) Orbital precession at 24° South between 1.52 Ma and 1.98 Ma based on the orbital solution of Berger and Loutre (1991).

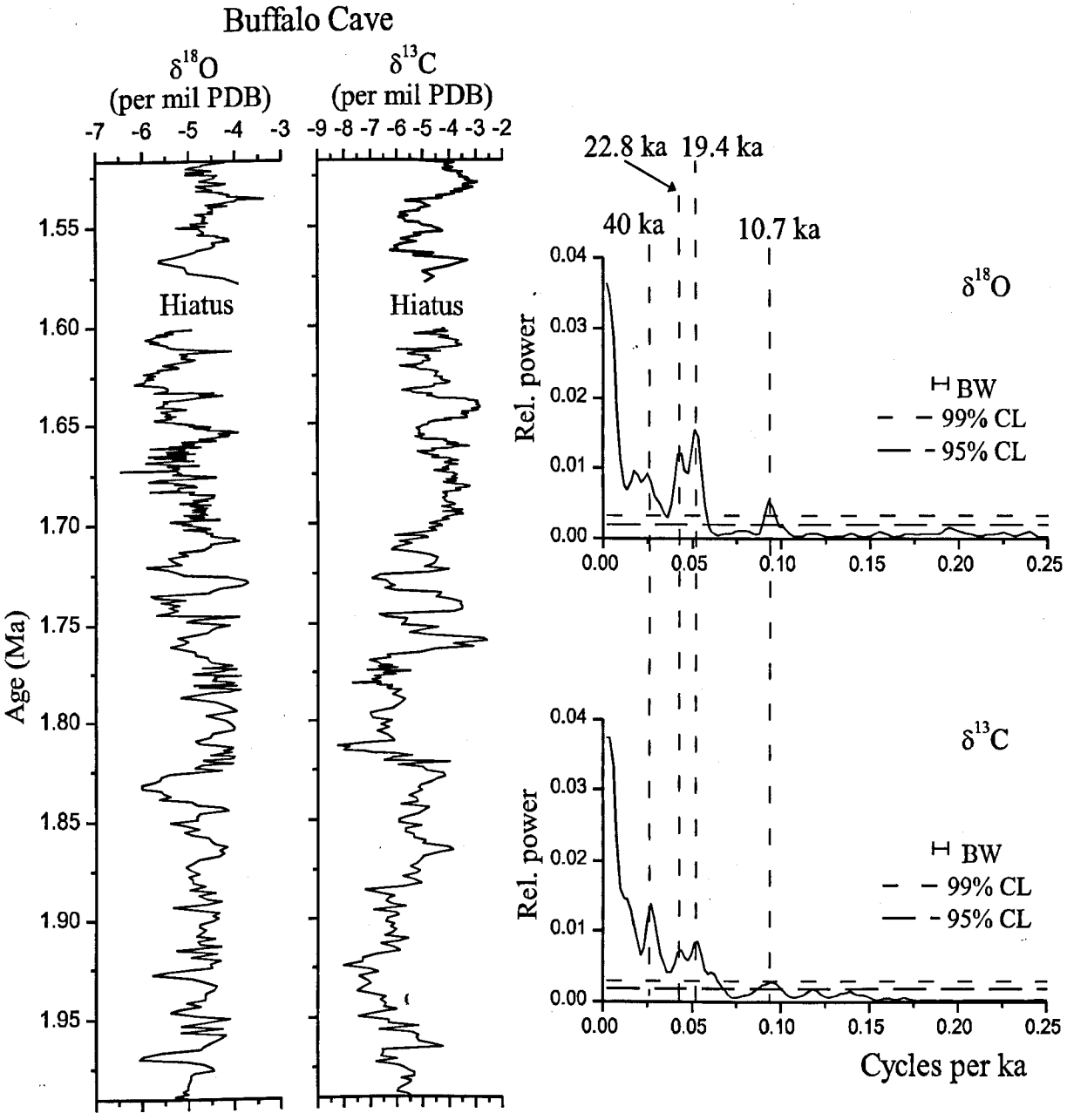

Figure 5.7. Buffalo Cave flowstone $\delta^{18}O$ and $\delta^{13}C$ time series, and spectral analysis of the orbitally-tuned time-series. Well-defined spectral peaks at 40 ka and 19-23 ka are not a function of the tuning process (Pisias, 1983) and represent a genuine orbital signal. The 40 ka obliquity cycle is the dominant periodicity in the $\delta^{13}C$ record whereas the ca. 20 ka precessional cycles dominate the $\delta^{18}O$ record. See Section 5.8.3. for a discussion of the different forcing mechanisms controlling these two climatic proxies. BW = bandwidth; CL = confidence level.

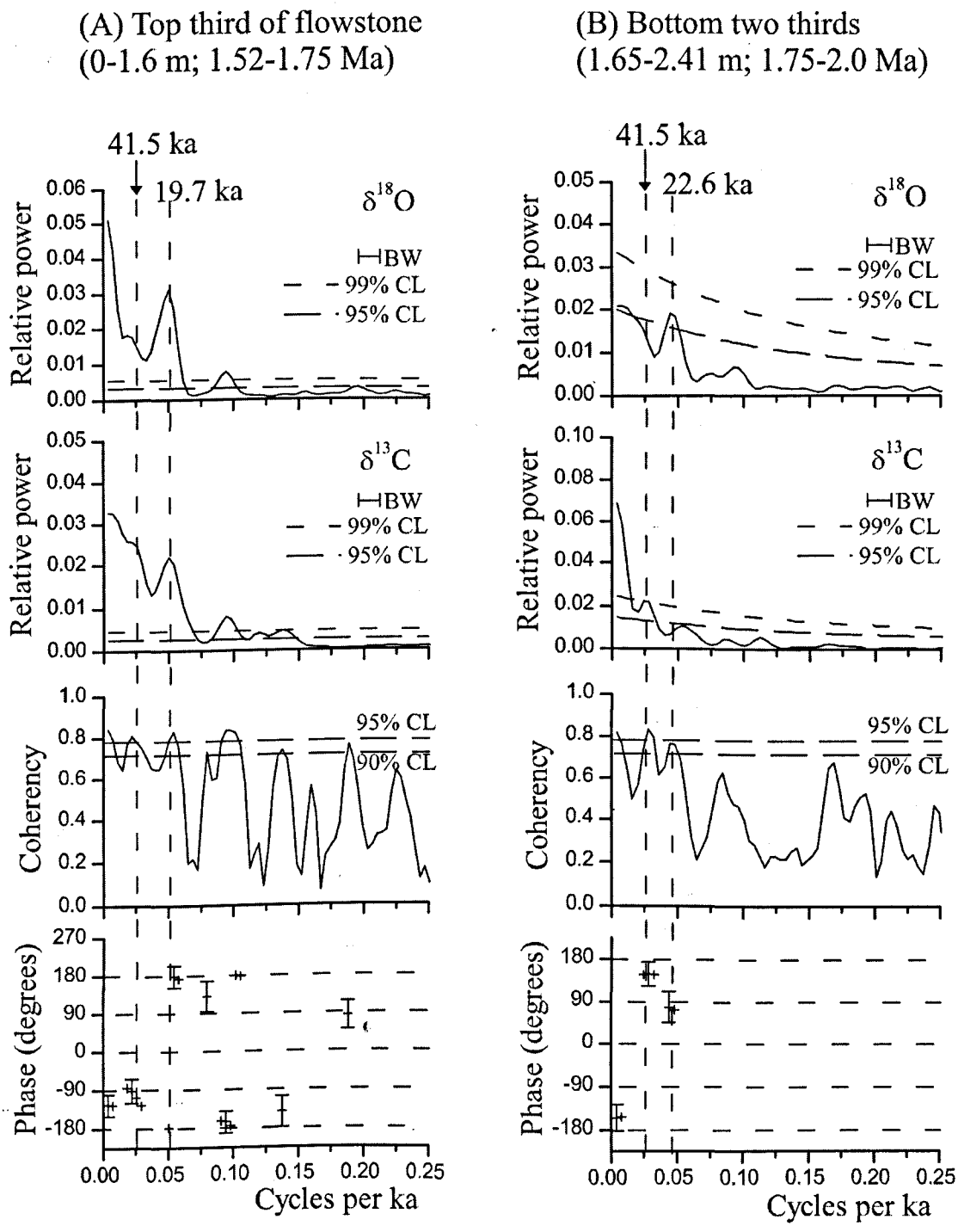

Figure 5.8. Coherency and phase relationships between $\delta^{18}O$ and $\delta^{13}C$ of the Buffalo Cave flowstone in (a) the top two thirds of the flowstone (0-1.6 m; 1.52 - 1.75 Ma) and (b) the bottom third of the flowstone (1.65-2.41 m; 1.75 – 2.0 Ma). Phase relationships occur above the 90% confidence level above and below the 1.29 m datum at both the ca. 20 ka and 40 ka periodicities. (a) indicates an anti-phase relationship at the ca. 20 ka periodicity. At the 40 ka periodicity, $\delta^{13}C$ leads $\delta^{18}O$ by approximately half a cycle. (b) At the ca. 20 ka periodicity, $\delta^{18}O$ leads $\delta^{13}C$ by approximately half a cycle. There is an approximately anti-phase relationship at the 40ka periodicity. BW = bandwidth; CL = confidence level.

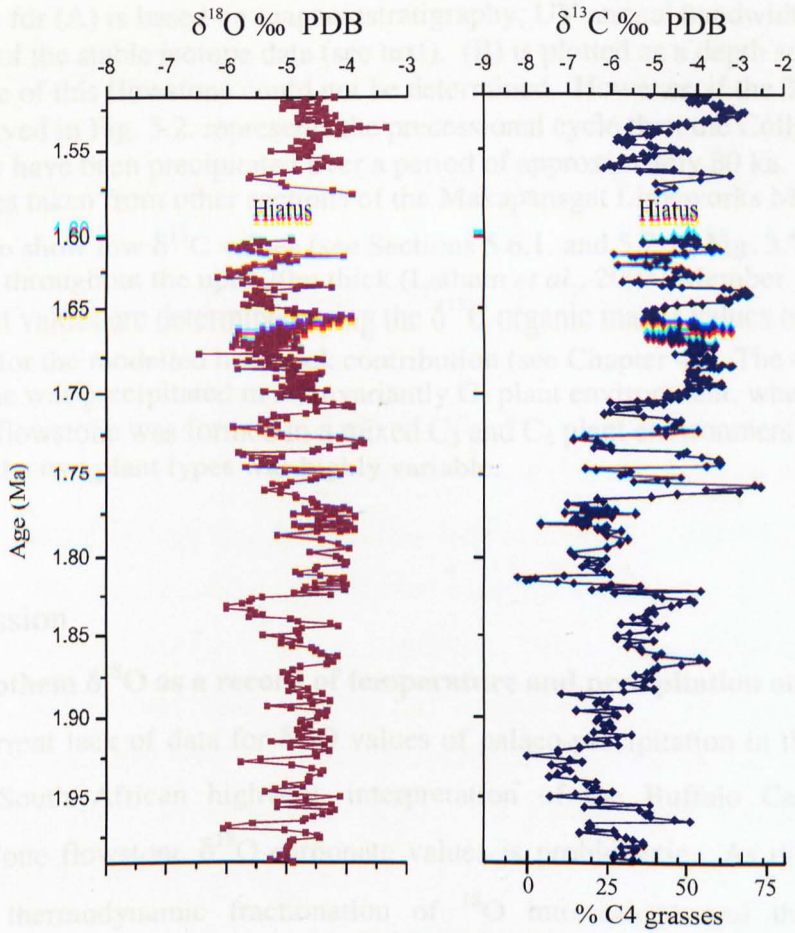

(A) lower Pleistocene

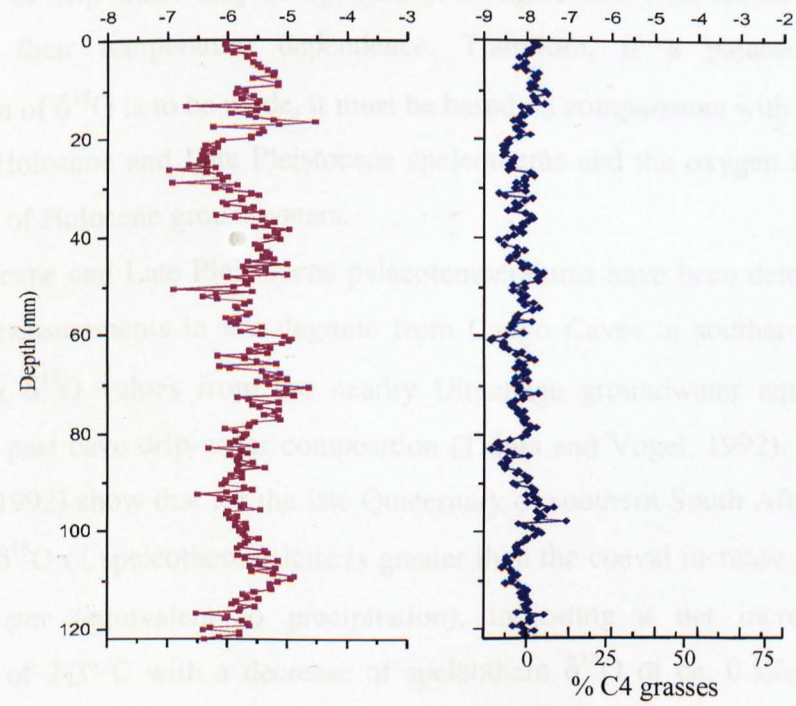

(B) late Miocene / early Pliocene

Figure 5.9. (A) Buffalo Cave flowstone and (B) Collapsed Cone flowstone stable isotope time-series and inferred proportions of C_4 grasses determined from $\delta^{13}C$ values. (continued..)

The time scale for (A) is based on magnetostratigraphy, UV annual bandwidths and orbital tuning of the stable isotope data (see text). (B) is plotted as a depth series because the growth-rate of this flowstone could not be determined. However, if the 33.8 cm cyclicity observed in Fig. 5.2. represents the precessional cycle then the Collapsed Cone flowstone may have been precipitated over a period of approximately 80 ka. Stable isotope samples taken from other sections of the Makapansgat Limeworks Member1 flowstones also show low $\delta^{13}C$ values (see Sections 5.6.1. and 5.7.1.; Fig. 3.7.) indicating invariant $\delta^{13}C$ throughout the upto 20m thick (Latham *et al.*, 2003) Member 1 sequence. The % C_4 plant values are determined using the $\delta^{13}C$ organic matter values of Chapter 4 and corrected for the modelled host-rock contribution (see Chapter 4.). The Collapsed Cone flowstone was precipitated in an invariantly C_3 plant environment, whereas the Buffalo Cave flowstone was formed in a mixed C_3 and C_4 plant environment in which the proportion of the two plant types was highly variable.

5.8. Discussion

5.8.1. Speleothem $\delta^{18}O$ as a record of temperature and precipitation amount

With the current lack of data for $\delta^{18}O$ values of palaeo-precipitation in the Plio-Plestocene South African highveld, interpretation of the Buffalo Cave and Collapsed Cone flowstone $\delta^{18}O$ carbonate values is problematic. As discussed above, the thermodynamic fractionation of ^{18}O into calcite and the $\delta^{18}O$ composition of drip water may be opposed or in agreement with respect to the polarity of their temperature dependence. Therefore, if a palaeoclimatic interpretation of $\delta^{18}O$ is to be made, it must be based on comparisons with oxygen isotopes in Holocene and Late Pleistocene speleothems and the oxygen isotopic composition of Holocene groundwaters.

Holocene and Late Pleistocene palaeotemperatures have been determined from $\delta^{18}O$ measurements in a stalagmite from Cango Caves in southern South Africa using $\delta^{18}O$ values from the nearby Uitenhage groundwater aquifer as estimates of past cave drip-water composition (Talma and Vogel, 1992). Talma and Vogel (1992) show that for the late Quaternary of southern South Africa, the decrease in $\delta^{18}O$ of speleothem calcite is greater than the coeval increase in $\delta^{18}O$ of groundwater (equivalent to precipitation), indicating a net increase in temperature of 2-3° C with a decrease of speleothem $\delta^{18}O$ of ca. 0.5‰. This speleothem palaeotemperature calibration indicates a 7° C temperature increase between the last glacial maximum and the Holocene, in general agreement with other palaeotemperature estimates during this period. For example,

palaeotemperature estimates for the Stampriet aquifer, Namibia, indicate that the LGM was 5-6° C cooler than the Holocene (Stute and Talma, 1997).

The Cold Air Cave stalagmite, T8, is the only Makapansgat stalagmite to date back to the last glacial maximum (Holmgren *et al.*, 2003). This stalagmite stable isotope record has been supplemented with Holocene and Late Pleistocene groundwater $\delta^{18}O$ data from the nearby Bela Bela spring (formerly Warmbaths). The mean groundwater $\delta^{18}O$ values are 0.8‰ depleted in the Late Pleistocene compared to the Holocene values, whereas the mean speleothem $\delta^{18}O$ values 0.65‰ heavier over this same period. By assuming that the groundwater $\delta^{18}O$ values approximate $\delta^{18}O$ drip-water values, Holmgren *et al.* (2003) have been able to show that the thermodynamic fractionation function dominated over the drip-water function, resulting in a negetative relationship between $\delta^{18}O$ speleothem and temperature over this timescale. The calculated palaeotemperatures show that the Late Pleistocene was on average 5.7° C cooler than the Holocene, in broad agreement with the Cango Cave and Stampriet aquifer palaeotemperature estimates (Talma and Vogel, 1992; Stute and Talma, 1997).

In contrast to the temperature fractionation effect observed in the Cango Cave and Cold Air Cave T8 stalagmites, the Holocene portion of stalagmites, T7 and T8, from Cold Air Cave show $\delta^{18}O$ depletion during periods of known cooling such as the Little Ice Age (Holmgren *et al.*, 1999 and 2003 and Repinski *et al.*, 1999). Holmgren *et al.* (1999) suggest that changes in $\delta^{18}O$ of rainfall (the drip-water function) have overridden the temperature fractionation effect during small, non-glacial/interglacial-scale temperature changes. Since precipitation source and transport effects are unlikely to have changed during the Holocene, shifts in the temperature at which water or hail condensation occurs (related to higher-altitude convective rain events) are suggested as the most likely cause for the $\delta^{18}O$ depletion of rainfall. Convective rain and hail originating in the upper troposphere are markedly depleted in $\delta^{18}O$ (Dansgaard, 1964; Rozanski *et al.*, 1993), and such intense thunderstorms are known to increase in frequency during dry spells in South Africa (Olivier, 1989; Tyson, 2000). Therefore, Holmgren *et al.* (1999) conclude that cooler and drier conditions are likely to be associated

with a decrease in $\delta^{18}O$ of precipitation and warmer and wetter conditions with an increase in $\delta^{18}O$ of precipitation (and therefore speleothem drip water $\delta^{18}O$).

The late Quaternary Makapansgat stalagmites therefore seem to show a positive correlation between $\delta^{18}O$ speleothem and temperature over short (100 year) timescales but a negative correlation over glacial-interglacial cycles. This is likely to be a result of the temperature change between glacials and interglacials dominating the large-scale speleothem $\delta^{18}O$ variations, and the $\delta^{18}O$ values of precipitation dominating the small-scale speleothem $\delta^{18}O$ variations. If the negative correlation observed between temperature and $\delta^{18}O$ over the Late Pleistocene to Holocene transition in Cold Air Cave (Holmgren *et al.*, 2003) is typical of all previous glacial-interglacial cycles in the South African highveld, then perhaps this negative correlation is controlling the Buffalo Cave flowstone and Collapsed Cone flowstone $\delta^{18}O$ variations. This can be tested by applying the Holmgren *et al.* (2003) palaeotemperature calibration to the Plio-Pleistocene speleothem $\delta^{18}O$ data obtained in this study.

If the $\delta^{18}O$ of precipitation is primarily dependant on the changes in atmospheric circulation patterns over glacial-interglacial cycles, it may be reasonable to assume that the range of $\delta^{18}O$ values of Pliocene and Early Pleistocene precipitation was essentially similar to that of the range determined for late Pleistocene and Holocene precipitation. If so, then the measured values of Holocene and last glacial maximum groundwater $\delta^{18}O$ (Holmgren *et al.*, 2003) from Bela Bela spring (ranging from –5‰ to –4‰), can be used as an estimate of precipitation $\delta^{18}O$ in the Pliocene and Early Pleistocene. Inputting these palaeo-precipitation values into the Craig (1965) palaeotemperature equation along with the range of $\delta^{18}O$ values measured in this study (-3.4‰ to -7‰) produces palaeotemperature estimates from 14.4° C to 30.7° C with the precipitation $\delta^{18}O$ value of –4‰, and from 10.5° C to 25.8° C with the precipitation $\delta^{18}O$ value of –5‰. These lower palaeotemperature estimates lie within potential mean annual temperature for sub-tropical Africa in the late Neogene whereas the higher palaeotemperatures (upto 30° C) are highly unlikely. To achieve more realistic palaeotemperature estimates, it is nessesary to alter the $\delta^{18}O$ palaeo-precipitation values. Therefore it is likely that changes in the $\delta^{18}O$ values of palaeo-

precipitation combined with changes in palaeotemperature were responsible for the wide range of measured speleothem $\delta^{18}O$ values.

Global ice volume was lower in the early Pleistocene than in the Late Pleistocene and even lower still in the Late Miocene/Early Pliocene. This reduction in global ice volume resulted in oceanic water that was depleted in $\delta^{18}O$ by approximately 1.2‰ in the late Miocene, relative to modern day values (Shackleton and Kennett, 1975; Shackleton, 1995). The ^{18}O depleted oceanic water would have lead to the depletion of ^{18}O in Late Neogene precipitation, assuming that the precipitation source, transport and temperature of precipitation remained constant. It is likely that the reduction of global ice volume in the Late Neogene is at least partly responsible for the reduction in $\delta^{18}O$ values with increasing age observed when comparing the mean $\delta^{18}O$ values of the Cold Air Cave stalagmite T8 (~3.7‰), the Buffalo Cave flowstone (-4.9‰) and the Collapsed Cone flowstone (-5.7‰), all from the Makapansgat Valley. As the precise nature of $\delta^{18}O$ values and variation in precipitation and its magnitude relative to the global ice volume effect is unknown, it is not possible to convert the Buffalo Cave and Collapsed Cone flowstone $\delta^{18}O$ records into records of palaeotemperature.

Irrespective of the difficulties in quantifying the $\delta^{18}O$ values in terms of palaeotemperature, it is apparent that the negative correlation between $\delta^{18}O$ and $\delta^{13}C$ from the late glacial maximum to the present day at Makapansgat (Holmgren *et al.*, 2003) is analogous to the negative relationship between $\delta^{18}O$ and $\delta^{13}C$ observed over glacial-interglacial cycles in the early Pleistocene of Buffalo Cave. Although the relative magnitudes of variation in the drip-water $\delta^{18}O$ and thermodynamic fractionation of $\delta^{18}O$ over glacial-interglacial cycles in the South African highveld are currently uncertain, it is clear that there is a strong and repeated relationship between glacial-interglacial climate change and speleothem carbonate $\delta^{18}O$.

5.8.2. Carbon isotopes as a proxy for palaeovegetation

Organic carbon $\delta^{13}C$ data from the Buffalo Cave flowstone ranges from –20‰ to –26‰ and is indicative of a mixed C_3 and C_4 palaeovegetation (see Figure 4.3.). These values can be used to determine the proportion of carbon within speleothem

carbonate that is derived from host-rock dissolution, thereby calibrating the carbonate $\delta^{13}C$ palaeovegetation signal (as discussed in Chapter 4). With a mean modelled host-rock proportion of 47%, the $\delta^{13}C$ values have been converted into an index of the percentage of C_4 plants within the local palaeovegetation (as shown in Fig. 5.9.). The estimated percentage of C_4 plants in the palaeoenvironment of the Buffalo Cave flowstone ranges from 0% (–8.2‰) to 73% (–2.6‰) with an uncertainty of approximately 10%. The Collapsed Cone flowstone organic matter $\delta^{13}C$ and carbonate $\delta^{13}C$ values are indicative of a purely C_3 vegetation. The low degree of carbonate $\delta^{13}C$ variation (range of 1.7‰) in the Collapsed Cone flowstone occurs despite more variable $\delta^{18}O$ values (see Figs. 5.2. and 5.9.). This is a pattern typically observed in a purely C_3 environment (e.g. Quade *et al.*, 1989; Cerling, 1992; Cerling *et al.*, 1993; France-Lanord and Derry, 1994). The marked difference in the isotopic composition and isotopic variability of the two flowstones is indicative of deposition under two contrasting climatic regimes, before and after the development of C_4 grass ecosystems.

The accuracy of the speleothem $\delta^{13}C$ palaeovegetation proxy can be tested by comparison with other vegetation proxy records for the Late Neogene of Southern Africa. Carbon isotopes in fossil teeth from the South African Plio-Pleistocene hominin sites have been used to investigate changes in C_4 plant proportions over time (Luyt, 2001; Luyt and Lee-Thorp, 2003). Luyt and Lee-Thorp (2003) classified fossil individuals and species as either browsers, mixed feeders or grazers, on the basis of the $\delta^{13}C$ value of their enamel carbonate. They observed an increase in the proportion of grazers between Sterkfontein Member 4 (35% grazers) and Member 5 (68% grazers) and suggested that this shift is indicative of an increase in the proportion of C_4 grasses at approximately 1.7 Ma (age-estimate based on faunal correlation with east African hominin sites). Such a marked shift in the proportion of grazers is not observed within the older South African fossil faunas (Luyt, 2001; Sponheimer and Lee-Thorp, 2003). Given the small sample sizes and possible taphonomic biases (Vrba, 1980), the percentage of grazers represents a qualitative rather than quantitative indicator of changes in the proportion of C_4 grasses in the local palaeoenvironment.

The increase in C_4 vegetation at ca. 1.7 Ma described by Luyt and Lee-Thorp (2003) is also observed in the Buffalo Cave flowstone (see Figs. 5.7 and 5.9). This shift is the only non-stationary trend within the Buffalo Cave flowstone $\delta^{13}C$ time-series and occurs over a period of approximately 15 ka, centred at precisely 1.7 Ma. The shift is marked by the increase in mean $\delta^{13}C$ values from -5.7‰ (n = 224) before 1.7 Ma to –4.4‰ (n = 259) after 1.7 Ma. These mean $\delta^{13}C$ values correspond to mean palaeovegetation reconstructions of 30% C_4 plants before 1.7 Ma and 49% C_4 plants after 1.7 Ma (see Fig. 5.9.), which are not dissimilar to the increase in the proportion of grazers at Sterkfontein over this period (Luyt and Lee-Thorp, 2003). The rapid increase in C_4 plant proportions at 1.7 Ma is recorded in the Sterkfontein and Makapansgat valleys, indicating that the Buffalo Cave record reflects regional as well as local palaeoenvironmental change. This vegetational shift at approximately 1.7 Ma (1.6-1.8 Ma) has also been recorded in a number of palaeoclimatic records in equatorial Africa (Cerling, 1992; Bonnefille *et al.*, 1987; deMenocal and Bloemendal, 1995) and has been linked to a period of faunal turnover (Turner and Anton, 1998; Vrba, 1995).

5.8.3. Climatic forcing of the oxygen and carbon isotope time-series

The negative correlation between $\delta^{13}C$ and $\delta^{18}O$ observed in the majority of the Buffalo Cave flowstone (see Figs. 5.7 and 5.8) is unusual within speleothem records and must relate to the orbitally-forced interactions of vegetation and climate in the sub-tropical environment of Southern Africa. The Devils Hole calcite vein in Nevada (Coplen *et al.*, 1994) also shows a negative correlation between $\delta^{13}C$ and $\delta^{18}O$ over Milankovitch periodicities. In the case of the Devils Hole calcite, the lack of C_4 grasses in the present day environment lead the authors to suggest that changes in vegetation density were responsible for the carbon isotope variation rather than changes in the proportion of C_3 and C_4 vegetation (Coplen *et al.*, 1994). The strong negative correlation between $\delta^{13}C$ and $\delta^{18}O$ in both the Devils Hole calcite and the Buffalo Cave flowstone demonstrates the control of global climate on terrestrial vegetational changes.

The Buffalo Cave $\delta^{18}O$ time-series is dominated by the 19 ka and 23 ka precession signal, and also contains a minor 40 ka obliquity component (see Fig. 5.6.). Precessional forcing of precipitation and temperature in sub-tropical

terrestrial environments is both an observed and modelled phenomenon (Rossignol-Strick, 1983; Prell and Campo, 1986; Pokras and Mix, 1987; Clemens *et al.*, 1991; Partridge *et al.*, 1997; Tyson *et al.*, 2001). This study is the first to show precessional forcing of climate in the early Pleistocene of Southern Africa.

In contrast to the $\delta^{18}O$ record, the $\delta^{13}C$ time-series of the Buffalo Cave flowstone is dominated by the obliquity cycle (40 ka), with the 23 ka and 19 ka precessional cycles occuring as minor components (see Fig. 5.7.). The obliquity cycle is known to force high latitude climates, as variation in insolation over the obliquity cycle is greatest at high latitudes (Ruddiman *et al.*, 1986; Raymo and Nisancioglu, 2003). For this reason, the obliquity cycle is rarely seen in low latitude climate proxies, except in the chemically mixed oceans where it is indicative of high-latitude ice-sheet dynamics (Ruddiman *et al.*, 1986). Obliquity is the dominant periodicity in marine $\delta^{18}O$ variation during the late Pliocene and early Pleistocene (Ruddiman *et al.*, 1986; Raymo and Nisancioglu, 2003), rather than the dominant eccentricity cycles observed in the late Pleistocene (Shackleton, 1995). There are currently no high-resolution proxy records for atmospheric pCO_2 in the early Pleistocene, but it is likely that the dominant periodicity of pCO_2 variation corresponds to the obliquity cycle observed in the marine environment at this time. This is because variations in atmospheric pCO_2 are thought to lead and drive marine $\delta^{18}O$ variations (Petit *et al.*, 1999; Shackleton, 2000).

It is well known that an increase in the proportion of C_4 grasses in a tropical ecosystem is controlled either by an increase in temperature, a decrease in atmospheric pCO_2 or both (Ehleringer *et al.*, 1991; Ehleringer and Monson, 1993; Ehleringer *et al.*, 1997). It has been demonstrated in the Late Pleistocene that the reduced levels of atmospheric pCO_2 in glacial periods have a greater impact on vegetation than the corresponding reduction of tropical temperatures, resulting in a net increase in C_4 grasses during glacial periods (Jolly and Haxeltine, 1997; Collatz *et al.*, 1998; Cowling and Sykes, 1999; Boom *et al.*, 2001; Boom *et al.*, 2002). Long records of Late Pleistocene vegetation change (Hooghiemstra, 1995; Boom *et al.*, 2001; Boom *et al.*, 2002) are shown to closely resemble the corresponding records of atmospheric pCO_2 (Petit *et al.*, 1999) and marine $\delta^{18}O$ (Shackleton *et al.*, 1995) and are therefore dominated by the Late Pleistocene

eccentricity cycle. In contrast, a Pliocene and Early Pleistocene pollen record from marine sediments off the coast of west Africa (Dupont and Leroy, 1995) is dominated by an obliquity (41 ka) periodicity, the dominant orbital parameter within marine $\delta^{18}O$ records at this time (Ruddiman *et al.*, 1986; Raymo and Nisancioglu, 2003).

In agreement with the west African palaeovegetation record of Dupont and Leroy (1995), the early Pleistocene palaeovegetation of South Africa recorded in the Buffalo Cave flowstone is dominated by the obliquity signal, suggesting that both vegetation records are forced by the obliquity frequency of atmospheric pCO_2 variation. The presence of the obliquity cycle in the Buffalo Cave $\delta^{13}C$ time-series suggests that the proportion of C_4 grasses is responding to changes in the atmospheric partial pressure of CO_2, in agreement with carbon isotope proxies from the Late Pleistocene (Collatz *et al.*, 1998; Boom *et al.*, 2001).

The Buffalo Cave flowstone demonstrates that independent orbital periodicities can dominate co-occurring temperature/precipitation and palaeovegetation proxies. This indicates the dominant control of temperature/ precipitation by local variations in sub-tropical precessional forcing, whereas tropical vegetation is controlled by high-latitude variations in orbital obliquity that force the variation in Early Pleistocene atmospheric pCO_2. Both proxy records also show significant periodicity at both the obliquity and precession frequencies (see Fig. 5.7), indicating the coupling of the vegetation and climate systems. With the current uncertainties in interpreting the $\delta^{18}O$ values in terms of palaeotemperature, it is not possible to identify whether shifts in temperature or atmospheric pCO_2 or both are controlling the C_4 plant proportion of the Buffalo Cave flowstone record.

5.8.4. Climatic variability and early hominin habitats in South Africa

The high degree of resolution of the Buffalo Cave Flowstone record indicates that climatic variability on the short time-scale of orbital cycles can be as great as long-term climatic changes such as the climate before and after 1.7 Ma (see Figs. 5.7. and 5.9.). The high temporal resolution shows that South African Plio-Pleistocene climatic variability is far greater in magnitude and frequency than that

determined from previous studies of faunal deposits (e.g. Luyt and Lee-Thorp, 2003).

Each faunal deposit or Member within the Transvaal palaeokarst is time-averaged, representing tens or hundreds of thousands of years of deposition (Herries, 2003; McFadden *et al.*, 1979). Therefore, only the broadest, time-averaged trends in vegetation composition can be identified from the stable isotope record of fossil teeth from the South African hominin sites (Sponheimer *et al.*, 1999; Luyt *et al.* 2001; Luyt and Lee-Thorp, 2003; Sponheimer and Lee-Thorp, 2003) such as the increase of C_4 grass proportions after 1.7 Ma. Care must be taken when making palaeoclimatic inferences based on the South African faunal deposits, because climatic variations occurring at Milankovitch periodicities will be subsumed within a given faunal assemblage to create an averaged climatic signal.

Previous data on carbon isotopes and ecomorphology in fossil mammals in the Makapansgat Limeworks have shown the Member 3 fauna dated at 3 Ma to be composed of both grazers and browsers (Sponheimer *et al.*, 1999; Sponheimer *et al.*, 2001; Reed, 1997; 1998). By assuming that the faunal deposit was formed under constant ecological conditions, it has been concluded that the South African palaeoenvironment was a highly mixed "riparian forest bordered with edaphic grasslands and nearby wetlands" (Reed, 2002). Based on the insights into secular variations in the C_3/C_4 plant ratio provided by speleothem isotope data, it is now possible to state that the same faunal deposit represents a climatic trend from a forest-dominated to grass-dominated environment or oscillation between these two end-members. Independant evidence for the variability in proportion of savannah grasses relative to woodland in the Pliocene comes from high-resolution faunal data from East Africa (Bobe *et al.*, 2002) that indicates cyclicity in the percentage of arboreal versus terrestrial taxa. It is therefore important to recognise that an individual faunal deposit from the South African cave breccias may not represent a single environment or fossil community.

If the vegetation cover at a specific locality is oscillating between woodland-dominated and grassland-dominated, two possibilities exist for the habitat specifities and adaptive strategies of the fauna living in this environment. (1) Savannah adapted and woodland adapted species can migrate with their favoured habitat as both vegetative components shrink and expand over

Milankovitch periodicities. (2) Generalised species can remain in one locality over the precessional change, as they are able to exploit both grassland and woodland environments. The former scenario is envisaged in the Habitat Theory model of Vrba (1995) and the latter scenario is more in line with the Varibility Selection model of Potts (1998).

Between 1.5 Ma and 2.0 Ma, the period represented by the Buffalo Cave flowstone, there were two contemporaneous early hominin species in South Africa, *Australopithecus robustus* and *Homo* sp. (Tobias, 2000). Both of these species had a diet partly dependent on C_4 plant-derived foodstuffs (Sillen, 1992; Lee-Thorp *et al.*, 1994; Sillen *et al.*, 1998; Lee-Thorp *et al.*, 2003), indicating that they exploited both the grassland and woodland components of their mosaic environment. It is currently unknown to what extent each species was able to transgress vegetation zones or how dependent they were on either vegetation component.

5.9. Conclusions

This study has developed a high-resolution 1.5-2.0 Ma record of continuous climatic and vegetation change in South Africa from an early Pleistocene flowstone. The dominant orbital parameter differs between the vegetation and climate proxy records – vegetation is responding to the obliquity forcing of early Pleistocene global climate, whereas the precipitation/temperature signal is responding to low latitude precessional variation in temperature and rainfall amount. This precessional component to sub-tropical terrestrial climate is absent from marine records of early Pleistocene climate change.

Two vegetational shifts are observed within the South African flowstones; between the Late Miocene/Early Pliocene and at 1.7 Ma. Both of these events would have lead to a restructuring of terrestrial ecosystems of importance to mammalian evolution, but pass largely un-noticed in the marine $\delta^{18}O$ record. The causes of these vegetational shifts have not been determined, but they are likely to reflect the combined affect of changes in temperature and atmospheric pCO_2 (Cerling *et al.*, 1997). The differences in the tempo, timing and magnitude of marine and tropical terrestrial climate change indicate that the marine $\delta^{18}O$ record

does not precisely describe changes in hominin habitat, and should not be used as a proxy for African terrestrial climate change.

5.10. References

Baker, A., Smart, P. L., Edwards, R. L., and Richards, D. A. (1993). Annual growth banding in a cave stalagmite. *Nature* **364,** 518-520.

Baker, A., Proctor, C. J., and Barnes, W. L. (1999). Variations in stalagmite luminescence laminae structure at Poole's Cavern, England, AD 1910-1996: calibration of a palaeoprecipitation proxy. *Holocene* **9,** 683-688.

Bamford, M. (1999). Pliocene fossil woods from an early hominid cave deposit, Sterkfontein, South Africa. *South African Journal of Science* **95,** 231-237.

Barry, J. C., Morgan, M. L. E., Flynn, L. J., Pilbeam, D., Behrensmeyer, A. K., Raza, S. M., Khan, I. A., Badgley, C., Hicks, J., and Kelley, J. (2002). Faunal and environmental change in the late Miocene Siwaliks of northern Pakistan. *Paleobiology* **28,** 1-71.

Berger, A., and Loutre, M. F. (1991). Insolation values for the climate of the last 10 million years. *Quaternary Science Reviews* **10,** 297-317.

Bloomfield, P. (1976). "Fourier analysis of time series: an introduction." Wiley, London.

Bobe, R., and Eck, G. G. (2001). Responses of African bovids to Pliocene climatic change. *Paleobiology Memoirs* **27,** 1-47.

Bobe, R., Behrensmeyer, A. K., and Chapman, R. E. (2002). Faunal change, environmental variability and late Pliocene hominin evolution. *Journal of Human Evolution* **42,** 475-497.

Bonnefille, R., Vincens, A., and Buchet, G. (1987). Palynology, stratigraphy and palaeoenvironment of a Pliocene hominid site (2.9-3.3 M.Y.) at Hadar, Ethiopia. *Palaeogeography, Palaeoclimatology, Palaeoecology* **60,** 249-281.

Boom, A., Mora, G., Cleef, A. M., and Hooghiemstra, H. (2001). High altitude C4 grasslands in the northern Andes: relicts from glacial conditions? *Review of Palaeobotany and Palynology* **115,** 147-160.

Boom, A., Marchant, R., Hooghiemstra, H., and Sinninghe Damste, J. S. (2002). CO_2-and temperature-controlled altitudinal shifts of C4- and C3-dominated grasslands allow reconstruction of palaeoatmospheric pCO_2. *Palaeogeography, Palaeoclimatology, Palaeoecology* **177,** 151-168.

Bromage, T. G., and Schrenk, F. (1995). Biogeographic and climatic basis for a narrative of early hominid evolution. *Journal of Human Evolution* **28,** 109-114.

Cerling, T. E., Quade, J., Wang, Y., and Bowman, J. R. (1989). Carbon isotopes in soils and paleosols as ecology and paleoecology indicators. *Nature* **341,** 138-139.

Cerling, T. E. (1992). Development of grasslands and savannas in east-Africa during the Neogene. *Palaeogeography, Palaeoclimatology, Palaeoecology (Global and Planetary Change Section)* **97,** 241-247.

Cerling, T. E., Wang, Y., and Quade, J. (1993). Expansion of C4 ecosystems as an

indicator of global ecological change in the Late Miocene. *Nature* **361,** 344-345.

Cerling, T. E., Harris, J. M., MacFadden, B. J., Leakey, M. G., Quade, J., Eisenmann, V., and Ehleringer, J. R. (1997). Global vegetation change through the Miocene/Pliocene boundary. *Nature* **389,** 153-158.

Cerling, T. E., Ehleringer, J. R., and Harris, J. M. (1998). Carbon dioxide starvation, the development of C-4 ecosystems, and mammalian evolution. *Philosophical Transactions of the Royal Society of London Series B-Biological Sciences* **353,** 159-170.

Clemens, S., Prell, W., Murray, D., Shimmield, G., and Weedon, G. (1991). Forcing mechanisms of the Indian Ocean monsoon. *Nature* **353,** 720-725.

Collatz, G. J., Berry, J. A., and Clark, J. S. (1998). Effects of climate and atmospheric CO_2 partial pressure on the global distribution of C4 grasses: present, past, and future. *Oecologia* **114,** 441-454.

Coplen, T. B., Winograd, I. J., Landwehr, J. M., and Riggs, A. C. (1994). 500,000-year stable carbon isotopic record from Devils Hole, Nevada. *Science* **263,** 361-365.

Coplen, T. B. (1995). Reporting of stable carbon, hydrogen, and oxygen isotopic abundances. *In* "Reference and intercomparison materials for stable isotopes of light elements." pp. 31-34. International Atomic Energy Agency, TECDOC.

Cowling, S. A., and Sykes, M. T. (1999). Physiological significance of low atmospheric CO_2 for plant-climate interactions. *Quaternary Research* **52,** 237-242.

Craig, H. (1957). Isotopic standards for carbon and oxygen and correction factors for mass-spectrometric analysis of carbon dioxide. *Geochemica et Cosmochimica Acta* **12,** 133-149.

Craig, H. (1965). The measurements of oxygen isotope paleotemperature: stable isotopes in oceanographic studies and paleotemperatures. *In* "Proceedings of the Third Spoleto Conference, Spoleto, Italy." (E. Tongiori, Ed.), pp. 161-182. Sischi and Figli, Pisa.

Dansgaard, W. (1964). Stable isotopes in precipitation. *Tellus* **16,** 436-468.

deMenocal, P. B., and Bloemendal, J. (1995). Plio-Pleistocene climatic variability in subtropical African and the paleoenvironment of hominid evolution. *In* "Paleoclimate and evolution with emphasis on human origins." (E. S. Vrba, G. H. Denton, T. C. Partridge, and L. H. Burckle, Eds.), pp. 262-288. Yale University Press, New Haven.

Dennis, P. F., Rowe, P. J., Atkinson, T. C. (2001). The recovery and isotopic measurement of water from fluid inclusions in speleothems. *Geochimica et Cosmochimica Acta* **65**: 871-884.

Dupont, L. M., and Leroy, S. A. G. (1995). Steps toward drier climatic conditions in Northwestern Africa during the Upper Pliocene. *In* "Paleoclimate and evolution with emphasis on human origins." (E. S. Vrba, G. H. Denton, T. C. Partridge, and L. H. Burckle, Eds.), pp. 289-298. Yale University Press, New Haven.

Ehleringer, J. R., Sage, R. F., Flanagan, L. B., and Pearcy, R. W. (1991). Climate Change and the evolution of C4 photosynthesis. *Trends in Ecology & Evolution* **6,** 95-99.

Ehleringer, J. R., and Monson, R. K. (1993). Evolutionary and ecological aspects of photosynthetic pathway variation. *Annual Review of Ecology and*

Systematics **24,** 411-439.

Ehleringer, J. R., Cerling, T. E., and Helliker, B. R. (1997). C-4 photosynthesis, atmospheric CO_2 and climate. *Oecologia* **112,** 285-299.

Fleitmann, D., Burns, S. J., Neff, U., Mangini, A., and Matter, A. (2003). Changing moisture sources over the last 330,000 years in Northern Oman from fluid-inclusion evidence in speleothems. *Quaternary Research* **60,** 223-232.

France-Lanord, C., and Derry, L. A. (1994). $\delta^{13}C$ of organic carbon in the Bengal Fan: source evolution and transport of C3 and C4 plant carbon to marine sediments. *Geochimica et Cosmochimica Acta* **58,** 4809-4814.

Herries, A. I. R. (2003). "Magnetostratigraphic seriation of South African hominin palaeocaves." Unpublished PhD thesis, University of Liverpool.

Herries, A. I. R., Reed, K., Latham, A. G., and Kuykendall, K. L. (in press). The age of the Buffalo palaeocave fossil locality, Makapansgat, South Africa as determined by faunal correlation and magnetostratigraphy. *Quaternary Science Reviews.*

Holmgren, K., Karlen, W., Lauritzen, S. E., Lee-Thorp, J. A., Partridge, T. C., Piketh, S., Repinski, P., Stevenson, C., Svanered, O., and Tyson, P. D. (1999). A 3000-year high-resolution stalagmite-based record of palaeoclimate for northeastern South Africa. *Holocene* **9,** 295-309.

Holmgren, K., Lee-Thorp, J. A., Cooper, G. R. I., Lundblad, K., Partridge, T. C., Scott, L., Sithaldeen, R., Talma, A. S., Tyson, P. D. (2003). Persistent millennial-scale climatic variability over the past 25,000 years in Southern Africa. *Quaternary Science Reviews* **22**: 2311-2326.

Hooghiemstra, H. (1995). Enivironmental and paleoclimatic evolution in Late Pliocene - Quaternary Colombia. *In* "Paleoclimate and evolution with emphasis on human origins." (E. S. Vrba, G. H. Denton, T. C. Partridge, and L. H. Burckle, Eds.), pp. 249-261. Yale University Press, New Haven.

Ifeachor, E. C., and Jervis, B. W. (1993). "Digital signal processing. A practical approach." Addison-Wesley, Harlow.

Jolly, D., and Haxeltine, A. (1997). Effects of low glacial atmospheric CO_2 on tropical African montane vegetation. *Science* **276,** 786-788.

Kominz, M. A., and Pisias, N. G. (1979). Pleistocene Climate: deterministic or stochastic? *Science* **204,** 171-173.

Kominz, M. A., Heath, G. R., Ku, T.-L., and Pisias, N. G. (1979). Brunhes time scales and the interpretation of climatic change. *Earth and Planetary Science Letters* **45,** 394-410.

Kuykendall, K. L., Toich, C. A., and McKee, J. K. (1995). Preliminary analysis of the fauna from Buffalo cave, northern transvaal, South Africa. *Palaeontologia Africana* **32,** 27-31.

Latham, A. G., Herries, A., Quinney, P., Sinclair, A., and Kuykendall, K. (1999). The Makapansgat Australopithecine site from a speleological perspective. In, Pollard, A. M. (ed.) Geoarchaeology: exploration, environments, resources. *Geological Society of London, Special Publications* **165,** 61-77.

Latham, A. G., Herries, A., and Kuykendall, K. (2003). The formation and sedimentary infilling of the Limeworks cave, Makapansgat, South Africa. *Palaeontologia Africana* **39**: 69-82.

Lauritzen, S.-E. (1995). High-resolution paleotemperature proxy record for the last interglaciation based on Norwegian speleothems. *Quaternary Research* **43,** 133-146.

Lee-Thorp, J. A., van der Merwe, N. J., and Brain, C. K. (1994). Diet of *Australopithecus-robustus* at Swartkrans from stable carbon isotopic analysis. *Journal of Human Evolution* **27,** 361-372.

Lee-Thorp, J. A., and Talma, A. S. (2000). Stable light isotopes and environments in the Southern African Quaternary and Late Pliocene. *In* "The Cenozoic of Southern Africa." pp. 406. Oxford Monographs on Geology and Geophysics. Oxford University Press, Oxford.

Lee-Thorp, J. A., Thackeray, J. F., and van der Merwe, N. (2000). The hunters and the hunted revisited. *Journal of Human Evolution* **39,** 565-576.

Lee-Thorp, J. A., Sponheimer, M., and Van der Merwe, N. H. (2003). What do stable isotopes tell us about hominid dietary and ecological niches in the Pliocene? *Internation Journal of Osteoarchaeology* **13,** 104-113.

Luyt, J. (2001). "Revisiting the palaeoenvironments of the South African hominid-bearing Plio-Pleistocene sites: New isotopic evidence from Sterkfontein." Unpublished MSc thesis, University of Cape Town.

Luyt, C. J., and Lee-Thorp, J. A. (2003). Carbon isotope ratios of Sterkfontein fossils indicate a marked shift to open environments c. 1.7 Myr ago. *South African Journal of Science* **99,** 273-275.

Mann, M. E., and Lees, J. (1996). Robust estimation of background noise and signal detection in climatic time series. *Climate Change* **33,** 409-445.

Matthews, A., Ayalon, A., and Bar-Matthews, M. (2000). D/H ratios of fluid inclusions of Soreq cave (Israel) speleothems as a guide to the Eastern Mediterranean Meteoric Line relationships in the last 120 ky. *Chemical Geology* **166,** 183-191.

McClellan, J. H., Parks, T. W., and Rabiner, L. R. (1973). A computer program for designing optimum FIR linear phase digital filters. *IEEE Transactions on audio and electroacoustics* **21,** 506-526.

McFadden, P. L., Brock, A., and Partridge, T. C. (1979). Palaeomagnetism and the age of the Makapansgat hominid site. *Earth and Planetary Science Letters* **44,** 373-382.

O'Leary, M. H. (1981). Carbon isotope fractionation in plants. *Phytochemistry* **20,** 553-567.

O'Leary, M. H. (1988). Carbon isotopes in photosynthesis. *BioScience* **38,** 328-336.

Olivier, J. (1989). Some temporal aspects of hail in the Transvaal. *South African Geographer* **16,** 39-52.

Partridge, T. C. (1978). Re-appraisal of lithostratigraphy of Sterkfontein hominid site. *Nature* **275,** 282-287.

Partridge, T. C. (1979). Re-appraisal of lithostratigraphy of Makapansgat Limeworks hominid site. *Nature* **279,** 484-488.

Partridge, T. C., deMenocal, P. B., Lorentz, S., Paiker, M. J., and Vogel, J. C. (1997). Obital forcing of climate over South Africa: a 200,000-year rainfall record from the Pretoria Saltpan. *Quaternary Science Reviews* **16,** 1125-1133.

Partridge, T. C. (2000). Hominid-bearing cave and tufa deposits. *In* "The Cenozoic of Southern Africa." (T. C. Partridge, and R. R. Maud, Eds.), pp. 100-130. Oxford University Press, Oxford.

Partridge, T. C., Latham, A. G., and Heslop, D. (2000). Appendix on magnetostratigraphy of Makapansgat, Sterkfontein, Taung and Swartkrans. *In* "The Cenozoic of Southern Africa." (T. C. Partridge, and

R. R. Maud, Eds.), pp. 126-129. Oxford University Press, Oxford.

Petit, J. R., Jouzel, J., Raynaud, D., Barkov, N. I., Barnola, J.-M., Basile, I., Bender, M., Chappellaz, J., Davis, M., Delaygue, G., Delmotte, M., Kotlyakov, V. M., Legrand, M., Lipenkov, V. Y., Lorius, C., Pepin, L., Ritz, C., Saltzman, E., and Stievenard, M. (1999). Climate and atmospheric history of the past 420,000 years from the Vostok ice core, Antarctica. *Nature* **399,** 429-436.

Pisias, N. G. (1983). Geologic time series from deep-sea sediments: time scales and distortion by bioturbation. *Marine Geology* **51,** 99-113.

Pokras, E. M., and Mix, A. C. (1987). Earth's precession cycle and Quaternary climatic change in tropical Africa. *Nature* **326,** 486-487.

Potts, R. (1996). Evolution and climate variability. *Science* **273,** 922-923.

Potts, R. (1998). Variability selection in hominid evolution. *Evolutionary Anthropology* **7,** 81-96.

Prell, W. L., and Van Campo, E. (1986). Coherent response of Arabian Sea upwelling and pollen transport to late Quaternary monsoonal winds. *Nature* **323,** 526-528.

Prell, W., and Kutzbach, J. E. (1987). Monsoon variability over the past 150,000 years. *Journal of Geophysical Research* **92,** 8411-8425.

Press, W. H., Teukolsky, S. A., Vetterling, W. T., and Flannery, B. P. (1992). "Numerical recipes, the art of scientific computing." Cambridge University Press, Cambridge.

Quade, J., Cerling, T. E., and Bowman, J. R. (1989). Development of the Asian monsoon revealed by marked ecological shift during the latest Miocene in northern Pakistan. *Nature* **342,** 163-166.

Raymo, M. E., and Nisancioglu, K. (2003). The 41 kyr world: Milankovitch's other unsolved mystery. *Paleoceanography* **18,** 1011(1-6).

Reed, K. E. (1997). Early hominid evolution and ecological change through the African Plio-Pleistocene. *Journal of Human Evolution* **32,** 289;322.

Reed, K. E. (1998). Using large mammal communities to examine ecological and taxonomic structure and predict vegetation in extant and extinct assemblages. *Paleobiology* **24,** 384-408.

Reed, K. (2002). The use of paleocommunity and taphonomic studies in reconstructing primate behavior. *In* "Reconstructing Behavior in the primate fossil record." (Plavcan, Ed.), pp. 217-259. Kluwer Academic/Plenum Publishers, New York.

Repinski, P., Holmgren, K., Lauritzen, S. E., and Lee-Thorp, J. A. (1999). A late Holocene climate record from a stalagmite, Cold Air Cave, Northern Province, South Africa. *Palaeogeography, Palaeoclimatology, Palaeoecology* **150,** 269-277.

Rossignol-Strick, M. (1983). African monsoons, an immediate climate response to orbital insolation. *Nature* **304,** 46-49.

Rozanski, K., Araguas-Araguas, L., and Gonfiantini, R. (1992). Relation between long-term trends of oxygen-18 isotope composition of precipitation and climate. *Science* **258,** 981-985.

Ruddiman, W. F., Raymo, M. E., and McIntyre, A. (1986). Matuyama 41,000-year cycles: North Atlantic Ocean and northern hemisphere ice sheets. *Earth and Planetary Science Letters* **80,** 117-129.

Schwarcz, H. P., Harmon, R. S., Thompson, P., and Ford, D. C. (1976). Stable isotope studies of fluid inclusions in speleothems and their paleoclimatic

significance. *Geochemica et Cosmochimica Acta* **40,** 657-665.

Schwarcz, H. P. (1986). Geochronology and isotopic geochemistry of speleothems. *In* "Handbook of Environmental Isotope Geochemistry." (P. Fritz, and J. C. Fontes, Eds.), pp. 271-303. Elsevier, Amsterdam.

Scott, L. (1995). Pollen evidence for vegetational and climatic change in southern Africa during the Neogene and Quaternary. *In* "Paleoclimate and evolution with emphasis on human origins." (E. S. Vrba, G. H. Denton, T. C. Partridge, and L. H. Burckle, Eds.), pp. 65-76. Yale University Press, New Haven.

Scott, L. (2002). Grassland development under glacial and interglacial conditions in southern Africa: review of pollen, phytolith and isotope evidence. *Palaeogeography, Palaeoclimatology, Palaeoecology* **177,** 47-57.

Shackleton, N. J., and Kennett, J. P. (1975). Late Cenozoic oxygen and carbon isotopic changes at DSDP site 284: implications for glacial history of the Northern Hemisphere and Antarctica. *Initial Reports of the Deep Sea Drilling Project* **29,** 801-807.

Shackleton, N. J. (1995). New data on the evolution of Pliocene climatic variability. *In* "Paleoclimate and evolution with emphasis on human origins." (E. S. Vrba, G. H. Denton, T. C. Partridge, and L. H. Burckle, Eds.), pp. 242-248. Yale University Press, New Haven.

Shackleton, N. J. (2000). The 100,000-year ice-age cycle identified and found to lag temperature, carbon dioxide, and orbital eccentricity. *Science* **289,** 1897-1902.

Shopov, Y. Y., Ford, D. C., and Schwarcz, H. P. (1994). Luminescent microbanding in speleothems: high resolution chronology and palaeoclimate. *Geology* **22,** 407-410.

Sillen, A. (1992). Strontium calcium ratios (Sr/Ca) of *Australopithecus robustus* and associated fauna from Swartkrans. *Journal of Human Evolution* **23,** 495-516.

Sillen, A., Hall, G., Richardson, S., and Armstrong, R. (1998). Sr^{87}/Sr^{86} ratios in modern and fossil food-webs of the Sterkfontein Valley: Implications for early hominid habitat preference. *Geochimica et Cosmochimica Acta* **62,** 2463-2473.

Sponheimer, M., Reed, K. E., and Lee-Thorp, J. A. (1999). Combining isotopic and ecomorphological data to refine bovid paleodietary reconstruction: a case study from the Makapansgat Limeworks hominin locality. *Journal of Human Evolution* **36,** 705-718.

Sponheimer, M., Reed, K., and Lee-Thorp, J. A. (2001). Isotopic palaeoecology of Makapansgat Limeworks Perissodactyla. *South African Journal of Science* **97,** 327-329.

Sponheimer, M., and Lee-Thorp, J. A. (2003). Using carbon isotope data of fossil bovid communities for palaeoenvironmental reconstruction. *South African Journal of Science* **99,** 273-275.

Stute, M., and Talma, A. S. (1997). Glacial temperatures and moisture transport regimes reconstructed from noble gases and $\delta^{18}O$, Stampriet Aquifer, Namibia. *In* "Isotope techniques in the study of environmental change: proceedings of an international symposium on isotope techniques in the study of past and current environmental changes in the hydrosphere and the atmosphere." (IAEA, Ed.), pp. 307-318. IAEA, Vienna.

Talma, A. S., and Vogel, J. C. (1992). Late Quaternary paleotemperatures derived

from Cango Caves, Cape Province, South Africa. *Quaternary Research* **37,** 203-213.

Tobias, P. V. (2000). The fossil hominids. *In* "The Cenozoic of Southern Africa." (T. C. Partridge, and R. R. Maud, Eds.), pp. 252-276. Oxford University Press, Oxford.

Turner, A., and Anton, M. (1998). Climate and evolution: implications of some extinction patterns in African and European Machairodontine cats of the Plio-Pleistocene. *Estudios Geologicos* **54,** 209-230.

Tyson, P. D. (1999). Atmospheric circulation changes and palaeoclimates of southern Africa. *South African Journal of Science* **95,** 194-201.

Tyson, P. D., and Preston-Whyte, R. A. (2000). "The weather and climate of southern Africa." Oxford University Press, Oxford.

Tyson, P. D., Odada, E. O., and Partridge, T. C. (2001). Late Quaternary environmental change in southern Africa. *South African Journal of Science* **97,** 139-150.

van der Merwe, N. J., and Thackeray, J. F. (1997). Stable carbon isotope analysis of Plio-Pleistocene ungulate teeth from Sterkfontein, South Africa. *South African Journal of Science* **93,** 194-194.

Vogel, J. C., Fuls, A., and Ellis, R. P. (1978). The geographical distribution of Kranz grasses in South Africa. *South African Journal of Science* **74,** 209-215.

Vrba, E. S. (1980). The significance of bovid remains as indicators of environment and predation patterns. *In* "Fossils in the making. Vertebrate taphonomy and paleoecology." (A. K. Behrensmeyer, and A. P. Hill, Eds.), pp. 247-271. University of Chicago Press, Chicago.

Vrba, E. S. (1992). Mammals as a key to evolutionary theory. *Journal of Mammalogy* **73,** 1-28.

Vrba, E. S. (1995). The fossil record of African Antelopes (Mammalia, Bovidae) in relation to human evolution and paleoclimate. *In* "On the connections between paleoclimate and evolution." (E. S. Vrba, G. H. Denton, T. C. Partridge, and L. H. Burckle, Eds.), pp. 385-424. Yale University Press, New Haven.

Vrba, E. S. (1995). On the connections between paleoclimate and evolution. *In* "Paleoclimate and evolution with emphasis on human origins." (E. S. Vrba, G. H. Denton, T. C. Partridge, and L. H. Burckle, Eds.). Yale University Press, New Haven.

Weedon, G. P., and Jenkyns, H. C. (1999). Cyclostratigraphy and the Early Jurassic timescale: data from the Belemnite Marls, Dorset, southern England. *Geological Society of America Bulletin* **111,** 1823-1840.

Weedon, G. (2003). "Time-series analysis and cyclostratigraphy." Cambridge University Press, Cambridge.

Yonge, C. J., Ford, D. C., Gray, J., and Schwarcz, H. P. (1985). Stable isotope studies of cave seepage water. *Chemical Geology* **58,** 97-105.

Zeitoun, V. (2000). Adequation entre changements environnementaux et speciations humaines au Plio-Pleistocene. *C.R.Acad.Sci.Paris,Sciences de la Terre et des planetes* **330,** 161-166.

Chapter 6. Palaeoenvironment and palaeodiet of mid-Pliocene micromammals from Makapansgat Limeworks, South Africa: stable isotope and dental microwear approach

6.1. Abstract

The origin of C_4 grasses occurred at low latitudes in the mid-Miocene after which they spread towards mid-latitudes by approximately the Miocene-Pliocene boundary. In an attempt to determine of the timing of this event in the South African highveld, a carbon isotope study of some of the oldest faunal deposits in the region (mid-Pliocene) was undertaken to reconstruct the palaeoenvironment of this period. The combination of carbon isotope and dental microwear analysis of micromammals from the Rodent Corner and the Exit Quarry repositories of the Makapansgat Limeworks has enabled the determination of the relative proportions of C_4 grass, C_3 grass and C_3 browse in the diets of two extinct herbivorous rodent species, *Otomys* cf. *gracilis* and *Mystromys* cf. *hausleitneri*. M. cf. *hausleitneri* is shown to have a similar diet to the extant M. *albicaudatus* whereas O. cf. *gracilis* is shown to be less reliant on grazing than the extant O. *irroratus* despite its specialised hypsodont molars. The lack of a grazing specialist amongst the most common species in the Makapansgat micromammal assemblages is suggestive of a local palaeo-environment that was more wooded than the present day woodland-savannah mosaic. The presence of C_4 grasses in the mid-Pliocene of Makapansgat indicates that the origin of C_4 grasses in the South African highveld occurred prior to the mid-Pliocene.

6.2. Introduction

Between the mid-Miocene and early Pliocene (15 to 4 Ma) a large-scale vegetation shift occurred when C_4 grasses began a global expansion. It has been suggested that the origin and spread of the C_4 grasses was triggered by a decrease in atmospheric CO_2 levels to below 500 parts per million by volume (p.p.m.v.), which would have been of advantage to C_4 grasses which out-compete C_3 grasses under conditions of low atmospheric CO_2 and high temperatures (Ehleringer *et*

al., 1991, 1997; Cerling, 1993; Cerling *et al.*, 1997). However, the evidence for a decrease in the partial pressure of atmospheric CO_2 (pCO_2) during the mid-Miocene is disputed (Pagani *et al.*, 1999) and the ultimate cause for the spread of C_4 grasses remains unresolved. The C_4 global-expansion model (Cerling *et al.*, 1997) predicts a latitudinal gradient in the proportions of C_4 versus C_3 plants, as is seen today and in the Quaternary (MacFadden *et al.*, 1999), with C_4 grasses dominating over C_3 grasses in the low latitudes. Latitudinal gradients in C_4 grass distribution at any given time are a function of growing season temperature, with the magnitude of the gradient dependant on atmospheric pCO_2. The Cerling *et al.* (1997) model also predicts that the earliest records of C_4 grasses will occur in low latitudes and that the expansion of C_4 grasses into mid-latitudes will be accompanied by either an increase in global temperature or a decrease in pCO_2 (Cerling *et al.*, 1997). In support of the Cerling *et al.* (1997) model, there is evidence that the first record of C_4 grasses in mid-latitude sites can be as late at the Miocene-Pliocene boundary in Namibia (Segalen *et al.*, 2002), China (Ding *et al.*, 1997 and Ding and Yang, 2000) and northern North America (Cerling *et al.*, 1997). Therefore, the mid-Pliocene rodent faunas of Makapansgat (latitude 24° south) in South Africa offer the opportunity to determine the distribution of C_4 grasses close to the proposed transition from a C_3 to C_4 ecosystem. The aim of this study was to use carbon isotopes in fossil micromammal teeth and combine this data with dental microwear analysis, to determine the approximate proportions of C_4 grasses, C_3 grasses and C_3 trees and bushes in the local palaeoenvironment.

The present day vegetation of the southwestern parts of the subcontinent are dominated by "fynbos" (see Fig. 6.1.), a unique sclerophyllous shrubland vegetation in which grasses are a very minor component and when present are predominately cool-season C_3 grasses. One of the features of fynbos is that it can grow in the sandy, low-nutrient soils found in this region and as a result has low nutritional content and supports few large mammals. In contrast, the subcontinent to the east of the Cape Fold Mountains experiences a largely summer rainfall, a vegetation dominated by woodlands and C_4 grasslands (see Fig. 6.1.), and can support a rich mammalian fauna. Exactly when these two distinct climate and floral systems developed is not well understood, but limited marine evidence

suggests that early forms of the Benguella Upwelling System may have been present in the late Miocene (Siesser, 1980), which would imply the existence of a dry summer / wet winter regime in southwestern Southern Africa since this time. This is supported by the lack of C_4 grasses in the winter rainfall region since the early Pliocene, as determined from carbon isotopes in the Langebaanweg macrofauna (Franz-Odendaal *et al.*, 2002; see Fig. 6.1.). It has been suggested (Cockcroft *et al.*, 1987) that the winter rainfall zone extended northwards well into the present day summer rainfall zone during glacial periods. However, this model has been refuted based on evidence from stable isotopes in the grazing fauna from Equus Cave, located to the south of the present summer rainfall zone (see Fig. 6.1.), which indicates that only a limited expansion of the winter rainfall zone occurred during the late Pleistocene (Lee-Thorp and Beaumont, 1995).

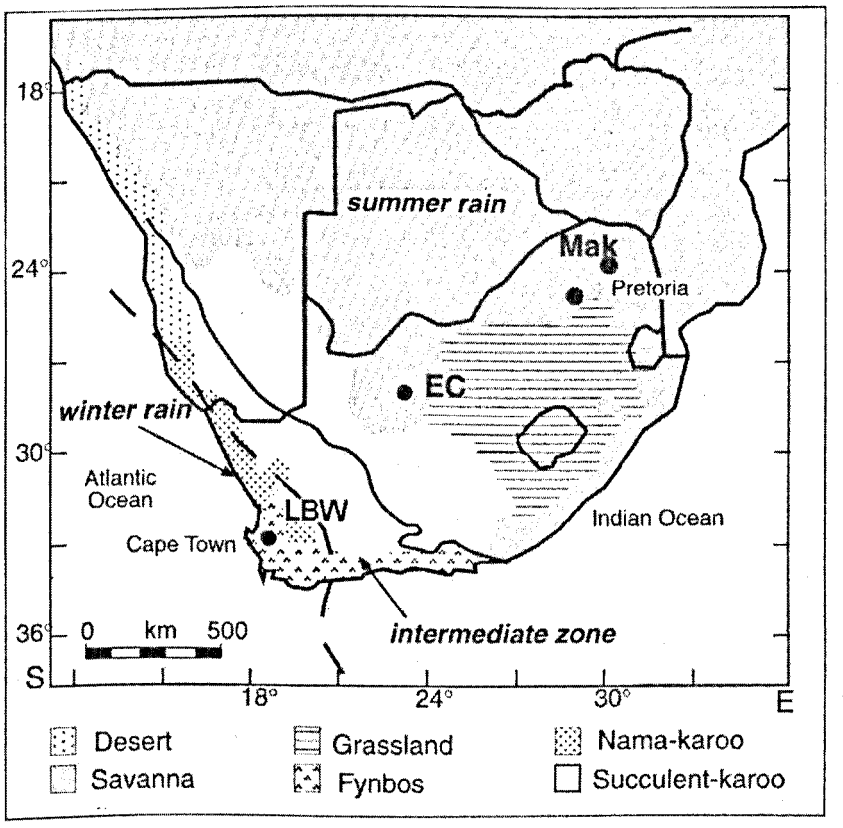

Figure 6.1. Map of Southern Africa showing the present distribution of the main vegetation biomes, summer and winter rainfall regimes, and the position of Makapansgat (Mak), Langebaanweg (LBW) and Equus Cave (EC). Figure modified from Lee-Thorp and Talma (2000).

The origins of the savannah environment of the South African highveld (north east South Africa) is poorly understood. The Quaternary isotopic (Repinski *et al.*, 1999, Holmgren *et al.*, 1999, Scott and Vogel, 2000) and palynological (Scott, 1986 & 2002) records indicate a mixture of C_4 grasses and bushes that is essentially the same as the present day southern savannahs. The evidence for the timing of the origins of the savannah biome in Southern Africa is currently elusive and at present can only be estimated using the model of Cerling *et al.* (1997) as discussed above. There is also uncertainty as to the nature of the vegetation preceeding the savannah biome in the South African highveld which is currently hindered by the lack of data. Two end-member possibilities for this pre-savannah vegetation include a montane C_3 grassland or a C_3 woodland / forest.

6.3. Environment and Palaeoenvironment of Makapansgat

The Makapansgat valley is situated in the north east of South Africa (latitude 24° South), at an altitude of approximately 1400 meters. It is located within the summer rainfall zone and today has a mean annual temperature of 19°C. The modern vegetation in the mountain range in the vicinity of the Makapansgat Valley is a mixture of riparian woodland, bushland and savannah grass. This region is transitional between Sourish Mixed Bushveld and North-Eastern Sourveld type as classified by Acocks (1953). The modern-day vegetation has also been classified as *Loudetia simplex-Diheteropogon filifolius* grassland (O'Connor and Bredenkamp, 1997) or Mixed-Savanna (Scholes, 1997). Both vegetation types are dominated by grasses using the C_4 photosynthetic pathway (Vogel *et al.*, 1978). It is likely that the tree and bush cover was greater prior to the deforestation of the valley by farmers.

Previous faunal and palaeoenvironmental studies at the Makapansgat Limeworks have focused on the australopithecine-bearing bone breccias, Members 3 and 4. These late-Pliocene members are thought to be the oldest macrofaunal deposits in the South African Transvaal cave-systems. Palaeoenvironmental interpretations of these deposits have ranged from fairly shrub-like with open grassland nearby (Wells and Cooke, 1956) to sub-tropical forest (Rayner at al., 1993). However, in the light of recent ecomorphological and stable isotope data, these deposits have most recently been interpretated as

representing a bush and woodland environment (Reed, 1998; Sponheimer *et al.*, 1999). Therefore, despite the greater woodland cover in Member 3 times, it appears that the Pliocene to recent climate of Makapansgat and other regions of the South African highveld was located within the summer rainfall regime and had a mixed C_3 and C_4 vegetation.

The Cerling *et al.* (1997) model for the global expansion of C_4 grasses predicts that C_4 plants were likely to have first arrived in the South African highveld close to the Miocene-Pliocene boundary at ~5 Ma. This prediction is based on the latitude of Makapansgat (24°South) and the assumption that palaeotemperatures were approximately equivalent to present day mean annual temperatures (18°C - the high altitude of Makapansgat gives it lower than average annual temperatures for this latitude). By investigating the palaeoecology of the oldest Makapansgat faunas, the Exit Quarry and Rodent Corner micromammal assemblages, the palaeoenvironmental data will be extended into the mid-Pliocene, possibly towards the putative origin of C_4 grasses in South Africa. By combining stable isotope data and dental microwear, it should be possible to identify the presence of C_3 grasses in the diet of herbivorous rodents. Given the suggested temporal links between the Makapansgat and the Langebaanweg rodent faunas (Pocock, 1987; Denys, 1999), it is possible that the two faunas will share a C_3 grass dominated palaeoenvironment.

Reconstructing the palaeodiets of extinct species has traditionally been determined by taxonomic uniformitarianism, the assumption that extinct species share the same dietary preferences as their extant relatives. However, it has been demonstrated that the habitat and dietary preferences of closely related extant taxa are not always similar to their extinct cogeners (Sponheimer *et al.*, 2001). The study of dental morphology has also been used as an indication of dietary adaptations, however it has been shown that generalist adaptations may mask specific dietary behaviour (Feranec, 2003). Denys (1994) used dental morphology to infer extinct rodent palaeodiets, and stressed the importance of additional palaeodietary data sources, such as stable isotopes and dental microwear. These techniques provide semi-quantitative dietary information for individuals within a population, independently of morphological assumptions.

Previous palaeoclimatic reconstructions using micromammals as environmental proxies (e.g. Avery, 1995, Wesselman, 1995, Denys, 1999) have been based on the premise that extinct taxa shared the same dietary and habitat preferences as their extant cogeners. This approach is appropriate for Pleistocene faunas from South Africa, such as Swartkrans, where only one rodent species out of 29 is extinct (Avery, 1998). However, in the Makapansgat Limeworks faunas, where two of the three most common micromammal species (*Otomys* cf. *gracilis* and *Mystromys* cf. *hausleitneri*) are extinct, dental morphology and uniformitarianism cannot be relied upon. Therefore, this study has used stable isotopes and dental microwear techniques on three of the most common micromammals from the Makapansgat Limeworks, to investigate palaeodietary and palaeoenvironmental conditions in the mid-Pliocene.

6.4. Introduction to stable isotopes and dental microwear

This study uses stable isotopes and dental microwear analysis to reconstruct the diet and palaeoenvironment of the Rodent Corner and Exit Quarry microfaunas and to compare it to the younger highveld sites (Lee-Thorp *et al.*, 1994; Van der Merwe *et al.*, 2003) and to the older lowveld site of Langebaanweg (Franz-Odendaal *et al.*, 2002). Stable carbon and oxygen isotope analyses of tooth enamel carbonate and dental microwear analysis of molar occlusal surfaces were used to obtain two independent palaeodietary assessments. By combining these two techniques, a more detailed palaeodietary reconstruction can be obtained than by using either technique in isolation. The use of stable carbon isotopes in tooth enamel is a well established technique that has been used to provide dietary and ecological information about animals living in savannah environments today and in the past (Vogel, 1978; Lee-Thorp *et al.*, 1997; Cerling *et al.*, 1997; Cerling *et al.*, 1999). The method relies on the fact that C_3 plants (trees, shrubs and high-latitude/altitude grasses preferring wet and cool growing seasons) and C_4 plants (savanna grasses and sedges growing in hot, arid habitats) use different photosynthetic pathways. The C_4 photosynthetic pathway is a CO_2-concentrating mechanism, a modification of the C_3 photosynthetic pathway, which increases the carbon fixing efficiency during photosynthesis, enabling a C_4 plant to tolerate higher temperatures, drier conditions and lower atmospheric pCO_2 levels than C_3

species. C_4 photosynthesis is energetically more costly (Salisbury and Ross, 1985) and C_4 vegetation is out-competed by C_3 plants at lower temperatures and higher pCO_2 levels. A consequence of the C_4 photosynthetic pathway is that the carbon isotope composition of plant tissue produced by C_4 plants is approximately 10-12‰ heavier than that of C_3 plants (O'Leary, 1981). When a mammal consumes plant matter, the $\delta^{13}C$ value of the vegetation it consumes is incorporated into its tissue such that the $\delta^{13}C$ of tooth enamel reflects its diet, with an additional fractionation. The enrichment in $\delta^{13}C$ between diet and tooth enamel is between 12 and 14‰ (Lee-Thorp *et al.*, 1989; Cerling and Harris, 1999). Typically, tooth enamel from herbivores eating C_3 vegetation have $\delta^{13}C$ values between –15‰ and –10‰ whereas those feeding on C_4 tropical grasses have $\delta^{13}C$ values between –2‰ and +2‰. Mixed feeders have values between these extremes. The diets of several fossil species have been investigated using stable carbon isotopes (e.g. Cerling *et al.*, 1999; Lee-Thorp *et al.*, 1989, 1994 and 2000). While the majority of studies have focused on macrofauna, stable isotope studies of microvertebrates offer further opportunities for palaeodietary and palaeoenvironmental research (Rogers and Wang, 2002). Due to taphonomic factors, macro and micro-vertebrates are often found in separate faunal assemblages, so the expansion of stable isotope studies into micromammal faunas can increase the number of sites available for isotopic investigation.

A complicating factor in stable isotope biogeochemistry is the potential for diagenetic alteration of both the $\delta^{13}C$ and $\delta^{18}O$ signal in fossil tooth enamel carbonate. Several authors have shown that carbon isotopes in enamel survive largely unaltered and that the distinction between C_3 browsers and C_4 grazers is preserved back to the Miocene and beyond (Lee-Thorp and van der Merwe, 1987; MacFadden and Cerling, 1994). It is often assumed that oxygen isotopes are more susceptible than carbon isotopes to diagenetic alteration in fossil enamel due to the availability of other sources of oxygen. Theoretical and empirical studies show that structural carbonate isotopic signals are seriously altered in fossil bone because it is highly porous and poorly crystalline (Koch *et al.*, 2001; Lee-Thorp *et al.*, 1989; Wang and Cerling, 1994). In contrast, the greater density and crystallinity of enamel enables biogenic oxygen isotopes signals to be better preserved (Sponheimer and Lee-Thorp, 1999). Comparisons of fossil enamel

carbonate $\delta^{18}O$ and phosphate oxygen $\delta^{18}O$ can be used to determine the degree of carbonate diagenesis (Bryant *et al.*, 1996; Iacumin *et al.*, 1996).

Dental microwear analysis has been proven as a valuable technique in the reconstruction of diet in a wide range of mammals. Microwear analysis has been used to distinguish various aspects of a mammalian diet such as browsing versus grazing (Solounias *et al.*, 1988; Walker *et al.*, 1978); frugivory versus folivory (Teaford and Walker *et al.*, 1984; Teaford, 1994); faunivore (i.e. invertebrates and reptiles) versus frugivore/folivore (Strait, 1993). Most explanations for microwear formation have focused on factors intrinsic to food such as the presence of opal phytoliths in grasses (Walker *et al.*, 1978) or the "hardness" of nuts (Teaford and Walker, 1984) and insect carapaces (Strait, 1993). However, there is also some indication that extraneous factors, such as soil or grit particles ingested with food may be important agents in the modification of dental microwear (Ward and Mainland, 1999; Walker, 1976 and Ungar and Teaford, 1996).

Two key dental microwear features in relation to diet are striations and pits. Striations on the wear facets of enamel are caused by small inorganic particles of greater hardness than the enamel, that have been drawn across the enamel surface at a pressure not so great as to cause the particle to be crushed (Rensberger, 1978). The striations are randomly spaced but are often sub-parallel, indicating the dominant direction of jaw movement. The particles responsible for the formation of striations are likely to be either soil derived quartz or opal phytoliths. Phytoliths occur in much larger concentrations in grasses than in many dicotyledonous plants (Baker, 1959) and the proximity of grasses to the soil increases the likelihood of soil derived quartz ingestion. Therefore the formation of striations on wear facets is associated with a grazing behaviour, as indicated by the dominance of striations on wear facets of grazing herbivores (Walker *et al.*, 1978; Solounias *et al.*, 1988; Solounias and Hayek, 1993; Rivals and Deniaux, 2003).

Pits tend to be created by food items that require more masticatory demand and/or are inherently hard enough to cause microscopic fractures of the tooth surface. The hard-objects responsible for the pitting of the enamel are likely

to be hard fruits or seeds in the case of frugivores and granivores or chitin or bone in the case of faunivores. Strait (1993) indicates that it is not possible on the basis of dental microwear to distinguish hard-object frugivores from hard-object faunivores within the studied sample of primates and microchiropterans. Such studies indicate that the proportion of pits relative to striations on the occlusal surface is a qualitative indication of the proportion of grass versus hard-objects in the diet of omnivores and herbivores and can be used successfully to predict the diet of modern species and reconstruct the diet of extinct species (Teaford, 1988; Rafferty *et al.*, 2002). This proportion can be measured semi-quantitatively using image analysis softwear (Ungar *et al.*; 1991, Ungar, 1995).

A number of microwear studies on modern small mammals (Rensberger, 1978; Walker *et al.*, 1978; Lee and Houston, 1993; Silcox and Teaford, 2002) and on fossil rodents (Lewis *et al.*, 2000) indicate the potential for palaeodietary reconstruction in rodents using dental microwear.

6.5. Locality and Materials

The teeth analysed in this study were taken from the Pocock collection of micromammals housed at the Bernard Price Institute of Palaeontology (BPI) at the University of the Witswatersrand and described in Pocock (1985; 1987). The Pocock collection is taken from two *in situ* deposits of the Makapansgat Limeworks, the Makapansgat Rodent Corner *in situ* (MRCIS) Pink Breccia and the Exit Quarry Basal Red Mud (EXQRM). The EXQRM collection comes from large blocks of dry red mud collected in 1973 from the back of the Exit or North-East Quarry (Maguire, 1980) and by further collections in 1980-1983 (Pocock, 1987). The skeletal elements present, the degree of disarticulation and the lack of bone digestion indicate that both the deposits are calcified owl pellet accumulations (Levinson, 1982; Brain, 1981). The most likely accumulator was the Barn Owl, *Tyto alba* (Levinson, 1982). The three genera of micromammals that dominate the faunas, *Otomys* sp., *Mystromys* sp. and *Myosorex* sp., are represented by 150 to 500 minimum number of individuals at each site, which together constitutes 40% and 52% of the total number of micromammals collected at MRICS and EXQRM respectively (Pocock, 1987).

Dating of the South African Plio-Pleistocene cave faunas has been a problem since their first discovery. Makapansgat has been classified as the oldest of the South African cave deposits on the basis of faunal seriation (McKee *et al.*, 1995 and Mckee 1995) and by palaeomagnetism which places Member 3 at 3.1-3.2 Ma (Partridge *et al.*, 2000). This is in broad agreement with faunal correlation with the radiometrically dated biostratigraphy of the Plio-Pleistocene of east Africa which places Makapansgat Member 3 at approximately 3 Ma (Vrba, 2000). The Rodent Corner and Exit Quarry faunas have traditionally been included within Makapansgat Member 4 (McKee *et al.*, 1995). However, as discussed in Maguire *et al.* (1985), Latham *et al.* (1999) and Latham *et al.* (2003), Makapansgat Members 3 and 4 and the Rodent Corner and Exit Quarry deposits are best viewed as separate repositories with uncertain temporal relationships.

The establishment of a biostratigraphic framework based on east African Plio-Pleistocene rodents has been hampered by the lack of phyletic lineages, the slow rate of morphological change and the high degree of endemism (Denys and Jaeger, 1986). The Makapansgat rodent faunas do however share common species with other South African Plio-Pleistocene cave deposits, especially with the lower Pliocene Langebaanweg from the Cape Province of South Africa. For example, *Stenodontomys* (Mystromys) *darti*, a common species from Makapansgat MRCIS, is known elsewhere only from Langebaanweg (Pocock, 1976 and 1987). *Proodontomys cooki* (Pocock, 1987) is an extinct Cricetine rodent species and genus from MRCIS and EXQRM that also occurs in the majority of the South African Plio-Pleistocene rodent faunas. On the basis of the micro- and macro-faunal correlations, it is widely accepted that Makapansat is the oldest of the highveld faunas, with the possible exception of the recent discovery of a lower Pliocene rodent fauna from Waypoint 160 in the Bolt's Farm area (Sénégas and Michaux, 2000; Sénégas and Avery, 1998). The age often quoted for the Makapansgat MRCIS and EXQRM microfauna is 3.3-3.5 Ma (Denys, 1999; Partridge *et al.*, 2000; Herries, 2003).

The Grand Canyon locality (GRCAN) is an Iron-Age rock shelter deposit on the western slope of the northern end of the Makapansgat (Zwartkrans) valley. It contains a micromammal assemblage accumulated by Owl predation (Bray, 2001) and is used in this study as a modern analogue to the accumulation of the MRCIS and EXQRM micro-faunas. The most common components of the

microfauna include *Otomys* cf. *irroratus*, *Mastomys* (Praomys) sp., *Myosorex* sp. and *Cryptomys* sp. (Bray, 2001). The GRCAN fauna accumulated prior to deforestation and farming in the Makapansgat valley and therefore represents a more natural late Holocene palaeoclimate than the farmed valley of the present day.

6.6. The micromammals

6.6.1. *Mystromys cf. hausleitneri*

The genus *Mystromys* is the single extant African representative of the subfamily Cricetinae and is represented by a single extant species that is endemic to South Africa, *Mystromys albicaudatus* (Smith, 1834), the White Tailed Rat. M. *albicaudatus* lives today to the south of latitude 25° South where it is confined to highveld and montane grassland in small fragmented populations. It is locally absent from the Makapansgat Valley (24° South) in the present day. It is nocturnal, occupies burrows and has an omnivorous diet of plant food, seeds and insects (Perrin and Maddock, 1983). This omnivorous diet is evident in the molar teeth which are cusped, not flattened, and in the lengths of the small and large intestines which are typical of an omnivore (Perrin and Curtis, 1980). Brain (1985) suggested that today's relict population was linked to a larger population during previous episodes of cold-induced grassland expansion and that it is isolated today because of Holocene inter-glacial conditions. The northern Cricetine relatives of *Mystromys* (including the voles and hamsters) are generally considered to be "cold-adapted" and Down and Perrin (1995) show that M. *albicaudatus* has maintained the thermal characteristics of typical cold-adapted rodents, without adapting to the warmer temperature regimes of Africa. M. *albicaudatus* remains inactive diurnally in the thermally buffered microenvironment of a burrow and is active during the cold nights of the South African highveld (Down and Perrin, 1995).

The fossil record of the Cricetinae indicates a more diverse clade in the late Neogene, represented by the extinct species *Proodontomys cookei* (Pocock, 1987), M*ystromys Pocockei* (Denys, 1991) and *Mystromys hausleitneri* (Broom, 1937). M. *Pocockei* has only been securely identified from the type locality of Langebaanweg although it has been suggested that it is synonymous with the

undescribed "dwarf" species of *Mystromys* from Makapansgat MRCIS (Pocock, 1987 and Denys, 1991). If M. *Pocockei* is shown to be present at MRCIS then this is more evidence to suggest that components of the microfauna are shared between Langebaanweg and Makapansgat MRCIS. *Proodontomys cooki* first occurs at Makapansgat (Pocock, 1987) and is also known from the younger sites of Kromdraai A & B and Sterkfontein (Member 5), Swartkrans, Gladysvale and Taung. M. *hausleitneri* is present in the Plio-Pleistocene at Langebaanweg (Hendey, 1976, Pocock, 1976) and Makapansgat MRCIS and EXQRM (Pocock, 1987) and at Swartkrans Members 1,2 & 3 (Avery, 1995) and in the Pleistocene at the Cave of Hearths (de Graaff, 1960).

6.6.2. *Otomys* cf. *gracilis*

The Otomyinae are tropical myomorph rodents called African swamp rats or groove-toothed rats, characterised by high crowned lamellar teeth. They are represented today by nine pan-African species of *Otomys* (Cuvier, 1823) and two endemic South African species of *Parotomys* (Thomas, 1918). The very derived morphology of the *Otomyinae* hides their phylogenetic affinities (cricetid versus murid) and the systematic position of this subfamily has been extensively debated (Misonne, 1969, Pocock, 1976, Denys *et al.*, 1987). However, recent molecular and palaeontological evidence has come to the consensus that the *Otomyinae* constitute a monophyletic clade within the Murinae (Chevret *et al.*, 1993; Senegas and Avery, 1998). The typical high-crowned lamellar teeth of *Otomys* are associated with the strict herbivorous diet observed in extant *Otomys* (Kerley, 1992; Perrin and Curtis, 1980) so it is assumed that the similar dental morphology of the extinct *Otomys* species is also indicative of a highly fibrous diet.

Kerley (1992) in a study of modern *Otomys unisulcatus* from the semi-arid Karoo of South Africa and Monadjem (1997) in a study of modern O. *angoniensis* and O. *irroratus* from the moist savannahs of Swaziland and O. *angoniensis* from the highlands of Kenya (Taylor and Green, 1976) all found that stomach contents were exclusively herbivorous (excluding seeds). Perrin and Curtis (1980) in a study of the digestive morphology of modern myomorph rodents concluded that *Otomys* shows a high level of adaptation to a herbivorous diet in terms of gut morphology (microbial fermentation) and dental morphology (laminate, hypsodont molars with flat crowns and open roots), but has a stomach typical of a

more generalised diet. They suggest that the more specialised gut and dental morphologies compensate for the less specialised stomach. Perrin and Curtis (1980) also suggest that this mosaic of specialisations has prevented *Otomys* from reaching an extreme level of specialisation, which enables it to cope with potential changes in environmental conditions. If *Otomys* is forced to change its diet, the generalised stomach will compensate for the specialised dentition and gut. The present study of the palaeodiet of the extinct *Otomys* cf. *gracilis* may indicate that the varied morphology of modern *Otomys* is indicative of a more varied or different diet in its recent evolutionary history.

6.6.3. *Myosorex* cf. *varius*

The extant genus *Myosorex* is a member of the African shrews (Insectivora: Soricidae). The Soricidae is traditionally divided into two subfamilies, the Soricinae and Crocidurinae, but based on recent morphological and genetic evidence (Bedford *et al.*, 1998; Maddalena and Bronner, 1992; Querouil *et al.*, 2001) *Myosorex* is now placed in a separate subfamily called Myosoricinae. Makapansgat is the earliest record of *Myosorex* cf. *varius*, the extant forest shrew. It is the most abundant taxon at EXQRM and the fourth most abundant taxon at MRCIS. Its extinct cogener *Myosorex robinsoni* (Meester, 1955) is also found in the Plio-Pleistocene of South Africa (Meester, 1955) and East Africa (Wesselman, 1995).

M. *varius* is usually considered to live in moist coastal and temperate forest (Brown *et al.*, 1997). However, Fuller and Perrin (2001) show that M. *varius* is also common in South African grasslands. The diet of modern M. *varius* is predominantly insectivorous although there is evidence of a more omnivorous dietary behaviour. Monadjem (1997) in a study of stomach contents in Savannah dwelling M. *varius* from Swaziland found 97% arthropods, 3% foliage and no seeds. Earthworms are also a significant dietary component of M. *varius* (Reinecke *et al.*, 2000) and it is also known to consume some plant and fruit material (Wirminghaus and Perrin, 1992).

6.6.4. *Mastomys* (Praomys) sp.

The genus *Mastomys* belongs to the *Praomys* group of murine rodents and has been included in the present study because *Mystromys albicaudatus* is rare in the Holocene and is missing from the GRCAN fauna (see above). *Mastomys* is a common component of the GRCAN fauna (Bray, 2001) and is an omnivore-insectivore that has a very similar dietary niche to that of *M. albicaudatus*. Therefore, in terms of carbon isotope composition and dental microwear analyses, *Mastomys* sp. is an appropriate modern analogue for the Makapansgat M. *hausleitneri*. *Mastomys* (Praomys) sp. is present only in small numbers at Makapansgat MRCIS and EXQRM (Pocock, 1987), perhaps indicating that it was outcompeted at this time by M. *hausleitneri*. The extinct species M. *minor* and M. *cinereus* are known from the Plio-Pleistocene of east Africa (Denys, 1986; Wesselman, 1985) but the South African specimens have not been identified to the species level (Pocock, 1987; Avery, 1995).

There are two modern *Mastomys* species common in South Africa, the multimammate mice, M. *natalensis* and M. *coucha*. Morphologically, both species are almost identical and were originally regarded as one (De Graaf, 1981), M. *natalensis*. However, ethologic, morphometric and genetic characteristics have aided in the identification of the two species (Smit *et al.*, 2001; Dippenaar *et al.*, 1993) and enabled their habitat range to be determined. Smit *et al.* (2001) indicate that M. *natalensis* inhabits the savannah biome whereas M. *coucha* inhabits the montane grassland biome.

M. *natalensis* has been described as omnivorous (Smithers, 1983). Seeds, insects and other plant and animal matter are important food sources for *Mastomys* (Monadjem, 1997). Termites and insect larvae are commonly featured in the diet, and the skin and muscles of frogs and rodents have also been found in its stomach contents (Taylor and Green, 1976). The soil fungus Endogene (mixed with particles of grit) was also found when cereals were scarce (Taylor and Green 1976). However, M. *natalensis* has been shown to be primarily granivorous in the Zimbabwean Highlands (Swanepoel, 1980) and in the Kenyan Highlands (Taylor and Green, 1976), with seasonal increases in the consumption of insects and herbage. Kerley (1992) in a study of modern *Mastomys natalensis* from the semi-arid Karoo of South Africa found that stomach contents contained mainly herbage and insects and no seeds. The unspecialised digestive morphology of M.

natalensis described by Perrin and Curtis (1980) is related to the dietary opportunism observed in this species.

6.7. Methods

Pocock (1987) states that the EXQRM fauna was prepared using water to disintegrate the dried mud whereas the MRCIS fauna had been prepared using acid dissolution of the calcified breccia. The prior use of acid preparation on the MRCIS fauna requires caution in the interpretation of dental microwear in this study. However, the acid-etched microwear pattern was easily identified and teeth with obvious acid-etching were removed from the analysis. Based on experimental studies (Nielson-Marsh and Hedges, 2000) it has been shown that acid exposure does not have a significant effect on the stable isotope composition of enamel. King *et al.* (1999) show that acid dissolution is readily identifiable in dental microwear studies, and tends to obliterate rather than alter microwear features.

a) Stable Isotopes

Incisors from the fossil and recent micromammals were cleaned of any adhering matrix and the enamel was mechanically separated from the dentine. The enamel was ground to a fine powder and was of sufficient mass to provide adequate CO_2 for isotopic measurement following the standard method out-lined in Lee-Thorp *et al.* (1997). Due to the small size of insectivore teeth, the insectivore mandibles (*Myosorex* sp.) were cleaned of any adhering matrix and the cheek teeth and incisors were removed from the mandible and ground to a fine powder. This method inevitably leads to an enamel/dentine mixture. For one sample, cheek teeth powder from two Rodent Corner *Myosorex* sp. individuals was combined in order to generate enough CO_2 for analysis (see Table 6.1.).

To remove organic matter, samples were reacted with 2% NaOCl overnight and washed 5 times by centrifugation. To remove all the carbonate adsorbed onto apatite crystal surfaces, the residue was then reacted with 1M acetic acid for 15 minutes and washed 5 times. This preparation procedure has been shown to have minimal effects on the isotopic values of structural carbonate (Koch *et al.*, 1997; Nielsen-Marsh *et al.*, 2000). The remaining structural

carbonate in the enamel samples was converted to CO_2 by reaction with 100% phosphoric acid at 90°C for 10 minutes using an automated VG Isocarb common acid-bath preparation system. Blank samples were run between each enamel sample to ensure that there was no cross-contamination between adjacent samples. All blank samples evolved quantities of CO_2 below the routine detection limits of the mass spectrometer.

The CO_2 released by the enamel reaction was cryogenically purified prior to the measurement of carbon and oxygen isotope ratios on an automated VG SIRA 12 mass spectrometer at the University of Liverpool. All data were corrected for ^{17}O effects following Craig (1957). Carbon and oxygen isotope data are reported in conventional delta (δ) notation in "parts per mil" (‰) relative to V-PDB (Coplen, 1995). Accuracy and reproducibility of the isotopic analyses was assessed by replicate analysis of BCS2 (internal calcite standard) against NBS-19 and two internal enamel standards. Analytic precision (σ) determined from the enamel standards is ±0.22‰ and ±0.62‰ for $\delta^{13}C$ and $\delta^{18}O$ respectively. The lower precision of $\delta^{18}O$ is attributed to the heterogeneity of $\delta^{18}O$ in the enamel standards. Long-term laboratory reproducibility (σ) is better than ±0.1‰ for both isotope ratios.

b) Dental Microwear

The molar specimens of *Mystromys* (EXQRM and MRCIS) and *Otomys* EXQRM were taken from a collection of mandibles and lower dentitions whereas the *Otomys* MRCIS specimens were taken from a collection of mixed, isolated first molars. Any adhering matrix was removed from the teeth and mandibles in an ultrasonic bath. The dried samples were then given a gold/palladium coating and viewed under the Scanning Electron Microscope (SEM).

The occlusal surface of worn molars from at least 9 individuals of each species was investigated (see Table 6.2.). At least two photomicrographs were taken from each individual at a magnification of x1000. The digital images were then analysed using the semi-automated image analysis software Microwear 4.0 (Ungar, 1991, 1995). The dimensions and orientation of each microwear feature was measured and the length to breadth ratio of 4:1 was used to distinguish striations from pits.

6.8. Results

6.8.1. Stable Isotope Results

The $\delta^{13}C$ values of the fossil micromammal teeth analysed in this study ranged from -10.0 ‰ to –3.5 ‰ with a mean value of –6.5 ‰ (n=25) whereas the modern micromammal teeth $\delta^{13}C$ values ranged from –7.3 ‰ to –2.2 ‰ with a mean value of –4.1 ‰ (n=9). Therefore, the $\delta^{13}C$ values in this study indicate a range in consumption from an almost pure C_3-plant diet to an almost pure C_4-plant diet. The carbon isotope composition of the insectivore enamel is similar in the fossil and modern samples, whereas the rodents show more enriched $\delta^{13}C$ values (greater proportion of C_4 grass consumption) in the modern samples relative to the fossil samples (see Fig. 6.2.) The $\delta^{18}O$ values of the fossil rodent teeth ranged from –4.2 ‰ to 0.9 ‰ with a mean value of –1.9 ‰ whereas the $\delta^{18}O$ values of the modern rodent teeth ranged from –7.6 ‰ to 0.6 ‰ with a mean value of –3.3 ‰. There are no observable species-specific trends in the $\delta^{18}O$ data, and there is no simple relationship between the $\delta^{18}O$ and $\delta^{13}C$ values. Given the complexity of $\delta^{18}O$ interpretation in fossil enamel carbonate (Wang and Cerling, 1994; Sponheimer and Lee-Thorp, 1999; Lindars *et al.*, 2001), the $\delta^{18}O$ values obtained in this study are not discussed further.

LOCALITY	$\delta^{13}C$	$\delta^{18}O$
Rodent Corner (MRCIS)		
Otomys cf. *gracilis* (i)	-7.0	0.9
Otomys cf. *gracilis* (i)	-5.8	-1.0
Otomys cf. *gracilis* (i)	-8.1	-1.0
Otomys cf. *gracilis* (i)	-4.5	-3.0
Otomys cf. *gracilis* (i)	-5.6	-4.4
Mystromys cf. *hausleitneri* (i)	-7.7	-1.1
Mystromys cf. *hausleitneri* (i)	-8.9	-2.3
Mystromys cf. *hausleitneri* (i)	-10.0	-4.2
Mystromys cf. *hausleitneri* (i)	-7.9	-2.3
Myosorex cf. *varius* (c)	-5.5	-2.7
Myosorex cf. *varius* (c)*	-8.4	-3.7
Exit Quarry (EXQRM)		
Otomys cf. *gracilis* (i)	-3.6	-1.1
Otomys cf. *gracilis* (i)	-9.6	0.6
Otomys cf. *gracilis* (i)	-5.6	-3.0
Otomys cf. *gracilis* (i)	-4.3	-2.7
Otomys cf. *gracilis* (i)	-4.5	-1.6
Otomys cf. *gracilis* (i)	-4.9	-2.2
Mystromys cf. *hausleitneri* (i)	-6.3	-0.4
Mystromys cf. *hausleitneri* (i)	-6.7	-1.1
Mystromys cf. *hausleitneri* (i)	-7.6	-1.1
Mystromys cf. *hausleitneri* (i)	-6.6	-1.4
Mystromys cf. *hausleitneri* (i)	-5.6	-2.6
Myosorex cf. *varius* (c)	-5.5	-1.5
Myosorex cf. *varius* (c)	-6.4	-1.1
Myosorex cf. *varius* (c)	-6.5	-3.0
Grand Canyon (GRCAN)		
Otomys sp. (i)	-3.6	0.6
Otomys sp. (i)	-2.8	-0.4
Otomys sp. (i)	-2.8	-7.6
Mastomys sp. (i)	-2.2	-6.5
Mastomys sp. (i)	-7.3	-3.4
Mastomys sp. (i)	-2.2	-3.6
Myosorex sp. (c)	-6.8	-3.5
Myosorex sp. (c)	-6.0	-3.5
Myosorex sp. (c)	-3.0	-1.4

Table 6.1. Carbon and oxygen isotope values for Rodent Corner, Exit Quarry and Grand Canyon micromammals. (i) = incisor; (c) = cheek teeth. *enamel sampled from two individuals

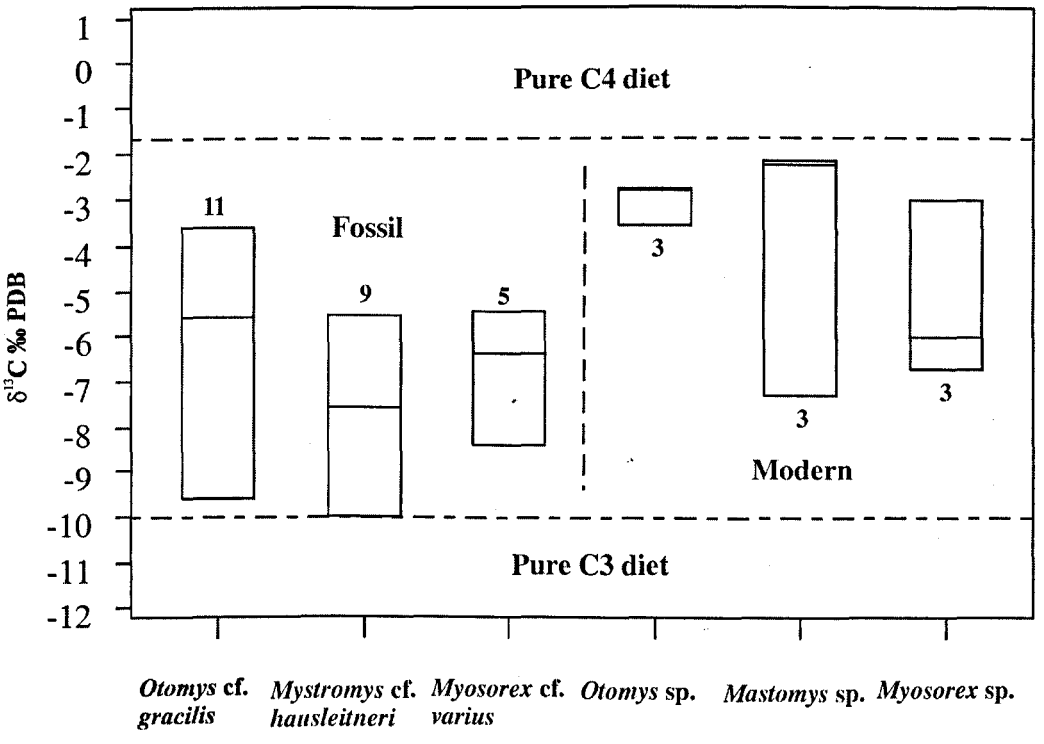

Figure 6. 2. Range charts showing the median and range of carbon isotope values for the studied fossil and modern rodent species. The fossil sites are EXQRM and MRCIS combined and the recent site is GRCAN. The number within each box refers to the number of individuals analysed within each species. C_3 and C_4 diet end-members for Makapansgat are from Sponheimer *et al.* (1999).

6.8.2. Dental Microwear Results

Each occlusal surface examined under the SEM showed a combination of pits and striations with the number of pits as a percentage of the total number of microwear features (averaged over two micrographs from the same individual) ranging from 3.9% to 67.9%. The precision of the semi-quantitative Microwear analysis (Ungar *et al.*, 1991 and Ungar, 1995) was determined by comparing the percentage of pits in 34 duplicate micrographs from the same individual. The mean difference in % pits for duplicate micrographs is 8.4% with 97% of individuals showing a difference of less than 15% (see Fig. 6.4.). This is similar to the 7% intra-observer error rate quoted by Grine *et al.* (2002). The quantification of microwear features can only be regarded as an approximation due to individual biases in the identification and recording of microwear features - Grine *et al.* (2002) quote a 9% inter-observer error. The significant differences in

mean % pits (see Table 6.2.) between species and sites is considered indicative of dietary changes.

The mean pit length per micrograph ranges from 3 μm to 9 μm and there is no significant variation in pit length between species. The mean percentage of pits differs significantly between species, with *Mystromys* and *Mastomys* showing the greatest proportion of pits at 45.4% and 33.7% respectively (Table 6.2.). The microwear features of *Otomys* sp. from GRCAN are dominated by striations although there is also a substantial proportion of pits (17.1%). The microwear of *Otomys* sp. from EXQRM and MRCIS has a low percentage of pits (8.2% and 27.8%) and is characterised by the presence of furrows as discussed below.

	No. of Individuals	Min % Pits	Max % Pits	Mean % Pits	Mean $\delta^{13}C$
Otomys cf. *gracilis* MRCIS	5	22.0	38.5	27.8	-6.2
Otomys cf. *gracilis* EXQRM	4	3.9	10.7	8.2	-5.4
Otomys sp. GRCAN	9	5.1	37.3	17.1	-3.1
Mystromys cf. *hausleitneri* MRCIS	6	29.4	51.1	42.4	-8.6
Mystromys cf. *hausleitneri* EXQRM	7	26.6	67.9	48.3	-6.1
Mastomys sp. GRCAN	9	24.5	43.2	33.7	-3.9

Table 6.2. Molar microwear results for Exit Quarry, Rodent Corner and Grand Canyon. Mean $\delta^{13}C$ values are presented for comparison – an increased percentage of pits is expected to correspond with lower $\delta^{13}C$ values. Exceptions are discussed in the text.

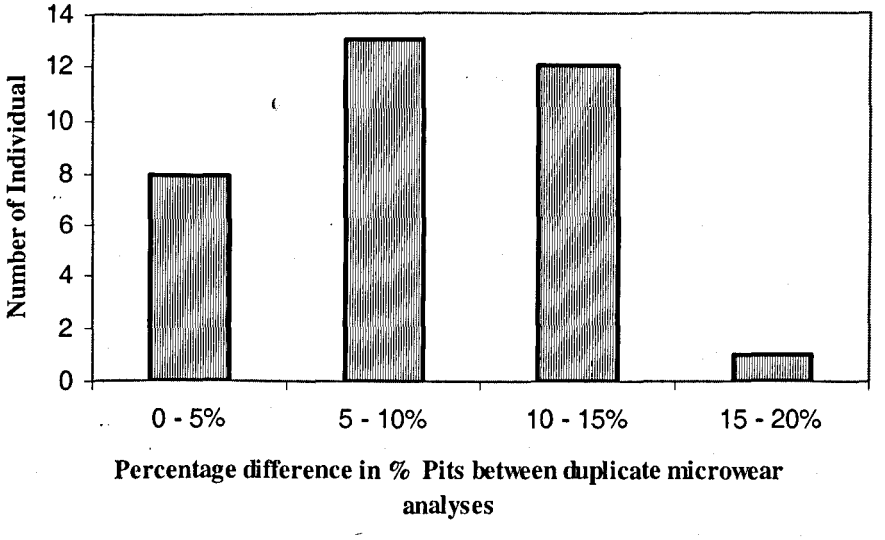

Figure 6.4. Precision of molar microwear analysis determined from duplicate micrographs. Duplicate micrographs taken from different wear facets of the same individual.

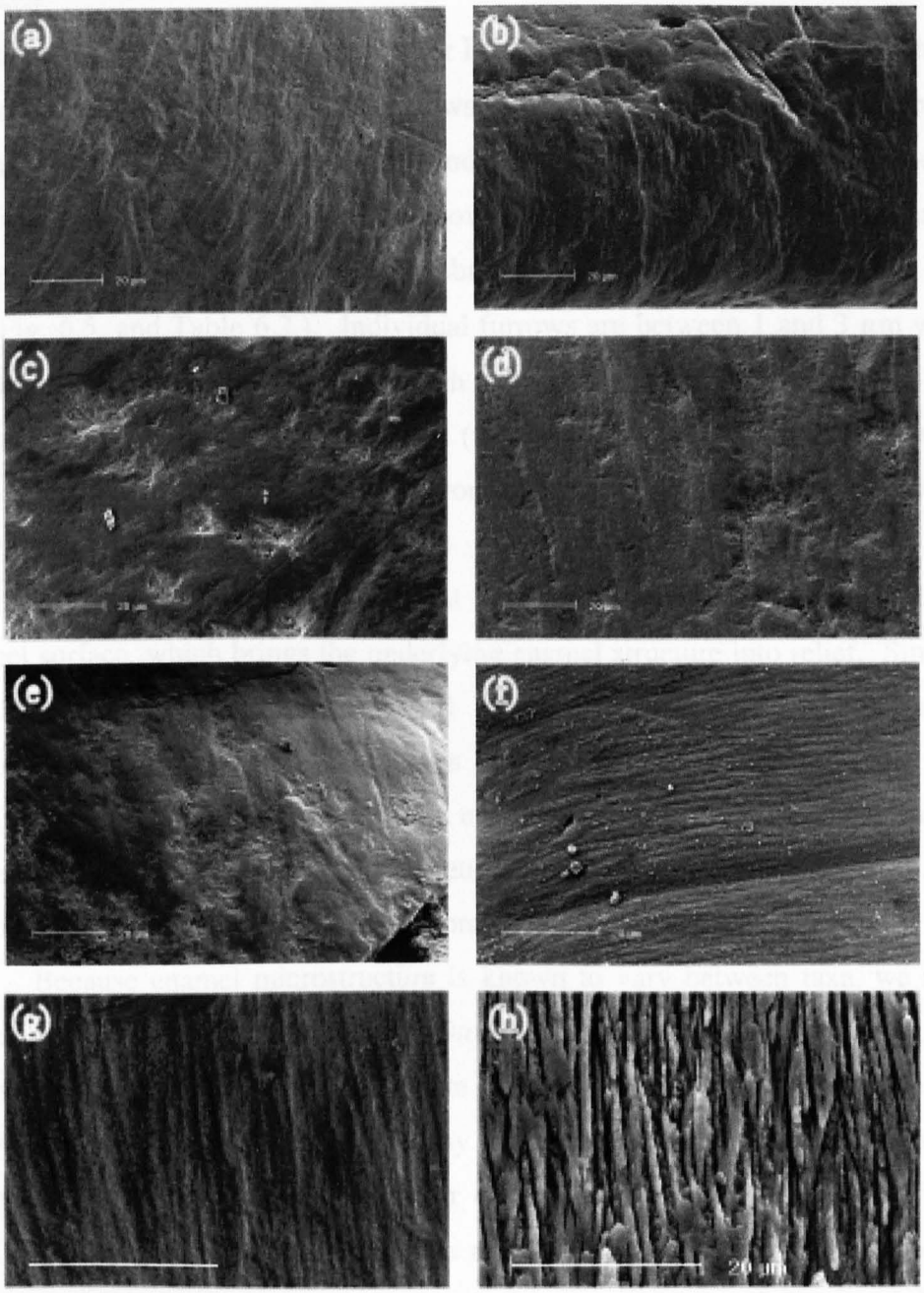

Figure 6.3. – Scanning electron micrographs of microwear on the occlusal surface of fossil and modern rodent molars and the enamel microstructure of modern *Otomys* sp. molar (a) Modern *Otomys* sp. from GRCAN. Striations indicative of a grass dominated diet. (b) *Otomys* cf. *gracilis* from MRCIS. Pits and striations indicative of a mixed diet of grass and hard objects (e.g. seeds). This micrograph shows remnants of a furrowed surface. (c) *Mystromys* cf. *hausleitneri* from EXQRM. Dominated by pits, indicating a diet of hard objects such as seeds. (d) *Mystromys* cf. *hausleitneri* from MRCIS. Mixture of pits and striations indicating a diet of hard objects and grass. (e) Modern *Mastomys* sp. from GRCAN. Pits and striations indicative of a mixed diet of grass and hard objects. (f & g) *Otomys* cf. *gracilis* from EXQRM. Dominated by polishing of the occlusal surface which highlights the underlying enamel microstructure, resulting in furrows. The high degree of polishing indicates a soft diet of leaves and perhaps fruit. (h) Acid etched occlusal surface of *Otomys* sp. from GRCAN. Radial enamel adjacent to the outer enamel surface. The position, orientation and spacing of the enamel prisms is identical to the microwear of f & g. Scale bars are 20 microns.

Furrows

The dental microwear of each of the four EXQRM *Otomys* cf. *gracilis* individuals studied was dominated by parallel furrows (grooves) that run perpendicular to the enamel dentine junction (EDJ) and are more prominent towards the leading edge. The ridges that occur between the grooves generally lack microwear features, except for occasional striations. This fabric is also associated with a lack of pits (see Fig. 6.5. and Table 6.2.). Individual furrows are between 1 and 3 μm wide and are usually less than 20 μm in length and are often tapered at each end. The term *furrow* is taken from Rensberger (1978) who used it to describe a very similar microwear fabric in the herbivorous *Microtus townsendi* (Arvicolidae, Rodentia).

Rensberger (1978) suggested that furrows are a result of polishing of the enamel surface, which brings the underlying enamel structure into relief. Similar polished fabrics have been observed in *Heterohyrax brucei* (Procaviidae, Hyracoidea) and they have been shown to be associated with a browsing diet (Walker *et al.*, 1978). It is unlikely that enamel dissolution is responsible for the presence of furrows as there is no indication of the characteristic patterns of acid etching and the EXQRM fauna was not prepared using acid dissolution.

Because enamel microstructure is known to vary between taxa, we acid etched the lower molars of a modern *Otomys* sp. following the methodology of Koenigswald *et al.* (1994) to investigate the possibility that the furrows in the microwear of *Otomys* cf. *gracilis* may be reflecting the underlying enamel structure. The etched surface of molar enamel of a modern *Otomys* sp. from GRCAN is shown in Figure 6.3.h. The radial enamel prisms towards the outer enamel surface are of approximately the same average spacing (2-5μm) and show the same tapering pattern (Fig. 6.3.h) as the furrows on the occlusal surface of *Otomys* cf. *gracilis* (Fig. 6.3.f,g). Therefore it seems likely that the furrowed pattern of the wear facets is formed by the combination of chemical corrosion and physical abrasion described by Rensberger *et al.* (1978).

There is evidence of faint and worn furrows in some MRCIS *Otomys* cf. *gracilis* specimens (Fig. 6.3.b), indicating a significant proportion of soft food material in the diet in the months prior to death. In contrast, the recent GRCAN *Otomys* sp. shows no evidence of furrows (Fig. 6.3.a) on the wear facets.

6.9. Discussion

6.9.1. Palaeodietary Reconstruction

The combined approach of isotopic and microwear analysis used in this study has successfully reconstructed the known diets of the two modern species *O. irroratus* and *Mastomys* sp. as graminivory and omnivory respectively (see Table 6.3.). The insectivorous modern shrew *Myosorex* sp. was not studied using dental microwear analysis as the identification of insectivorous palaeodiets was not a primary concern of this study. The carbon isotopic composition of modern *Myosorex* from GRCAN (mean $\delta^{13}C$ = -5.3) and fossil *Myosorex* from EXQRM and MRCIS (mean $\delta^{13}C$ = -6.5) is consistent with an insectivorous diet derived from a mixture of C_3 and C_4 plant consuming invertebrates.

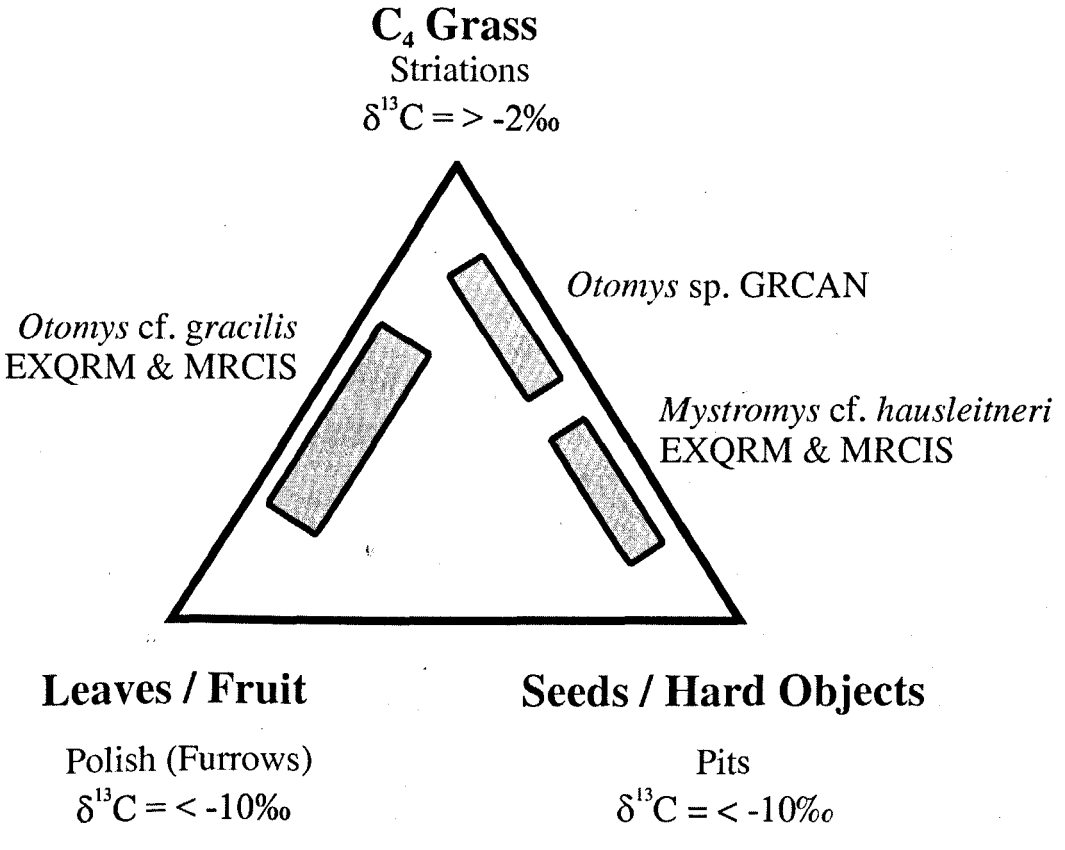

Figure 6.5. Triangular plot illustrating the results of the combined stable isotope and molar microwear study of palaeodiet in modern and fossil rodents from Makapansgat. The inferred dietary components in bold are determined from the labelled microwear and isotopic evidence.

The extinct species *Mystromys* cf. *hausleitneri* is reconstructed as a seed and grass eater on the basis of the mixture of striations and pits on the molar occlusal surfaces (see Table 6.3.). It is also possible that some of the pits observed are the result of alternative sources of hard objects such as bark or invertebrate consumption, as is observed in some extant rodents species (Baxter and Hansson, 2001; Perrin and Maddock, 1983). The carbon isotope data indicates a mixed C_3 and C_4 plant diet that varies among individuals from an almost pure C_3 diet to an almost pure C_4 diet which is likely to represent the variation from seed-dominated to grass-dominated diets. Modern *Mystromys albicaudatus* is known to consume invertebrates (Perrin and Maddock 1983), so based on the similar omnivorous dentition of M. *hausleitneri* it was also likely have to consumed invertebrates, although there are no microwear or isotopic indicators available to qualify this assumption. Based on the evidence presented in this study, it is apparent that M. *hausleitneri* shared similar dietary preferences to that of its extant cogener M. *albicaudatus*.

Species	Modern Diet[1]	Dental Morphology	Carbon Isotopes[2]	Molar Microwear[3]	Palaeodiet Reconstruction	
					Composite	Summary
Modern						
Otomys sp.	G (S)	G	G	G (S)	G (S)	G (S)
Mastomys sp.	O	O	M-F	G - S	S - G (?I)	O
Myosorex sp.	I	I	M-F	-	I	I
Fossil						
Otomys cf. *gracilis*	-	G	M-F	B (G,S)	B - G (S)	M-F (S)
Mystromys cf. *hausleitneri*	-	O	M-F	S - G	S - G (?I)	O

Table 6.3. Comparison of dietary indicators derived from dental morphology, carbon isotopes and molar microwear. There is strong agreement between the dietary reconstruction and known diet in the modern taxa, indicating the accuracy of the combined technique. There is close agreement between the carbon isotope and molar microwear data in the fossil taxa. B = Browse, G = Graze, I = Insectivory, M-F = Mixed-Feeding on Browse and Graze, O = Omnivory, S = seeds. Dietary components separated by a hyphen indicate that both components represent a major proportion of the diet, with the larger proportion listed first. Dietary components in brackets indicate a minor constituent of the diet. [1]Data from Monadjem (1997). [2]Mean carbon isotope values are divided in three catagories – C_4 Graze (> -3.5‰), C_3 Browse (< -8‰) and Mixed-Feeder (-3‰ to -8‰). [3]Assuming that pits are caused primarily by seeds, striations by grass and polish by browse.

The extinct species *Otomys* cf. *gracilis* is reconstructed as a leaf or soft fruit consumer on the basis of microwear analysis (as indicated by the presence of furrows), with a significant component of grass in its diet (as indicated by striations). A small proportion of seeds or bark were also contributing to the diet of this species as indicated by the small proportion of pitting of the molar occlusal surfaces. This microwear interpretation is supported by the carbon isotope data, which indicates a mixed C_3 and C_4 plant diet that can vary between individuals from close to the C_3 plant end-member to close to the C_4 plant end-member as the proportion of grass in the diet of each individual varies. The carbon isotope values are significantly lighter than those of the extant specialist herbivore O. *irroratus*, indicating that O. *gracilis* had a more varied diet and greater browse component to its diet than that of O. *irroratus*, despite its hypsodont and laminate molar morphology. Based on the carbon isotope and microwear data and known dietary preferences of extant *Otomys* (Taylor and Green, 1976; Kerley, 1992; Monadjem, 1997), it is evident that O. cf. *gracilis* from the mid-Pliocene was a less specialised graminivore than its present day cogeners. The consumption of soft food particles, as indicated by furrows on the molar occlusal surface of *Otomys* cf. *gracilis*, may be a species-specific dietary adaptation or may be broader feature of the Otomyinae. The recent placement of *Otomys* within the murinae and the presence of vestigial molar cusps in its sister taxon *Euryotomys bolti* (Senegas and Avery, 1998) is suggestive of the evolution of the Otomyinae from a more omnivorous ancestor. The data from this study indicates that while the specialised molar morphology of O. *gracilis* was an adaptation to the grassy component of its diet, it also maintained a browsing dietary component. This is in agreement with recent morphological and isotopic evidence (Jernvall and Fortelius, 2002; Feranec, 2003) suggesting that hypsodonty can be indicative of a generalised diet in addition to its traditional interpretation as a grazing adaptation.

6.9.2. Palaeoenvironmental Reconstruction

As discussed in Kingston (1999), the isotopic composition of herbivore enamel cannot simply be interpreted as a proxy for the isotopic composition of palaeovegetation. In general terms, browsers inhabit forested ecosystems and grazers inhabit more open woodland and grassland habitats, and mixed feeders are ecotonal. However, selective feeding, competitive exclusion, migration and immigration should all be considered if palaeodietary signals are to be translated into palaeoecological reconstructions (Kingston, 1999). Selective feeding is perhaps the greatest of these problems, and it can only be addressed by comparing taxa with a range of dietary strategies. Taxa were chosen for inclusion in the present study on the basis of dental morphology, with each site represented by a species that was considered to be a grazer, omnivore and insectivore. The apparent grazing specialist *Otomys* cf. *gracilis* has been reinterpreted as a mixed-feeder. Therefore, neither of the three dominant species in the Makapansgat Pliocene micromammal faunas had a predominately grazing diet. This suggests either that the necessary adaptations to an exclusively graminivorous diet had yet to develop in the fossil faunas, or that there were not sufficient grasslands to support a wholly graminivorous life-style. Although the proportion of grasses in the Pliocene flora was lower than in the present day, the presence of some C_4 grasses in the diet of each of the Makapansgat Limeworks micromammal individuals studied, indicates that C_4 grasses were a small but consistent presence in the mid-Pliocene of Makapansgat. Similarly, stable isotope studies of the macrofaunas from the late-Pliocene Member 3 of the Makapansgat Limeworks, indicate that browsing and mixed-feeding were the dominant dietary strategies but that C_4 grasses were also present. Sponheimer *et al.* (1999) found that of the seven fossil bovid species studied from Makapansgat Member 3, carbon isotopes indicated that two species, *Aepyceros* sp. and *Gazella vanhoepeni*, were found to have exclusively browsing diets when on the basis of ecomorphology they were considered to be mixed-feeders. The mixed-feeding diet of the supposed rodent grazer *Otomys* cf. *gracilis*, is more evidence to suggest that the late Neogene Makapansgat palaeoenvironments were more wooded than is the modern day Makapansgat valley.

The data from this study clearly indicate the presence of C_4 grasses in the EXQRM and MRCIS ecosystems. It is possible to indicate the approximate

proportion of C_3 grasses in an ecosystem by comparing the carbon isotope and microwear dietary reconstructions. For example, in a highly C_3 environment, the dental microwear of herbivores will indicate a grass diet whereas the carbon isotopes will indicate $\delta^{13}C$ values that indicate the absence of C_4 grasses (and by inference, the presence of C_3 grasses). In contrast, when C_4 grasses are the dominant grass-type, both the dental microwear and the $\delta^{13}C$ value will indicate approximately the same proportion of grass in the diet. In the case of the Makapansgat Limeworks microfauna, the good agreement between the dietary reconstruction based on dental microwear and the reconstruction based on carbon isotope values (Table 6.3.) indicates that the C_3 grass contribution to the ecosystem was not significant. Because dental microwear analysis cannot determine the absolute proportion of grass in the diet, only a relative proportion, it is difficult to assess any subtle discrepancies between the isotopic and microwear approaches. Therefore, while it is highly unlikely that C_3 grasses constituted a significant component of the EXQRM and MRCIS flora, it has not been possible to identify whether C_3 grasses were present in small quantities.

The evidence presented in this study indicates that in the mid-Pliocene, the boundary between the C_3 grass dominated winter rainfall zone and the C_4 grass dominated summer rainfall zone of South Africa lay between the sites Makapansgat and Langebaanweg, as is the case in the modern day (Fig. 6.1.). As suggested by Franz-Odendaal *et al.* (2002), the presence of the Benguela Upwelling System in the Cape Region of South Africa has maintained a Mediterranean climate since its early development in the Late Miocene (Siesser, 1980) and is responsible for the lack of C_4 grasses in this region. The underlying reasons for the presence of C_4 grasses in the mid-Pliocene of Makapansgat are a function of growth-season temperature and atmospheric pCO_2. As measurements of both of these parameters are currently lacking for the South African highveld, it cannot be indicated whether these aspects of regional and global climate were significantly different from that of the modern day. For example, based on the Cerling *et al.* (1997) model, the mixed C_3 and C_4 environment of the mid-Pliocene could be maintained by a combination of increased temperatures in an atmosphere of increased pCO_2 or reduced temperatures in an atmosphere of reduced pCO_2. However with existing data, the most parsimonious interpretation

of the carbon isotope data is that the mid-Pliocene temperature and atmospheric pCO_2 of the South African highveld was essentially similar to modern day conditions.

Because the mid-Pliocene microfaunal assemblages of Makapansgat indicate that the South African highveld was located within the zone of C_4 grasses at this time, the timing of the origin of C_4 grasses in this region remains unresolved at pre mid-Pliocene. Older South African highveld deposits such as Bolt's Farm Waypoint 160 (Sénégas and Avery, 1998) and the Mio-Pliocene speleothem at the base of the Makapansgat sedimentary sequence (Member 1 of Partridge 2000; Partridge *et al.* 2000; see Chapter 5.), may provide the opportunity for identifying the timing of the origin of C_4 grasses in this region.

6.10. Conclusions

The combined approach of stable isotope and microwear analysis has enabled a more detailed and more accurate reconstruction of palaeodiet than either technique in isolation. This study has successfully reconstructed the diet of modern species with known dietary preferences and has shown that the diet of extinct rodents cannot always be assumed from dental morphology. The use of micromammals in palaeodietary and palaeoecological research also offers a new and useful addition to similar studies based on large mammals.

The extinct *Mystromys* cf. *hausleitneri* had a diet similar to that of the extant M. *albicaudatus*, suggesting that it occupied a similar dietary niche. In contrast, the extinct *Otomys* cf. *gracilis* had a greater browse or frugivorous component to its diet than the extant species of *Otomys*. Therefore, the specialised dental morphology of the early Otomyinae is not an *a priori* indication of a grazing niche.

The mid-Pliocene palaeoenvironment of Makapansgat EXQRM and MRCIS was a mixture of C_3 browse and C_4 grasses, probably dominated by woodland. C_3 grasses were not a significant component of the vegetation. The EXQRM and MRCIS deposits are two of the oldest faunal assemblages in the South African highveld, and indicate an essentially modern palaeoenvironment in the mid-Pliocene. This is in marked contrast to the pure C_3 environment of the early Pliocene to recent of the Cape Province of South Africa.

6.11. References

Acocks, J. P. H. (1953). Veld types of South Africa. *Memoirs of the Botanical Survey of South Africa* **28,** 1-192.

Avery, D. M. (1995). Southern savannas and Pleistocene hominid adaptations: the micromammalian perspective. *In* "Paleoclimate and evolution with emphasis on human origins." (E. S. Vrba, G. H. Denton, T. C. Partridge, and L. H. Burckle, Eds.), pp. 459-478. Yale University Press, New Haven and London.

Avery, D. M. (1998). An assessment of the Lower Pleistocene micromammalian fauna from Swartkrans Members 1-3, Gauteng, South Africa. *Geobios* **31,** 393-414.

Baker, G., Jones, L. H. P., and Wardrop, I. D. (1959). Cause of wear in sheep's teeth. *Nature* **184,** 1583-1584.

Baxter, R., and Hansson, L. (2001). Bark consumption by small rodents in the northern and southern hemispheres. *Mammal Review* **31,** 47-59.

Bedford, J. M., Bernard, R. T. F., and Baxter, R. M. (1998). The 'hybrid' character of the gametes and reproductive tracts of the African shrew, *Myosorex varius*, supports its classification in the Crocidosoricinae. *Journal of Reproductive Fertility* **112.**

Brain, C. K. (1981). "The hunters or the hunted? An introduction to African Cave Taphonomy." The University of Chicago Press, Chicago and London.

Brain, C. K. (1985). Temperature-induced environmental changes in Africa as evolutionary stimuli. *In* "Species and Speciation." (E. S. Vrba, Ed.), pp. 45-52, Pretoria.

Bray, K. (2001). "The use of micro-mammal accumulations as Palaeoecological indicators with respect to environmental change in the Makapan Valley from the Iron Age to present." Unpublished MSc thesis, University of Liverpool.

Broom, R. (1937). Notices of a few more new fossil mammals from the caves of the Transvaal. *Annals and Magazine of Natural History* **Series 10, vol 20,** 509-514.

Bryant, J. D., Koch, P. L., Froelich, P. N., Showers, W. J., and Genna, B. J. (1996). Oxygen isotope partitioning between phosphate and carbonate in mammalian apatite. *Geochemica et Cosmochimica Acta* **60,** 5145-5148.

Cerling, T. E., and Harris, J. M. (1999). Carbon isotope fractionation between diet and bioapatite in ungulate mammals and implications for ecological and paleoecological studies. *Oecologia* **120,** 347-363.

Cerling, T. E., Harris, J. M., and Leakey, M. G. (1999). Browsing and grazing in elephants: the isotope record of modern and fossil proboscideans. *Oecologia* **120,** 364-374.

Cerling, T. E., Harris, J. M., MacFadden, B. J., Leakey, M. G., Quade, J., Eisenmann, V., and Ehleringer, J. R. (1997). Global vegetation change through the Miocene/Pliocene boundary. *Nature* **389,** 153-158.

Cerling, T. E., Wang, Y., and Quade, J. (1993). Expansion of C4 ecosystems as an

indicator of global ecological change in the late Miocene. *Nature* **361,** 344-345.

Chevret, P., Denys, C., Jaeger, J.-J., Michaux, J., and Catzeflis, F. (1993). Molecular and paleontological aspects of the tempo and mode of evolution in Otomys (Otomyinae: Muridae: Mammalia). *Biochemical Systematics and Ecology* **21,** 123-131.

Cockcroft, M. J., Wilkinson, M. J., and Tyson, P. D. (1987). The application of a present-day climatic model to the Late Quaternary in Southern Africa. *Climatic Change* **10,** 161-181.

Coplen, T. B. (1995). Reporting of stable carbon, hydrogen, and oxygen isotopic abundances. *In* "Reference and intercomparison materials for stable isotopes of light elements." pp. 31-34. International Atomic Energy Agency, TECDOC.

Craig, H. (1957). Isotopic standards for carbon and oxygen and correction factors for mass-spectrometric analysis of carbon dioxide. *Geochemica et Cosmochimica Acta* **12,** 133-149.

de Graaff, G. (1960). A preliminary investigation of the Mammalian microfauna in Pleistocene deposits of caves in the Transvaal system. *Palaeontologia Africana* **7,** 59-118.

Denys, C. (1991). A new rodent *Mystromys pocockei* sp. nov. (Cricetinae) from the Lower Pliocene site of Langebaanweg (Cape Region, South Africa). *C.R.Acad.Sci.Paris,Sciences de la Terre et des planetes* **313 serie II,** 1335-1341.

Denys, C. (1994). Diet and dental morphology of two coexisting Aethomys species (Rodentia) in Mozambique. Implications for diet reconstruction in related extinct species from South Africa. *Acta Theriologica* **39,** 357-364.

Denys, C. (1999). Of mice and men: evolution in East and South Africa during Plio-Pleistocene times. *In* "African biogeography, climate change & human evolution." (T. G. Bromage, and F. Schrenk, Eds.), pp. 226-252. Oxford University Press, Oxford.

Denys, C., and Jaeger, J. J. (1986). A biostratigraphic problem: the case of the east African Plio-Pleistocene rodent faunas. *Modern Geology* **10,** 215-233.

Denys, C., Michaux, J., and Hendey, B. (1987). Les rongeurs (Mammalia) *Euryotomys* et *Otomys*: un exemple d'evolution parallèle en Afrique tropicale? *C. R. Acad. Sci. Paris, Sciences de la Terre et des planetes Series II* **305,** 1389-1395.

Ding, Z. L., Rutter, N. W., and Liu, T. S. (1997). The onset of extensive loess deposition around the G/M boundary in China and its palaeoclimatic implications. *Quaternary International* **40,** 53-60.

Ding, Z. L., and Yang, S. L. (2000). C3/C4 vegetation evolution over the last 7.0 Myr in the Chinese Loess Plateau: evidence from pedogenic carbonate $\delta^{13}C$. *Palaeogeography, Palaeoclimatology, Palaeoecology* **160,** 291-299.

Dippenaar, N. J., Swanepoel, P., and Gordon, D. H. (1993). Diagnostic morphometrics of 2 medically importanct southern African rodents, *Mastomys Natalensis* and *Mastomys coucha* (Rodentia, Muridae). *South African Journal of Science* **89,** 300-303.

Downs, C. T., and Perrin, M. R. (1995). The thermal biology of the white-tailed rat *Mystromys albicaudatus*, a cricetine relic in southern temperate African grassland. *Comparative Biochemistry and Physiology A* **110,** 65-69.

Ehleringer, J. R., Cerling, T. E., and Helliker, B. R. (1997). C-4 photosynthesis,

atmospheric CO_2 and climate. *Oecologia* **112,** 285-299.

Ehleringer, J. R., Sage, R. F., Flanagan, L. B., and Pearcy, R. W. (1991). Climate Change and the evolution of C4 photosynthesis. *Trends in Ecology & Evolution* **6,** 95-99.

Feranec, R. S. (2003). Stable isotopes, hypsodonty, and the paleodiet of Hemiauchenia (Mammalia: Camelidae): a morphological specialization creating ecological generalization. *Paleobiology* **29,** 230-242.

Franz-Odendaal, T. A., Lee-Thorp, J. A., and Chinsamy, A. (2002). New evidence for the lack of C_4 grassland expansions during the early Pliocene at Langebaanweg, South Africa. *Paleobiology* **28,** 378-388.

Fuller, J. A., and Perrin, M. R. (2001). Habitat assessment of small mammals in the Umvoti Vlei Conservancy, KwaZulu-Natal, South Africa. *South African Journal of Wildlife Research* **31,** 1-12.

Grine, F. E., Ungar, P. S., and Teaford, M. F. (2002). Error rates in dental microwear quantification using Scanning Electron Microscopy. *Scanning* **24,** 144-153.

Hendey, Q. B. (1976). The Pliocene fossil occurrences in 'E' Quarry, Langebaanweg, South Africa. *Annals of the South African Museum* **69,** 215-247.

Herries, A. I. R. (2003). "Magnetostratigraphic seriation of South African hominin palaeocaves." Unpublished PhD thesis, University of Liverpool.

Holmgren, K., Karlen, W., Lauritzen, S. E., Lee-Thorp, J. A., Partridge, T. C., Piketh, S., Repinski, P., Stevenson, C., Svanered, O., and Tyson, P. D. (1999). A 3000-year high-resolution stalagmite-based record of palaeoclimate for northeastern South Africa. *Holocene* **9,** 295-309.

Iacumin, P., Bocherens, H., Mariotti, A., and Longinelli, A. (1996). Oxygen isotope analyses of co-existing carbonate and phosphate in biogenic apatite: a way to moniter diagenetic alteration of bone phosphate? *Earth and Planetary Science Letters* **142,** 1-6.

Jernvall, J., and Fortelius, M. (2002). Common mammals drive the evolutionary increase of hypsodonty in the Neogene. *Nature* **417,** 538-540.

Kerley, G. I. H. (1992). Trophic Status of Small Mammals in the Semiarid Karoo, South- Africa. *Journal of Zoology* **226,** 563-572.

King, T., Andrews, P., and Boz, B. (1999). Effect of taphonomic processes on dental microwear. *American Journal of Physical Anthropology* **108,** 359-373.

Kingston, J. D. (1999). Isotopes and environments of the Baynunah Formation, Emirate of Abu Dhabi, United Arab Emirates. *In* "Fossil Vertebrates of Arabia." (P. J. Whybrow, and A. Hill, Eds.), pp. 523. Yale University Press.

Koch, P. L., Behrensmeyer, A. K., Stott, A. W., Tuross, N., Evershed, R. P., and Fogel, M. L. (2001). The effects of weathering on the Stable Isotope composition of bones. *Ancient Biomolecules* **3,** 117-134.

Koch, P. L., Tuross, N., and Fogel, M. L. (1997). The effects of sample treatment and diagenesis on the isotopic integrity of carbonate in biogenic hydroxylapatite. *Journal of Archaeological Science* **24,** 417-429.

Koenigswald, v., W., Sander, P. M., Leite, M., Mörs, T., and Santel, W. (1994). Functional symmetries in the schmelzmuster and morphology of rootless rodent molars. *Zoological Journal of the Linnean Society* **110,** 141-179.

Latham, A. G., Herries, A., and Kuykendall, K. (2003). The formation and

sedimentary infilling of the Limeworks cave, Makapansgat, South Africa. *Palaeontologia Africana* **39**: 69-82.

Latham, A. G., Herries, A., Quinney, P., Sinclair, A., and Kuykendall, K. (1999). The Makapansgat Australopithecine site from a speleological perspective. In, Pollard, A. M. (ed.) Geoarchaeology: exploration, environments, resources. *Geological Society of London, Special Publications* **165,** 61-77.

Lee Thorp, J., and Van der Merwe, N. J. (1987). Carbon isotope analysis of fossil bone apatite. *South African Journal of Science* **83,** 712-715.

Lee, W. B., and Houston, D. C. (1993). Tooth wear patterns in voles (*Microtus agrestis* and *Clethrionomys glareolus*) and efficiency of dentition in preparing food for digestion. *Journal of Zoology* **231,** 301-309.

Lee-Thorp, J., Manning, L., and Sponheimer, M. (1997). Problems and prospects for carbon isotope analysis of very small samples of fossil tooth enamel. *Bulletin De La Societe Geologique De France* **168,** 767;773.

Lee-Thorp, J. A., and Beaumont, P. B. (1995). Vegetation and seasonality shifts during the Late Quaternary deduced from $^{13}C/^{12}C$ ratios of grazers at Equus Cave, South Africa. *Quaternary Research* **43,** 426-432.

Lee-Thorp, J. A., Sealy, J. C., and van der Merwe, N. J. (1989). Stable carbon isotope ratio differences between bone collagen and bone apatite, and their relationship to diet. *Journal of Archaeological Science* **16,** 585-599.

Lee-Thorp, J. A., and Talma, A. S. (2000). Stable light isotopes and environments in the Southern African Quaternary and Late Pliocene. *In* "The Cenozoic of Southern Africa." pp. 406. Oxford Monographs on Geology and Geophysics. Oxford University Press, Oxford.

Lee-Thorp, J. A., Thackeray, J. F., and van der Merwe, N. (2000). The hunters and the hunted revisited. *Journal of Human Evolution* **39,** 565-576.

Lee-Thorp, J. A., van der Merwe, N. J., and Brain, C. K. (1989). Isotopic evidence for dietary differences between two extinct baboon species from Swartkrans. *Journal of Human Evolution* **18,** 183-190.

Lee-Thorp, J. A., van der Merwe, N. J., and Brain, C. K. (1994). Diet of *Australopithecus-robustus* at Swartkrans from stable carbon isotopic analysis. *Journal of Human Evolution* **27,** 361-372.

Levinson, M. (1982). Taphonomy of microvertebrates - from owl pellets to cave breccia. *Annals of the Transvaal Museum* **33,** 115-121.

Lewis, P. J., Gutierrez, M., and Johnson, E. (2000). *Ondatra zibethicus* (Arvicolinae, Rodentia) dental microwear patterns as a potential tool for palaeoenvironmental reconstruction. *Journal of Archaeological Science* **27,** 789-798.

Lindars, E. S., Grimes, S. T., Mattey, D. P., Collinson, M. E., Hooker, J. J., and Jones, T. P. (2001). Phosphate delta ^{18}O determination of modern rodent teeth by direct laser fluorination: An appraisal of methodology and potential application to palaeoclimate reconstruction. *Geochemica et Cosmochimica Acta* **65,** 2535-2548.

Macfadden, B. J., and Cerling, T. E. (1994). Fossil horses, carbon isotopes and global change. *Trends in Ecology & Evolution* **9,** 481-486.

MacFadden, B. J., Cerling, T. E., Harris, J. M., and Prado, J. (1999). Ancient latitudinal gradients of C_3/C_4 grasses interpreted from stable isotopes of New World Pleistocene horse (*Equus*) teeth. *Global Ecology and Biogeography* **8,** 137-149.

Maddalena, T., and Bronner, G. (1992). Biochemical systematics of the endemic

African genus *Myosorex* Gray, 1838 (Mammalia, Soricidae). *Israel Journal of Zoology* **38,** 245-252.

Maguire, B. (1980). Further observations on the nature and provenance of the lithic artefacts from the Makapansgat Limeworks. *Palaeontologia Africana* **23,** 127-151.

Maguire, J. M., Schrenk, F., and Stanistreet, I. G. (1985). The lithostratigraphy of the Makapandsgat Limeworks Australopithecine site: some matters arising. *Annals of the geological survey of South Africa* **19,** 37-51.

McKee, J. K. (1995). Further chronological seriations of southern African Pliocene and Pleistocene mammalian faunal assemblages. *Palaeontologia Africana* **32,** 11-16.

McKee, J. K., Thackeray, J. F., and Berger, L. R. (1995). Faunal assemblage seriation of southern African Pliocene and Pleistocene fossil deposits. *American Journal of Physical Anthropology* **96,** 235-250.

Meester, J. (1955). Fossil shrews of South Africa. *Annals of the Transvaal Museum* **22,** 271-278.

Misonne, X. (1969). African and Indo-Australian Muridae. Evolutionary trends. *Annales Musee Republique d'Afrique Centrale, Tervuren* **172,** 1-219.

Monadjem, A. (1997). Stomach contents of 19 species of small mammals from Swaziland. *South African Journal of Zoology* **32,** 23-26.

Nielsen-Marsh, C. M., and Hedges, R. E. M. (2000). Patterns of diagenesis in bone II: effects of acetic acid treatment and the removal of diagenetic CO_3^{2-}. *Journal of Archaeological Science* **27,** 1151-1159.

O'Connor, T. G., and Bredenkamp, G. J. (1997). Grassland. *In* "Vegetation of Southern Africa." (R. M. Cowling, D. M. Richardson, and S. M. Pierce, Eds.), pp. 215-257. Cambridge University Press, Cambridge.

O'Leary, M. H. (1981). Carbon isotope fractionation in plants. *Phytochemistry* **20,** 553-567.

Partridge, T. C. (2000). Hominid-bearing cave and tufa deposits. *In* "The Cenozoic of Southern Africa." (T. C. Partridge, and R. R. Maud, Eds.), pp. 100-130. Oxford University Press, Oxford.

Partridge, T. C., Latham, A. G., and Heslop, D. (2000). Appendix on magnetostratigraphy of Makapansgat, Sterkfontein, Taung and Swartkrans. *In* "The Cenozoic of Southern Africa." (T. C. Partridge, and R. R. Maud, Eds.), pp. 126-129. Oxford University Press, Oxford.

Perrin, M. R., and Curtis, B. A. (1980). Comparative morphology of the digestive system of 19 species of Southern Afircan myomorph rodents in relation to diet and evolution. *South African Journal of Zoology* **15,** 22-33.

Perrin, M. R., and Maddock, A. H. (1983). Preliminary investigations of the digestive processes of the white-tailed rat *Mystromys albicaudatus* (Smith 1834). *South African Journal of Zoology* **18,** 128-133.

Pocock, T. N. (1976). Pliocene mammalian microfauna from Langebaanweg: A new fossil genus linking the Otomyinae with the Murinae. *South African Journal of Science* **72,** 58-60.

Pocock, T. N. (1985). Plio-Pleistocene mammalian microfauna in southern Africa. *Annals of the geological survey of South Africa* **19,** 65-67.

Pocock, T. N. (1987). Plio-Pleistocene fossil mammalian microfauna of Southern Africa - a preliminary report including description of two new fossil muroid genera (Mammalia: Rodentia). *Palaeontologia Africana* **26,** 69-91.

Quérouil, S., Hutterer, R., Barrière, P., Colyn, M., Kerbis Peterhans, J. C., and

Verheyen, E. (2001). Phylogeny and evolution of African shrews (Mammalia: Soricidae) inferred from 16s rRNA sequences. *Molecular Phylogenetics and Evolution* **20,** 185-195.

Rafferty, K. L., Teaford, M. F., and Jungers, W. L. (2002). Molar microwear of subfossil lemurs: improving the resolution of dietary inferences. *Journal of Human Evolution* **43,** 645-657.

Rayner, R. J., Moon, B. P., and Masters, J. C. (1993). The Makapansgat Australopithecine environment. *Journal of Human Evolution* **24,** 219-231.

Reed, K. E. (1998). Using large mammal communities to examine ecological and taxonomic structure and predict vegetation in extant and extinct assemblages. *Paleobiology* **24,** 384-408.

Reinecke, A., Reinecke, S., Musilbono, D., and Chapman, A. (2000). The transfer of lead (Pb) from earthworms to shrews (Myosorex varius). *Archives of Environmental contamination and Toxicology* **39,** 392-397.

Rensberger, J. M. (1978). Scanning electron microscopy of wear and occlusal events in some small herbivores. *In* "Development, Function and Evolution of teeth." (P. M. Butler, and K. A. Joysey, Eds.), pp. 415-438. Academic Press, London.

Repinski, P., Holmgren, K., Lauritzen, S. E., and Lee-Thorp, J. A. (1999). A late Holocene climate record from a stalagmite, Cold Air Cave, Northern Province, South Africa. *Palaeogeography, Palaeoclimatology, Palaeoecology* **150,** 269-277.

Rogers, K. L., and Wang, Y. (2002). Stable isotopes in pocket gopher teeth as evidence of a Late Matuyama climate shift in the Southern Rocky mountains. *Quaternary Research* **57,** 200-207.

Salisbury, F. B., and Ross, C. W. (1985). "Plant Physiology." Wadsworth Publishing, Belmont.

Scholes, R. J. (1997). Savanna. *In* "Vegetation of Southern Africa." (R. M. Cowling, D. M. Richardson, and S. M. Pierce, Eds.), pp. 258-277. Cambridge University Press, Cambridge.

Scott, L. (1986). The late Tertiary and Quaternary pollen record in the interior of South-Africa. *South African Journal of Science* **82,** 73-73.

Scott, L. (2002). Grassland development under glacial and interglacial conditions in southern Africa: review of pollen, phytolith and isotope evidence. *Palaeogeography, Palaeoclimatology, Palaeoecology* **177,** 47-57.

Scott, L., and Vogel, J. C. (2000). Evidence for environmental conditions during the last 20 000 years in Southern Africa from C^{13} in fossil hyrax dung. *Global and Planetary Change* **26,** 207-215.

Segalen, L., Renard, M., Pickford, M., Senut, B., Cojan, I., Le Callonnec, L., and Rognon, P. (2002). Environmental and climatic evolution of the Namib Desert since the Middle Miocene: the contribution of carbon isotope ratios in ratite eggshells. *Comptes Rendus Geoscience* **334,** 917-924.

Sénégas, F., and Avery, D. M. (1998). New evidence for the murine origins of the Otomyinae (Mammalia, Rodentia) and the age of Bolt's Farm (South Africa). *South African Journal of Science* **94,** 503-507.

Sénégas, F., and Michaux, J. (2000). *Boltimys broomi* gen. nov., sp. nov. (Rodentia, Mammalia), nouveau Muridae d'affinité incertaine du Pliocène inférieur d'Afrique du Sud. *C.R.Acad.Sci.Paris,Sciences de la Terre et des planetes* **330,** 521-525.

Siesser, W. G. (1980). Late Miocene origin of the Benguela upswelling system off

Northern Namibia. *Science* **208,** 283-285.
Silcox, M. T., and Teaford, M. F. (2002). The diet of worms: an analysis of mole dental microwear. *Journal of Mammalogy* **83,** 804-814.
Smit, A., van der Bank, H., Falk, T., and de Castro, A. (2001). Biochemical genetic markers to identify two morphologically similar South African *Mastomys* species (Rodentia: Muridae). *Biochemical Systematics and Ecology* **29,** 21-30.
Smithers, R. H. N. (1983). "The mammals of the southern African subregion." University of Pretoria, Pretoria.
Solounias, N., and Hayek, L.-A. C. (1993). New methods of tooth microwear analysis and application to dietary determination of two extinct antelopes. *Journal of Zoology* **229,** 421-445.
Sponheimer, M., and Lee-Thorp, J. A. (1999). Oxygen isotopes in enamel carbonate and their ecological significance. *Journal of Archaeological Science* **26,** 723-728.
Sponheimer, M., Reed, K. E., and Lee-Thorp, J. A. (1999). Combining isotopic and ecomorphological data to refine bovid paleodietary reconstruction: a case study from the Makapansgat Limeworks hominin locality. *Journal of Human Evolution* **36,** 705-718.
Strait, S. G. (1993). Molar microwear in extant small-bodied faunivorous mammals: an analysis of feature density and pit frequency. *American Journal of Physical Anthropology* **92,** 63-79.
Swanepoel, C. M. (1980). Some factors influencing the breeding-season of *Praomys natalensis*. *South African Journal of Zoology* **15,** 95-98.
Taylor, K. D., and Green, M. G. (1976). The influence of rainfall on diet and reproduction in four African rodent species. *Journal of Zoology* **180,** 367-389.
Teaford, M. F. (1988). A review of dental microwear and diet in modern mammals. *Scanning Microscopy* **2,** 1149-1166.
Teaford, M. F. (1994). Dental microwear and dental function. *Evolutionary Anthropology* **17,** 17-30.
Teaford, M. F., and Walker, A. (1984). Quantitative differences in dental microwear between primate species with different diets and a comment on the presumed diet of *Sivapithecus*. *American Journal of Physical Anthropology* **64,** 191-200.
Ungar, P. S. (1995). A semiautomated image analysis procedure for the quantification of dental microwear II. *Scanning* **17,** 57-59.
Ungar, P. S., Simon, J.-C., and Cooper, J. W. (1991). A semiautomated image analysis procedure for the quantification of dental microwear. *Scanning* **13,** 31-36.
van der Merwe, N., Thackeray, F., Lee-Thorp, J. A., and Luyt, J. (2003). The carbon isotope ecology and diet of *Australopithecus africanus* at Sterkfontein, South Africa. *Journal of Human Evolution* **44,** 581-597.
Vogel, J. C. (1978). Isotopic assessment of the dietary habits of ungulates. *South African Journal of Science* **74,** 298-301.
Walker, A., Hoeck, H. N., and Perez, L. (1978). Microwear of mammalian teeth as an indicator of diet. *Science* **201,** 908-910.
Wang, Y., and Cerling, T. E. (1994). A model of fossil tooth and bone diagenesis -implications for paleodiet reconstruction from stable isotopes. *Palaeogeography, Palaeoclimatology, Palaeoecology* **107,** 281-289.

Ward, J., and Mainland, I. L. (1999). Microwear in modern rooting and stall-fed pigs: the potential of dental microwear analysis for exploring pig diet and management in the past. *Environmental Archaeology* **4,** 25-32.

Wesselman, H. B. (1995). Of mice and almost-men: regional paleoecology and human evolution in the Turkana Basin. *In* "Paleoclimate and evolution with emphasis on human origins." (E. S. Vrba, G. H. Denton, T. C. Partridge, and L. H. Burckle, Eds.), pp. 356-368. Yale University Press, New Haven and London.

Wirminghaus, J. O., and Perrin, M. R. (1992). Diets of small mammals in a southern African temperate forest. *Israel Journal of Zoology* **38,** 353-361.

Chapter 7. Late Neogene spread of savannah grasses and the origins of hominin bipedalism

7.1. Abstract

There has been a long history of linking the late Neogene replacement of tropical forests by savannah grasses to events in early hominin evolution. Here it is shown, based on carbon isotope evidence, that the late Neogene global expansion of savannah grasses occurred gradually from approximately 15 to 4 Ma, occurring first at low latitudes and later at mid-latitudes. This spread of C_4 grasses overlaps both temporally and spatially with the origins of bipedalism in Africa at approximately 5 Ma. A causal relationship between these two events is suggested.

7.2. Introduction

Previous studies linking global climatic change with episodes of early hominin evolution have focused on the Plio-Pleistocene onset and intensification of glacial conditions at 2.5 Ma and 1.7 Ma as the stimulus for hominin speciation and migration (Vrba *et al.*, 1995, Bobe and Eck, 2001, Bobe *et al.*, 2002, Zeitoun, 2000, Foley, 1994, Stanley, 1995). This study however, focuses on late Miocene climatic change in relation to the evolution of the Hominini and the earliest stages of savannah grassland development. Bipedalism, the defining characteristic of the hominini, is unique among the predominantly arboreal primates, and is usually recognised as a locomotory adaptation to open environments. Since Darwin (1874), most hypotheses for the origins of bipedalism have included an element of ecological change from forest to savannah conditions that is viewed as the forcing mechanism behind this change in locomotion (e.g. Pickford, 1990; Tobias, 1991; Bromage and Schrenk, 1995; Owen-Smith, 1999; Foley, 2002). By inference, such hypotheses considered the earliest hominins to be more or less adapted to a savannah environment (e.g. Dart, 1953; Bromage and Schrenk, 1995; Tobias, 1991; Owen-Smith, 1999). The postulated savannah adaptations of the earliest hominins and the role of spreading savannah environments in the origins of the hominins are two paradigms that are loosely referred to as the Savannah

Hypothesis. These two aspects of the Savannah Hypothesis can be considered independently - this study addresses the evidence for spreading savannah grasslands rather than aspects of hominin adaptations.

As new Late Neogene palaeoenvironmental evidence from east and South Africa has emerged, it has become apparent that there has been a strong association between savannah grassland and forest in eastern Africa, known as the savannah-mosaic, since the Late Miocene (Kingston *et al.*, 1994; 2002; Cerling *et al.*, 1997; 1988; 2003; Jacobs, 2002). An entirely open savannah environment is considered to be unique to the middle and late Pleistocene (Cerling, 1992). The dominance of the Late Neogene savannah-mosaic has lead some authors to question the validity of the Savannah Hypothesis (Hill, 1987; Kingston *et al.*, 1994). The lack of evidence for a marked shift in vegetation type in the Miocene to Pliocene (Kingston *et al.*, 1994; Jacobs, 2002) has lead authors to discount the role of spreading savannah grasslands in the origins of bipedalism. However, other authors have stressed the importance of the late Miocene global development of the savannah ecosystem and its role in the restructuring of mammalian faunas at this time (Leakey and Harris, 2003). In this study we review the recent evidence for the origin and spread of savannah grasses in Africa, and assess its implications for the origins of bipedalism.

7.3. The ecophysiology and distribution of savannah grasses

There are two main photosynthetic pathways among the higher plants, the C_3 and C_4 pathways (O'Leary, 1981; 1988). The C_3 pathway, or Calvin-Benson cycle, is the most primitive mode of photosynthesis and has been the dominant pathway since the evolution of land plants in the Palaeozoic, under conditions of high atmospheric concentrations of CO_2 (Cerling *et al.*, 1998). Under low atmospheric concentrations of CO_2 and high growth-season temperatures photorespiration, the release of CO_2 during photosynthesis, increases, reducing the net efficiency of C_3 photosynthesis (Ehleringer *et al.*, 1991; Ehleringer and Monson, 1993). The low ratio of CO_2/O_2 in the present day atmosphere reduces the photosynthetic efficiency of C_3 plants by approximately one third (Ehleringer and Monson, 1993).

C_4 photosynthesis (the Hatch-Slack cycle) acts as a CO_2 concentrating mechanism, resulting in CO_2 concentrations within the chloroplasts that are an order of magnitude higher than in C_3 plants, thereby reducing the effects of photorespiration (Ehleringer and Monson, 1993). The C_4 photosynthetic pathway is a simple modification of the C_3 photosynthetic pathway and has arisen independently in at least 18 families of angiosperms since the mid-Miocene (Ehleringer *et al.*, 1991). As a consequence of the different photosynthetic reactions, C_4 plants (savannah grasses) discriminate less between the stable isotopes of carbon, resulting in significantly heavier carbon isotope ratios (Hatch, 1987). C_4 plants typically have a $\delta^{13}C$ value of approximately –13‰ whilst C_3 plants have a value of –27‰ (O'Leary, 1988; Farquhar *et al.*, 1989).

The present day distribution of C_4 plants is restricted to tropical and sub-tropical regions, consistent with the observation that C_3 plant distribution is restricted by photorespiration at high temperatures. C_3 plants dominate at higher latitudes/lower temperatures (between 30° and 45° latitude in the present day) because they out-compete C_4 plants when photorespiration is reduced (Carter and Peterson, 1983). The crossover point (50% C_3 grasses, 50% C_4 grasses) has been experimentally modelled for a range of temperature and atmospheric pCO_2 conditions (Cerling *et al.*, 1997; Collatz *et al.*, 1998). When atmospheric CO_2 levels are high, above about 500 p.p.m.v., the C_3 photosynthetic pathway is favoured in all conditions, except those with extremely high temperatures. The crossover temperature at pre-industrial pCO_2 (280 p.p.m.v.) is between 16° and 20°C (daytime growing temperature), with C_3 grasses being favoured in cooler regions such as higher latitudes and altitudes (Cerling *et al.*, 1997). Quaternary records are expected to show a net expansion of C_4 grasses during glacial periods, because the reduction in atmospheric pCO_2 has a greater negative impact on the photosynthetic yield of C_3 vegetation than the positive impact of reduction in temperature over the same period (Cerling *et al.*, 1997). This expected expansion of C_4 grasses during glacial periods has been observed in numerous Late Quaternary sedimentary records (e.g. Talbot and Johannessen, 1992; Giresse *et al.*, 1994; Jolly and Haxeltine, 1997; Street-Perrott *et al.*, 1997; Boom *et al.*, 2002).

The world-wide expansion of C_4 plant biomass during the late Miocene has been investigated using the carbon isotope composition of fossil herbivore enamel (Cerling *et al.*, 1997), palaeosol carbonate (Cerling *et al.*, 1986; 1989) and sedimentary organic matter (France-Lanord and Derry, 1994). The first evidence of C_4 grasses comes from east Africa at 15 Ma (Kingston *et al.*, 1994) and the most significant period of global increase in C_4 grass biomass occurs between 8 and 6 Ma (Cerling *et al.*, 1997). There is also evidence for the spread of C_4 grasses into higher latitudes until 4 Ma (Cerling *et al.*, 1997; Ding and Yang, 2000). Cerling *et al.* (1997) have suggested that the mid-Miocene origin and spread of C_4 grasses was forced by the late Neogene decline in atmospheric pCO_2, as determined from models of the global carbon cycle (Berner and Kothavala, 2001). However, this gradual reduction in late Neogene pCO_2 has been questioned (Pagani *et al.*, 1999; Pearson and Palmer, 2000) based on the evidence from geochemical pCO_2 proxies such as $\delta^{11}B$.

Inherent in the Cerling *et al.* (1997) model of C_4 grass expansion is a reduction in the latitudinal range of C_4 grass distribution with reducing atmospheric pCO_2. A carbon isotope transect across the Americas show that the Quaternary latitudinal range of C_4 grasses (time-averaged over glacial-interglacial cycles) was essentially the same as in the present day (MacFadden *et al.*, 1999). Cerling *et al.* (1997) suggest that under the postulated late Miocene conditions of higher pCO_2, the latitudinal range of C_4 grasses is expected to contract, as only the hottest temperatures will favour C_4 grasses. If the Cerling *et al.* (1997) model is correct, then it is to be expected that C_4 grasses occurred first at low latitudes (high temperatures) and later at mid latitudes (lower temperatures) after a reduction in pCO_2 reduced the crossover temperature. This study uses new and published carbon isotope data from fossil teeth and carbonate deposits from the mid-Miocene to Recent to test the latitude and age relationships predicted by the Cerling *et al.* (1997) model of C_4 grass origins.

An increase in the latitudinal range of C_4 grasses can be attributed to either an increase in tropical temperatures or a decrease in atmospheric pCO_2 or both (e.g. Cerling *et al.*, 1997; Collatz *et al.*, 1998; Cowling and Sykes, 1999). With the current lack of quantitative palaeotemperature data for terrestrial tropical environments, the temperature component of C_4 grass distribution can be

identified based on the predictable negative relationship between latitude and temperature (MacFadden *et al.*, 1999). An increase in the latitudinal range of C_4 grass distribution can be used to indicate that C_4 grasses were migrating into lower temperature environments. The use of latitude as an indication of palaeotemperature is based on the following two assumptions: (1) there is a negative relationship between temperature and latitude (2) modern day temperatures approximate palaeotemperatures.

While there is generally a negative relationship between temperature and latitude due to the latitudinal insolation gradient, assumption (1), other factors such as altitude and continentality distort this relationship (Rozanski *et al.*, 1993). The second assumption (2), that modern day temperatures approximate Miocene and Pliocene palaeotemperatures, is not always valid. Areas that have undergone significant late Neogene uplift will have experienced higher palaeotemperatures in the past when the altitude was lower. The altitudinal effect is responsible for the low and variable temperatures within these regions. It is likely that palaeotemperatures in these regions were higher during earlier stages of uplift due to the lower elevations at this time.

Fundamental aspects of late Neogene terrestrial palaeoclimate such as absolute palaeotemperature, the degree of seasonality and the amount of precipitation are not precisely known. Therefore, with the lack of any substantial evidence to the contrary, this study assumes that modern day mean annual temperature for each of the studied regions approximates late Neogene palaeotemperature.

7.4. Methods

Published records of late Neogene C_3 and C_4 plant distributions determined from various sources (tooth enamel, palaeosols, speleothems and organic matter) were collected and sorted into geographic region. Geographical regions in which an isotopic shift from exclusively C_3 values to values that indicate the presence of C_4 grasses within the local environment were termed transitional records. Most of these transitional records were found in single studies that had attempted to pinpoint the timing of C_4 grass origins in that region, although some transitional records were made by combining studies by different authors. The age, in Ma,

when C_4 grasses are first observed in these records is noted and is termed the "transition age". The other two types of records were classified as geographical regions in which C_4 grasses are always present in the data collected ("C_4 present" records) and geographical regions in which C_4 grasses are always absent in the data collected ("C_4 absent" records). The age range of the deposits and the mean latitude of the sites were recorded for each study.

Present day mean annual surface temperature and precipitation data for each geographical region was collected from the University of Delaware Air Temperature and Precipitation dataset (Legates and Willmott, 1990a,b), provided by the NOAA-CIRES Climate Diagnostics Center, Boulder, Colorado, USA, from their Web site at http://www.cdc.noaa.gov/. Values quoted represent mean values from 1990 to 1996 and were taken from the locality of the fossil sites, not the regional mean.

7.5. Localities

Carbon isotope records of late Neogene C_4 grass proportions come from each continent except Antarctica (see Fig. 7.1.). The low-latitude data comes from a number of studies at hominin sites in the east African Rift Valley (Cerling, 1992; Cerling *et al.*, 1997a,b; Kingston *et al.*, 1994; Morgan *et al.*, 1994). There is currently no equivalent low latitude data from equatorial South America (see Fig. 7.1.). Assigning a single transition age to the east African data was problematic due to the conflicting evidence between the numerous east African carbon isotope studies. For example, Cerling *et al.* (1997b) shows the lack of C_4 grasses at Fort Ternan in Kenya at 13.9-14.0 Ma whereas Kingston *et al.* (1994) show the presence of C_4 grasses at the Tugen Hills in Kenya as early as 15.3 Ma. Cerling *et al.* (1997 and 1992) quote 9-10 Ma as the time of C_4 grass expansion in east Africa. It is likely that this variability is related to local differences in temperature and rainfall which control vegetation distribution both in the present day and in the past. There is also evidence for variability of C_4 grass proportions within these sites, indicating a degree of vegetation change over glacial-interglacial cycles (Cerling *et al.*, 2003; Kingston *et al.*, 2002; 1994, Cerling, 1992). As the data for the earliest evidence of C_4 grasses at 15.3 Ma in east Africa (Kingston *et al.*, 1994; Morgan *et al.*, 1994) comes from only one locality,

the Tugen Hills, the mid-point value between 15.3 Ma and 10 Ma of 12.65 Ma has been taken here as the transition age in east Africa.

In the Siwaliks sequence of Pakistan, palaeosol evidence indicates the origin of C_4 grasses to have occurred between 7 and 5 Ma (Quade *et al.*, 1989; Cerling *et al.*, 1993) and this is in general agreement with the shift in enamel carbon isotope values documented in Morgan *et al.* (1994). However, the earliest record of C_4 grasses as a dietary component in the Siwaliks is at 9.4 Ma (Morgan *et al.*, 1994) and this is the value used here.

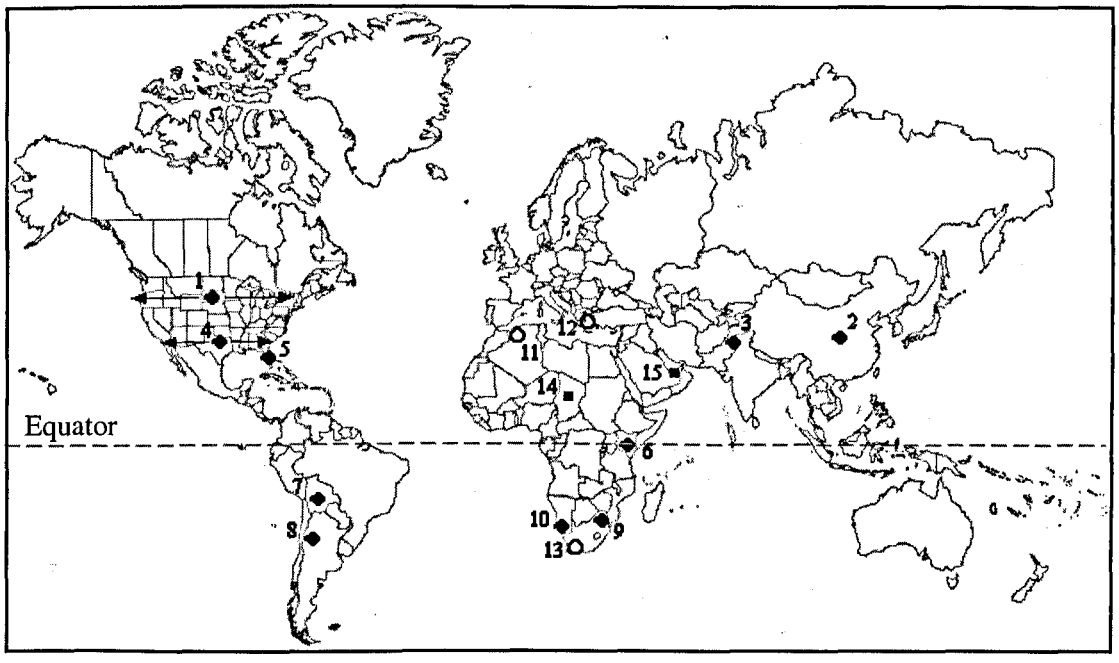

Figure 7.1. Map of the world showing the localities discussed in this study. Black diamonds indicate the localities where long carbon isotope records have enabled the first occurrence of C_4 grasses to be dated. These records show the transition from a C_3 vegetation to a mixed C_3 and C_4 vegetation and are referred to as transition records in this study. Empty circles indicate late Neogene records in which C_4 grasses are absent. Regions at higher latitudes than these "C_4 absent" records also lack C_4 grasses in the present day and in the late Neogene. Black squares indicate localities where C_4 grasses are present but where data is lacking regarding the timing of C_4 grass origins. [1]Northern North America (Cerling, 1997); [2]Northern China (Ding and Yang, 2000; Jiang *et al.*, 2002); [3]Northern Pakistan (Quade *et al.*, 1992; Cerling *et al.*, 1993); [4]Southern North America (Cerling *et al.*, 1997); [5]Florida (MacFadden and Cerling, 1996; Cerling *et al.*, 1997); [6]East Africa (Cerling *et al.*, 1997; Cerling, 1992); [7]Bolivia (MacFadden *et al.*, 1994); [8]Argentina (Latorre *et al.*, 1997); [9] Northern South Africa (Chapters 5 and 6); [10]Namibia (Segalen *et al.*, 2002); [11]Algeria (Bocherans *et al.*, 1996); [12]Greece (Quade *et al.*, 1994); [13]Southern South Africa (Franz-Odendaal *et al.*, 2002); [14]Chad (Zazzo *et al.*, 2000); [15]United Arab Emirates (Kingston, 1999).

The present day southerly extent of C_4 grasses in Africa reaches central South Africa (see Fig. 7.1.). The southern tip of the continent is devoid of C_4 grasses today and has been since at least the early Pliocene (Franz-Odendaal *et al.*, 2002). The lack of C_4 grasses in the early Pliocene site of Langebaanweg (latitude 33° South), Cape Province of South Africa, is attributed to its location within the winter rainfall zone (Franz-Odendaal *et al.*, 2002). In contrast, Namibia is located within the summer rainfall zone and the modern day Namib Desert contains a mixture of C_3 and C_4 vegetation. The carbon isotope data from Namibia (Segalen *et al.*, 2002) is derived from ratite eggshell over the last 20 Ma and indicates that for the vast majority of this time, Namibia was essentially free of C_4 grasses. There is a lack of temporal resolution in the ratite biostratigraphy, but the shift to a mixed C_3 / C_4 environment occurred between the Upper Pliocene and lower Pleistocene (3.5 -2 Ma). Ratites are known to feed selectively on C_3 plants (Segalen *et al.*, 2002) so the shift to an observable component of C_4 grass in the diet may be less pronounced. However, Stern *et al.* (1994) in a study of ratite eggshell from the Siwalik sequence of Pakistan, show that the timing of C_4 grass origins based on ratite eggshell isotopic composition approximates that determined from co-occurring mammal enamel. Also within the summer rainfall zone of southern Africa is the late Miocene to recent sequence at Makapansgat, South Africa (see Chapters 5 & 6). The Makapansgat valley (latitude 24° South) is a high altitude site (1400m above sea level) and therefore has a low present day mean annual temperature (18° C), when compared with sites from similar latitudes in the Northern hemisphere (United Arab Emirates, 28° C; Florida, USA, 20-24° C). It is suggested that this reduced temperature is a possible cause of the later origin of C_4 grasses at Makapansgat compared to the northern hemisphere sites from similar latitudes.

The data from the Chinese Loess Plateau is a 7.0 Ma palaeosol carbon isotope record from Lingtai (35° North) in which the first evidence for C_4 grasses occurs at 4 Ma (Ding and Yang, 2000). Although Lingtai is of similar latitude to the Siwalik sequence from Pakistan (33° North), the origin of C_4 grasses occurs approximately 3 Ma years later than in Pakistan (7 Ma). Ding and Yang (2000) explain this disparity in terms of a reduced temperature over the Loess Plateau during the late Miocene due to the uplift of the Tibetan Plateau. The northern North American (>37° North) record of Cerling *et al.* (1997) also has the origin of

C_4 grasses at approximately 4 Ma, indicating another case of the late origin of C_4 grasses at mid-latitude sites.

The South American data comes from Argentina and Bolivia. One Argentinian study (MacFadden *et al.*, 1996) includes samples from the whole of Argentina with a wide latitudinal range from 20° South to 50° South and quotes 8 Ma as the origin of C_4 grasses over this region. However, Latorre *et al.* (1997) focus on North Western Argentina (latitude of 28-30° South) and quote 7.3 to 6.7 Ma as the origin of C_4 grasses in this restricted region of Argentina. Because of the higher degree of latitudinal resolution, we have used the data of Latorre *et al.* (1997) in Table 7.1. and Figure 7.1. A lower latitude South American carbon isotope sequence from the Bolivian Andes (latitude 16-22° South) is documented in MacFadden *et al.* (1994). The sample sizes at each stratigraphic level are small but C_4 grasses are clearly present at 10 Ma, and this is the date used in this study for the origin of C_4 grasses in Bolivia. The present day elevation of these sites varies between 500 m and 4000 m, which is reflected in the modern day annual temperatures that range from 5 to 25°C. However, palaeoelevation estimates quoted in MacFadden *et al.* (1994) are between 500 m and 2800 m indicating that altitude and temperature gradients would have had less impact on the palaeovegetation than on modern day vegetation.

7.6. Results

The data compiled for use in this study of the distribution of C_4 grasses from the mid-Miocene to recent are shown in Figure 7.2. The latitudinal distribution of C_4 grasses ranges from the equator to 35°-40° North and South in the present day. Transition ages range from approximately 12 Ma in equatorial eastern Africa to approximately 4 Ma in the mid-latitude sites of Namibia, South Africa, northern North America and China. Each of these four mid-latitude regions have modern day mean annual temperatures below 19° C (see Table 7.1.), whereas the sites with older transition ages have modern-day mean annual temperatures greater than 20° C.

Site	Data Source	Latitude	Age Range (Ma)	Date of Transition (Ma)	Present Day Temp° C	Precipitation mm/year
Transition Records						
Northern North America (>37° N)[1]	E	37-~45° N	18-0	4	8-13	360 - 720
Northern China[2]	P	35° N	5.2-2.4	4	9	480
Siwaliks, Pakistan[3]	P, E, O	?	16-0	7–5	21	480
Siwaliks, Pakistan[4]	E	~32° N	13-4	9.4	21	480
Southern North America (<37° N)[1]	E	37-~30° N	20-0	8-7	12-21	360 - 960
Florida, USA[5]	E	25-30° N	9.5-0.1	~7	20-24	1200 - 1560
East Africa[1,6]	P, E	10° S - 4° N	19-0	9-10	25-30	
Bolivia, South America[7]	E	16–22° S	25-0	15-7.5	5-25	360 - 1080
Northern South Africa[8]	SC, E, O	24° S	5-0	5-4	18	840
Namibia[9]	ES	25–28° S	20–0	5-3	15-19	84 - 144
N.W. Argentina[10]	P, E	28–30° S	9.2–3.5	7.3-6.7	13-18	
Argentina, South America*[11]	E	20–50° S	28–0	8		
Presence of C4 grasses						
Tugen Hills, Kenya[12]	E, P	0.5° N	7-6	>6.5	18	1200
Omo, Ethiopia[13]	E	?			28	<480
Tugen Hills, Kenya[14]	E, O	0.5° N	15.3-0	>15.3	18	1200
Koobi Fora, Turkana Basin, Kenya[15]	LC	4° N	4–0.7	>4	28	<480
Abu Dhabi, United Arab Emirates[16]	P, E	24° N	8-6	>8	26	96
Chad, Central Africa[17]	E	16° N	6–3	>6	28	<720
Arizona, North America[18]	E, P, O	32 ° N	3.4-0.8	>3.4	20	480
Absence of C4 grasses						
Fort Ternan, Kenya[19]	E, P		13.9-14.0	<14	21	1200
Langebaanweg, South Africa[20]	E	33° S	~5	-	16	840
Western Europe[1, 21]	E	38–48° N	18–0	-	<16	480–960
Tighenif, Algeria[22]	E	35° N	0.7	<0.7	15	360

Table 7.1. Pubished records of C_4 grass distribution from the mid-Miocene to recent. E = enamel; ES = eggshell; LC = lake carbonate; O = organic matter; P = palaeosol; SC = speleothem carbonate. [1]Cerling *et al.* (1997); [2]Ding and Yang (2000), Jiang *et al.* (2002); [3]Quade *et al.* (1992), Cerling *et al.* (1993); [4]Morgan *et al.*, 1994; [5]MacFadden and Cerling (1996); [6]Cerling (1992); [7]MacFadden *et al.* (1994); [8]Chapters 5 and 6; [9]Segalen *et al.* (2002); [10]Latorre *et al.* (1997); [11]MacFadden *et al.* (1996); [12]Kingston *et al.* (2002); [13]Ericson *et al.* (1981); [14]Kingston *et al.* (1994), Morgan *et al.* (1994); [15]Cerling *et al.* (1988); [16]Kingston (1999); [17]Zazzo *et al.* (2000); [18]Wang *et al.* (1993); [19]Cerling *et al.* (1997b); [20]Franz-Odendaal *et al.* (2002); [21]Quade *et al.* (1994); [22]Bocherens *et al.* (1996).

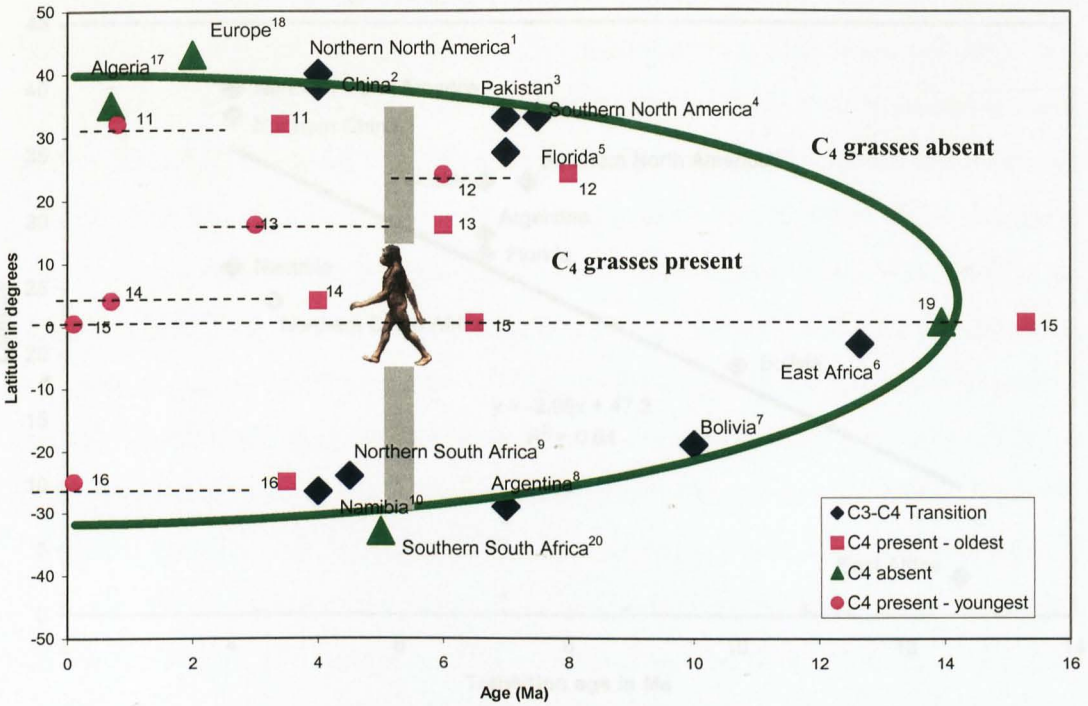

Figure. 7.2. Distribution of C_4 grasses from mid-Miocene onwards. Curved line shows the relationship between latitude and the age of the first occurrence of C_4 (savannah) grasses. This relationship is in agreement with existing models of C_4 grass origins and distribution (Cerling *et al.*, 1997; 1998; Collatz *et al.*, 1998). Hominin graphic indicates the origins of bipedalism at ca. 5-6 Ma in Africa (see Section 7.7.4.). Data for transition records from: [1]Cerling *et al.* (1997); [2]Ding and Yang (2000), Jiang *et al.* (2002); [3]Quade *et al.* (1992), Cerling *et al.* (1993); [4]Cerling *et al.* (1997); [5]MacFadden and Cerling (1996); [6]Cerling *et al.*, 1997; Cerling (1992); [7]MacFadden *et al.* (1994); [8]Latorre *et al.* (1997); [9]Chapters 5 and 6; [10]Segalen *et al.* (2002). Data for C_4 grasses present records from: [11]Wang *et al.* (1993); [12]Kingston (1999); [13]Zazzo *et al.* (2000); [14]Cerling *et al.* (1988); [15]Kingston *et al.* (1994; 2002); [16]Sponheimer *et al.* (2001), van der Merwe *et al.* (2003), Lee-Thorp *et al.* (2000), Lee-Thorp and Talma (2000). Data for C_4 absent records from: [17]Bocherans *et al.* (1996) [18]Cerling *et al.*, 1997; Quade *et al.* (1994); [19]Cerling *et al.* (1997b); [20]Franz-Odendaal *et al.* (2002).

Despite the inaccuracies of the temperature/latitude relationship (as discussed in Section 7.3.), there is a significant relationship ($p>0.01$) between latitude and the age of the C_3 to C_4 plant transition ($r = -0.8$; $n = 10$), with younger ages occurring at higher latitudes (see Fig. 7.3.). "C_4 absent" records plot either at the mid to high latitudes in the present day or at lower latitudes in the late Miocene, and show the same temporal / latitudinal trends as the transition records. This indicates that through the latitude/temperature relationship, C_4 plants were increasing their geographic range into lower temperature regions throughout the late Neogene. It is likely that a gradual reduction in atmospheric pCO_2 was

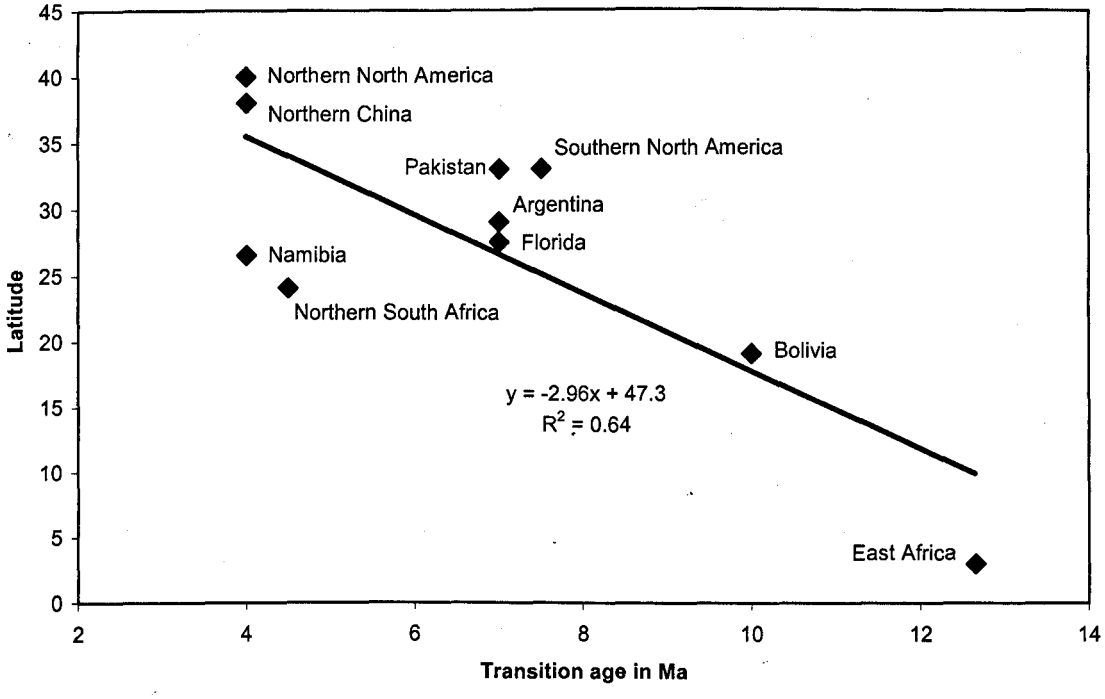

Figure 7.3. Relationship between latitude and the age of the C_3 to C_4 plant transition. See Section 7.7.1. for discussion. Data and sources listed in Table 7.1.

controlling this gradual spread of C_4 grasses, following the models and evidence of (Cerling *et al.*, 1997; Collatz *et al.*, 1998). This postulated gradual increase in the latitudinal range of C_4 plants over millions of years contrasts with the rapid shift in vegetation between 8 Ma and 6 Ma suggested by Cerling *et al.* (1997).

7.7. Discussion

7.7.1. Late Neogene spread of C_4 grasses across Africa

The incorporation here of new palaeoclimatic data from Northern China, Namibia and South Africa (Ding and Yang, 2000; Segalen *et al.*, 2002; Chapters 5 and 6) increases the database of mid-latitude carbon isotope data and indicates that the origin of C_4 grasses in these regions occurred as late as 4 Ma. Of particular relevance to early hominin evolution in Africa is the latitudinal increase of C_4 plant distribution over time. Langebaanweg in the Cape Province of South Africa and Tighenif in Algeria both had a Mediterranean climate throughout the late Neogene and were essentially lacking in C_4 grasses during this period (Bocherens *et al.*, 1996; Franz-Odendaal *et al.* 2002). The equatorial sites in east Africa have had a small and increasing proportion of C_4 grasses in the local vegetation since

15 Ma (Kingston *et al.*, 1994) and since this time have been mixed environments with the proportions of C_3 versus C_4 vegetation varying both spatially and temporally. In between these two extremes are the mid latitude hominin sites. Koro-Toro in Chad at 16° North has high modern day mean annual temperatures (28 °C) and has had C_4 grasses present in the local environment since at least 6 Ma (in the absence of data from any older sites). Data from Makapansgat in South Africa (24° South) is determined from speleothem and enamel data that suggest an age of approximately 4-5 Ma for the origin of C_4 grasses (Chapters 5 and 6; Sponheimer *et al.*, 2001). A similar late occurrence of C_4 grasses occurs at 2-3.5 Ma in Namibia at a latitude of 25-28 ° South (Segalen *et al.*, 2002). There is no stable isotope data from the Miocene to recent of North African mid-latitude faunas. However, the trend between latitude and the timing of C_4 grass origins shown in Figure 7.2., predicts a north African origin of C_4 grasses at 4-5 Ma. Future work on more African sites will help to confirm the latitudinal pattern discussed in this study.

7.7.2. Faunal response to a gradual spread of C_4 grasses

It is widely accepted that the mid-Miocene African faunas differ significantly from the Plio-Pleistocene African faunas in terms of their species composition and habitat preferences (e.g. Hill, 1987; Andrews, 1992; Vrba *et al.*, 1995), and that the interim period represents a gross restructuring of the African terrestrial communities. However, refining the details of the transition from the mid-Miocene "C_3-world" to the Plio-Pleistocene "C_4-world" has been problematic. The Cerling *et al.* (1997) interpretation of the carbon isotope data from fossil herbivore teeth restricts the global expansion of C_4 biomass to one event between 8 Ma and 6 Ma. However, as noted by Köhler *et al.* (1998), this single pulse of C_4 grass expansion is not always accompanied by an increase in faunal turnover in the "C_4 world". Köhler *et al.* (1998) also argue that an increase in faunal turnover in the purely C_3 environment of Spain at 7-6 Ma indicates that faunal turnover is not always directly associated with savannah grass environments. The gradual expansion model presented in this study predicts a period of extended faunal turnover, rather than the shorter vegetation shift and turnover pulse of Cerling *et al.* (1997).

Numerous episodes of increased rates of faunal turnover have been identified within terrestrial late Neogene mammalian sequences, each showing replacement of woodland fauna by more savannah adapted species. These events occur at different times in different regions of the world and are regularly distributed within the last 10 million years. Examples of documented late Neogene faunal turnover events have been recorded at 10 Ma, 7.8 Ma and 7.3-7.0 Ma in Pakistan (Barry *et al.*, 2002; Patnaic, 2003; Raza *et al.*, 2002); 10-9 Ma and 6.5 Ma in Spain (Köhler *et al.*, 1998; Pickford *et al.*, 1995); approximately 7.4 Ma – 6.0 Ma in the Nawata Formation of the Lothagam succession, Kenya (Leakey and Harris, 2003; McDougall and Feibel, 2003); between 2.8 and 2.3 Ma in the Omo sequence of Ethiopia (Bobe and Eck, 2001; Bobe *et al.*, 2002). These records indicate a series of turnover events, which if they are linked with episodes of climatic change, are related to local rather than global events. There is no global faunal turnover event significantly above background rates at 8-6 Ma (Köhler *et al.*, 1998) that can be related to the rapid global expansion of C_4 grasses as described by Cerling *et al.* (1997). The more gradual spread of C_4 grasses shown in this study shows greater correspondence with the evidence for smaller sequential faunal turnover events throughout the late Neogene.

The evidence for a gradual expansion of C_4 grasses shown in Figures 7.2. and 7.3 is supported by faunal evidence for prolonged faunal turnover (Köhler *et al.* 1998; Barry *et al.* 2002) and gradual increases in hypsodonty (Jernvall and Fortelius, 2002) in the Late Neogene. The faunal evidence indicates that the late Neogene faunal response to the spread of the savannah biome is gradual over millions of years with periods of peak turnover that can vary in timing between regions. The overall result of this gradual change is a Plio-Pleistocene savannah-woodland adapted fauna that differs markedly from the mid-Miocene forest adapted faunas.

7.7.3. Hominin habitats and adaptations

The current distribution of Miocene and Pliocene hominin discoveries ranges from South Africa in the South to Chad in the North and is similar to the contemporaneous extent of C_4 grasses (see Figs. 7.2). This may suggest that the early hominins were restricted to the woodland-savannah mosaic of Africa.

Direct evidence for the reliance of early hominins on the savannah biome comes from carbon isotope analysis of *Australopithecus* and *Homo* teeth from South Africa which indicates a significant component of food containing a C_4 grass signature (e.g. termites – d'Errico *et al.* 2001) in the diet of these taxa (Sponheimer and Lee-Thorp, 1999; van der Merwe *et al.*, 2003; Lee-Thorp *et al.*, 1994). It is currently unknown whether the same is true for earlier hominin species, but future carbon isotope studies of the earliest hominins have the potential to provide important clues for determining the diets and habitats of the earliest bipeds.

7.7.4. Origins of Bipedalism

Recent finds from Chad (Brunet *et al.* 2002) and Kenya (Senut *et al.* 2001) have pushed back the earliest evidence of hominins well into the late Miocene at 6-7 Ma. *Sahelanthropus tchadensis* is lacking conclusive evidence for a bipedal posture (Brunet *et al.* 2002), whereas the femur morphology of *Orrorin tugenensis* (Senut *et al.*, 2001) has been used as evidence of bipedalism at ca. 6 Ma. More post-cranial evidence for a bipedal gait comes from *Australopithecus anamensis* at 4 Ma (Leakey *et al.*, 1995). These new finds have expanded species-diversity at the base of the hominin tree and have lead authors to suggest that there was an adaptive radiation of early hominins in the late Miocene to early Pliocene (Wood, 2002; Foley, 2002). If this is the case, then bipedalism can be considered as the principal adaptation to an increasingly open environment that lead to the rapid speciation of early hominins. The gradual spread of C_4 grassland and the mosaics of woodland-savannah in transitional zones provides ample opportunity for allopatric speciation in small reproductively-isolated populations (Vrba, 1992; Vrba, 1995), and it is within such populations that the earliest bipedal hominins are envisaged to have evolved. The gradual expansion of the new savannah-grass ecosystem is consistent with the evolution of morphological novelty such as bipedalism. In contrast, a rapid shift in vegetation is more likely to lead to extinction and faunal turnover rather than adaptive radiation (Foley, 1994; 2002).

7.8. Conclusions

This review of published palaeoenvironmental records shows that the spread of savannah grasses started in the mid-Miocene at low latitudes and continued to spread to mid latitudes into the Pliocene. This gradual expansion of savannah grasses was forced by decreasing concentrations of atmospheric CO_2, in agreement with the Cerling *et al.* (1997) model of C_4 grass distribution over time. Recent evidence for the origins of bipedalism between 7 and 4 Ma, places the early hominins within this major global expansion of savannah environments for the first time. It is likely that the mosaic of woodland and grassland environments in Africa since the mid-Miocene provided ample opportunity for the development of locomotory and dietary adaptations that enabled the earliest hominins to survive in more open environments. Beyond this assertion, many aspects of the origins of bipedalism remain unknown. Proving the causal relationship between spreading savannahs and the origins of bipedalism will be a challenge, but in the light of the new palaeoclimatic data presented here, the Savannah Hypothesis of human origins cannot yet be discounted.

7.9. References

Andrews, P. (1992). Evolution and environment in the Hominoidea. *Nature* **360,** 641-646.

Barry, J. C., Morgan, M. L. E., Flynn, L. J., Pilbeam, D., Behrensmeyer, A. K., Raza, S. M., Khan, I. A., Badgley, C., Hicks, J., and Kelley, J. (2002). Faunal and environmental change in the late Miocene Siwaliks of northern Pakistan. *Paleobiology* **28,** 1-71.

Berner, R. A., and Kothavala, Z. (2001). GEOCARB III: a revised model of atmospheric CO_2 over Phanerozoic time. *American Journal of Science* **301,** 182-204.

Bobe, R., and Eck, G. G. (2001). Responses of African bovids to Pliocene climatic change. *Paleobiology Memoirs* **27,** 1-47.

Bobe, R., Behrensmeyer, A. K., and Chapman, R. E. (2002). Faunal change, environmental variability and late Pliocene hominin evolution. *Journal of Human Evolution* **42,** 475-497.

Bocherens, H., Koch, P. L., Mariotti, A., Geraads, D., and Jaeger, J.-J. (1996). Isotopic biogeochemistry (^{13}C, ^{18}O) of mammalian enamel from African Pleistocene Hominid sites. *Palaios* **11,** 306-318.

Boom, A., Marchant, R., Hooghiemstra, H., and Sinninghe Damste, J. S. (2002). CO_2-and temperature-controlled altitudinal shifts of C4- and C3-dominated grasslands allow reconstruction of palaeoatmospheric pCO_2. *Palaeogeography, Palaeoclimatology, Palaeoecology* **177,** 151-168.

Bromage, T. G., and Schrenk, F. (1995). Biogeographic and climatic basis for a narrative of early hominid evolution. *Journal of Human Evolution* **28,**

109-114.

Brunet, M., Guy, F., Pilbeam, D., Mackaye, H. T., Likius, A., Ahounta, D., Beauvilain, A., Blondel, C., Bocherens, H., Boisserie, J. R., De Bonis, L., Coppens, Y., Dejax, J., Denys, C., Duringer, P., Eisenmann, V. R., Fanone, G., Fronty, P., Geraads, D., Lehmann, T., Lihoreau, F., Louchart, A., Mahamat, A., Merceron, G., Mouchelin, G., Otero, O., Campomanes, P. P., De Leon, M. P., Rage, J. C., Sapanet, M., Schuster, M., Sudre, J., Tassy, P., Valentin, X., Vignaud, P., Viriot, L., Zazze, A., and Zellikefer, C. (2002). A new hominid from the Upper Miocene of Chad, Central Africa (vol 419, pg 145, 2002). *Nature* **418,** 801-801.

Carter, D. R., and Peterson, K. M. (1983). Effects of a CO_2-enriched atmosphere on the growth and competitive interaction of a C_3 and a C_4 grass. *Oecologia* **58,** 188-193.

Cerling, T. E., and Hay, R. L. (1986). An isotopic study of paleosol carbonates from olduvai gorge. *Quaternary Research* **25,** 63-78.

Cerling, T. E., Bowman, J. R., and Oneil, J. R. (1988). An isotopic study of a fluvial lacustrine sequence - the Plio-Pleistocene Koobi Fora sequence, east-Africa. *Palaeogeography, Palaeoclimatology, Palaeoecology* **63,** 335;356.

Cerling, T. E., Quade, J., Wang, Y., and Bowman, J. R. (1989). Carbon isotopes in soils and paleosols as ecology and paleoecology indicators. *Nature* **341,** 138-139.

Cerling, T. E. (1992). Development of grasslands and savannas in east-Africa during the Neogene. *Palaeogeography, Palaeoclimatology, Palaeoecology (Global and Planetary Change Section)* **97,** 241-247.

Cerling, T. E., Wang, Y., and Quade, J. (1993). Expansion of C4 ecosystems as an indicator of global ecological change in the late miocene. *Nature* **361,** 344-345.

Cerling, T. E., Harris, J. M., MacFadden, B. J., Leakey, M. G., Quade, J., Eisenmann, V., and Ehleringer, J. R. (1997). Global vegetation change through the Miocene/Pliocene boundary. *Nature* **389,** 153; 158.

Cerling, T. E., Harris, J. M., Ambrose, S. H., Leakey, M. G., and Solounias, N. (1997b). Dietary and environmental reconstruction with stable isotope analyses of herbivore tooth enamel from the Miocene locality of Fort Ternan, Kenya. *Journal of Human Evolution* **33,** 635-650.

Cerling, T. E., Ehleringer, J. R., and Harris, J. M. (1998). Carbon dioxide starvation, the development of C-4 ecosystems, and mammalian evolution. *Philosophical Transactions of the Royal Society of London Series B-Biological Sciences* **353,** 159-170.

Cerling, T. E., Harris, J. M., Leakey, M. G., and Mudida, N. (2003). Stable isotope ecology of northern Kenya, with emphasis on the Turkana Basin. *In* "Lothagam: the dawn of humanity in eastern Africa." (M. G. Leakey, and J. M. Harris, Eds.), pp. 583-604. Columbia University Press, New York.

Cerling, T. E., Harris, J. M., and Leakey, M. G. (2003). Isotope paleoecology of the Nawata and Nachukui Formations at Lothagam, Turkana Basin, Kenya. *In* "Lothagam: the dawn of humanity in eastern Africa." pp. 605-624. Columbia University Press, New York.

Collatz, G. J., Berry, J. A., and Clark, J. S. (1998). Effects of climate and atmospheric CO_2 partial pressure on the global distribution of C4 grasses:

present, past, and future. *Oecologia* **114,** 441-454.
Cowling, S. A., and Sykes, M. T. (1999). Physiological significance of low atmospheric CO_2 for plant-climate interactions. *Quaternary Research* **52,** 237-242.
d'Errico, F., Backwell, L. R., and Berger, L. R. (2001). Bone tool use in termite foraging by early hominids and its impact on our understanding of early hominid behaviour. *South African Journal of Science* **97,** 71-75.
Dart, R. A. (1953). The predatory transition from ape to man. *International Anthropology and Linguistics Review* **1,** 201-219.
Darwin, C. (1874). "The descent of man; and selection in relation to sex." Crowell, New York.
Ding, Z. L., and Yang, S. L. (2000). C3/C4 vegetation evolution over the last 7.0 Myr in the Chinese Loess Plateau: evidence from pedogenic carbonate $\delta^{13}C$. *Palaeogeography, Palaeoclimatology, Palaeoecology* **160,** 291-299.
Ehleringer, J. R., Sage, R. F., Flanagan, L. B., and Pearcy, R. W. (1991). Climate Change and the evolution of C4 photosynthesis. *Trends in Ecology & Evolution* **6,** 95-99.
Ehleringer, J. R., and Monson, R. K. (1993). Evolutionary and ecological aspects of photosynthetic pathway variation. *Annual Review of Ecology and Systematics* **24,** 411-439.
Ericson, J. E., Sullivan, C. H., and Boaz, N. T. (1981). Diets of Pliocene mammals from Omo, Ethiopia, deduced from carbon isotopic ratios in tooth apatite. *Palaeogeography, Palaeoclimatology, Palaeoecology* **36,** 69-73.
Farquhar, G. D., Ehleringer, J. R., and Hubick, K. T. (1989). Carbon isotope discrimination and photosynthesis. *Annual Review of Plant Physiology and Plant Molecular Biology* **40,** 503-537.
Foley, R. A. (1994). Speciation, extinction and climatic change in hominid evolution. *Journal of Human Evolution* **26,** 275-289.
Foley, R. A. (2002). Adaptive radiations and dispersals in Hominin evolutionary ecology. *Evolutionary Anthropology* **11,** 32-37.
France-Lanord, C., and Derry, L. A. (1994). Delta-^{13}C of organic carbon in the Bengal Fan: source evolution and transport of C3 and C4 plant carbon to marine sediments. *Geochimica et Cosmochimica Acta* **58,** 4809-4814.
Franz-Odendaal, T. A., Lee-Thorp, J. A., and Chinsamy, A. (2002). New evidence for the lack of C_4 grassland expansions during the early Pliocene at Langebaanweg, South Africa. *Paleobiology* **28,** 378-388.
Giresse, P., Maley, J., and Brenac, P. (1994). Late Quaternary palaeoenvironments in the Lake Barombi Mbo (West Cameroon) deduced from pollen and carbon isotopes of organic matter. *Palaeogeography, Palaeoclimatology, Palaeoecology* **107,** 65-78.
Hatch, M. D. (1987). C4 photosynthesis: a unique blend of modified biochemistry, anatomy and ultrastructure. *Biochimica et Biophysica Acta* **895,** 81-106.
Hill, A. (1987). Causes of perceived faunal change in the later Neogene of East Africa. *Journal of Human Evolution* **16,** 583-596.
Jacobs, B. F. (2002). Estimation of low-latitude paleoclimates using fossil angiosperm leaves: examples from the Miocene Tugen Hills, Kenya. *Paleobiology* **28,** 399-421.
Jernvall, J., and Fortelius, M. (2002). Common mammals drive the evolutionary

increase of hypsodonty in the Neogene. *Nature* **417,** 538-540.

Jiang, W., Peng, S., Hao, Q., and Liu, D. (2002). Carbon isotopic records in paleosols over the Pliocene in Northern China: Implication on vegetation development and Tibetan uplift. *Chinese Science Bulletin* **47,** 687-690.

Jolly, D., and Haxeltine, A. (1997). Effects of low glacial atmospheric CO_2 on tropical African montane vegetation. *Science* **276,** 786-788.

Kingston, J. D., Marino, B. D., and Hill, A. (1994). Isotopic evidence for Neogene Hominid paleoenvironments in the Kenya rift valley. *Science* **264,** 955-959.

Kingston, J. D. (1999). Isotopes and environments of the Baynunah Formation, Emirate of Abu Dhabi, United Arab Emirates. *In* "Fossil Vertebrates of Arabia." (P. J. Whybrow, and A. Hill, Eds.), pp. 523. Yale University Press.

Kingston, J. D., Jacobs, B. F., Hill, A., and Deino, A. (2002). Stratigraphy, age and environments of the late Miocene Mpesida Beds, Tugen Hills, Kenya. *Journal of Human Evolution* **42,** 95-116.

Köhler, M., Moyà-Solà, S., and Agusti, J. (1998). Miocene/Pliocene shift: one step or several? *Nature* **393,** 126-128.

Latorre, C., Quade, J., and McIntosh, W. C. (1997). The expansion of C-4 grasses and global change in the late Miocene: Stable isotope evidence from the Americas. *Earth and Planetary Science Letters* **146,** 83-96.

Leakey, M. G., Feibel, C. S., McDougall, I., and Walker, A. (1995). New four-million-year-old hominid species from Kanapoi and Allia Bay, Kenya. *Nature* **376,** 565-571.

Leakey, M. G., and Harris, J. M. (2003). Lothagam: its significance and contributions. *In* "Lothagam: the dawn of humanity in eastern Africa." (M. G. Leakey, and J. M. Harris, Eds.), pp. 625-660. Columbia University Press, New York.

Lee-Thorp, J. A., van der Merwe, N. J., and Brain, C. K. (1994). Diet of *Australopithecus-robustus* at Swartkrans from stable carbon isotopic analysis. *Journal of Human Evolution* **27,** 361-372.

Lee-Thorp, J. A., Thackeray, J. F., and van der Merwe, N. (2000). The hunters and the hunted revisited. *Journal of Human Evolution* **39,** 565-576.

Lee-Thorp, J. A., and Talma, A. S. (2000). Stable light isotopes and environments in the Southern African Quaternary and Late Pliocene. *In* "The Cenozoic of Southern Africa." pp. 406. Oxford Monographs on Geology and Geophysics. Oxford University Press, Oxford.

Legates, D. R., and Willmott, C. J. (1990a). Mean seasonal and spatial variability global surface air temperature. *Theoretical and Applied Climatology* **41,** 11-21.

Legates, D. R., and Willmott, C. J. (1990b). Mean seasonal and spatial variability in gauge-corrected, global precipitation. *International Journal of Climatology* **10.**

MacFadden, B. J., Wang, Y., Cerling, T. E., and Anaya, F. (1994). South-American fossil mammals and carbon isotopes - a 25-million-year sequence from the Bolivian andes. *Palaeogeography, Palaeoclimatology, Palaeoecology* **107,** 257-268.

MacFadden, B. J., Cerling, T. E., and Prado, J. (1996). Cenozoic terrestrial ecosystem evolution in Argentina: Evidence from carbon isotopes of fossil mammal teeth. *Palaios* **11,** 319-327.

MacFadden, B. J., and Cerling, T. E. (1996). Mammalian herbivore communities, ancient feeding ecology, and carbon isotopes: a 10 million-year sequence from the Neogene of Florida. *Journal of Vertebrate Paleontology* **16,** 103-115.

MacFadden, B. J., Cerling, T. E., Harris, J. M., and Prado, J. (1999). Ancient latitudinal gradients of C-3/C-4 grasses interpreted from stable isotopes of New World Pleistocene horse (Equus) teeth. *Global Ecology and Biogeography* **8,** 137-149.

Marchant, R., Boom, A., and Hooghiemstra, H. (2002). Biome reconstructions for the past 450,000 years from the Funza-II core, Colombia: comparisons with model-based vegetaion reconstructions and $\delta^{13}C$ record ecosystem relationships to Late Quaternary environmental change. *Palaeogeography, Palaeoclimatology, Palaeoecology* **177,** 29-45.

McDougall, I., and Feibel, C. S. (2003). Numerical age control for the Miocene-Pliocene succession at Lothagam, a Hominoid-bearing sequence in the Northern Kenya rift. *In* "Lothagam: the dawn of humanity in eastern Africa." pp. 43-66. Columbia University Press, New York.

Morgan, M. E., Kingston, J. D., and Marino, B. D. (1994). Carbon isotopic evidence for the emergence of C4 plants in the Neogene from Pakistan and Kenya. *Nature* **367,** 162-165.

O'Leary, M. H. (1981). Carbon isotope fractionation in plants. *Phytochemistry* **20,** 553-567.

O'Leary, M. H. (1988). Carbon isotopes in photosynthesis. *BioScience* **38,** 328-336.

Owen-Smith, N. (1999). Ecological links between African savanna environments, climate change, and early hominid evolution. *In* "African biogeography, climate change and human evolution." (T. G. Bromage, and F. Schrenk, Eds.), pp. 138-149. Oxford University Press, Oxford.

Pagani, M., Freeman, K. H., and Arthur, M. A. (1999). Late Miocene atmospheric CO_2 concentrations and the expansion of C4 grasses. *Science* **285,** 876-879.

Patnaik, R. (2003). Reconstruction of Upper Siwalik palaeoecology and palaeoclimatology using microfossil palaeocommunities. *Palaeogeography, Palaeoclimatology, Palaeoecology* **197,** 133-150.

Pearson, P. N., and Palmer, M. R. (2000). Atmospheric carbon dioxide concentrations over the past 60 million years. *Nature* **406,** 695-699.

Pickford, M. (1990). Uplift of the roof of Africa and its bearing on the evolution of mankind. *Human Evolution* **5,** 1-20.

Pickford, M., Morales, J., and Soria, D. (1995). Fossil camels from the Upper Miocene of Europe: implications for biogeography and faunal change. *Geobios* **28,** 641-650.

Quade, J., Cerling, T. E., and Bowman, J. R. (1989). Development of Asian monsoon revealed by marked ecological shift during the latest Miocene in northern Pakistan. *Nature* **342,** 163-166.

Quade, J., Cerling, T. E., Barry, J. C., Morgan, M. E., Pilbeam, D. R., Chivas, A. R., Leethorp, J. A., and Vandermerwe, N. J. (1992). A 16-Ma record of paleodiet using carbon and oxygen isotopes in fossil teeth from Pakistan. *Chemical Geology* **94,** 183-192.

Quade, J., Solounias, N., and Cerling, T. E. (1994). Stable isotopic evidence from paleosol carbonates and fossil teeth in Greece for forest or woodlands over

the past 11 Ma. *Palaeogeography, Palaeoclimatology, Palaeoecology* **108,** 41-53.

Raza, S., Cheema, I., Downs, W., Rajpar, A., and Ward, S. (2002). Miocene stratigraphy and mammal fauna from the Sulaiman Range, Southwestern Himalayas, Pakistan. *Palaeogeography, Palaeoclimatology, Palaeoecology* **186,** 185-197.

Rozanski, K., Araguas-Araguas, L., and Gonfiantini, R. (1993). Isotopic patterns in modern global precipitation. *In* "Climate change in continental isotopic records." (P. K. Swart, K. C. Lohmann, J. McKenzie, and S. Savin, Eds.), pp. 1-36. Geophysical Monograph. American Geophysical Union, Washington.

Segalen, L., Renard, M., Pickford, M., Senut, B., Cojan, I., Le Callonnec, L., and Rognon, P. (2002). Environmental and climatic evolution of the Namib Desert since the Middle Miocene: the contribution of carbon isotope ratios in ratite eggshells. *Comptes Rendus Geoscience* **334,** 917-924.

Senut, B., Pickford, M., Gommery, D., Mein, P., Cheboi, K., and Coppens, Y. (2001). First hominid from the Miocene (Lukeino Formation, Kenya). *Comptes Rendus De L Academie Des Sciences Serie Ii Fascicule a-Sciences De La Terre Et Des Planetes* **332,** 137-144.

Sponheimer, M., and Lee-Thorp, J. A. (1999). Isotopic evidence for the diet of an early hominid, *Australopithecus africanus*. *Science* **283,** 368-370.

Sponheimer, M., Reed, K., and Lee-Thorp, J. A. (2001). Isotopic palaeoecology of Makapansgat Limeworks Perissodactyla. *South African Journal of Science* **97,** 327-329.

Stanley, S. M. (1995). Climatic forcing and the origin of the human genus. *In* "Effects of past global change on life." (S. M. Stanley, and others, Eds.), pp. 233-243. Studies in Geophysics.

Stern, L. A., Johnson, G. D., and Chamberlain, C. P. (1994). Carbon isotope signature of environmental change found in fossil ratite eggshells from a South Asian Neogene sequence. *Geology* **22,** 419-422.

Street-Perrott, F. A., Huang, Y., Perrott, R. A., Eglinton, G., Barker, P., Khelifa, L. B., Harkness, D. D., and Olago, D. O. (1997). Impact of lower atmospheric carbon dioxide on tropical mountain ecosystems. *Science* **278,** 1422-1426.

Talbot, M. R., and Johannessen, T. (1992). A high resolution palaeoclimatic record for the last 27,500 years in tropical West Africa from the carbon and nitrogen isotopic composition of lacustrine organic matter. *Earth and Planetary Science Letters* **110,** 23-37.

Tobias, P. V. (1991). The environmental background of Hominid emergence and the appearance of the genus *Homo*. *Human Evolution* **6,** 129-142.

van der Merwe, N., Thackeray, F., Lee Thorp, J. A., and Luyt, J. (2003). The carbon isotope ecology and diet of *Australopithecus africanus* at Sterkfontein, South Africa. *Journal of Human Evolution* **44,** 581-597.

Vrba, E. S. (1992). Mammals as a key to evolutionary theory. *Journal of Mammalogy* **73,** 1-28.

Vrba, E. S., Denton, G. H., Partridge, T. C., and Burckle, L. H. (1995). "Paleoclimate and evolution with emphasis on human origins." Yale University Press, New Haven.

Vrba, E. S. (1995). On the connections between paleoclimate and evolution. *In* "Paleoclimate and evolution with emphasis on human origins." (E. S.

Vrba, G. H. Denton, T. C. Partridge, and L. H. Burckle, Eds.). Yale University Press, New Haven.

Wang, Y., Cerling, T. E., Quade, J., Bowman, J. R., Smith, G. A., and Lindsay, E. H. (1993). Stable isotopes of paleosols and fossil teeth as paleoecology and paleoclimate indicators: an example from the St. David Formation, Arizona. *In* "Climate change in continental isotopic records." (P. K. Swart, K. C. Lohmann, J. McKenzie, and S. Savin, Eds.), pp. 241-248. Geophysical Monograph. American Geophysical Union.

Wood, B. (2002). Palaeoanthropology: Hominid revelations from Chad. *Nature* **418,** 133-135.

Zazzo, A., Bocherens, H., Brunet, M., Beauvilain, A., Billiou, D., Mackaye, H. T., Vignaud, P., and Mariotti, A. (2000). Herbivore paleodiet and paleoenvironmental changes in Chad during the Pliocene using stable isotope ratios of tooth enamel carbonate. *Paleobiology* **26,** 294-309.

Zeitoun, V. (2000). Adequation entre changements environnementaux et speciations humaines au Plio-Pleistocene. *C.R.Acad.Sci.Paris,Sciences de la Terre et des planetes* **330,** 161-166.

Chapter 8. Conclusions and Future Work

8.1. Conclusions

This thesis has shown that there are at least two long records of primary calcite flowstone within the South African palaeocaves suitable for creating long records of Plio-Pleistocene climate change (see Chapter 3.). These are the Buffalo Cave flowstone and the Member 1 deposits (including the Collapsed Cone flowstone) of the Makapansgat Limeworks. There may be further suitable deposits to be discovered within the numerous South African palaeocaves. While not the focus of this study, thinner pieces of primary calcite flowstone (a few cm thick) can be found in the proximity of early hominin finds, and may offer further insights into hominin palaeoenvironments. However, identifying the chronological and environmental context of these shorter flowstones may prove difficult. The remainder of the South African Plio-Pleistocene speleothems examined here have been diagenetically altered and cannot provide palaeoclimatic evidence (see Chapter 3.).

Chapter 4 of this study utilised recent developments in the extraction and isotopic analysis of organic matter within speleothems. The organic matter $\delta^{13}C$ values of the Collapsed Cone and Buffalo Cave flowstones have been used as an indicator of palaeovegetation and have been used to model the relative proportions of host-rock derived carbon and palaeovegetation derived carbon within speleothem carbonate. This has enabled the speleothem carbonate $\delta^{13}C$ values to be converted into an index of palaeovegetation change. It has also been demonstrated that both the flowstones were precipitated in isotopic equilibrium with the cave waters and were not affected by kinetic isotopic effects during the precipitation of calcite. This indicates that both the carbon and oxygen isotopic variation within these flowstones reflects local or regional climatic change.

Given the evidence for the suitability of the Collapsed Cone and Buffalo Cave flowstones for palaeoclimatic reconstruction, high-resolution sampling of both speleothems was undertaken (see Chapter 5.). The resulting stable isotopic depth-series were 2.4 m and 1.2 m long respectively. The chronology of the Collapsed Cone flowstone could not be constrained using growth banding or time-series analysis so it is assigned to the late Miocene / early Pliocene (ca. 4-5

Ma) on the basis of magnetostratigraphy. Carbon isotope values are light and invariant indicating a predominantly C_3 palaeoenvironment. The Buffalo Cave flowstone chronology was constrained to between 2.0 Ma and 1.5 Ma using a combination of UV bandwidth measurement, magnetostratigraphy and time-series analysis. A carbon isotope shift at 1.7 Ma indicates an increase in the percentage of C_4 grasses in the local palaeoenvironment from approximately 25% to 50%. The carbon isotope oscillations in the Buffalo Cave flowstone occur over precession (19-23 ka) and obliquity (41 ka) periodicities indicating rapid fluctuations in vegetation cover from grass-dominated to woodland-dominated ecosystems.

The timing of the origin of C_4 plants was further investigated using fossil micromammal teeth from the oldest faunal cave-deposits in the Makapansgat Valley – the mid-Pliocene Rodent Corner and Exit Quarry repositories (see Chapter 6). Carbon isotope and dental microwear evidence indicates the presence of C_4 grasses in the diet of these micromammals. Therefore, C_4 grasses first appeared in the Makapansgat Valley before the mid-Pliocene of Rodent Corner and after the late Miocene / early Pliocene of the Collapsed Cone flowstone (between 5 Ma and 3.5 Ma).

This age estimate for the origin of C_4 plants in South Africa is younger than the mid to late Miocene age for the origin of C_4 grasses in east African hominin sites. By collecting previously published data on the late Neogene origin and distribution of C_4 grasses it is evident that it took millions of years for C_4 grasses to spread from low-latitude (e.g. east Africa) to mid-latitude sites such as South Africa (see Chapter 7.). This gradual spread of C_4 plants throughout the late Neogene coincides with the evolution of hominin bipedalism in the late Miocene. A causal relationship between these two events is suggested.

8.2. Future Work

This thesis has generated a number of questions that remain to be fully answered. This section poses these questions and suggests avenues of research that may help to provide some answers.

Creation of $\delta^{18}O$ palaeotemperature records

Palaeotemperature estimates require an estimate of the $\delta^{18}O$ composition of cave drip-water that cannot be obtained from conventional isotopic analysis of speleothem carbonate (see Section 5.4.). Recent developments in fluid-inclusion analysis can be used to determine the D/H and $\delta^{18}O$ values of fossil drip-water (see Section 5.4.). By inputting the fluid-inclusion $\delta^{18}O$ and speleothem carbonate $\delta^{18}O$ data into the equation for the temperature-dependant fractionation of $\delta^{18}O$ between water and calcite it is possible to determine the absolute palaeotemperature of speleothem formation. It would therefore be possible to convert the Buffalo Cave and Collapsed Cone flowstone $\delta^{18}O$ carbonate time-series into palaeotemperature records. These temperature records could also be used to determine the dominant control on C_4 grass proportions in the time-series – either temperature or pCO_2. Work is currently underway at the University of East Anglia.

Establishing a chronology for the Collapsed Cone flowstone

The Member 1b flowstone of the Makapansgat Limeworks (from where the Collapsed Cone flowstone was sampled) has been dated by palaeomagnetism to older than 4 Ma. While the top of the flowstone is unlikely to be much older than this date, the age of the base of the flowstone and the rate of precipitation is unknown. U/Pb dating of the flowstone may be able to provide absolute dates for this deposit. Work is currently underway at the University of Leeds.

When did C_4 grasses first arrive in Southern Africa?

This thesis has only constrained the evolution of C_4 grasses in South Africa to between 3.5 and 5 Ma. A carbon isotope study of rodent teeth in the oldest faunal deposit in the South African hominin sites (Bolt's Farm rodent deposit – c.a. 4.5-5 Ma) may help to determine the timing of this event more precisely.

Can the latitudinal expansion of C_4 grasses across Africa be observed at a finer resolution?

North Africa (Libya), Southern Africa (Namibian caves) and central eastern Africa (Malawi) all contain late Neogene faunal deposits that have yet to be studied for carbon isotopes. Future investigation of these deposits will further test the existing models of C_4 grass expansion.

Are early hominins savannah adapted?

Existing carbon isotope data from hominin teeth come from the South African hominins, *A. africanus*, *A. robustus* and *Homo sp.* (Lee-Thorp *et al.*, 1994; Sponheimer and Lee-Thorp, 1999). Each of these species shows a proportion of some savannah-based foods in their diet. It would be of great interest to determine whether there is also a savannah component to the diet of the earlier hominins (e.g. east African australopithecines and *Orrorin tugenensis* and *Sahelanthropus tchadensis*), as this would determine the degree to which these very early hominins were savannah adapted. This would help to evaluate the validity of the competing hypotheses of hominin evolution and climate change.

Appendices

Appendix 1. – Photographs of sampled flowstone sequences and maps of cave sites

a. Buffalo Cave flowstone, Buffalo Cave

b. Collapsed Cone flowstone, Makapansgat Limeworks

c. Swartkrans Lower Bank (Hanging Remnant) flowstone, Swartkrans

d. Map of the Makapansgat Limeworks site

e. Map of Buffalo Cave, Makapansgat Valley

Appendix 1a – Photo-map of the Buffalo Cave flowstone showing sampling strategy. Samples from A to N were sub-sampled for stable isotope and trace element analysis (see Chapter 5). Horizontal broken line indicates a change in the colour of the flowstone, and this datum is marked by the observed shift in carbon isotope values, trace element ratios and growth-rate of the flowstone at approx. 1.7Ma (see Chapter 5). The flowstone is the basal unit of the Buffalo Cave infill sequence, and on the basis of magnetostratigraphy is between 1 and 2Ma. Chapter 5 discusses the development of a more precise chronology based on annual growth banding and orbital tuning of stable isotope data. Photograph facing east.

Appendix 1b. (next page) Collapsed Cone flowstone in the Makapansgat Limeworks showing the sampling strategy. This block of flowstone fell from the roof of the mined cave and is unconformably overlain by the Member 5 breccia of Partridge (2000). The flowstone belongs to the upper (younger) layers of the stalagmitic boss (Latham *et al.*, 1999) of Member 1b (Partridge *et al.*, 2000). Member 1b directly underlies the Member 2 red mud deposits dated by magnetostratigraphy to 4 Ma (Herries, 2003). Samples A-C were subsampled for stable isotope and trace element analysis (see Chapters 3 and 5) and a climatic time-series was developed (see Chapter 5). Photograph facing west.

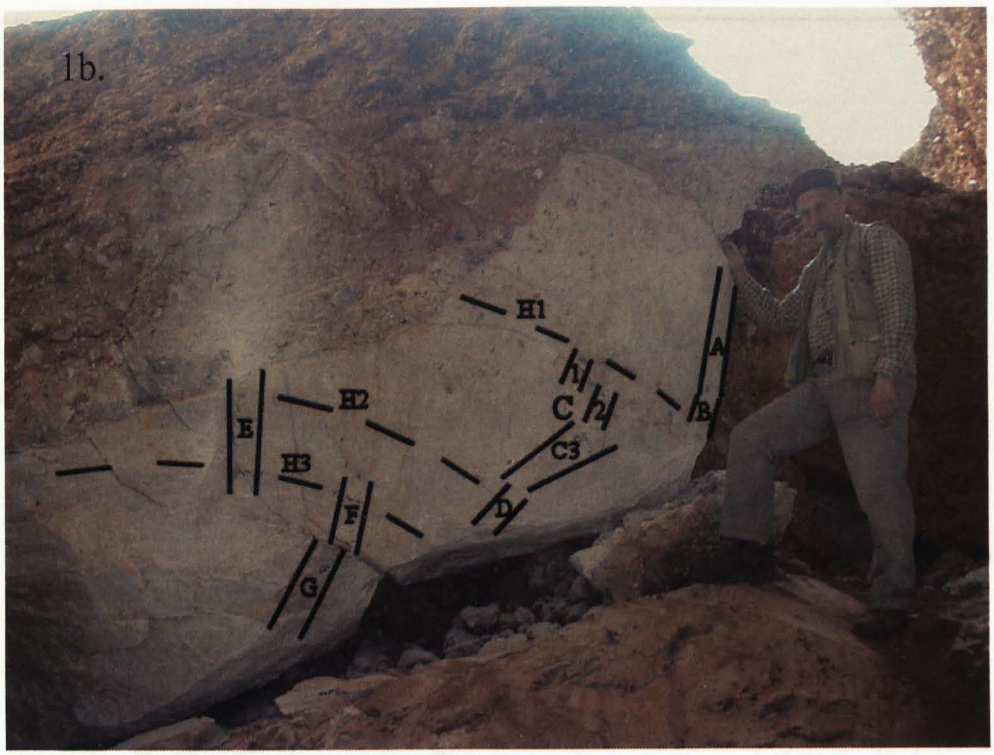

Appendix 1c. Swartkrans Member 1A (Partridge, 2000) basal flowstone of the Inner Cave Lower Bank deposits. The photograph is facing south at the southerly limit of the "floor block" of the Inner Cave (Brain, 1981), adjacent to the Hanging Remnant of Member 1C. Samples A-D were analysed for stable isotope and petrological analysis. The flowstone is composed of inter-bedded primary columnar calcite and secondary equant calcite (formerly aragonite). The primary and secondary calcites can also be identified by their largely independent carbon isotope compositions (see Chapter 3). The presence of secondary calcite prevents the development of a continuous palaeoclimate record from Swartkrans.

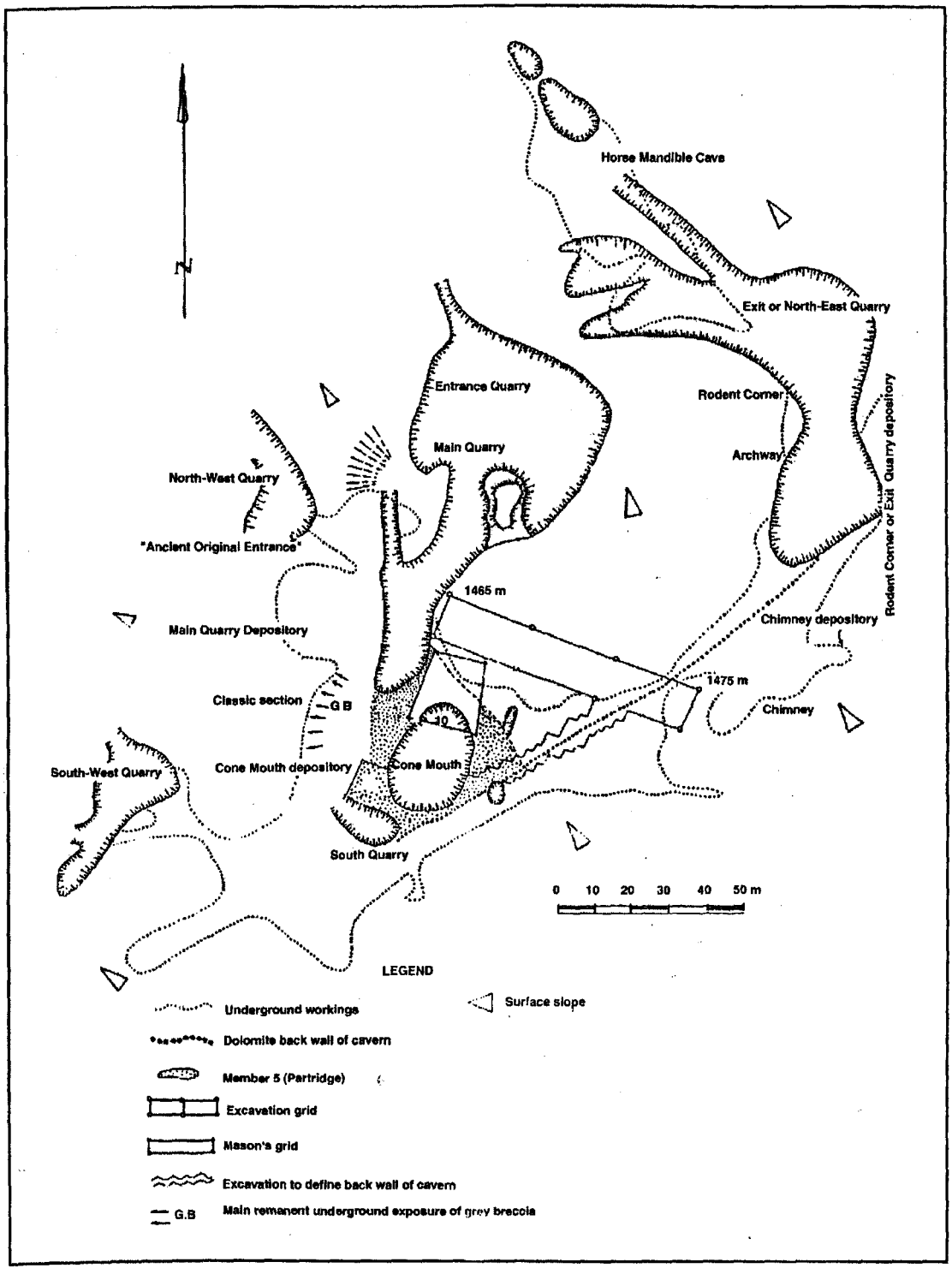

Appendix 1d. – Map of the Makapansgat Limeworks site (after Maguire *et al.*, 1980, *Palaeontolgia Africana* **23**: 75-98); site locations as referred to in the text. See Figure 4.1. for location of the Limeworks within the Makapansgat Valley. The Collapsed Cone flowstone (discussed in Chapters 3, 4, 5 & 7; see Appendix 1b) outcrops on the mined floor to the north-west of the Cone Mouth.

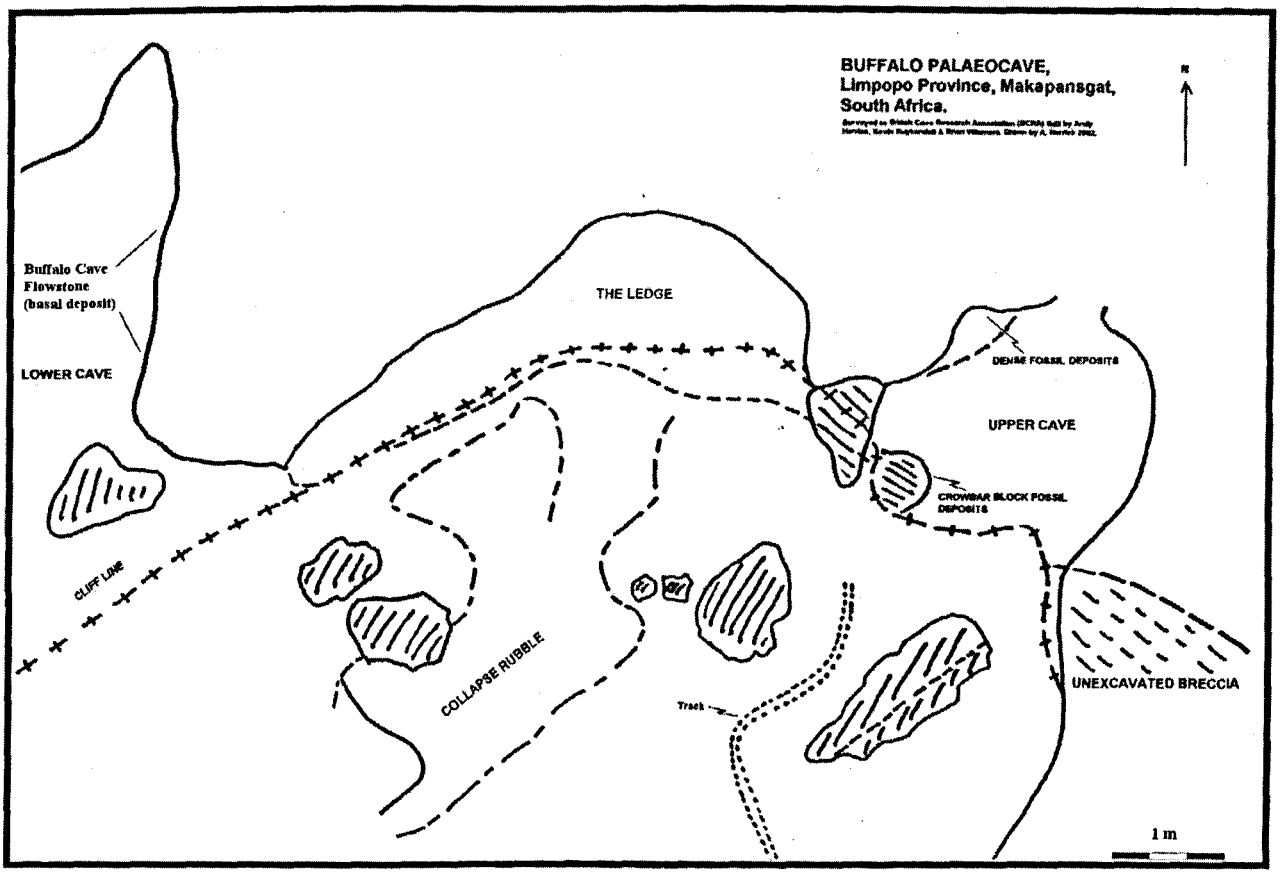

Appendix 1e. – Map of Buffalo Cave, Makapansgat Valley (after Herries 2003, Unpublished PhD Thesis, University of Liverpool). See Figure 4.1. for location of Buffalo Cave within the Makapansgat Valley.

Appendix 2. – Stable isotope and trace element data (also on attached disk).

Appendix 2.1. Stable isotope and trace element data for speleothems described in Chapter 3.

Sample	$\delta^{13}C$ ‰ PDB	$\delta^{18}O$ ‰ PDB	1000 Mg/Ca molar ratio	1000 Sr/Ca molar ratio
MAK OAE B2 - 1	-6.84	-5.20	19.15	0.103
MAK OAE B2 - 2	-7.01	-5.12	18.79	0.134
MAK OAE B2 - 3	-7.10	-5.08	25.41	0.104
MAK OAE B2 - 4	-7.53	-5.00	24.60	0.036
MAK OAE B2 - 5	-7.45	-5.46	20.57	0.070
MAK OAE B2 - 6	-7.72	-5.49	25.06	0.052
MAK OAE B2 - 7	-7.54	-5.55	18.79	0.043
MAK OAE B2 - 8	-7.44	-5.40	19.42	0.045
MAK OAE B2 - 9	-7.43	-5.62	19.37	0.061
MAK OAE B2 - 10	-7.40	-5.51	18.20	0.068
MAK OAE B2 - 11	-7.56	-5.14	17.05	0.019
MAK OAE B2 - 12	-7.60	-5.00	17.10	0.013
MAK OAE B2 - 13	-7.55	-5.25	17.98	0.030
MAK OAE B2 - 14	-7.58	-5.25	18.15	0.026
MAK OAE B2 - 15	-7.59	-5.16	17.31	0.019
MAK OAE B2 - 16	-7.26	-5.45	20.73	0.052
MAK OAE B2 - 17	-7.21	-5.35	20.31	0.053
MAK OAE B2 - 18	-7.30	-5.41	19.49	0.043
MAK OAE B2 - 19	-7.62	-5.07	16.36	0.012
MAK OAE B2 - 20	-7.53	-5.00	15.85	0.016
MAK LC04 - 1	-5.96	-4.77	1.38	0.175
MAK LC04 - 2	-6.14	-4.90	1.28	0.178
MAK LC04 - 3	-6.12	-4.77	1.24	0.180
MAK LC04 - 4	-6.14	-4.82	1.30	0.167
MAK LC04 - 5	-6.24	-4.85	1.26	0.140
MAK LC04 - 6	-6.25	-4.72	1.26	0.140
MAK LC04 - 7	-6.23	-4.69	1.23	0.138
MAK LC04 - 8	-6.37	-4.77	1.70	0.157
MAK LC04 - 9	-6.41	-4.71	1.46	0.161
MAK LC04 - 10	-6.36	-4.73	1.41	0.167
SWART HR D4 - 1	-1.26	-5.86	9.95	0.081
SWART HR D4 - 2	-1.54	-5.80	8.58	0.082
SWART HR D4 - 3	-1.77	-4.95	5.63	0.201
SWART HR D4 - 4	-4.57	-5.33	41.76	0.009
SWART HR D4 - 5	-4.22	-5.41	42.65	0.010
SWART HR D4 - 6	-4.35	-5.46	42.46	0.010
SWART HR D4 - 7	-5.26	-5.47	38.49	0.011
SWART HR D4 - 8	-4.44	-5.20	43.43	0.025
SWART HR D4 - 9	-2.46	-5.14	32.18	0.024

SWART HR D4 - 10	-2.42	-5.18	25.60	0.017
SWART HR D4 - 11	-2.02	-5.09	19.66	0.027
SWART HR D4 - 12	-2.01	-4.76	21.61	0.035
SWART HR D4 - 13	-1.60	-4.78	33.50	0.030
BUFF A - 71			37.49	0.024
BUFF A - 72	-3.49	-4.25	55.06	0.031
BUFF A - 73			54.82	0.033
BUFF A - 74	-3.62	-4.33	57.29	0.034
BUFF A - 75	-3.85	-4.39	56.29	0.052
BUFF A - 76	-3.91	-4.34	44.05	0.050
BUFF A - 77	-3.42	-4.16	54.19	0.047
BUFF A - 78	-3.81	-4.47	58.60	0.082
BUFF A - 79	-3.89	-4.08	61.36	0.042
BUFF A - 80	-3.83	-4.11	55.34	0.032
BUFF A - 81	-4.16	-4.23	58.66	0.035
BUFF A - 82	-3.80	-3.79	58.61	0.034
BUFF A - 83	-4.30	-4.16	52.88	0.030
BUFF A - 84	-4.08	-4.18	49.65	0.032
BUFF A - 85	-4.24	-4.37	51.20	0.033
BUFF A - 86	-4.39	-3.95	48.78	0.031
BUFF A - 87	-4.48	-3.80	49.96	0.032
BUFF A - 88	-4.38	-3.65	54.78	0.036
BUFF A - 89	-4.63	-3.71	56.16	0.038
BUFF A - 90	-4.36	-4.05	38.40	0.027
BUFF A - 91	-4.28	-3.36	26.09	0.025
BUFF C1 - 137	-4.57	-5.46	45.20	0.033
BUFF C1 - 138.5	-5.79	-5.74	42.55	0.031
BUFF C1 - 140	-4.64	-4.25	39.21	0.042
BUFF C2 - 141.5	-4.59	-4.89	62.80	0.042
BUFF C2 - 143	-3.48	-5.37	55.75	0.034
BUFF C2 - 144.5	-3.14	-5.47	56.82	0.032
BUFF C2 - 146	-2.85	-5.17	52.15	0.029
BUFF C2 - 147.5	-3.07	-5.72	49.04	0.028
BUFF C2 - 149	-3.61	-5.65	54.72	0.029
BUFF C2 - 150.5	-3.49	-5.55	46.78	0.027
BUFF C2 - 152	-3.35	-5.79	46.75	0.030
BUFF C2 - 153.5	-4.22	-5.88	48.14	0.026
BUFF C2 - 155	-4.03	-5.57	49.43	0.029
MAK M1 CC A1 - 1			38.47	0.010
MAK M1 CC A1 - 2			42.45	0.010
MAK M1 CC A1 - 3			43.64	0.010
MAK M1 CC A1 - 4			43.63	0.010
MAK M1 CC A1 - 5			43.86	0.010
MAK M1 CC A1 - 6			45.13	0.010
MAK M1 CC A1 - 7	-7.92	-5.31	45.77	0.010
MAK M1 CC A1 - 8	-7.22	-5.39	46.16	0.010
MAK M1 CC A1 - 9	-7.76	-5.17	47.68	0.010
MAK M1 CC A1 - 10	-7.94	-4.89	48.76	0.010

MAK M1 CC A1 - 11	-8.18	-5.46	47.72	0.009
MAK M1 CC A1 - 12	-8.11	-5.44	47.78	0.009
MAK M1 CC A1 - 13	-7.70	-5.34	42.94	0.009
MAK M1 CC A1 - 14	-8.07	-5.36	41.66	0.009
MAK M1 CC A1 - 15	-8.09	-5.43	41.77	0.009
MAK M1 CC A1 - 16	-7.88	-5.36	42.90	0.012
MAK M1 CC A1 - 17	-7.85	-5.28	44.49	0.010
MAK M1 CC A1 - 18	-7.83	-5.31	41.27	0.010
MAK M1 CC A1 - 19	-7.79	-5.36	43.08	0.009
MAK M1 CC A1 - 20	-7.93	-5.47	49.33	0.010
MAK M1 CC A1 - 21	-7.93	-5.54	44.39	0.008
MAK M1 CC A1 - 22	-7.90	-5.54	42.31	0.007
MAK M1 CC A1 - 23	-8.04	-5.68	39.01	0.009
MAK M1 CC A1 - 24	-8.20	-5.60	36.70	0.009
MAK M1 CC A1 - 25	-8.33	-5.75	38.05	0.009
MAK M1 CC A1 - 26	-8.13	-6.06	37.02	0.008
MAK M1 CC A1 - 27	-7.87	-6.12	35.40	0.008
MAK M1 CC A1 - 28	-7.97	-5.87	33.87	0.008
MAK M1 CC A1 - 29	-7.88	-5.68	35.65	0.009
MAK M1 CC A1 - 30	-7.82	-5.83	37.29	0.008
MAK M1 CC A1 - 31			36.43	0.008
MAK M1 CC A1 - 32			38.05	0.008
MAK M1 CC A1 - 33			40.33	0.009
MAK M1 CC A1 - 34			40.07	0.008
MAK M1 CC A1 - 35			39.72	0.008
MAK M1 CC A1 - 36			39.58	0.008
MAK M1 CC A1 - 37			38.59	0.008
MAK M1 CC A1 - 38			37.76	0.007
MAK M1 CC A1 - 39			40.09	0.008
MAK M1 CC A1 - 40			38.93	0.007
MAK AM01 - 1	-7.31	-4.93	46.54	0.006
MAK AM01 - 2	-7.23	-4.86		
MAK AM01 - 3	-7.74	-4.99	44.82	0.006
MAK AM01 - 4	-7.02	-5.14	38.35	0.006
MAK AM01 - 5	-7.17	-5.28	42.80	0.005
MAK AM01 - 6	-7.26	-5.34	44.25	0.004
MAK AM01 - 7	-7.39	-5.05	44.85	0.005
MAK AM01 - 8	-7.90	-5.48	46.17	0.006
MAK AM01 - 9	-7.58	-5.28	41.57	0.005
MAK AM01 - 10	-7.48	-5.26	46.90	0.005
MAK AM01 - 11	-7.77	-5.00		
MAK AM01 - 12	-7.83	-5.55		
MAK AM01 - 13	-7.62	-5.35		
MAK AM01 - 14	-7.57	-5.20		
MAK AM01 - 15	-7.26	-4.92		
MAK AM01 - 16	-7.22	-5.32		
MAK AM01 - 17	-7.21	-4.85		
MAK AM01 - 18	-7.51	-4.69		
MAK AM01 - 19	-6.66	-5.51		
MAK AM01 - 20	-7.41	-5.31		

MAK AM01 - 21	-7.27	-5.27		
MAK AM01 - 22	-6.94	-4.83		
MAK AM01 - 23	-6.66	-5.55		
MAK AM01 - 24	-6.57	-5.41		
MAK AM01 - 25	-6.86	-4.92		
MAK AM01 - 26	-7.61	-5.17		
MAK AM01 - 27	-7.48	-4.89		
MAK H03 - 1	-1.27	-4.88		
MAK H03 - 2	-1.16	-4.88		
MAK H03 - 3	-0.82	-4.97		
MAK H03 - 4	-1.78	-4.67		
MAK H03 - 5	-1.51	-4.80		
MAK H03 - 6	-1.87	-4.75		
MAK H03 - 7	-1.79	-4.73		
MAK H03 - 8	-2.30	-4.92		
MAK H03 - 9	-2.29	-4.84		
MAK H03 - 10	-2.32	-5.06		
MAK H03 - 11	-1.70	-5.30		
MAK H03 - 12	-1.72	-5.70		
MAK H03 - 13	-1.86	-4.80		
MAK H03 - 14	-2.33	-5.16		
MAK H03 - 15	-1.69	-5.14		
MAK H03 - 16	-1.31	-4.58		
MAK H03 - 17	-1.75	-4.89		
MAK H03 - 18	-4.19	-4.30		
MAK H03 - 19	-4.23	-4.36		
MAK LC03 - 29	-5.63	-2.15		
MAK LC03 - 30	-6.41	-3.62		
MAK LC03 - 31	-6.31	-4.17		
MAK LC03 - 32	-6.48	-3.82		
MAK LC03 - 33	-7.08	-4.85		
MAK LC03 - 34	-7.09	-4.55		
MAK LC03 - 35	-7.13	-4.07		
MAK LC03 - 36	-7.69	-4.70		
MAK LC03 - 37	-7.50	-4.80		
MAK M1 NA - 1	-8.26	-6.05		
MAK M1 NA - 2	-8.41	-6.01		
MAK M1 NA - 3	-8.57	-6.00		
MAK M1 EQ - 1	-7.94	-5.69		
MAK M1 EQ - 2	-7.79	-5.57		
RAINB - 1	-3.05	-4.89		
RAINB - 2	-4.37	-4.89		
RAINB - 3	-4.54	-5.35		
RAINB - 4	-3.71	-4.82		
RAINB - 5	-3.46	-5.43		
RAINB - 6	-3.15	-4.90		

RAINB - 7	-2.90	-4.57		
RAINB - 8	-3.47	-5.11		
RAINB - 9	-2.63	-4.89		
RAINB - 10	-5.39	-4.62		
RAINB - 11	-2.99	-4.39		
STERK 20 - 1	-1.60	-5.04		
STERK 20 - 2	-0.90	-5.09		
STERK 20 - 3	-1.22	-5.06		
STERK 20 - 4	-1.98	-4.92		
STERK 20 - 6	-2.22	-5.14		
STERK 20 - 7	-2.89	-4.86		
STERK 20 - 8	-3.32	-4.48		
STERK 20 - 9	-3.49	-4.89		
STERK 20 - 10	-3.36	-4.60		
STERK 20 - 11	-3.30	-4.49		
STERK 21 - 1	-3.13	-4.37		
STERK 21 - 3	-3.50	-4.88		
STERK 21 - 4	-3.39	-4.96		
STERK 21 - 5	-3.30	-4.76		
STERK 21 - 6	-3.92	-4.33		
STERK 22 - 1	-0.59	-4.21		
STERK 22 - 2	0.25	-4.21		
STERK 22 - 3	-1.00	-4.36		
STERK 22 - 4	-1.01	-4.35		
STERK 22 - 5	-0.79	-4.83		
STERK 22 - 6	-0.79	-4.41		
STERK 22 - 7	-0.78	-5.23		
STERK 22 - 8	-0.74	-5.19		
STERK 22 - 9	0.88	-4.29		
STERK 22 - 10	0.44	-4.65		
STERK 16 - 1	-5.00	-5.46		
STERK 16 - 2	-4.50	-5.64		
STERK 16 - 3	-5.19	-5.40		
STERK 16 - 4	-5.27	-6.68		
STERK 16 - 5	-5.39	-5.55		
DRIM D1 - 1	-4.27	-6.20		
DRIM D1 - 2	-3.69	-6.36		
DRIM D1 - 3	-4.25	-6.30		
DRIM D1 - 4	-4.71	-6.34		
DRIM D1 - 5	-4.45	-5.97		
DRIM D1 - 6	-4.42	-5.83		
DRIM D1 - 7	-5.07	-5.91		
DRIM D1 - 8	-5.96	-5.88		
DRIM D1 - 9	-5.47	-5.44		
DRIM D1 - 10	-3.76	-5.28		
DRIM D1 - 11	-4.16	-5.50		

DRIM D1 - 12	-3.85	-5.40		
DRIM D1 - 13	-4.03	-5.34		
DRIM D1 - 14	-4.46	-5.21		
DRIM D1 - 15	-5.41	-6.28		
DRIM D1 - 16	-5.15	-6.24		
DRIM D1 - 17	-5.12	-6.19		
DRIM D1 - 18	-5.34	-6.21		
DRIM D1 - 19	-4.70	-6.11		
DRIM D1 - 20	-4.33	-6.23		
DRIM D1 - 21	-4.65	-6.33		
DRIM D1 - 22	-4.26	-5.92		
DRIM D1 - 23	-4.69	-6.33		
DRIM D1 - 24	-4.87	-6.44		
DRIM D1 - 25	-4.27	-6.24		
DRIM D1 - 26	-4.01	-6.36		
DRIM D1 - 27	-3.82	-6.24		
DRIM D1 - 28	-3.50	-6.03		
DRIM D1 - 29	-4.20	-6.14		
DRIM D1 - 30	-5.48	-5.83		
GOND GB01 - 1	1.32	-3.39		
GOND GB01 - 2	0.86	-3.47		
GOND GB01 - 3	0.82	-4.56		
GOND GB01 - 4	-1.25	-4.98		
GOND GB01 - 5	0.74	-3.73		
GOND GB01 - 6	0.71	-4.08		
GOND GB01 - 7	0.31	-5.03		
GOND GB01 - 8	0.00	-5.34		
GOND GB01 - 9	-1.12	-5.32		
GOND GB01 - 10	0.66	-4.06		
GOND GB01 - 11	2.09	-3.69		
GOND GB01 - 12	2.19	-3.87		
GOND GB01 - 13	1.60	-3.88		
GOND GB01 - 14	1.03	-3.63		
GOND GB01 - 15	1.54	-3.81		
GOND GB01 - 16	1.79	-3.70		
GOND GB01 - 17	3.17	-3.27		
GOND GB01 - 18	2.47	-3.51		
GOND GB01 - 19	1.39	-4.39		
GOND GB01 - 20	-1.31	-4.42		
GOND GB01 - 21	2.24	-2.72		
GOND GB01 - 22	4.21	-1.90		
GOND GB01 - 23	4.20	-2.42		
GOND GB01 - 24	5.15	-2.23		
GOND GB01 - 25	5.23	-2.78		
GOND GB01 - 26	2.80	-3.52		
SWART HR A1 - 1	-2.49	-5.45		
SWART HR A1 - 2	-2.03	-4.74		
SWART HR A1 - 3	-2.11	-4.80		
SWART HR A1 - 4	-3.31	-4.97		

SWART HR A1 - 5	-3.04	-4.93		
SWART HR A1 - 6	-1.39	-4.85		
SWART HR A1 - 7	-2.68	-5.17		
SWART HR A1 - 8	-2.20	-5.61		
SWART HR A1 - 9	-2.30	-5.70		
SWART HR A1 - 10	-1.54	-5.43		
SWART HR A1 - 11	-0.90	-4.71		
SWART HR A1 - 12	0.81	-5.26		
SWART HR A1 - 13	0.03	-5.18		
SWART HR A1 - 14	-0.02	-5.15		
SWART HR A1 - 15	0.40	-5.20		
SWART HR A2 - 16	-1.49	-5.10		
SWART HR A2 - 17	-1.48	-4.85		
SWART HR A2 - 18	-0.57	-5.37		
SWART HR A2 - 19	-2.20	-5.55		
SWART HR A2 - 20	-0.84	-5.59		
SWART HR A2 - 21	-0.76	-5.38		
SWART HR A2 - 22	0.15	-4.88		
SWART HR A2 - 23	-0.87	-4.93		
SWART HR A2 - 24	-1.62	-4.59		
SWART HR A2 - 25	-1.05	-5.54		
SWART HR A2 - 26	-2.50	-5.73		
SWART HR A2 - 27	-1.04	-5.32		
SWART HR A2 - 28	0.18	-5.41		
SWART HR A2 - 29	-2.42	-5.04		
SWART HR A2 - 30	-1.96	-5.19		
SWART HR A2 - 31	-2.79	-5.76		
SWART HR A3 - 32	-1.85	-5.42		
SWART HR A3 - 33	-2.02	-4.97		
SWART HR A3 - 34	-2.77	-5.09		
SWART HR A3 - 35	-1.49	-5.18		
SWART HR A3 - 36	-3.93	-5.56		
SWART HR A3 - 37	-3.22	-5.72		
SWART HR A3 - 38	-3.18	-5.12		
SWART HR A3 - 39	-1.99	-5.30		
SWART HR A3 - 40	-1.35	-4.60		
SWART HR A3 - 41	-3.25	-5.39		
SWART HR A3 - 42	-3.05	-5.50		
SWART HR A3 - 43	-3.38	-5.85		
SWART HR A3 - 44	-2.94	-5.97		
SWART HR A3 - 45	-3.36	-6.24		
SWART HR A3 - 46	-3.11	-5.94		
SWART HR A3 - 47	-3.60	-5.53		
SWART HR A3 - 48	-3.51	-5.46		
SWART HR A3 - 49	-3.62	-5.86		
SWART HR A3 - 50	-3.79	-6.22		
SWART HR B - 51	-3.82	-6.06		
SWART HR B - 52	-3.59	-6.07		
SWART HR B - 53	-3.37	-6.24		
SWART HR B - 54	-2.83	-5.87		
SWART HR B - 55	-2.53	-5.92		

SWART HR B - 56	-3.34	-5.65		
SWART HR B - 57	-2.83	-5.86		
SWART HR B - 58	-2.62	-5.68		
SWART HR B - 59	-2.68	-5.77		
SWART HR B - 60	-2.13	-5.84		
SWART HR B - 61	-3.77	-4.92		
SWART HR B - 62	-4.21	-5.24		
SWART HR B - 63	-2.17	-4.78		
SWART HR B - 64	-1.60	-5.12		
SWART HR B - 65	-1.21	-5.01		
SWART HR B - 66	-1.96	-4.59		
SWART HR B - 67	-2.00	-4.81		
SWART HR B - 68	-1.44	-5.12		
SWART HR B - 69	-1.68	-5.35		
SWART HR B - 70	-1.05	-5.42		
SWART HR B - 71	-1.70	-5.08		
SWART HR B - 72	-1.87	-5.70		
SWART HR B - 73	-1.68	-5.44		
SWART HR B - 74	-1.80	-5.93		
SWART HR B - 75	-2.28	-5.91		
SWART HR C - 76	-2.17	-5.73		
SWART HR C - 77	-1.29	-5.80		
SWART HR C - 78	-1.20	-5.67		
SWART HR C - 79	-0.93	-5.55		
SWART HR C - 80	-1.02	-5.48		
SWART HR C - 81	-1.32	-5.58		
SWART HR C - 82	-1.30	-5.37		
SWART HR C - 83	-1.61	-5.51		
SWART HR C - 84	-2.70	-5.33		
SWART HR C - 85	-2.34	-5.87		
SWART HR C - 86	-2.21	-5.59		
SWART HR C - 87	-2.57	-5.28		
SWART HR C - 88	-2.62	-5.61		
SWART HR C - 89	-2.49	-5.84		
SWART HR C - 90	-2.12	-5.14		
SWART HR C - 91	-2.12	-4.93		
SWART HR C - 92	-1.26	-4.86		

Appendix 2.2. - Buffalo Cave flowstone trace element and stable isotope depth series (Figure 4.6.)

Sample	$\delta^{13}C$ ‰ PDB	$\delta^{18}O$ ‰ PDB	1000 Mg/Ca molar ratio	1000 Sr/Ca molar ratio	Distance from top of flowstone (cms)
BUFF D - 156.5	-4.86	-4.82	70.89	0.060	63.5
BUFF D - 158	-3.44	-5.53	57.89	0.038	65
BUFF D - 159.5	-3.01	-5.53	58.90	0.033	66.5
BUFF D - 161	-2.85	-5.40	49.37	0.031	68
BUFF D - 162.5	-2.90	-5.59	51.45	0.031	69.5
BUFF D - 164	-3.28	-5.50	52.96	0.028	71
BUFF D - 165.5	-3.32	-5.36	49.99	0.027	72.5
BUFF D - 167	-3.93	-5.31	54.88	0.028	74
BUFF D - 168.5	-4.78	-4.98	56.99	0.038	75.5
BUFF D - 170	-5.07	-4.54	65.00	0.064	77
BUFF D - 171.5	-5.12	-3.92	29.40	0.027	78.5
BUFF DD - 173	-5.08	-4.32	38.54	0.029	80
BUFF DD - 174.5	-4.96	-4.30	36.49	0.024	81.5
BUFF DD - 176	-5.08	-4.63	39.78	0.029	83
BUFF DD - 177.5	-4.46	-4.80	44.10	0.035	84.5
BUFF DD - 179	-4.09	-4.87	42.83	0.040	86
BUFF DD - 180.5	-3.69	-5.23	42.04	0.042	87.5
BUFF DD - 182	-3.46	-5.81	45.50	0.044	89
BUFF DD - 183.5	-3.92	-5.14	42.19	0.040	90.5
BUFF DD - 185	-4.52	-4.99	39.62	0.035	92
BUFF DD - 186.5	-5.20	-5.46	37.28	0.036	93.5
BUFF DEF - 188	-4.83	-5.03	39.11	0.035	95
BUFF DEF - 189.5	-4.40	-5.04	44.50	0.040	96.5
BUFF DEF - 191	-4.23	-5.35	40.71	0.037	98
BUFF DEF - 192.5	-3.92	-5.92	42.22	0.035	99.5
BUFF DEF - 194	-4.03	-5.19	40.55	0.034	101
BUFF DG - 195.5	-3.92	-5.45	42.69	0.039	102.5
BUFF DG - 197	-4.04	-5.19	42.51	0.038	104
BUFF DG - 198.5	-4.26	-6.46	40.86	0.033	105.5
BUFF DG - 200	-4.19	-5.23	41.68	0.032	107
BUFF DG - 201.5	-4.14	-4.95	38.85	0.035	108.5
BUFF DG - 203	-3.69	-4.41	42.50	0.035	110
BUFF DG - 204.5	-3.70	-5.85	45.45	0.038	111.5
BUFF DG - 206	-3.95	-5.30	30.89	0.028	113
BUFF DG - 207.5	-3.48	-5.19	46.91	0.036	114.5
BUFF E - 209	-3.76	-5.82	39.89	0.036	116
BUFF E - 210.5	-4.04	-4.97	36.40	0.034	117.5
BUFF E - 212	-4.15	-4.45	25.06	0.020	119
BUFF E - 213.5	-4.24	-4.58	23.93	0.021	120.5
BUFF E - 215	-4.06	-4.52	24.83	0.020	122
BUFF E - 216.5	-3.96	-4.59	28.23	0.023	123.5
BUFF E - 218	-3.84	-4.92	31.94	0.026	125
BUFF E - 219.5	-3.55	-5.08	39.57	0.032	126.5

BUFF E - 221	-4.00	-4.81	44.18	0.035	128
BUFF E - 222.5	-4.01	-5.36	48.12	0.038	129.5
BUFF E - 224	-4.75	-4.83	49.15	0.040	131
BUFF E - 225.5	-4.47	-5.11	50.05	0.042	132.5
BUFF E - 227	-4.48	-4.62	57.08	0.043	134
BUFF E - 228.5	-5.44	-4.52	63.90	0.056	135.5
BUFF E - 230	-4.83	-4.04	70.81	0.074	137
BUFF E - 231.5	-5.43	-4.51	76.01	0.076	138.5
BUFF E - 233	-5.30	-5.00	55.38	0.041	140
BUFF E - 234.5	-4.54	-5.15	44.35	0.030	141.5
BUFF E - 236	-4.04	-5.27	51.03	0.024	143
BUFF E - 237.5	-6.94	-3.77	65.37	0.060	144.5
BUFF E - 239	-6.07	-4.29	68.43	0.056	146
BUFF E - 240.5	-4.31	-5.80	47.75	0.025	147.5
BUFF F - 242	-3.95	-5.59	46.82	0.028	149
BUFF F - 243.5	-3.50	-5.23	49.46	0.028	150.5
BUFF F - 245	-6.65	-3.90	84.74	0.049	152
BUFF F - 246.5	-5.72	-4.11	60.31	0.040	153.5
BUFF F - 248	-4.99	-4.60	74.56	0.043	155
BUFF F - 249.5	-2.73	-5.00	59.79	0.036	156.5
BUFF F - 251	-3.08	-5.11	48.80	0.029	158
BUFF F - 252.5	-6.38	-4.59	55.02	0.026	159.5
BUFF F - 254	-6.69	-4.05	72.19	0.028	161
BUFF F - 255.5	-6.71	-3.96	72.56	0.036	162.5
BUFF F - 257	-7.13	-4.65	45.88	0.014	164
BUFF F - 258.5	-6.52	-3.87	89.18	0.054	165.5
BUFF F - 260	-6.65	-4.47	53.76	0.021	167
BUFF F - 261.5	-6.87	-4.01	61.31	0.031	168.5
BUFF F - 263	-6.61	-3.95	72.75	0.050	170
BUFF F - 264.5	-6.21	-3.88	60.55	0.037	171.5
BUFF H - 266	-5.82	-4.50	57.87	0.015	173
BUFF H - 267.5	-5.87	-4.14	65.78	0.024	174.5
BUFF H - 269	-6.91	-4.19	54.84	0.017	176
BUFF H - 270.5	-6.29	-4.04	72.86	0.032	177.5

Appendix 2.3. Buffalo Cave growth layer analyses and duplicate depth series – Chapter. 4

Growth Layer tests (Figure 4.4.)

Sample	$\delta^{13}C$ ‰ PDB	$\delta^{18}O$ ‰ PDB	Sample	$\delta^{13}C$ ‰ PDB	$\delta^{18}O$ ‰ PDB
(a)			(b)		
BUFF A GL1	-4.00	-4.37	CC A1-GL1	-8.14	-5.12
BUFF A GL2	-3.91	-3.58	CC A1-GL2	-8.24	-5.32
BUFF A GL3	-3.91	-4.39	CC A1-GL3	-8.33	-5.21
BUFF A GL4	-3.95	-4.43	CC A1-GL4	-8.34	-5.12
BUFF A GL5	-3.79	-4.19	CC A1-GL5	-8.26	-5.16
BUFF A GL6	-3.67	-4.00	CC A1-GL6	-8.38	-5.18
BUFF A GL7	-3.61	-3.92	CC A1-GL7	-8.38	-5.33
BUFF A GL8	-3.45	-3.86	CC A1-GL8	-8.13	-5.10
			CC A1-GL9	-8.08	-5.08

Depth Series A - duplicate analyses (Figure 4.5a)

Sample	$\delta^{13}C$ ‰ PDB	$\delta^{18}O$ ‰ PDB	Distance from top of flowstone (cms)	Sample	$\delta^{13}C$ ‰ PDB	$\delta^{18}O$ ‰ PDB
BUFF C2-140.5	-4.74	-4.60	63.5	BUFF D-156.5	-4.86	-4.82
BUFF C2-141	-4.47	-4.74	64	BUFF D-157	-4.65	-4.87
BUFF C2-141.5	-4.59	-4.89	64.5	BUFF D-157.5	-4.40	-5.21
BUFF C2-142	-3.97	-5.35	65	BUFF D-158	-3.44	-5.53
BUFF C2-142.5	-3.62	-5.43	65.5	BUFF D-158.5	-3.30	-5.44
BUFF C2-143	-3.48	-5.37	66	BUFF D-159	-2.93	-5.53
BUFF C2-143.5	-3.24	-5.60	66.5	BUFF D-159.5	-3.01	-5.53
BUFF C2-144	-2.83	-5.34	67	BUFF D-160	-2.89	-5.53
BUFF C2-144.5	-3.14	-5.47	67.5	BUFF D-160.5	-2.99	-5.68
BUFF C2-145	-2.92	-5.32	68	BUFF D-161	-2.85	-5.40
BUFF C2-145.5	-2.97	-5.62	68.5	BUFF D-161.5	-2.83	-5.04
BUFF C2-146	-2.85	-5.17	69	BUFF D-162	-3.15	-5.45
BUFF C2-146.5	-2.95	-5.25	69.5	BUFF D-162.5	-2.90	-5.59
BUFF C2-147	-3.33	-5.53	70	BUFF D-163	-3.10	-5.44
BUFF C2-147.5	-3.07	-5.72	70.5	BUFF D-163.5	-3.50	-5.39
BUFF C2-148	-3.00	-5.46	71	BUFF D-164	-3.28	-5.50
BUFF C2-148.5	-3.22	-5.76	71.5	BUFF D-164.5	-3.52	-5.27
BUFF C2-149	-3.61	-5.65	72	BUFF D-165	-3.37	-5.47
BUFF C2-149.5	-3.40	-5.65	72.5	BUFF D-165.5	-3.32	-5.36
BUFF C2-150	-3.36	-5.69	73	BUFF D-166	-3.31	-5.72
BUFF C2-150.5	-3.49	-5.55	73.5	BUFF D-166.5	-4.18	-5.64
BUFF C2-151	-3.38	-5.83	74	BUFF D-167	-3.93	-5.31
BUFF C2-151.5	-3.37	-5.88	74.5	BUFF D-167.5	-4.50	-5.25
BUFF C2-152	-3.35	-5.79	75	BUFF D-168	-4.78	-4.86
BUFF C2-152.5	-3.30	-5.91	75.5	BUFF D-168.5	-4.78	-4.98

BUFF C2-153	-4.37	-5.72		76		BUFF D-169	-4.82	-4.52
BUFF C2-153.5	-4.22	-5.88		76.5		BUFF D-169.5	-5.01	-4.88
BUFF C2-154	-4.32	-5.56		77		BUFF D-170	-5.07	-4.54
BUFF C2-154.5	-3.90	-5.33		77.5		BUFF D-170.5	-5.24	-4.60
BUFF C2-155	-4.03	-5.57		78		BUFF D-171	-5.20	-4.10
BUFF D-155.5	-5.02	-4.92		78.5		BUFF D-171.5	-5.12	-3.92
BUFF D-156	-4.28	-4.38		79		BUFF D-172	-5.13	-4.36

Depth Series B - duplicate analyses (Figure 4.5b)

Sample	$\delta^{13}C$ ‰ PDB	$\delta^{18}O$ ‰ PDB	Distance from top of flowstone (cms)	Sample	$\delta^{13}C$ ‰ PDB	$\delta^{18}O$ ‰ PDB
BUFF L-290.5	-5.47	-5.11	216.5	BUFF N1-309.5	-5.64	-5.09
BUFF L-291	-5.68	-4.92	217	BUFF N1-310	-5.68	-4.92
BUFF L-291.5	-5.32	-5.05	217.5	BUFF N1-310.5	-5.38	-4.58
BUFF L-292	-5.12	-4.83	218	BUFF N1-311	-5.35	-4.51
BUFF L-292.5	-5.04	-4.87	218.5	BUFF N1-311.5	-4.90	-4.43
BUFF L-293	-4.55	-4.49	219	BUFF N1-312	-5.02	-4.16
BUFF L-293.5	-3.88	-4.23	219.5	BUFF N1-312.5	-4.03	-4.32
BUFF L-294	-4.06	-4.37	220	BUFF N1-313	-3.86	-4.22
BUFF L-294.5	-5.16	-4.28	220.5	BUFF N1-313.5	-4.45	-4.33
BUFF L-295	-4.57	-4.23	221	BUFF N1-314	-4.98	-4.78
BUFF L-295.5	-5.79	-4.45	221.5	BUFF N1-314.5	-5.10	-4.90
BUFF L-296	-5.12	-4.60	222	BUFF N1-315	-5.24	-5.06
BUFF L-296.5	-5.10	-4.62	222.5	BUFF N1-315.5	-5.50	-4.98
BUFF L-297	-5.53	-4.80	223	BUFF N2-316	-5.12	-4.77
BUFF L-297.5	-5.39	-5.09	223.5	BUFF N2-316.5	-5.27	-5.00
BUFF M-298	-5.35	-4.87	224	BUFF N2-317	-5.78	-4.92
BUFF M-298.5	-5.15	-4.80	224.5	BUFF N2-317.5	-5.32	-4.92
BUFF M-299	-5.31	-4.47	225	BUFF N2-318	-5.07	-4.64
BUFF M-299.5	-7.47	-4.40	225.5	BUFF N2-318.5	-5.77	-4.98
BUFF M-300	-6.73	-4.78	226	BUFF N2-319	-7.22	-4.42
BUFF M-300.5	-6.68	-4.91	226.5	BUFF N2-319.5	-6.74	-4.78
BUFF M-301	-6.02	-4.54	227	BUFF N2-320	-6.11	-4.61
BUFF M-301.5	-6.97	-4.50	227.5	BUFF N2-320.5	-6.33	-4.29
BUFF M-302	-6.46	-4.63	228	BUFF N3-321	-6.40	-4.57
BUFF M-302.5	-6.16	-5.17	228.5	BUFF N3-321.5	-6.19	-5.33
BUFF M-303	-5.77	-4.69	229	BUFF N3-322	-5.65	-4.93
BUFF M-303.5	-6.54	-4.27	229.5	BUFF N3-322.5	-6.87	-4.33
BUFF M-304	-5.96	-4.53	230	BUFF N3-323	-6.01	-4.48
BUFF M-304.5	-5.91	-4.40	230.5	BUFF N3-323.5	-5.92	-4.36
BUFF M-305	-5.91	-4.29	231	BUFF N3-324	-6.34	-4.49
BUFF M-305.5	-6.34	-4.60	231.5	BUFF N3-324.5	-6.41	-4.75
BUFF M-306	-6.07	-4.65	232	BUFF N3-325	-6.09	-4.77
BUFF M-306.5	-5.98	-5.03	232.5	BUFF N4-325.5	-6.24	-4.62
BUFF M-307	-5.98	-4.61	233	BUFF N4-326	-6.02	-4.71
BUFF M-307.5	-6.13	-4.53	233.5	BUFF N4-326.5	-6.22	-4.84
BUFF M-308	-6.30	-4.66	234	BUFF N4-327	-6.46	-4.43

Appendix 2.4. Buffalo Cave and Collapsed Cone flowstones depth series (Figures 5.2 & 5.3.)

Sample	$\delta^{13}C$ ‰ PDB	$\delta^{18}O$ ‰ PDB	Distance from top of flowstone (cms)
BUFF A-1	-5.13	-4.21	0
BUFF A-3	-3.81	-4.47	0.5
BUFF A-5	-4.11	-4.71	1
BUFF A-7	-4.18	-4.70	1.5
BUFF A-9	-4.08	-4.96	2
BUFF A-11	-3.88	-5.06	2.5
BUFF A-13	-4.23	-4.75	3
BUFF A-15	-4.16	-4.49	3.5
BUFF A-18	-4.02	-5.06	4
BUFF A-21	-3.52	-4.66	4.5
BUFF A-24	-3.69	-5.08	5
BUFF A-27	-3.64	-4.37	5.5
BUFF A-30	-3.52	-4.47	6
BUFF A-33	-3.63	-4.43	6.5
BUFF A-36	-3.31	-4.52	7
BUFF A-39	-3.26	-4.75	7.5
BUFF A-42	-3.39	-4.76	8
BUFF A-45	-2.96	-4.37	8.5
BUFF A-48	-3.03	-4.19	9
BUFF A-51	-3.45	-4.34	9.5
BUFF A-54	-3.48	-4.83	10
BUFF A-58	-3.48	-4.74	10.5
BUFF A-61	-3.12	-4.64	11
BUFF A-65	-3.40	-4.49	11.5
BUFF A-69	-3.78	-4.83	12
BUFF A72	-3.49	-4.25	12.5
BUFF A76	-3.91	-4.34	13
BUFF A80	-3.83	-4.11	13.5
BUFF A83	-4.30	-4.16	14
BUFF A87	-4.48	-3.80	14.5
BUFF A91	-4.28	-3.36	15
BUFF B(small)91.5	-4.60	-3.94	15.5
BUFF B(small)92	-5.60	-4.01	16
BUFF B(small)92.5	-5.65	-4.14	16.5
BUFF B(small)93	-5.06	-4.31	17
BUFF B(small)93.5	-4.96	-4.63	17.5
BUFF B(small)94	-4.94	-4.16	18
BUFF B(small)94.5	-4.72	-4.57	18.5
BUFF B(small)95	-5.07	-4.47	19
BUFF B(small)95.5	-5.22	-4.47	19.5
BUFF B(small)96	-5.13	-4.56	20
BUFF B(small)96.5	-5.66	-4.47	20.5
BUFF B(small)97	-5.89	-4.85	21
BUFF B - 98	-5.85	-4.74	21.5

Sample (MAK M1)	$\delta^{13}C$ ‰ PDB	$\delta^{18}O$ ‰ PDB	Distance from top of flowstone (cms)
CC A1-40.5	-7.83	-6.04	0.5
CC A1-41	-7.74	-6.04	1
CC A1-41.5	-7.85	-5.68	1.5
CC A1-42	-7.95	-6.02	2
CC A1-42.5	-7.92	-5.91	2.5
CC A1-43	-8.03	-5.57	3
CC A1-43.5	-8.18	-5.68	3.5
			4
CC A1-44.5	-8.03	-5.58	4.5
CC A1-45	-8.09	-5.50	5
CC A1-45.5	-8.25	-5.46	5.5
CC A1-46	-8.02	-5.34	6
CC A1-46.5	-7.74	-5.22	6.5
CC A1-47	-7.83	-5.24	7
CC A1-47.5	-7.79	-5.59	7.5
			8
CC A2-48.5	-7.91	-5.17	8.5
CC A2-49	-7.82	-5.17	9
CC A2-49.5	-7.92	-5.84	9.5
CC A2-50	-7.57	-5.71	10
CC A2-50.5	-7.52	-5.87	10.5
CC A2-51	-7.86	-5.57	11
CC A2-51.5	-7.82	-5.76	11.5
CC A2-52	-7.79	-5.48	12
CC A2-52.5	-7.60	-5.52	12.5
CC A2-53	-8.13	-6.71	13
CC A2-53.5	-7.95	-5.36	13.5
CC A2-54	-7.92	-5.53	14
CC A2-54.5	-8.11	-5.95	14.5
CC A2-55	-8.07	-5.65	15
CC A2-55.5	-8.20	-5.54	15.5
CC A2-56	-8.32	-5.24	16
CC A2-56.5	-8.16	-4.54	16.5
CC A2-57	-8.10	-5.16	17
CC A2-57.5	-8.26	-6.25	17.5
CC A2-58	-8.25	-5.43	18
CC A2-58.5	-8.14	-5.41	18.5
CC A2-59	-7.92	-5.48	19
CC A2-59.5	-8.19	-5.62	19.5
CC A2-60	-8.41	-5.61	20
CC A2-60.5	-8.46	-6.09	20.5
CC A2-61	-8.43	-6.17	21
CC A2-61.5	-8.57	-6.38	21.5
CC A2-62	-8.51	-6.17	22

BUFF B - 98.5	-5.56	-4.63	22
BUFF B - 99	-5.92	-4.69	22.5
BUFF B - 100	-5.78	-4.65	23
BUFF B - 100.5	-5.67	-4.71	23.5
BUFF B - 101	-5.67	-4.58	24
BUFF B - 101.5	-5.17	-4.95	24.5
BUFF B - 102	-5.10	-4.93	25
BUFF B - 102.5	-5.01	-4.62	25.5
BUFF B - 103	-4.66	-5.27	26
BUFF B - 103.5	-4.60	-4.79	26.5
BUFF B - 104	-4.37	-4.74	27
BUFF B - 104.5	-4.27	-4.66	27.5
BUFF B - 105	-4.53	-4.65	28
BUFF B - 105.5	-5.31	-4.81	28.5
BUFF B - 106	-5.05	-4.35	29
BUFF B 106.5	-5.17	-4.38	29.5
BUFF B 107	-5.53	-4.12	30
BUFF B - 107.5	-5.81	-4.24	30.5
BUFF B - 108	-5.77	-4.12	31
BUFF B - 108.5	-5.27	-4.49	31.5
BUFF B - 109	-5.82	-4.41	32
BUFF B - 109.5	-6.07	-4.52	32.5
BUFF B - 110	-5.97	-4.81	33
BUFF B-110.5	-6.23	-4.85	33.5
BUFF B-111	-4.59	-5.06	34
BUFF B-111.5	-5.37	-5.30	34.5
BUFF B-112	-3.96	-5.61	35
BUFF B-112.5	-3.30	-5.64	35.5
BUFF B-113	-3.99	-5.09	36
BUFF B-113.5	-5.02	-5.02	36.5
BUFF B-114	-4.59	-4.25	37
BUFF B-114.5	-4.94	-3.91	37.5
BUFF B-115	-4.26	-4.93	38
BUFF B-115.5	-4.14	-5.41	38.5
BUFF B-116	-4.59	-5.51	39
BUFF B-116.5	-4.06	-5.32	39.5
BUFF B-117	-4.88	-5.69	40
BUFF B-117.5	-5.32	-5.46	40.5
BUFF B-118	-4.33	-5.72	41
BUFF B-118.5	-4.03	-5.79	41.5
BUFF B-119	-4.41	-5.93	42
BUFF B-119.5	-4.10	-5.81	42.5
BUFF B-120	-3.78	-5.63	43
BUFF B-120.5	-3.65	-5.82	43.5
BUFF B-121	-3.78	-5.59	44
BUFF B-121.5	-3.70	-5.46	44.5
BUFF B-122	-3.52	-5.46	45
BUFF B-122.5	-3.74	-5.36	45.5
BUFF B-123	-4.36	-4.97	46
BUFF B-123.5	-4.56	-4.65	46.5
BUFF B-124	-5.98	-4.07	47

CC A2-62.5	-8.54	-6.40	22.5
CC A2-63	-8.50	-6.24	23
CC A2-63.5	-8.55	-6.43	23.5
CC A2-64	-8.29	-6.37	24
CC A2-64.5	-8.33	-6.46	24.5
CC A2-65	-8.34	-6.35	25
CC A2-65.5	-8.44	-6.65	25.5
CC A2-66	-8.36	-6.20	26
CC A2-66.5	-8.42	-6.99	26.5
CC A2-67	-7.91	-6.36	27
CC A2-67.5	-7.83	-6.14	27.5
CC A2-68	-8.06	-6.00	28
CC A2-68.5	-8.05	-6.09	28.5
CC A2-69	-8.24	-6.94	29
CC A2-69.5	-8.04	-5.83	29.5
CC A2-70	-8.27	-6.22	30
CC A2-70.5	-8.04	-5.98	30.5
CC A2-71	-8.65	-5.61	31
CC A2-71.5	-8.50	-5.48	31.5
CC A2-72	-7.87	-5.79	32
CC A2-72.5	-8.06	-5.77	32.5
CC A3-73	-8.27	-6.09	33
CC A3-73.5	-8.18	-6.02	33.5
CC A3-74	-8.27	-5.57	34
CC A3-74.5	-8.44	-5.72	34.5
CC A3-75	-8.04	-5.43	35
CC A3-75.5	-7.90	-6.20	35.5
CC A3-76	-7.84	-5.88	36
CC A3-76.5	-7.97	-5.43	36.5
CC A3-77	-8.10	-5.23	37
CC A3-77.5	-8.09	-5.34	37.5
CC A3-78	-8.31	-5.56	38
CC B-78.5	-8.17	-4.97	38.5
CC B-79	-8.09	-5.23	39
CC B-79.5	-8.31	-5.17	39.5
CC B-80	-8.45	-5.35	40
CC B-80.5	-8.65	-5.13	40.5
CCTEST4.5			41
CC B-81.5	-8.52	-5.55	41.5
CC B-82	-8.23	-5.45	42
CC B-82.5	-8.05	-5.50	42.5
CC B-83	-8.24	-5.35	43
CC B-83.5	-8.26	-5.31	43.5
CC B-84	-8.38	-5.42	44
CC B-84.5	-8.42	-5.23	44.5
CC B-85	-8.14	-5.66	45
CC B-85.5	-7.96	-5.01	45.5
CC B-86	-8.09	-5.75	46
CC B-86.5	-7.78	-5.38	46.5
CC B-87	-7.62	-5.71	47
CC B-87.5	-7.69	-5.02	47.5

BUFF C1-124.5	-4.32	-5.00	47.5
BUFF C1-125	-5.24	-5.19	48
BUFF C1-125.5	-5.58	-5.03	48.5
BUFF C1-126	-5.49	-5.14	49
BUFF C1-126.5	-4.78	-5.15	49.5
BUFF C1-127	-4.90	-4.84	50
BUFF C1-127.5	-4.73	-4.97	50.5
BUFF C1-128	-4.77	-5.25	51
BUFF C1-128.5	-5.01	-5.28	51.5
BUFF C1-129	-5.00	-5.55	52
BUFF C1-129.5	-5.25	-5.23	52.5
BUFF C1-130	-5.89	-5.22	53
BUFF C1-130.5	-5.25	-5.66	53.5
BUFF C1-131	-5.15	-5.63	54
BUFF C1-131.5	-4.79	-5.71	54.5
BUFF C1-132	-4.43	-5.97	55
BUFF C1-132.5	-4.54	-5.72	55.5
BUFF C1-133	-4.48	-5.91	56
BUFF C1-133.5	-4.56	-5.75	56.5
BUFF C1-134	-4.25	-5.94	57
BUFF C1-134.5	-4.31	-5.94	57.5
BUFF C1-135	-4.30	-5.96	58
BUFF C1-135.5	-3.99	-6.16	58.5
BUFF C1-136	-4.13	-5.67	59
BUFF C1-136.5	-4.56	-5.55	59.5
BUFF C1-137	-4.57	-5.46	60
BUFF C1-137.5	-4.71	-5.44	60.5
BUFF C1-138	-5.41	-5.45	61
BUFF C1-138.5	-5.79	-5.74	61.5
BUFF C1-139	-5.50	-4.45	62
BUFF C1-139.5	-5.34	-4.78	62.5
BUFF C1-140	-4.64	-4.25	63
BUFF D-156.5	-4.86	-4.82	63.5
BUFF D-157	-4.65	-4.87	64
BUFF D-157.5	-4.40	-5.21	64.5
BUFF D-158	-3.44	-5.53	65
BUFF D-158.5	-3.30	-5.44	65.5
BUFF D-159	-2.93	-5.53	66
BUFF D-159.5	-3.01	-5.53	66.5
BUFF D-160	-2.89	-5.53	67
BUFF D-160.5	-2.99	-5.68	67.5
BUFF D-161	-2.85	-5.40	68
BUFF D-161.5	-2.83	-5.04	68.5
BUFF D-162	-3.15	-5.45	69
BUFF D-162.5	-2.90	-5.59	69.5
BUFF D-163	-3.10	-5.44	70
BUFF D-163.5	-3.50	-5.39	70.5
BUFF D-164	-3.28	-5.50	71
BUFF D-164.5	-3.52	-5.27	71.5
BUFF D-165	-3.37	-5.47	72
BUFF D-165.5	-3.32	-5.36	72.5

CC B-88	-7.76	-6.00	48
CC B-88.5	-7.73	-5.61	48.5
CC B-89	-8.05	-5.70	49
CC B-89.5	-8.32	-5.67	49.5
CC B-90	-8.06	-5.90	50
CC B-90.5	-8.33	-6.90	50.5
CC B-91	-8.15	-5.59	51
CC B-91.5	-8.00	-6.19	51.5
CC B-92	-8.06	-6.42	52
CC B-92.5	-8.14	-6.17	52.5
CC B-93	-7.84	-5.63	53
CC B-93.5	-8.06	-5.72	53.5
CC B-94	-7.72	-5.88	54
CC B-94.5	-7.87	-5.84	54.5
CCTEST6			55
CC B-95.5	-8.19	-5.63	55.5
CC B-96	-8.25	-5.68	56
CC B-96.5	-8.27	-6.02	56.5
CC Bblock-97	-7.88	-5.81	57
CC Bblock-97.5	-8.35	-5.95	57.5
CC Bblock-98	-8.31	-5.86	58
CC Bblock-98.5	-8.39	-5.43	58.5
CCTEST7			59
CC Bblock-99.5	-8.08	-5.78	59.5
CC Bblock-100	-8.49	-5.44	60
CC Bblock-100.5	-8.79	-5.06	60.5
CC Bblock-101	-8.83	-4.94	61
CC Bblock-101.5	-8.54	-4.98	61.5
CC Bblock-102	-8.53	-5.09	62
CC Bblock-102.5	-8.54	-5.51	62.5
CC Bblock-103	-8.41	-5.29	63
CC Bblock-103.5	-8.11	-5.64	63.5
CC Bblock-104	-8.24	-5.33	64
CC Bblock-104.5	-7.95	-6.16	64.5
CC Bblock-105	-7.82	-5.72	65
CC Bblock-105.5	-8.18	-5.51	65.5
CC Bblock-106	-8.07	-5.19	66
CC Bblock-106.5	-8.26	-6.14	66.5
CC Bblock-107	-8.08	-5.97	67
CC Bblock-107.5	-7.99	-5.43	67.5
CC Bblock-108	-8.08	-5.12	68
CC Bblock-108.5	-8.26	-5.36	68.5
CC Bblock-109	-7.98	-5.01	69
CC C1 1/2-109.5	-8.31	-5.51	69.5
CC C1 1/2-110	-8.20	-5.32	70
CC C1 1/2-110.5	-8.18	-4.66	70.5
CC C1 1/2-111	-8.20	-5.02	71
CC C1 1/2-111.5	-7.73	-5.22	71.5
CC C1 1/2-112	-8.08	-4.90	72
CC C1 1/2-112.5	-8.09	-5.84	72.5
CC C1 1/2-113	-8.27	-5.65	73

BUFF D-166	-3.31	-5.72	73
BUFF D-166.5	-4.18	-5.64	73.5
BUFF D-167	-3.93	-5.31	74
BUFF D-167.5	-4.50	-5.25	74.5
BUFF D-168	-4.78	-4.86	75
BUFF D-168.5	-4.78	-4.98	75.5
BUFF D-169	-4.82	-4.52	76
BUFF D-169.5	-5.01	-4.88	76.5
BUFF D-170	-5.07	-4.54	77
BUFF D-170.5	-5.24	-4.60	77.5
BUFF D-171	-5.20	-4.10	78
BUFF D-171.5	-5.12	-3.92	78.5
BUFF D-172	-5.13	-4.36	79
BUFF D-172.5	-5.14	-4.10	79.5
BUFF DD-173	-5.08	-4.32	80
BUFF DD-173.5	-5.14	-4.14	80.5
BUFF DD-174	-4.97	-4.35	81
BUFF DD-174.5	-4.96	-4.30	81.5
BUFF DD-175	-5.08	-4.63	82
BUFF DD-175.5	-5.29	-4.77	82.5
BUFF DD-176	-5.08	-4.63	83
BUFF DD-176.5	-5.07	-4.41	83.5
BUFF DD-177	-4.83	-5.13	84
BUFF DD-177.5	-4.46	-4.80	84.5
BUFF DD-178	-4.13	-5.12	85
BUFF DD-178.5	-4.21	-5.12	85.5
BUFF DD-179	-4.09	-4.87	86
BUFF DD-179.5	-4.03	-4.92	86.5
BUFF DD-180	-3.69	-5.17	87
BUFF DD-180.5	-3.69	-5.23	87.5
BUFF DD-181	-3.64	-5.41	88
BUFF DD-181.5	-4.09	-4.72	88.5
BUFF DD-182	-3.46	-5.81	89
BUFF DD-182.5	-3.26	-5.24	89.5
BUFF DD-183	-3.78	-5.08	90
BUFF DD-183.5	-3.92	-5.14	90.5
BUFF DD-184	-4.50	-5.40	91
BUFF DD-184.5	-4.66	-5.48	91.5
BUFF DD-185	-4.52	-4.99	92
BUFF DD-185.5	-4.56	-5.46	92.5
BUFF DEF-186	-4.71	-4.85	93
BUFF DEF-186.5	-5.20	-5.46	93.5
BUFF DEF-187	-5.07	-5.25	94
BUFF DEF-187.5	-4.94	-5.86	94.5
BUFF DEF-188	-4.83	-5.03	95
BUFF DEF-188.5	-4.87	-5.27	95.5
BUFF DEF-189	-4.59	-5.72	96
BUFF DEF-189.5	-4.40	-5.04	96.5
BUFF DEF-190	-4.48	-5.12	97
BUFF DEF-190.5	-4.65	-5.33	97.5
BUFF DEF-191	-4.23	-5.35	98

CC C1 1/2-113.5	-8.39	-5.15	73.5
CC C1 1/2-114	-8.36	-5.59	74
CC C1 1/2-114.5	-8.27	-5.48	74.5
CC C1 1/2-115	-8.07	-5.16	75
CC C1 1/2-115.5	-8.20	-5.23	75.5
CC C1 1/2-116	-8.14	-5.41	76
CC C1 2/2-116.5	-8.02	-5.16	76.5
CC C1 2/2-117	-8.08	-5.12	77
CC C1 2/2-117.5	-8.06	-5.56	77.5
CC C1 2/2-118	-7.92	-5.64	78
CC C1 2/2-118.5	-7.79	-5.65	78.5
CC C1 2/2-119	-7.96	-6.05	79
CC C1 2/2-119.5	-8.02	-5.87	79.5
CC C1 2/2-120	-7.99	-5.69	80
CC C1 2/2-120.5	-8.12	-5.73	80.5
CC C1 2/2-121	-8.40	-5.76	81
CC C1 2/2-121.5	-8.67	-5.87	81.5
CC C1 2/2-122	-8.71	-5.96	82
CC C1 2/2-122.5	-8.63	-5.53	82.5
CC C1 2/2-123	-8.83	-6.32	83
CC C1 2/2-123.5	-8.44	-5.77	83.5
CC C1 2/2-124	-8.30	-5.67	84
CC C1 2/2-124.5	-7.97	-5.97	84.5
CC C2-125	-8.49	-5.81	85
CC C2-125.5	-8.45	-5.85	85.5
CC C2-126	-8.59	-5.58	86
CC C2-126.5	-8.52	-5.81	86.5
CC C2-127	-8.51	-5.38	87
CC C2-127.5	-8.19	-5.84	87.5
CC C2-128	-8.25	-5.77	88
CC C2-128.5	-8.05	-5.95	88.5
CC C2-129	-7.94	-5.76	89
CC C2-129.5	-7.99	-6.03	89.5
CC C2-130	-8.32	-6.05	90
CC C2-130.5	-8.24	-6.10	90.5
CC C2-131	-7.89	-5.73	91
CC C2-131.5	-7.81	-5.59	91.5
CC C2-132	-7.85	-6.01	92
CC C3-132.5	-8.01	-6.50	92.5
CC C3-133	-7.82	-5.88	93
CC C3-133.5	-7.73	-6.13	93.5
CC C3-134	-7.98	-5.90	94
CC C3-134.5	-7.71	-5.73	94.5
CC C3-135	-7.37	-5.76	95
CC C3-135.5	-7.53	-5.46	95.5
CC C3-136	-7.77	-5.99	96
CC C3-136.5	-7.69	-6.02	96.5
CC C3-137	-7.64	-5.85	97
CC C3-137.5	-7.74	-5.97	97.5
CC C3-138	-7.08	-5.87	98
CC C3-138.5	-8.19	-5.70	98.5

BUFF DEF-191.5	-4.06	-4.88	98.5
BUFF DEF-192	-3.95	-5.51	99
BUFF DEF-192.5	-3.92	-5.92	99.5
BUFF DEF-193	-3.63	-5.64	100
BUFF DEF-193.5	-4.03	-5.50	100.5
BUFF DEF-194	-4.03	-5.19	101
BUFF DEF-194.5	-4.18	-5.23	101.5
BUFF DG-195	-3.95	-4.77	102
BUFF DG-195.5	-3.92	-5.45	102.5
BUFF DG-196	-3.68	-5.28	103
BUFF DG-196.5	-3.98	-5.33	103.5
BUFF DG-197	-4.04	-5.19	104
BUFF DG-197.5	-4.11	-5.36	104.5
BUFF DG-198	-4.03	-5.52	105
BUFF DG-198.5	-4.26	-6.46	105.5
BUFF DG-199	-4.07	-5.23	106
BUFF DG-199.5	-4.01	-5.21	106.5
BUFF DG-200	-4.19	-5.23	107
BUFF DG-200.5	-4.58	-5.14	107.5
BUFF DG-201	-4.20	-5.32	108
BUFF DG-201.5	-4.14	-4.95	108.5
BUFF DG-202	-3.82	-4.95	109
BUFF DG-202.5	-3.82	-4.49	109.5
BUFF DG-203	-3.69	-4.41	110
BUFF DG-203.5	-3.82	-5.01	110.5
BUFF DG-204	-3.89	-5.64	111
BUFF DG-204.5	-3.70	-5.85	111.5
BUFF DG-205	-4.09	-5.44	112
BUFF DG-205.5	-3.72	-5.04	112.5
BUFF DG-206	-3.95	-5.30	113
BUFF DG-206.5	-4.19	-4.90	113.5
BUFF DG-207	-3.72	-4.82	114
BUFF DG-207.5	-3.48	-5.19	114.5
BUFF DG-208	-3.24	-5.22	115
BUFF DG-208.5	-3.29	-5.18	115.5
BUFF E-209	-3.76	-5.82	116
BUFF E-209.5	-3.67	-4.86	116.5
BUFF E-210	-3.56	-4.96	117
BUFF E-210.5	-4.04	-4.97	117.5
BUFF E-211	-4.24	-4.43	118
BUFF E-211.5	-4.10	-4.50	118.5
BUFF E-212	-4.15	-4.45	119
BUFF E-212.5	-4.10	-4.66	119.5
BUFF E-213	-4.20	-4.90	120
BUFF E-213.5	-4.24	-4.58	120.5
BUFF E-214	-4.14	-4.96	121
BUFF E-214.5	-4.17	-5.18	121.5
BUFF E-215	-4.06	-4.52	122
BUFF E-215.5	-3.91	-4.96	122.5
BUFF E-216	-3.78	-4.81	123
BUFF E-216.5	-3.96	-4.59	123.5

CC C3-139	-8.04	-5.87	99
CC C3-139.5	-7.87	-5.69	99.5
CC C3-140	-7.73	-5.80	100
CC C3-140.5	-7.65	-5.74	100.5
CC C3-141	-7.82	-5.71	101
CC C3-141.5	-7.99	-5.48	101.5
CC C3-142	-7.99	-5.66	102
CC C3-142.5	-8.10	-5.71	102.5
CC C3-143	-8.21	-5.78	103
CC C3-143.5	-8.24	-5.84	103.5
CC C3-144	-8.23	-5.38	104
CC C3-144.5	-8.13	-5.33	104.5
CC C3-145	-8.27	-5.83	105
CC C3-145.5	-8.48	-5.71	105.5
CC C3-146	-8.48	-5.16	106
CC C3-146.5	-8.40	-5.48	106.5
CC C3-147	-8.53	-5.63	107
CC C3-147.5	-8.58	-5.20	107.5
CC C3-148	-8.37	-5.60	108
CC C3-148.5	-8.33	-5.24	108.5
CC C3-149	-8.21	-4.89	109
CC C3-149.5	-8.35	-4.95	109.5
CC C3-150	-8.34	-5.16	110
CC C3-150.5	-8.50	-5.30	110.5
CC C3-151	-8.20	-5.29	111
CC C3-151.5	-8.07	-5.27	111.5
CC C3-152	-7.98	-5.56	112
CC C3-152.5	-8.15	-5.75	112.5
CC C3-153	-8.04	-5.68	113
CC C3-153.5	-8.11	-5.48	113.5
CC C3-154	-7.98	-5.85	114
CC C3-154.5	-7.94	-5.92	114.5
CC C3-155	-8.04	-5.55	115
CC C3-155.5	-8.03	-5.79	115.5
CC C3-156	-7.97	-5.81	116
CC C3-156.5	-8.21	-6.52	116.5
CC C3-157	-7.59	-5.99	117
CC C3-157.5	-7.91	-6.04	117.5
CC C3-158	-7.93	-5.75	118
CC C3-158.5	-7.91	-5.66	118.5
CC C3-159	-8.11	-5.64	119
CC C3-159.5	-8.32	-6.30	119.5
CC C3-160	-8.06	-6.40	120
CC C3-160.5	-7.81	-5.80	120.5
CC C3-161	-8.08	-5.80	121
CC C3-161.5	-8.01	-6.14	121.5
CC C3-162	-8.04	-6.39	122

BUFF E-217	-4.29	-4.93	124
BUFF E-217.5	-4.00	-4.63	124.5
BUFF E-218	-3.84	-4.92	125
BUFF E-218.5	-3.50	-4.65	125.5
BUFF E-219	-4.25	-4.59	126
BUFF E-219.5	-3.55	-5.08	126.5
BUFF E-220	-3.48	-4.66	127
BUFF E-220.5	-3.79	-4.98	127.5
BUFF E-221	-4.00	-4.81	128
BUFF E-221.5	-4.15	-4.33	128.5
BUFF E-222	-4.27	-5.39	129
BUFF E-222.5	-4.01	-5.36	129.5
BUFF E-223	-4.34	-4.92	130
BUFF E-223.5	-4.49	-5.14	130.5
BUFF E-224	-4.75	-4.83	131
BUFF E-224.5	-4.34	-4.75	131.5
BUFF E-225	-4.29	-4.53	132
BUFF E-225.5	-4.47	-5.11	132.5
BUFF E-226	-4.78	-4.74	133
BUFF E-226.5	-4.66	-4.62	133.5
BUFF E-227	-4.48	-4.62	134
BUFF E-227.5	-4.68	-4.48	134.5
BUFF E-228	-5.20	-4.51	135
BUFF E-228.5	-5.44	-4.52	135.5
BUFF E-229	-6.08	-4.24	136
BUFF E-229.5	-4.99	-3.99	136.5
BUFF E-230	-4.83	-4.04	137
BUFF E-230.5	-5.09	-3.92	137.5
BUFF E-231	-5.91	-4.52	138
BUFF E-231.5	-5.43	-4.51	138.5
BUFF E-232	-6.08	-4.69	139
BUFF E-232.5	-6.22	-5.22	139.5
BUFF E-233	-5.30	-5.00	140
BUFF E-233.5	-4.75	-5.43	140.5
BUFF E-234	-4.44	-5.35	141
BUFF E-234.5	-4.54	-5.15	141.5
BUFF E-235	-4.59	-5.90	142
BUFF E-235.5	-4.97	-5.44	142.5
BUFF E-236	-4.04	-5.27	143
BUFF E-236.5	-4.79	-5.10	143.5
BUFF E-237	-6.65	-4.13	144
BUFF E-237.5	-6.94	-3.77	144.5
BUFF E-238	-6.40	-3.72	145
BUFF E-238.5	-6.30	-3.88	145.5
BUFF E-239	-6.07	-4.29	146
BUFF E-239.5	-6.46	-4.49	146.5
BUFF E-240	-6.05	-4.57	147
BUFF E-240.5	-4.31	-5.80	147.5
BUFF E-241	-4.37	-5.73	148
BUFF E-241.5	-4.50	-5.08	148.5
BUFF F-242	-3.95	-5.59	149

BUFF F-242.5	-3.56	-5.20	149.5
BUFF F-243	-3.59	-5.43	150
BUFF F-243.5	-3.50	-5.23	150.5
BUFF F-244	-3.54	-5.38	151
BUFF F-244.5	-3.84	-5.69	151.5
BUFF F-245	-6.65	-3.90	152
BUFF F-245.5	-6.40	-4.85	152.5
BUFF F-246	-5.61	-5.04	153
BUFF F-246.5	-5.72	-4.11	153.5
BUFF F-247	-5.83	-4.39	154
BUFF F-247.5	-4.44	-4.51	154.5
BUFF F-248	-4.99	-4.60	155
BUFF F-248.5	-5.53	-4.93	155.5
BUFF F-249	-4.75	-5.24	156
BUFF F-249.5	-2.73	-5.00	156.5
BUFF F-250	-2.59	-5.09	157
BUFF F-250.5	-3.86	-5.38	157.5
BUFF F-251	-3.08	-5.11	158
BUFF F-251.5	-4.52	-4.87	158.5
BUFF F-252	-5.12	-4.85	159
BUFF F-252.5	-6.38	-4.59	159.5
BUFF F-253	-6.24	-4.56	160
BUFF F-253.5	-7.06	-4.50	160.5
BUFF F-254	-6.69	-4.05	161
BUFF F-254.5	-6.63	-4.33	161.5
BUFF F-255	-6.14	-4.70	162
BUFF F-255.5	-6.71	-3.96	162.5
BUFF F-256	-5.97	-4.20	163
BUFF F-256.5	-6.38	-4.26	163.5
BUFF F-257	-7.13	-4.65	164
BUFF F-257.5	-5.49	-4.90	164.5
BUFF F-258	-6.35	-4.43	165
BUFF F-258.5	-6.52	-3.87	165.5
BUFF F-259	-6.04	-4.46	166
BUFF F-259.5	-6.86	-4.39	166.5
BUFF F-260	-6.65	-4.47	167
BUFF F-260.5	-6.61	-4.49	167.5
BUFF F-261	-6.95	-4.13	168
BUFF F-261.5	-6.87	-4.01	168.5
BUFF F-262	-6.59	-4.24	169
BUFF F-262.5	-7.69	-4.87	169.5
BUFF F-263	-6.61	-3.95	170
BUFF F-263.5	-6.73	-4.76	170.5
BUFF F-264	-6.15	-4.45	171
BUFF F-264.5	-6.21	-3.88	171.5
BUFF F-265	-6.38	-4.00	172
BUFF F-265.5	-6.26	-4.11	172.5
BUFF H-266	-5.82	-4.50	173
BUFF H-266.5	-6.16	-5.16	173.5
BUFF H-267	-5.67	-4.42	174
BUFF H-267.5	-5.87	-4.14	174.5

BUFF H-268	-6.15	-3.96	175
BUFF H-268.5	-7.01	-4.63	175.5
BUFF H-269	-6.91	-4.19	176
BUFF H-269.5	-6.19	-4.10	176.5
BUFF H-270	-6.61	-4.00	177
BUFF H-270.5	-6.29	-4.04	177.5
BUFF H-271	-6.73	-4.50	178
BUFF H-271.5	-6.39	-4.54	178.5
BUFF H-272	-6.22	-4.85	179
BUFF H-272.5	-6.09	-4.77	179.5
BUFF H-273	-7.14	-4.44	180
BUFF H-273.5	-8.24	-4.04	180.5
BUFF J-274	-7.81	-4.06	181
BUFF J-274.5	-7.94	-4.26	181.5
BUFF J-275	-8.02	-4.07	182
BUFF J-275.5	-7.31	-4.29	182.5
BUFF J-276	-6.92	-4.53	183
BUFF J-276.5	-6.06	-4.01	183.5
BUFF J-277	-5.39	-4.04	184
BUFF J-277.5	-6.17	-4.68	184.5
BUFF J-278	-6.28	-4.52	185
BUFF J-278.5	-6.50	-4.04	185.5
BUFF J-279	-3.99	-4.72	186
BUFF J-279.5	-5.97	-4.87	186.5
BUFF J-280	-5.02	-4.27	187
BUFF K-280.5	-4.88	-5.41	187.5
BUFF K-281	-4.23	-5.58	188
BUFF K-281.5	-4.14	-5.62	188.5
BUFF K-282	-4.46	-5.74	189
BUFF K-282.5	-4.66	-6.00	189.5
BUFF K-283	-5.08	-6.00	190
BUFF K-283.5	-5.18	-5.60	190.5
BUFF K-284	-5.03	-5.53	191
BUFF K-284.5	-5.25	-5.40	191.5
BUFF K-285	-5.54	-5.63	192
BUFF K-285.5	-5.27	-4.94	192.5
BUFF K-286	-5.20	-4.81	193
BUFF K-286.5	-5.82	-4.28	193.5
BUFF K-287	-4.79	-4.13	194
BUFF K-287.5	-4.96	-4.75	194.5
BUFF K-288	-5.18	-4.84	195
BUFF K-288.5	-5.63	-4.80	195.5
BUFF K-289	-5.92	-5.40	196
BUFF K-289.5	-5.92	-5.08	196.5
BUFF L-290	-5.06	-4.77	197
BUFF N1-309.5	-5.64	-5.09	197.5
BUFF N1-310	-5.68	-4.92	198
BUFF N1-310.5	-5.38	-4.58	198.5
BUFF N1-311	-5.35	-4.51	199
BUFF N1-311.5	-4.90	-4.43	199.5
BUFF N1-312	-5.02	-4.16	200

BUFF N1-312.5	-4.03	-4.32	200.5
BUFF N1-313	-3.86	-4.22	201
BUFF N1-313.5	-4.45	-4.33	201.5
BUFF N1-314	-4.98	-4.78	202
BUFF N1-314.5	-5.10	-4.90	202.5
BUFF N1-315	-5.24	-5.06	203
BUFF N1-315.5	-5.50	-4.98	203.5
BUFF N2-316	-5.12	-4.77	204
BUFF N2-316.5	-5.27	-5.00	204.5
BUFF N2-317	-5.78	-4.92	205
BUFF N2-317.5	-5.32	-4.92	205.5
BUFF N2-318	-5.07	-4.64	206
BUFF N2-318.5	-5.77	-4.98	206.5
BUFF N2-319	-7.22	-4.42	207
BUFF N2-319.5	-6.74	-4.78	207.5
BUFF N2-320	-6.11	-4.61	208
BUFF N2-320.5	-6.33	-4.29	208.5
BUFF N3-321	-6.40	-4.57	209
BUFF N3-321.5	-6.19	-5.33	209.5
BUFF N3-322	-5.65	-4.93	210
BUFF N3-322.5	-6.87	-4.33	210.5
BUFF N3-323	-6.01	-4.48	211
BUFF N3-323.5	-5.92	-4.36	211.5
BUFF N3-324	-6.34	-4.49	212
BUFF N3-324.5	-6.41	-4.75	212.5
BUFF N3-325	-6.09	-4.77	213
BUFF N4-325.5	-6.24	-4.62	213.5
BUFF N4-326	-6.02	-4.71	214
BUFF N4-326.5	-6.22	-4.84	214.5
BUFF N4-327	-6.46	-4.43	215
BUFF N4-327.5	-5.58	-4.81	215.5
BUFF N4-328	-5.92	-4.76	216
BUFF N4-328.5	-6.61	-4.29	216.5
BUFF N4-329	-6.14	-5.26	217
BUFF N4-329.5	-5.89	-4.37	217.5
BUFF N4-330	-6.78	-4.95	218
BUFF N4-330.5	-7.29	-4.30	218.5
BUFF N4-331	-7.29	-4.53	219
BUFF N4-331.5	-8.01	-4.50	219.5
BUFF N4-332	-7.02	-5.44	220
BUFF N4-332.5	-6.73	-5.77	220.5
BUFF N4-333	-7.44	-4.92	221
BUFF N4-333.5	-7.13	-4.58	221.5
BUFF N4-334	-7.00	-4.39	222
BUFF N4-334.5	-7.31	-4.45	222.5
BUFF N4-335	-7.50	-4.62	223
BUFF N4-335.5	-6.88	-4.65	223.5
BUFF N4-336	-6.40	-4.63	224
BUFF N4-336.5	-6.63	-5.04	224.5
BUFF N4-337	-6.41	-4.73	225
BUFF N4-337.5	-6.49	-5.19	225.5

BUFF N4-338	-6.02	-5.38	226
BUFF N4-338.5	-6.87	-4.85	226.5
BUFF N4-339	-7.48	-4.12	227
BUFF N4-339.5	-6.30	-4.68	227.5
BUFF N4-340	-6.34	-5.15	228
BUFF N4-340.5	-5.17	-4.26	228.5
BUFF N4-341	-6.67	-5.16	229
BUFF N4-341.5	-5.40	-4.20	229.5
BUFF N4-342	-5.18	-4.29	230
BUFF N4-342.5	-5.26	-4.40	230.5
BUFF N4-343	-5.16	-4.57	231
BUFF N4-343.5	-4.59	-4.69	231.5
BUFF N4-344	-4.24	-4.74	232
BUFF N4-344.5	-6.56	-5.57	232.5
BUFF N4-345	-6.52	-5.98	233
BUFF N4-345.5	-6.59	-6.06	233.5
BUFF N4-346	-6.00	-5.04	234
BUFF N4-346.5	-6.79	-4.68	234.5
BUFF N4-347	-5.92	-4.49	235
BUFF N4-347.5	-5.71	-4.46	235.5
BUFF N4-348	-5.54	-4.89	236
BUFF N4-348.5	-5.32	-4.94	236.5
BUFF N4-349	-5.31	-4.95	237
BUFF N4-349.5	-5.82	-4.97	237.5
BUFF N4-350	-5.45	-4.99	238
BUFF N4-350.5	-5.53	-5.00	238.5
BUFF N4-351	-5.79	-5.01	239
BUFF N4-351.5	-5.97	-5.11	239.5
BUFF N4-352	-5.99	-4.99	240
BUFF N4-352.5	-5.56	-5.27	240.5
BUFF N4-353	-5.42	-4.89	241